REVIEWS OF MODERN PHYSICS, VOLUME 73, OCTOBER 2001

Traffic and related self-driven many-particle systems

Dirk Helbing*

Institute for Economics and Traffic, Dresden University of Technology, Andreas-Schubert-Str. 23, D-01062 Dresden, Germany and Institute of Theoretical Physics, University of Stuttgart, Pfaffenwaldring 57/III, D-70550 Stuttgart, Germany and Collegium Budapest—Institute for Advanced Study, Szentháromság utca 2, H-1014 Budapest, Hungary

(Published 7 December 2001)

Since the subject of traffic dynamics has captured the interest of physicists, many surprising effects have been revealed and explained. Some of the questions now understood are the following: Why are vehicles sometimes stopped by "phantom traffic jams" even though drivers all like to drive fast? What are the mechanisms behind stop-and-go traffic? Why are there several different kinds of congestion, and how are they related? Why do most traffic jams occur considerably before the road capacity is reached? Can a temporary reduction in the volume of traffic cause a lasting traffic jam? Under which conditions can speed limits speed up traffic? Why do pedestrians moving in opposite directions normally organize into lanes, while similar systems "freeze by heating"? All of these questions have been answered by applying and extending methods from statistical physics and nonlinear dynamics to self-driven many-particle systems. This article considers the empirical data and then reviews the main approaches to modeling pedestrian and vehicle traffic. These include microscopic (particle-based), mesoscopic (gas-kinetic), and macroscopic (fluid-dynamic) models. Attention is also paid to the formulation of a micro-macro link, to aspects of universality, and to other unifying concepts, such as a general modeling framework for self-driven many-particle systems, including spin systems. While the primary focus is upon vehicle and pedestrian traffic, applications to biological or socio-economic systems such as bacterial colonies, flocks of birds, panics, and stock market dynamics are touched upon as well.

CONTENTS

*Electronic address: helbing@trafficforum.org

I. INTRODUCTION

A. Motivation: History of traffic modeling and the impact of traffic on society

The interest in the subject of traffic dynamics is surprisingly old. In 1935, Greenshields carried out early studies of vehicular traffic, and in the 1950s, there was considerable publication activity in journals on operations research and engineering. These papers introduced the fundamental diagram showing the relation between traffic flow and vehicle density or the instability of traffic flow, which are still relevant. The motivation for such studies was self-evident. As Greenberg wrote in 1959, "The volume of vehicular traffic in the past several years has rapidly outstripped the capacities of the nation's highways. It has become increasingly necessary to understand the dynamics of traffic flow and obtain a mathematical description of the process."

More than 40 years later, the situation has greatly deteriorated. Cities like Los Angeles and San Francisco suffer from heavy traffic congestion around the clock. In Europe, as well, the time that drivers spend standing in traffic jams amounts to several days each year. During holiday seasons, jams may grow up to more than 100 km in size. Vehicle emissions of SO_2, NO_x, CO, CO_2, dust particles, smog, and noise have reached or even exceeded levels comparable to those from industrial production or private households, and are harmful to the environment and human health. On average, every second driver is involved in one serious accident during his or her lifetime. In Germany alone, the financial damage from traffic due to accidents and environmental impact is estimated to be \$100 billion each year. The economic loss due to congested traffic is of the same order of magnitude. However, the volume of traffic is still growing because of increased demands for mobility and modern logistics.

Without doubt, an efficient transportation system is essential for the functioning and success of modern industrialized societies. But the days when freeways were free ways are over. The increasing problems of roadway traffic raise the following questions: Is it still affordable and publicly acceptable to expand the infrastructure? Will drivers still buy cars when streets are effectively turned into parking lots? Automobile companies, worried about their future market, have spent considerable amounts of money for research on traffic dynamics and on how the available infrastructure could be used more efficiently by new technologies (telematics).

Physicists have also addressed the problems of traffic dynamics. Although, among mathematicians, physicists, and chemists, there were some early pioneers like Whitham, Prigogine, Montroll, and Kühne, the primary research started in 1992 and 1993 with papers by Biham *et al.* (1992), Nagel and Schreckenberg (1992), and Kerner and Konhäuser (1993). These papers initiated an avalanche of publications in various international physics journals. Since then, it has been difficult to keep track of the scientific developments and literature. Therefore it is high time for a review on traffic that tries to bring together the different approaches and to show their inter-relations. In this review, I shall take into account many significant contributions by traffic engineers. I hope that this will stimulate discussion and cooperation among the different disciplines involved.

In the following sections, I shall try to give an overview of the field of traffic dynamics from the perspective of many-particle physics.

B. Driven many-particle systems in classical mechanics, fluids, and granular media

Dynamics and pattern formation in systems far from equilibrium, especially living systems, have long posed a challenge for physicists.[1] Nonequilibrium systems are characterized by not being closed, i.e., by having an exchange of energy, particles, and/or information with their environment. Consequently they often show complex behavior and, normally, there are no general results such as the laws of thermodynamics and statistical mechanics for closed systems of gases, fluids, or solids in equilibrium. Nevertheless, they can be cast in a general mathematical framework (Helbing, 2001) as I shall show here.

Let us start with Newton's equation of motion from classical mechanics, which describes the acceleration $\ddot{\mathbf{x}}_\alpha(t)$ of a body α of mass m_α subject to pair interactions with other bodies β:

$$m_\alpha \ddot{\mathbf{x}}_\alpha(t) = \sum_{\beta(\neq\alpha)} \mathbf{F}_{\alpha\beta}(t). \tag{1}$$

The interaction forces $\mathbf{F}_{\alpha\beta}(t)$ are mostly dependent on the locations $\mathbf{x}_\alpha(t)$ and $\mathbf{x}_\beta(t)$ of the interacting bodies α and β at time t. Often, they depend only on the distance vector $\mathbf{d}_{\alpha\beta}=(\mathbf{x}_\beta-\mathbf{x}_\alpha)$, but in special cases, they are also functions of the velocities $\mathbf{v}_\alpha(t)=\dot{\mathbf{x}}_\alpha(t)$ and $\mathbf{v}_\beta(t)=\dot{\mathbf{x}}_\beta(t)$. For potential forces, the above many-body system can be characterized by a Hamilton function. A typical example is the description of the motion of celestial bodies.

In *driven* many-body systems such as fluids under the influence of pressure gradients and boundary forces or vibrated granular media like sand, we have to consider additional interactions with the environment. Therefore we need to consider additional terms. This includes (external) driving forces $\mathbf{F}_0(\mathbf{x},t)$ due to boundary interactions and gravitational or electrical fields, (sliding) friction forces $\mathbf{F}_{\rm fr}(t)=-\gamma_\alpha \mathbf{v}_\alpha(t)$ with friction coefficient γ_α, and individual fluctuations $\boldsymbol{\zeta}_\alpha(t)$ reflecting thermal interactions with the environment (boundaries, air, etc.) or a variation of the surface structure of the particles:

$$m_\alpha \ddot{\mathbf{x}}_\alpha(t) = \mathbf{F}_0(\mathbf{x}_\alpha(t),t) - \gamma_\alpha \mathbf{v}_\alpha(t) + \sum_{\beta(\neq\alpha)} \mathbf{F}_{\alpha\beta}(t) + \boldsymbol{\zeta}_\alpha(t). \tag{2}$$

From this "microscopic," molecular-dynamics type of equation, one can systematically derive "macroscopic," fluid-dynamic equations for the spatio-temporal evolution of the particle density, the momentum density or average velocity, and the energy density or velocity variance (related to the temperature). The methods for the construction of this micro-macro link will be sketched in Sec. III.E.

In driven systems, the ongoing competition between the driving forces and the dissipative friction forces leads to a spatio-temporal redistribution of energy, which produces a great variety of self-organization phenomena. These result from nonlinearities in the equations of motion, which allow small initial perturbations to be enhanced and nonequilibrium patterns to be dynamically stabilized. In fluids one can find the formation of waves or vortices, bifurcation scenarios like period-doubling behavior, the Ruelle-Takens-Newhouse route to chaos, intermittency, or turbulence, depending on the particular boundary conditions (Joseph, 1976; Drazin and Reid, 1981; Swinney and Gollub, 1985; Landau and Lifshits, 1987; Schuster, 1988; Großmann, 2000). In this review, it is important to know that turbulence normally requires three- or higher-dimensional systems, so it is not expected to appear in one- or two-dimensional vehicle or pedestrian traffic. However, the instability mechanism which explains the *subcritical transition* to turbulence in the Hagen-Poiseuille experiment (Gebhardt and Großmann, 1994; Großmann, 2000) may also be relevant to traffic systems, as pointed out by Krug (see the discussion of metastability in Sec. IV.A.4).

In vibrated granular media, one can find emergent convection patterns (Bourzutschky and Miller, 1995; Ehrichs *et al.*, 1995; Pöschel and Herrmann, 1995), collective oscillating states (so-called *oscillons*; see Umbanhowar *et al.*, 1996), spontaneous segregation of different granular materials (Pöschel and Herrmann, 1995; Santra *et al.*, 1996; Makse *et al.*, 1997), or *self-organized criticality* with power-law distributed avalanche sizes in growing sand heaps (Bak *et al.*, 1987, 1988; Bak, 1996) or in the outflow from hoppers (Schick and Verveen, 1974; Peng and Herrmann, 1995).

In spite of the many differences between flows of fluids, granular media, and vehicles or pedestrians, due to different conservation laws and driving terms, one can apply similar methodological approaches. For example:

(i) microscopic, molecular dynamic models (see, for example, Hoover, 1986; Buchholtz and Pöschel, 1993; Goldhirsch *et al.*, 1993; Hirshfeld *et al.*, 1997; Sec. III.A);
(ii) lattice gas automata (Frisch *et al.*, 1986; Chen *et al.*, 1991; Peng and Herrmann, 1994; Tan *et al.*, 1995) or *cellular automata* (see Sec. III.B);
(iii) gas-kinetic (Boltzmann- and Enskog-like) models (Enskog, 1917; Chapman and Cowling, 1939; Boltzmann, 1964; Cohen, 1968, 1969; Lun *et al.*, 1984; Jenkins and Richman, 1985; Cercignani and Lampis, 1988; McNamara and Young, 1993; Dufty

[1] See, for example, Haken, 1977, 1983, 1988; Nicolis and Prigogine, 1977; Pasteels and Deneubourg, 1987; Feistel and Ebeling, 1989; Weidlich, 1991; DeAngelis and Gross, 1992; Kai, 1992; Vicsek, 1992; Vallacher and Nowak, 1994; Cladis and Palffy-Muhoray, 1995; Helbing, 1995a.

et al., 1996; Kobryn *et al.*, 1996; Sela *et al.*, 1996; Lutsko, 1997; see Sec. III.E);

(iv) fluid-dynamic models (Haff, 1983; Du *et al.*, 1995; Goldhirsch, 1995; Hayakawa *et al.*, 1995; Sela and Goldhirsch, 1995; see Sec. III.D).

C. Self-driven many-particle systems and the concept of social (behavioral) forces

In self-driven many-particle systems, the driving force is not of external origin (exerted from outside), but is associated with each single particle and self-produced. This requires each particle to have some kind of internal energy reservoir (Schweitzer, Ebeling, and Tilch, 1998; Ebeling *et al.*, 1999).

Self-driven "particles" are a paradigm for many active or living systems, in which they are a simplified and abstract representation of the most important dynamic behavior of cells, animals, or even humans. In order to reflect this, I shall generalize Eq. (2) a little, replacing the external driving force $\mathbf{F}_0(\mathbf{x}_\alpha,t)$ by an individual driving force $\mathbf{F}_\alpha^0(t)$. Moreover, *Newton's third law* $\mathbf{F}_{\beta\alpha}(t) = -\mathbf{F}_{\alpha\beta}(t)$ (*actio=reactio*) does not necessarily apply anymore to the self-driven, self-propelled, motorized, or active "particles" we have in mind. I shall show that these minor changes will imply various interesting phenomena observed in nature, for example in biological, traffic, or socioeconomic systems. In this context, the masses m_α are sometimes not well defined, and it is better to rewrite the resulting equation by means of the scaled quantities $\mathbf{F}_\alpha^0(t)=\gamma_\alpha v_\alpha^0(t)\mathbf{e}_\alpha^0(t)$, $\gamma_\alpha=m_\alpha/\tau_\alpha$, $\mathbf{F}_{\alpha\beta}(t)=m_\alpha\mathbf{f}_{\alpha\beta}(t)$, and $\boldsymbol{\zeta}_\alpha(t)=\gamma_\alpha\boldsymbol{\xi}_\alpha(t)$, where the accelerations $\mathbf{f}_{\alpha\beta}(t)$ are often loosely called forces as well:

$$\frac{d\mathbf{v}_\alpha(t)}{dt}=\frac{v_\alpha^0(t)\mathbf{e}_\alpha^0(t)+\boldsymbol{\xi}_\alpha(t)-\mathbf{v}_\alpha(t)}{\tau_\alpha}+\sum_{\beta(\neq\alpha)}\mathbf{f}_{\alpha\beta}(t). \quad (3)$$

From this equation we can see that, with a relaxation time of τ_α, the driving term $v_\alpha^0(t)\mathbf{e}_\alpha^0(t)/\tau_\alpha$ and friction term $-\mathbf{v}_\alpha(t)/\tau_\alpha$ together lead to an exponential-in-time adaptation of the velocity $\mathbf{v}_\alpha(t)$ to the desired speed $v_\alpha^0(t)$ and the desired direction $\mathbf{e}_\alpha^0(t)$ of motion. This is, however, disturbed by fluctuations $\boldsymbol{\xi}_\alpha(t)$ and interactions $\mathbf{f}_{\alpha\beta}(t)$ with other particles β. It is clear that attractive forces $\mathbf{f}_{\alpha\beta}(t)$ will lead to agglomeration effects. Therefore we shall usually investigate systems with vanishing or repulsive interactions, for which one can find various surprising effects.

A further simplification of the model equations can be achieved in the overdamped limit $\tau_\alpha\approx 0$ of fast (adiabatic) relaxation. In this case and with the abbreviations $\mathbf{v}_{\alpha\beta}(t)=\tau_\alpha\mathbf{f}_{\alpha\beta}(t)$, $\boldsymbol{\xi}_\alpha(t)=v_\alpha^0(t)\boldsymbol{\chi}_\alpha(t)$, we obtain

$$\mathbf{v}_\alpha(t)=v_\alpha(t)\mathbf{e}_\alpha(t)=v_\alpha^0(t)\mathbf{e}_\alpha^0(t)+\sum_{\beta(\neq\alpha)}\mathbf{v}_{\alpha\beta}(t)+\boldsymbol{\xi}_\alpha(t)$$
$$=v_\alpha^0(t)[\mathbf{e}_\alpha^0(t)+\boldsymbol{\chi}_\alpha(t)]+\sum_{\beta(\neq\alpha)}\mathbf{v}_{\alpha\beta}(t). \quad (4)$$

Human behavior often seems to be chaotic, irregular, and unpredictable. So why and under what conditions can we apply the above force equations? First of all, we need to consider a phenomenon of motion in some (quasi)continuous space, which may also be an abstract behavioral space or opinion scale (Helbing, 1992a, 1993b, 1994, 1995a). It is favorable to have a system in which the fluctuations due to unknown influences are not large compared to the systematic, deterministic part of the motion. This is usually the case in pedestrian and vehicle traffic, where people are confronted with standard situations and react automatically rather than making complicated decisions among various possible alternatives. For example, an experienced driver would not have to think about the detailed actions to be taken when turning, accelerating, or changing lanes.

This automatic behavior can be interpreted as the result of a learning process based on trial and error (Helbing, Molnar, *et al.*, 2001), which can be simulated with *evolutionary algorithms* (Klockgether and Schwefel, 1970; Rechenberg, 1973; Schwefel, 1977; Baeck, 1996). For example, pedestrians have a preferred side for walking (Oeding, 1963; Older, 1968; Weidmann, 1993), since an asymmetrical avoidance behavior turns out to be profitable (Bolay, 1998). The related formation of a behavioral convention can be described by means of *evolutionary game theory* (Helbing, 1990, 1991, 1992a, 1992c, 1993a, 1995a, 1996c).

Another requirement is the vectorial additivity of the separate force terms reflecting different environmental influences and psychological factors. This is probably an approximation, but there is some experimental evidence for it. Based on quantitative measurements of animals and human test subjects receiving separately or simultaneously applied stimuli of different natures and strengths, one has shown that behavior in conflict situations can be described by a superposition of forces (Miller, 1944, 1959; Herkner, 1975). This fits well with the concept of Lewin (1951), according to which behavioral changes are guided by *social fields or social forces*, an idea that has been put into mathematical terms by Helbing (1991, 1992a, 1993b, 1994, 1995a; see also Helbing and Molnár, 1995). Newton's third law, however, is usually not applicable.

D. What this review is about

In the following sections,

(i) I shall focus on the phenomena actually observed in traffic and their characteristic properties, and discuss models only to the extent to which they are helpful and necessary for an interpretation and a better understanding of the observations;

(ii) I shall discuss the main methods from statistical physics relevant for modeling and analyzing traffic dynamics (see the Table of Contents);

(iii) I shall discuss how far one can get with a physical, many-particle description of traffic, neglecting so-

ciopsychological factors and human behavior. The limitations of this approach will be briefly discussed in Sec. IV.F.

This review is intended to serve both experts and newcomers to the field, so some matters will be simplified or explained in greater detail for didactic reasons. Moreover, I shall try to identify open problems and to shed new light on some controversial topics currently under discussion. The main focus will be on the various kinds of phenomena occurring in self-driven many-particle systems and the conditions under which they appear. I shall start with the subject of one-dimensional vehicle traffic and continue with two-dimensional pedestrian traffic and three-dimensional air traffic by birds.

Those physicists who do not feel comfortable with such systems may instead imagine special kinds of granular, colloidal, or spin systems driven by gravitational or electrical forces, or imagine particular systems with Brownian motors (Hänggi and Bartussek, 1996; Astumian, 1997; Jülicher, Ajdari, and Prost, 1997; Reimann, 2000). Moreover, I would like to encourage everyone to perform analogous experiments in these related physical systems.

Despite the complexity of traffic with unknown, latent, or hardly measurable human factors, physical traffic theory is nonetheless a prime example of a highly advanced quantitative description of a living system. There is agreement between the theory and empirical data not only on a qualitative but also on a semiquantitative level (see Sec. IV.B.1). Moreover, there are even "natural constants" of traffic, emerging from nonlinear vehicle interactions; see Sec. IV.A.5. But, before getting into all this, I would like to mention some other interesting (self-)driven many-particle systems loosely related to traffic.

E. Particle hopping models, power-law scaling, and self-organized criticality

Many-particle systems in equilibrium can be well understood with methods from thermodynamics (Keizer, 1987) and statistical physics (Uhlenbeck and Ford, 1963; Landau and Lifshits, 1980; Ma, 1985; Klimontovich, 1986; Huang, 1987). Two examples are phase transitions between different aggregate states of matter like vapor, water, and ice, or the magnetization of spin systems composed of many "elementary magnets." It is known that the phase transition of disordered many-particle systems with short-range interactions into states with long-range order is easier in higher dimensions, because of the greater number of neighbors with which to interact. Often there is a certain upper dimension above which the system can be described by a mean-field approach so that the fluctuations can be neglected. For lower-dimensional spaces, one can usually develop approximate theories for the influence of noise by means of suitable expansions and renormalization-group treatments based on scaling arguments. These give universal power-law scaling exponents for the (critical) behavior of the system close to the phase-transition point (critical point; Stanley, 1971; Domb and Green, 1972–1976; Ma, 1976; Hohenberg and Halperin, 1977; Stinchcombe, 1983; Domb and Lebowitz, 1983–2000; Voss, 1985; Schuster, 1988). In nonequilibrium systems, one can frequently find *self-organized criticality* (Bak *et al.*, 1987, 1988; Bak, 1996) and *fractal properties* (Mandelbrot, 1983; Family and Vicsek, 1991; Vicsek, 1992; Barabási and Stanley, 1995). Self-organized criticality means that the respective system drives itself to the critical point, which is normally characterized by long-range correlations and scale-free power laws in analogy to thermodynamics.

In the considered many-particle systems, there is often also a certain lower dimension below which the system is always disordered because of the small number of neighbors. For example, it is known that neither ferromagnetic nor antiferromagnetic order is possible in one-dimensional equilibrium spin systems (Mermin and Wagner, 1966). The discovery that the situation can be very different in *driven* nonequilibrium spin systems has initiated intense research activity regarding the phase transitions in one-dimensional driven diffusive systems far from equilibrium. It turns out that many properties of equilibrium systems can be generalized to nonequilibrium systems, but others cannot.

By means of particle hopping models, it has been possible to gain a better understanding of *directed percolation* (Domany and Kinzel, 1984), *spontaneous structure formation* (Vilfan *et al.*, 1994), *spontaneous symmetry breaking* (Evans *et al.*, 1995), the *roughening transition* in certain growth processes (Alon *et al.*, 1996), the nonequilibrium *wetting transition* (Hinrichsen *et al.*, 1997), and *phase separation* (Evans *et al.*, 1998; Helbing, Mukamel, and Schütz, 1999). Nevertheless, for these nonequilibrium transitions there is still no general theory available that would be of comparable generality to that of equilibrium thermodynamics or statistical physics. For further reading, I recommend the books by Spohn (1991), Schmittmann and Zia (1995, 1998), Derrida and Evans (1997), Liggett (1999), and Schütz (2000a).

Note that the above-mentioned models usually assume a *random sequential (asynchronous) update*, i.e., the state of each particle is randomly updated after an exponentially distributed waiting time Δt. However, it is known that this is not realistic for traffic systems, which rather require a *parallel (synchronous) update* of the vehicle locations (Schreckenberg *et al.*, 1995), as in other flow problems. To reflect driver reaction to a change in the traffic situation, it is common to update the vehicle speeds synchronously as well. However, it would also be interesting to check out a random sequential velocity update, as some models of spatio-temporal interactions in social systems show artifacts if updated in parallel (Huberman and Glance, 1993). For example, a parallel update excludes dynamic attainment of certain states (Schadschneider and Schreckenberg, 1998), which are called paradisical or Garden of Eden states (Moore, 1962).

The only particle hopping model I shall discuss here is the asymmetric simple exclusion process.[2] For overviews see Spohn (1991), Schmittmann and Zia (1995, 1998), Liggett (1999), and Schütz (2000a). Here, I shall discuss only the totally asymmetric simple exclusion process (TASEP). This model is defined by L sites j of a one-dimensional lattice, which can be either empty (corresponding to the occupation number $n_j=0$) or occupied by one particle ($n_j=1$). The particle locations and occupation numbers are updated after every time step Δt. When updated, a particle in cell j hops to the right neighboring cell $(j+1)$ with probability q, if this is empty; otherwise it stays in cell j. The total rate of motion to the right is therefore given by $qn_j(1-n_{j+1})/\Delta t$. The boundaries are characterized as follows: A particle enters the system at the left-most cell $j=1$ with probability q_0, if this is empty. Moreover, a particle in the right-most cell $j=L$ leaves the system with probability q_L. This corresponds to particle reservoirs at the boundaries which can be described by constant occupation probabilities $n_0=q_0/q$ and $n_{L+1}=(1-q_L/q)$. Although it requires enormous effort, the stationary states and even the dynamics of a TASEP can be analytically determined. For this, one has to solve the corresponding master equation (see Secs. III.C.3 and III.D.1).

F. Active Brownian particles

Like ordinary Brownian particles, active Brownian particles perform a random walk. However, they are not only reactive to an external potential $U(\mathbf{x},t)$, but also driven by an internal energy reservoir ("pumped particles") or can actively change the potential $U(\mathbf{x},t)$ while moving ("active walkers"). Therefore I have recently suggested calling them *Brownian agents*. For an overview see Schweitzer (2001).

1. Pumped Brownian particles

Schweitzer, Ebeling, and Tilch (1998) suggest a model describing how self-driven particles may take up and consume the internal energy behind their driving force. Their model corresponds to Eq. (2) with the specifications $\mathbf{F}_{\alpha\beta}=0$ (i.e., no direct interactions), but $\mathbf{F}_0(\mathbf{x}_\alpha(t))$ is replaced by the expression $-\nabla U(\mathbf{x}_\alpha)+\gamma E_\alpha(t)\mathbf{v}_\alpha(t)$, where the first term is an external potential force and the last term an internal driving force (γ being the friction coefficient). The dimensionless (scaled) energy reservoir $E_\alpha(t)$ is assumed to follow the equation

$$\frac{dE_\alpha(t)}{dt}=Q_0(\mathbf{x}_\alpha(t))-\{c+d[\mathbf{v}_\alpha(t)]^2\}E_\alpha(t). \tag{5}$$

Herein $Q_0(\mathbf{x})$ reflects the exploitation rate of energy resources, while the last term describes the energy consumption rate, which grows quadratically with the speed (c and d being suitable parameter values). If the relaxation of this energy equation is fast, we can approximate the driving term by

$$\frac{v_\alpha^0(t)\mathbf{e}_\alpha^0(t)}{\tau_\alpha}=\frac{\gamma}{m_\alpha}E_\alpha(t)\mathbf{v}_\alpha(t)=\frac{\gamma}{m_\alpha}\frac{Q_0(\mathbf{x}_\alpha(t))\mathbf{v}_\alpha(t)}{c+d[\mathbf{v}_\alpha(t)]^2},$$

so that the internal driving and the dissipative friction together can be represented by an active friction coefficient $\gamma'(v)=\gamma[1-Q_0/(c+dv^2)]$. Moreover, the driving direction $\mathbf{e}_\alpha^0(t)$ is given by the normalized actual velocity $\mathbf{e}_\alpha(t)=\mathbf{v}_\alpha(t)/\|\mathbf{v}_\alpha(t)\|$, and the desired velocity $v_\alpha^0(t)$ depends on the speed as well: $v_\alpha^0(t)=Q_0\|\mathbf{v}_\alpha(t)\|/\{c+d[\mathbf{v}_\alpha(t)]^2\}\geqslant 0$. Notice that particle α takes up energy only when it moves with some finite speed $v_\alpha(t)=\|\mathbf{v}_\alpha(t)\|\neq 0$ (i.e., exploits its environment). Therefore, in the absence of a potential $U(\mathbf{x},t)$, we find the stationary solution $v_\alpha=v_\alpha^0=0$. However, this is stable only under the condition $\tau_\alpha\gamma Q_0<cm_\alpha$. Otherwise, particle α will spontaneously start to move with average speed

$$v_\alpha=v_\alpha^0=\left(\frac{\tau_\alpha\gamma Q_0}{m_\alpha d}-\frac{c}{d}\right)^{1/2}. \tag{6}$$

Depending on $Q_0(\mathbf{x})$ and $U(\mathbf{x})$, this spontaneous motion displays interesting dynamics such as limit cycles, deterministic chaos, or intermittency (Schweitzer, Ebeling, and Tilch, 1998; see also Chen, 1997). It also allows the particles to climb potential hills, e.g., in a periodic ratchet potential $U(\mathbf{x})$ (Schweitzer *et al.*, 2000).

2. Dissipative Toda and Morse chains

Toda and Morse chains are particles coupled to a heat bath and moving on a ring with particular asymmetrical springs among neighbors, which are described by nonlinear Toda or Morse potentials $U'(x_\beta-x_\alpha)$ (Bolterauer and Opper, 1981; Toda, 1983; Jenssen, 1991; Ebeling and Jenssen, 1992; Dunkel *et al.*, 2001). Assuming pumped particles with an active friction coefficient $\gamma'(v)$ similar to that described in the previous paragraph, Ebeling *et al.* (2000) have found interesting dynamical patterns for overcritical pumping. These include uniform rotations, one- and multiple-soliton-like excitations, and relative oscillations. For Morse potentials, one also observes clustering effects reminiscent of jamming (Dunkel *et al.*, 2001).

3. Active walker models

By modifying their environment locally, active walkers have indirect interactions with each other, which may lead to the formation of global structures. The versatility of this concept for the description of physical, chemical, biological, and socioeconomic systems is discussed by Schweitzer (2001). For example, a simple model is given

[2]Particularly relevant contributions to this model go back to the work of Spitzer (1970), Liggett (1975), Domany and Kinzel (1984), Katz *et al.* (1984), Liggett (1985), Krug (1991), Derrida *et al.* (1992, 1993), Janowski and Lebowitz (1992), Schütz and Domany (1993), Ferrari (1994), Stinchcombe and Schütz (1995a, 1995b), Kolomeisky *et al.* (1998), and Schütz (1998).

by $m_\alpha d\mathbf{v}_\alpha/dt=[-\nabla U(\mathbf{x}_\alpha,t)-\gamma\mathbf{v}_\alpha(t)+\zeta_\alpha(t)]$, while changes of the environmental potential $U(\mathbf{x},t)$ are described according to

$$\frac{\partial U(\mathbf{x},t)}{\partial t}=-\sum_\alpha B\,\delta(\mathbf{x}-\mathbf{x}_\alpha(t))-CU(\mathbf{x},t)+D\Delta U(\mathbf{x},t).$$

Here, C and D are constants, and $\delta(\mathbf{x}-\mathbf{x}_\alpha)$ denotes the Dirac delta function, giving contributions only at $\mathbf{x}=\mathbf{x}_\alpha$. Therefore the first term on the right-hand side reflects particles α leaving attractive markings at their respective locations $\mathbf{x}_\alpha$. The last term describes a diffusion of the field $U(\mathbf{x},t)$ (e.g., a chemical one), and the previous term its decay.

The result of the dynamics is a spatial agglomeration process. While in the first stage one finds the emergence of localized clusters at random locations, the clusters eventually merge with each other, resulting in one big cluster. The growth and competition of these clusters can be described by an Eigen-Fisher-like selection equation (Fisher, 1930; Eigen, 1971; Eigen and Schuster, 1979; Schweitzer and Schimansky-Geier, 1994).

4. Pattern formation of bacterial colonies

In 1994, Eshel Ben-Jacob *et al.* proposed a *communicating walker model* for the beautiful pattern formation in certain bacterial colonies (for reviews see Ben-Jacob, 1997; Ben-Jacob *et al.*, 2000). This model takes into account the consumption, diffusion, and depletion of food, multiplication under good growth conditions, and the transition to an immobile spore state under starvation, as well as the effect of *chemotaxis*, i.e., the attractive or repulsive reaction to self-produced chemical fields. The model allows one to reproduce the observed growth patterns of bacterial colonies as a function of the nutrient concentration and the agar concentration determining the mobility of the bacteria. The same bacterial patterns have recently been reproduced by means of a macroscopic reaction-diffusion model (Golding *et al.*, 1998). The formation of the observed dendritic structures is due to a diffusion instability (Ben-Jacob, 1993, 1997).

5. Trail formation by animals and pedestrians

Another example of an active walker model is the observed formation of trunk trail systems by certain ant species, which is also based on chemotaxis. It can be modeled by two kinds of chemical markings, one of which is dropped during the search for food, while the other is dropped on the way back to the nest of the ant colony (Schweitzer *et al.*, 1997). Other models for ant-like swarm formation have been developed by Deneubourg *et al.* (1989) and Bonabeau (1996).

Further kinds of active walker models have been proposed for the self-organization of trail systems by pedestrians or animals, where the markings correspond to "footprints" or other kinds of modifications of the ground that make it more comfortable to walk (Helbing, Keltsch, and Molnár, 1997; Helbing, Schweitzer, *et al.*, 1997; Helbing, 1998c). Interestingly enough, the model yields fair solutions and optimal compromises between short and comfortable ways; see Fig. 1 (Helbing, 1998c; Helbing and Vicsek, 1999). The corresponding computer simulations are therefore a valuable tool for developing optimized pedestrian facilities and way systems.

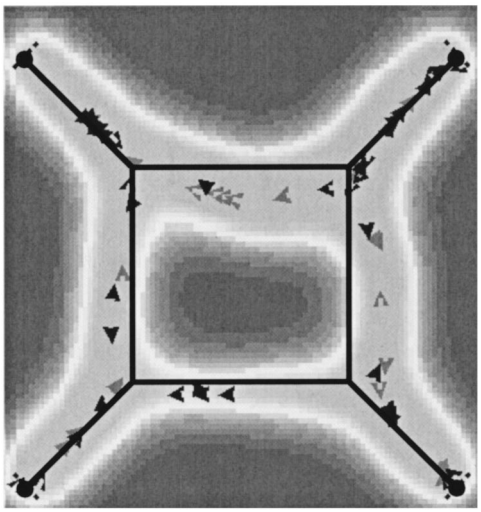

FIG. 1. Schematic representation of a human trail system (black solid lines) evolving between four entry points and destinations (solid circles) on an initially homogeneous ground. When the frequency of trail usage is small, the direct path system (consisting of the four paths along the edges and the two diagonal connections) is too long to be maintained in competition with the regeneration of the vegetation. Here, by bundling of trails, the frequency of usage becomes large enough to support the depicted trail system. It corresponds to the optimal compromise between the diagonal paths and those along the edges, supplying maximum walking comfort at a minimal detour of 22% for everyone, which is a fair solution. After Helbing, Keltsch, and Molnar, 1997; Helbing, Schweitzer, *et al.*, 1997; Helbing, 1998b; Helbing and Vicsek, 1999; Helbing, Molnar, *et al.*, 2001.

G. Vehicle and pedestrian traffic

The next sections will focus mainly on unidirectional freeway traffic, but bidirectional traffic and two-dimensional city traffic are briefly sketched as well. I shall start with an overview of the most important empirical findings. Then, I shall discuss the different modeling approaches, starting with one-lane traffic of identical vehicles and then adding more and more details including heterogeneous traffic on multilane roads. Finally, I shall discuss two-dimensional pedestrian traffic and three-dimensional flocks of birds.

II. EMPIRICAL FINDINGS FOR FREEWAY TRAFFIC

As physics deals with phenomena in our physical world, a physical theory must face comparison with empirical data. A good theory should not only reproduce all the empirically known properties of a system, but it

should also make predictions allowing us to verify or disprove the theory. To gain an overview of data analyses, I recommend the review articles and books by Gerlough and Huber (1975), Koshi *et al.* (1983), the Transportation Research Board (1985), May (1990), Daganzo (1997a, 1999a, 1999b), Bovy (1998), and Kerner (1998b, 1998c, 1999a, 1999b, 2000a, 2000b).

A. Measurement techniques

Probably the most refined technique for gathering empirical data on traffic is based on aerial photography or video recordings, allowing us to track the trajectories of many interacting vehicles and even their lane-changing maneuvers (Treiterer and Taylor, 1966; Treiterer and Myers, 1974). Another method suitable for experimental investigations uses car-following data. Depending on the equipment of the cars, it is possible to determine the location and speed, possibly the acceleration and clearance (the net or netto distance), and sometimes even lane-changing maneuvers of the equipped car or of a following vehicle (see, for example, Koshi *et al.*, 1983; Bleile, 1997, 1999; Manstetten *et al.*, 1997).

However, most data are obtained by detectors located at certain cross sections x of the freeway. For example, single induction-loop detectors measure the numbers ΔN of crossing vehicles α during a certain sampling interval ΔT as well as the times t_α^0 and t_α^1 when a vehicle α reaches and leaves the detector. This facilitates the determination of the *time headways* (the gross or brutto time separations)

$$\Delta t_\alpha = (t_\alpha^0 - t_{\alpha-1}^0)$$

and the *time clearances* (netto time separations) $t_\alpha^0 - t_{\alpha-1}^1$ including their respective distributions, as well as the *vehicle flow*

$$Q(x,t) = \frac{\Delta N}{\Delta T} \tag{7}$$

and the *time occupancy* $O(x,t) = \Sigma_\alpha (t_\alpha^1 - t_\alpha^0)/\Delta T$ (where $\alpha_0 < \alpha \leqslant \alpha_0 + \Delta N$ and α_0 denotes the last vehicle before the sampling interval begins). The newer double induction-loop detectors additionally measure the vehicle velocities v_α and the vehicle lengths l_α, allowing us to estimate the headways (brutto distances) $d_\alpha = v_\alpha \Delta t_\alpha$ (assuming constant vehicle speeds) and the clearances (netto distances) $s_\alpha = (d_\alpha - l_{\alpha-1})$. The velocity measurements are normally used to obtain the (arithmetic) average velocity

$$V(x,t) = \langle v_\alpha \rangle = \frac{1}{\Delta N} \sum_{\alpha=\alpha_0+1}^{\alpha_0+\Delta N} v_\alpha, \tag{8}$$

but the velocity variance

$$\theta(x,t) = \langle [v_\alpha - \langle v_\alpha \rangle]^2 \rangle = \langle (v_\alpha)^2 \rangle - \langle v_\alpha \rangle^2 \tag{9}$$

and the local velocity distribution may be determined as well. The vehicle density $\rho(x,t)$ is often calculated via the fluid-dynamic equation (46), i.e., $\rho(x,t) = Q(x,t)/V(x,t)$. Another method is to relate the density with the time occupancy, as in the formula $\rho(x,t) = O(x,t)/[L(x,t) + L_D]$, where $L(x,t)$ is the average vehicle length during the measurement interval and L_D the detector length (i.e., the loop extension) in the driving direction (May, 1990).

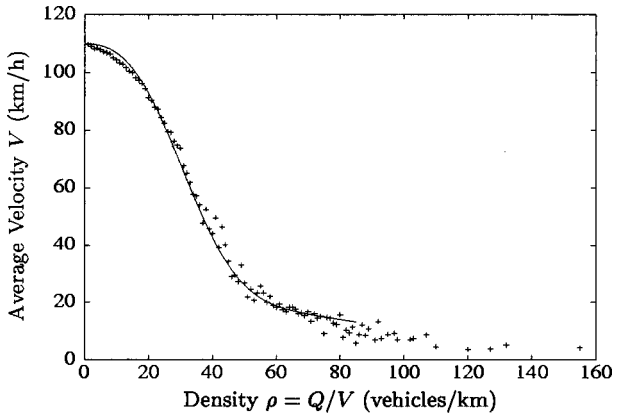

FIG. 2. Empirical velocity-density relations for different definitions of the average velocity. Symbols represent averages of one-minute data determined via the harmonic velocity formula $V = 1/\langle 1/v_\alpha \rangle$, while the solid line is a fit function to the velocity averages determined via the conventionally applied arithmetic formula $V = \langle v_\alpha \rangle$. After Helbing, 1997a.

The problem with the above measurement methods is that the velocity distribution measured over a time interval ΔT differs from that measured on a freeway section of length ΔX. In other words, temporal and spatial averaging yield different results, since fast vehicles cross a section of the freeway more frequently than slow ones, which is intuitive for a periodically closed multilane freeway with fast and slow lanes. The problem with determining the empirical density via the formula $\rho = Q/V$ is that it mixes a temporal average (the flow) with a spatial one (the density). This can be compensated for by the harmonic average velocity $V(x,t)$ defined by

$$\frac{1}{V(x,t)} = \left\langle \frac{1}{v_\alpha} \right\rangle, \tag{10}$$

giving a greater weight to small velocities (Gerlough and Huber, 1975; Leutzbach, 1988). Using Eq. (10) instead of the commonly applied equation (8) together with the relation $\rho = Q/V$ results in similarly shaped velocity-density relations, but the density range is much higher (see Fig. 2). Moreover, the velocity and flow values at high densities are somewhat lower. The disadvantage of Eq. (10) is its great sensitivity to errors in the measurement of small velocities v_α.

B. Fundamental diagram and hysteresis

Functional relations between the vehicle flow $Q(x,t)$, the average velocity $V(x,t)$, and the vehicle density $\rho(x,t)$ or occupancy $O(x,t)$ have been measured for decades, beginning with Greenshields (1935), who found a

linear velocity-density relationship. The name *fundamental diagram* is mostly used for some fit function

$$Q_e(\rho)=\rho V_e(\rho) \tag{11}$$

of the empirical flow-density relation, where $V_e(\rho)$ stands for the fitted empirical velocity-density relation (see Fig. 2), which is monotonically falling: $dV_e(\rho)/d\rho \leqslant 0$. Most measurements confirm the following features:

(i) At low densities ρ, there is a clear and quasi-one-dimensional relationship between the vehicle flow and the density. It starts almost linearly and is bent downwards. The slope at low densities corresponds to the average free velocity V_0, which can be sustained at finite densities as long as there are sufficient possibilities for overtaking. That is, the velocity-density relation of a multilane road starts horizontally, while it tends to have a negative slope on a one-lane road.

(ii) With growing density, the velocity decreases monotonically, and it vanishes together with the flow at some *jam density* ρ_{jam}, which is hard to determine because of the above-mentioned measurement problems. Estimates by different researchers from various countries extend from 120 to 200 vehicles per kilometer and lane, but values between 140 and 160 vehicles per kilometer are probably most realistic.

(iii) The vehicle flow has one maximum $Q_{\max}$ at medium densities.

(iv) The empirical flow-density relation is discontinuous and looks comparable to a mirror image of the Greek letter lambda. The two branches of this reverse lambda are used to define free low-density and congested high-density traffic (see, for example, Koshi *et al.*, 1983; Hall *et al.*, 1986; Neubert, Santen, *et al.*, 1999; Kerner, 2000a; see also Edie and Foote, 1958). In congested traffic, the average vehicle velocity is significantly lower than in free traffic. Therefore the free and congested part of the flow-density relation can be approximately separated by a linear flow-density relation ρV_{sep}, where V_{sep} is the average velocity below which traffic is characterized as congested. Around this line, the density of data points is reduced [see Fig. 3(a)]. The reverse-lambda-like structure of the flow-density data implies several things: First, we have a discontinuity at some critical density ρ_{cr} (Edie, 1961; Treiterer and Myers, 1974; Ceder and May, 1976; Payne, 1984), which has led researchers (Dillon and Hall, 1987; Hall, 1987; Gilchrist and Hall, 1989; Persaud and Hall, 1989) to relate traffic dynamics with catastrophe theory (Thom, 1975; Zeeman, 1977). Second, there is a certain density region $\rho_{c1} \leqslant \rho \leqslant \rho_{c2}$ with $\rho_{c2}=\rho_{\text{cr}}$, in which we can have either free or congested traffic, which points to hysteresis (Treiterer and Myers, 1974). The tip of the lambda corresponds to high-flow states of free traffic (in the passing lanes), which can last for many minutes (see, for example, Cassidy and Bertini, 1999).

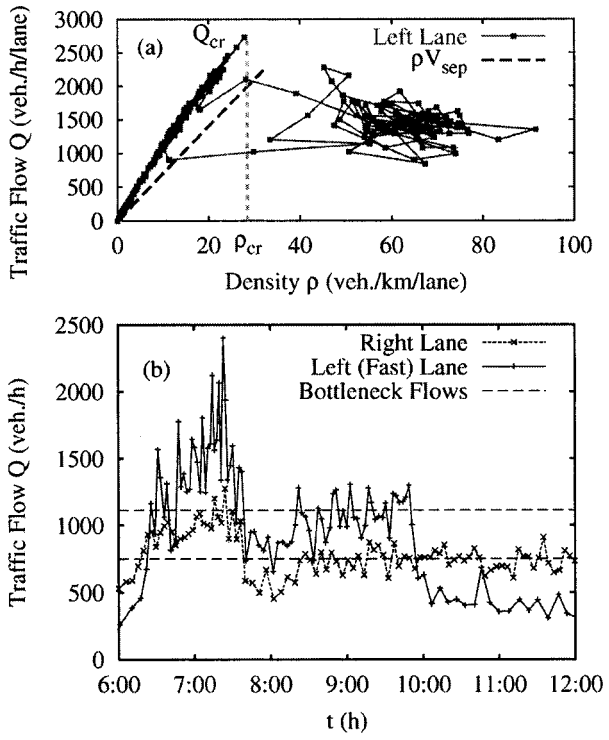

FIG. 3. Empirical time series of the hysteretic breakdown of traffic flow plotted (a) as a function of the density and (b) as a function of the time. High-flow states are observed only shortly before the breakdown of traffic. Note that, immediately after the breakdown, the flow drops temporarily below the typical bottleneck flow (see Persaud *et al.*, 1998; Cassidy and Bertini, 1999). While free traffic is characterized by a quasi-one-dimensional flow-density relationship, in the congested regime the flow-density data are widely scattered. The free and congested traffic regimes can be separated by a line ρV_{sep}; here we have chosen $V_{\text{sep}}=70$ km/h.

However, these are not stable, since it is only a matter of time until a transition to the lower, congested branch of the lambda takes place (Persaud *et al.*, 1998; see also Elefteriadou *et al.*, 1995). The

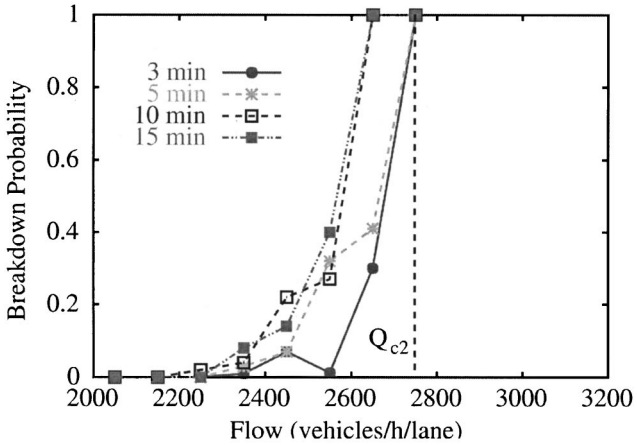

FIG. 4. Probability of breakdown of free traffic as a function of the flow for different waiting times. After Persaud *et al.*, 1998.

transition probability from a free to a congested state within a long time interval is 0 below the flow $Q_{c1}=Q_e(\rho_{c1})$ and 1 above the flow $Q_{c2}=Q_e(\rho_{c2})$. Between Q_{c1} and Q_{c2}, it is monotonically increasing; see Fig. 4 (Persaud *et al.*, 1998). The transition from congested to free traffic does usually not go back to high-flow states, but to flows $Q_e(\rho)$ belonging to densities $\rho<\rho_{c2}$, typically around ρ_{c1}. The high-flow states in the density range $\rho_{c1}\leqslant\rho\leqslant\rho_{c2}$ are only metastable (Kerner and Rehborn, 1996b, 1997; Kerner, 1998b, 1999a, 1999b, 1999c, 2000a, 2000b).

(v) The flow-density data in the congested part are widely scattered within a two-dimensional area (see, for example, Koshi *et al.*, 1983; Hall *et al.*, 1986; Kühne, 1991b). This complexity in traffic flow is usually interpreted as an effect of fluctuations, of jam formation, or of an instability of vehicle dynamics. The scattering is reduced by increasing the sampling interval ΔT of the data averaging (Leutzbach, 1988).

(vi) By removing the data belonging to wide moving jams (see Fig. 20 below), Kerner and Rehborn (1996b) could demonstrate that the remaining congested traffic data still display a wide and two-dimensional scattering [see Fig. 3(a)], thereby questioning the applicability of a fundamental diagram and defining the state of *synchronized flow* ["synchronized" because of the typical synchronization between lanes in congested traffic—see Fig. 15(a)—and "flow" because of flowing in contrast to standing traffic in fully developed jams]. Therefore Kerner suggests classifying three phases (see Sec. IV.A.6):
- free flow,
- synchronized flow (see Secs. II.C, II.D, and II.E.2 for details), and
- wide moving jams (moving jams whose longitudinal extension is considerably longer than their jam fronts).[3]

A wide moving jam propagates through free or synchronized flow and through bottlenecks with constant (phase) velocity (Kerner, 2000a, 2000b). In contrast, the downstream front of synchronized flow is normally fixed at the location of some bottleneck, e.g., an on-ramp. In initially free flow, two types of transitions are observed: either to synchronized flow or to a wide moving jam. Both of them appear to be first-order phase transitions accompanied by different hysteresis and nucleation effects (Kerner and Rehborn, 1997; Kerner, 1998a, 1999a, 2000c).

[3]The nonspecialist might find it more intuitive to refer to such jams as "long moving jams." However, the term "wide moving jam," introduced by Kerner, has become part of the technical vocabulary in the field. Width in this case is measured by an observer next to the highway and applies to the longitudinal extension along the road.

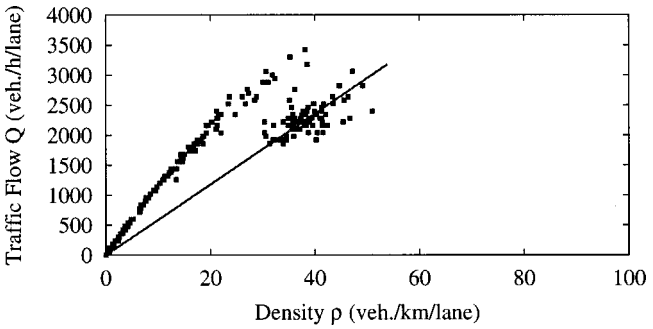

FIG. 5. Homogeneous-in-speed states scattered around a line through the origin, indicating constant speeds. The data are typical for "recovering traffic" at cross sections located downstream of a bottleneck, where congested traffic relaxes to free traffic.

(vii) The slopes $S_x^{\Delta T}(t)=[Q(x,t+\Delta T)-Q(x,t)]/[\rho(x,t+\Delta T)-\rho(x,t)]$ of the lines connecting successive data points are always positive in free traffic. In synchronized flow, however, they erratically take on positive and negative values, reflecting a complex spatiotemporal dynamics (Kerner and Rehborn, 1996b). This erratic behavior is quantitatively characterized by a weak cross correlation between flow and density (Neubert, Santen, *et al.*, 1999). Banks (1999) showed that it could be interpreted as a result of random variations in the time clearances (partly due to acceleration and deceleration maneuvers in unstable traffic flow). These variations are, in fact, very large [see Fig. 6(b)]. Banks points out that, if drivers would keep a safe clearance $s^*(v)=s'+Tv$ in congested traffic, the flow would grow with decreasing (effective) *safe time clearance* T according to

$$Q_e(\rho)=\frac{1}{T}\left(1-\frac{\rho}{\rho_{\rm jam}}\right), \tag{12}$$

where s' denotes the minimum rear-to-front distance kept and $\rho_{\rm jam}=1/l'=1/(l+s')$, the jam density with the (average) minimum space requirement $l'=(l+s')$. Simplifying his argument, in the congested regime positive slopes can result from a reduction in the safe time clearance T with growing density, while negative slopes normally correspond to a reduction in the speed. Hence the slopes $S_x^{\Delta T}(t)$ do not necessarily have the meaning of a wave propagation speed.

(viii) The flow-density data depend on the measurement cross section. While the congested branch is very pronounced upstream of a bottleneck, that is, in the traffic flowing towards it, it is virtually not present far downstream of it, that is, in the traffic that has proceeded past it. However, immediately downstream of a bottleneck, one finds a positively sloped congested area slightly below the free branch (*homogeneous-in-speed states*). It looks similar to the upper part of the free branch,

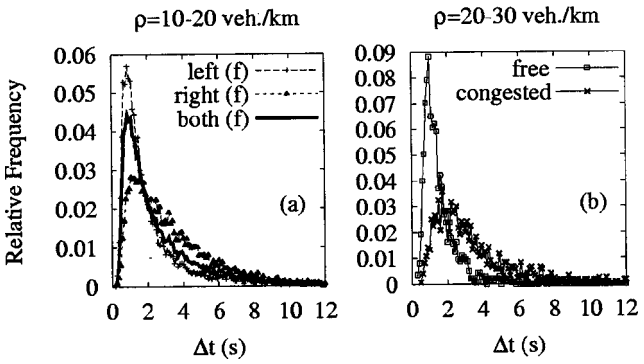

FIG. 6. Empirical time-headway distributions for different vehicle densities and traffic regimes: (a) Due to the larger proportion of long vehicles (see Sec. II.F), the time-headway distribution is broader in the right lane than in the left one; (b) before the breakdown of free traffic flow, the time-headway distribution is particularly narrow; afterwards it becomes wide. After Tilch and Helbing, 2000.

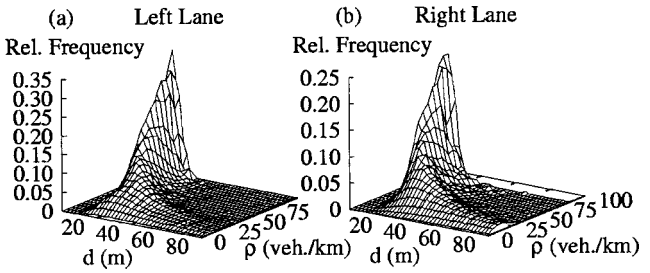

FIG. 7. The distribution of vehicle distances d is rather broad at all densities ρ, although the average vehicle distance decreases with the inverse density $1/\rho$. After Tilch and Helbing, 2000.

but with a somewhat lower desired velocity. I suggest that this indicates a transition to free traffic along a portion of the road [see Figs. 5 and 42(b)] and that this *recovering traffic* already bears some signatures of free traffic (see also Persaud and Hurdle, 1988; Hall *et al.*, 1992). For example, on-ramp flows just add to the flows on the freeway, which may produce states with high flows (Kerner, 2000b). Some observations, however, question the interpretation of homogeneous-in-speed states as recovering traffic, since they can extend over stretches of more than 3 km (Kerner, 1999a).

C. Time headways, headways, and velocities

Time headways show an astonishing individual variation, supporting Banks's theory discussed above. When distinguished for different density ranges, time-headway distributions have an interesting property. It turns out that the distribution becomes sharply peaked around approximately 1 s for densities close to congestion (Smulders, 1990; Hoogendoorn and Bovy, 1998; Neubert, Santen *et al.*, 1999). For lower and higher densities, the distribution is considerably broader; see Fig. 6 (Tilch and Helbing, 2000). This indicates that congestion is an overcritical phenomenon occurring when the maximum efficiency in terms of time headways (related to high-flow states) cannot be supported any longer. One may conclude that the effective time clearance has then reached the safe time clearance T_α. A further increase in the density forces a reduction in the speed, which automatically increases the time headway $\Delta t_\alpha = (T_\alpha + l'_\alpha / v_\alpha)$, even if the effective clearance remains T_α (see Banks, 1991b).

The distribution of vehicle headways $d_\alpha = v_\alpha \Delta t_\alpha$ can be determined as well, but it is always surprisingly broad (see Fig. 7). Therefore Bleile (1999) suggests considering this by an individual distance scaling of the velocity-clearance relation.

What are the reasons for the wide scattering of time headways and clearances, apart from driver-dependent preferences? By detailed investigations of clearance-over-speed relations, Koshi *et al.* (1983) have observed that vehicles keep larger distances in real congested traffic than in free traffic or (undisturbed) congested traffic under experimental conditions (see Fig. 8).

Plotting the speed over the vehicle distance, one can find a density-dependent reduction of the speed (see Fig. 9), which has been called the "frustration effect." In my opinion, this is partly an effect of a reduction in the vehicle speed with decreasing distance due to safety requirements, combined with the wide distance scattering illustrated in Fig. 7 (Tilch and Helbing, 2000). Another relevant factor is the influence of the relative velocity Δv on driver behavior (Bleile, 1997, 1999). The average clearances of vehicles that are driving faster or slower than the respective leading vehicles are naturally increased compared to vehicles driving at the same speed; see Fig. 10 (Neubert, Santen, *et al.*, 1999; Tilch, 2001). In summary, driver behavior is influenced not only by the clearance to the next car, but also by the relative velocity and the driver velocity (Koshi *et al.*, 1983; Bleile, 1997; 1999; Manstetten *et al.*, 1997; Dijker *et al.*, 1998; Neubert, Santen, *et al.*, 1999).

Note that the relative velocity in congested traffic is oscillating because of the instability of traffic flow; see Fig. 11 (Hoefs, 1972; Helbing and Tilch, 1998). As a consequence, the relative velocity variance θ, as compared to the average velocity V, is considerably higher in congested than in free traffic (see Figs. 12 and 17). I suggest that this, together with the factors mentioned in the previous paragraph, may explain the empirical relations depicted in Fig. 9. If this is confirmed, one may drop the assumption of driver frustration in congested traffic.

Measurements of velocity distributions for traffic with a small fraction of trucks are in good agreement with a Gaussian distribution; see Fig. 13 (Pampel, 1955; Leong, 1968; May, 1990). However, if the sampling intervals ΔT are taken too large, one may also observe bimodal distributions (Phillips, 1977; Kühne, 1984a, 1984b), reflecting a transition from free to congested traffic. As expected for a Gaussian distribution, one-minute averages of single-vehicle data for the skewness $\langle (v_\alpha - V)^3 \rangle / \theta^{3/2}$

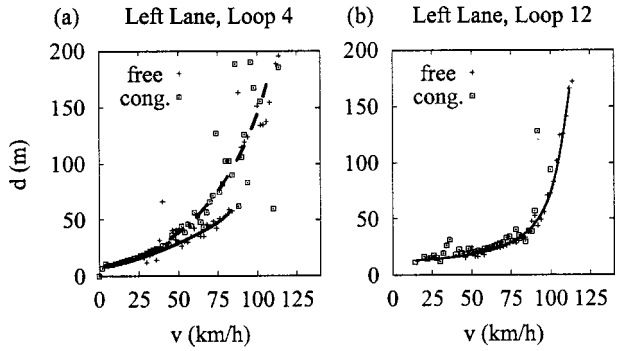

FIG. 8. Average vehicle distances d as a function of individual vehicle velocity v, shown separately for time intervals with free and congested traffic, according to the classification introduced in Fig. 3(a). Vehicles keep increased distances in congested traffic flow (dashed line) upstream of a bottleneck (a), but not in an undisturbed section (b) far enough away from it. The dashed and solid lines are fit curves in order to guide the eyes. After Tilch and Helbing, 2000 (note the related studies by Koshi *et al.*, 1983; Dijker *et al.*, 1998).

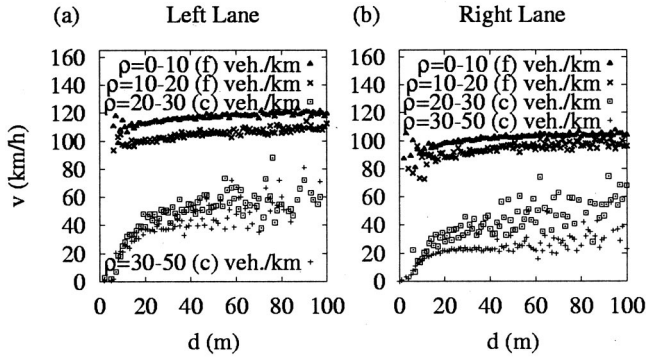

FIG. 9. Average vehicle velocities v as a function of the headways $d=v\Delta t$ for various density regimes, shown separately for free traffic (f) and congested traffic (c) in (a) the left and (b) the right lane for a cross section upstream of a bottleneck. Headways of less than 5 m are due to measurement errors. The dependence of the $v(d)$ relation on the vehicle density and traffic regime is called the *frustration effect* (see also Brilon and Ponzlet, 1996). From Tilch and Helbing, 2000; note the related study by Neubert, Santen, *et al.*, 1999.

and the kurtosis $[\langle(v_\alpha - V)^4\rangle/\theta^2 - 3]$ are scattered around the zero line (Helbing, 1997a, 1997c, 1997e, 1998a).

Like the velocity distribution itself, the higher-velocity moments are sensitive to the choice of the sampling interval ΔT. Large values of ΔT may lead to peaks in the variance θ when the average velocity V changes abruptly. The additional contribution can be estimated as $\overline{[\partial V(x,t)/\partial t]^2}(\Delta T)^2/4$, where the overbar indicates a time average over the sampling interval (Helbing, 1997a, 1997b, 1997e). One-minute data of the variance θ are more or less monotonically decreasing with the vehicle density (see Fig. 14), while five-minute data have maxima in the density range between 30 and 40 vehicles per kilometer and lane, indicating particularly unstable traffic (Helbing, 1997a).

Note that the average $\theta=\Sigma_i\rho_i\theta_i/(\Sigma_i\rho_i)$ of the velocity variances θ_i in the different lanes i is lower by an amount of $\langle(V_i-V)^2\rangle$ than the velocity variance evaluated over all lanes, which is particularly important at low densities ρ_i. This is due to the different average velocities V_i in the neighboring lanes. For a two-lane highway, the difference in average speeds decreases almost linearly up to a density of 35 to 40 vehicles per kilometer, while it fluctuates around zero at higher densities; see Fig. 15(a) (Helbing, 1997a, 1997b; Helbing *et al.*, 2001b). This reflects a synchronization of the velocities $V_i(x,t)$ in neighboring lanes in congested traffic, in both wide moving jams and synchronized flow (Koshi *et al.*, 1983; Kerner and Rehborn, 1996b; for reduced speed differences in congested traffic see also Edie and Foote, 1958; Forbes *et al.*, 1967; Mika *et al.*, 1969). However, according to Figs. 15(b) and 15(c), there is a difference between the speeds of cars and of long vehicles (trucks), which indicates that vehicles can still sometimes overtake, apart from a small density range around 25 vehicles per kilometer, where cars move as slowly as trucks (Helbing and Huberman, 1998). However, direct measurements of the number of lane changes or of overtaking maneuvers as a function of the macroscopic variables are rare (Sparmann, 1978; Hall and Lam, 1988; Chang and Kao, 1991). It would be particularly interesting to look at the dependence of lane-changing rates on the difference in velocities among lanes.

D. Correlations

In congested traffic, the average velocities in neighboring lanes are synchronized; see Fig. 16 (Mika *et al.*, 1969; Koshi *et al.*, 1983; see also Kerner and Rehborn, 1996b, for the complex features of synchronized flow). The synchronization is probably a result of lane changes to the faster lane, until the speed difference is equilibrated (for recent results see, for example, Lee *et al.*, 1998; Shvetsov and Helbing, 1999; Nelson, 2000). This

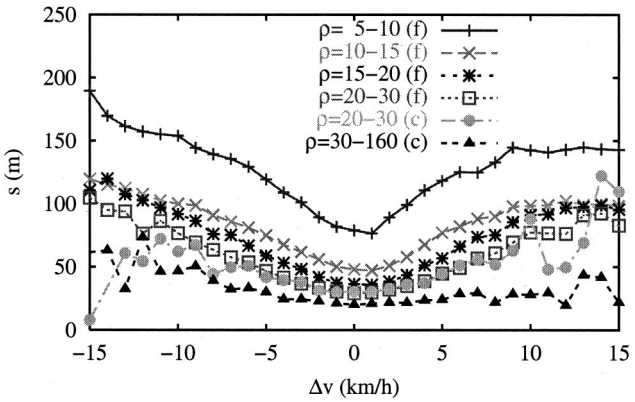

FIG. 10. Empirical clearance $s=(d-l)$ as a function of the relative velocity Δv, for free traffic (f) and congested traffic (c) in different density regimes. The clearance is minimal for identical vehicle velocities. From Tilch, 2001, after Neubert, Santen, *et al.*, 1999.

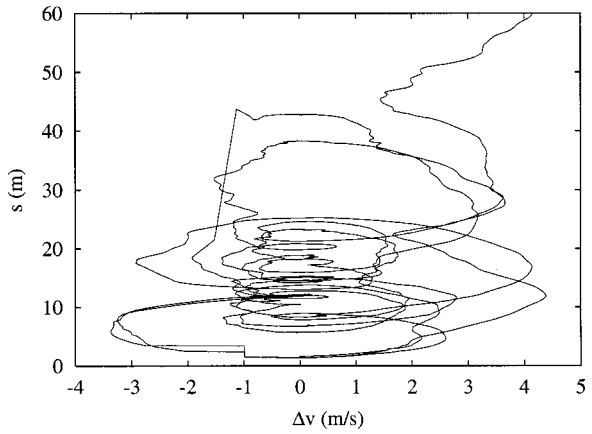

FIG. 11. Measured oscillations of the relative velocity Δv around $\Delta v = 0$ and of the clearance $s = (d - l)$ (cf. Hoefs, 1972), indicating an instability in car-following behavior. After Helbing and Tilch, 1998.

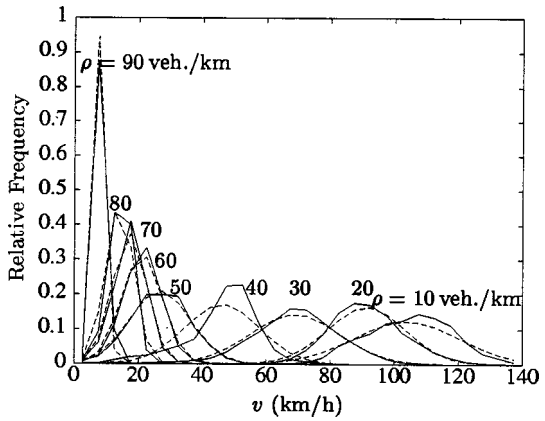

FIG. 13. Comparison of empirical velocity distributions at different vehicle densities ρ (solid curves) with frequency polygons of grouped normal distributions having the same mean value and variance (dashed curves). A significant deviation is observed only for $\rho = 40$ veh./km/lane, probably because of the instability of traffic flow. After Helbing, 1997a, 1997c, 1997e, 1998a.

equilibration process leads to a higher vehicle density in the so-called "fast" lane, which is used by fewer trucks (see, for example, Hall and Lam, 1988; Helbing, 1997a, 1997b). Nevertheless, density changes in congested neighboring lanes are correlated as well. Less understood and therefore even more surprising is the approximate synchronization of the lane-specific velocity variances θ_i over the whole density range; see Fig. 16(b) (Helbing, 1997a, 1997b, 1997e). It may be a sign of adaptive driver behavior.

Correlations are also found between the density and flow or average velocity. At low densities, there is a strong positive correlation with the flow, which is reflected by the almost linear free branch of the fundamental diagram. In contrast, at high densities, the velocity and density are strongly anticorrelated (see Fig. 16) because of the monotonically decreasing velocity-density relation (see Fig. 2). The average velocity and variance are positively correlated, since both quantities are related via a positive but density-dependent prefactor; see Fig. 17 (Helbing, 1996b, 1997a, 1997c; Shvetsov and Helbing, 1999; Treiber *et al.*, 1999; Helbing *et al.*, 2001a, 2001b).

Finally, it is interesting to look at the velocity correlations among successive cars. Neubert, Santen, *et al.* (1999) have found a long-range velocity correlation in synchronized flow, while in free traffic vehicle velocities are almost statistically independent. This finding is complemented by results from Helbing *et al.* (2001b); see Fig. 18. The observed velocity correlations may be interpreted in terms of vehicle platoons (Wagner and Peinke, 1997). Such vehicle platoons have been tracked by Edie and Foote (1958) and Treiterer and Myers (1974).

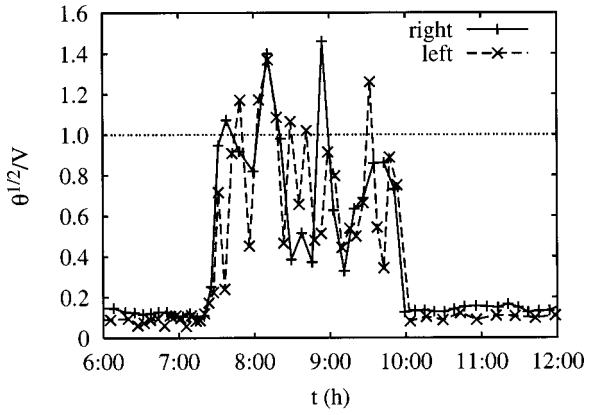

FIG. 12. Empirical standard deviation $\sqrt{\theta(t)}$ of vehicle velocities divided by the average velocity $V(t)$, as a function of time. The relative variation $\sqrt{\theta(t)}/V(t)$ is particularly large during the rush hour, when traffic is congested. This reflects oscillations in following behavior due to unstable traffic flow (cf. Fig. 11) and implies that measurements of average velocities V are unreliable in the congested traffic regime. From Tilch, 2001.

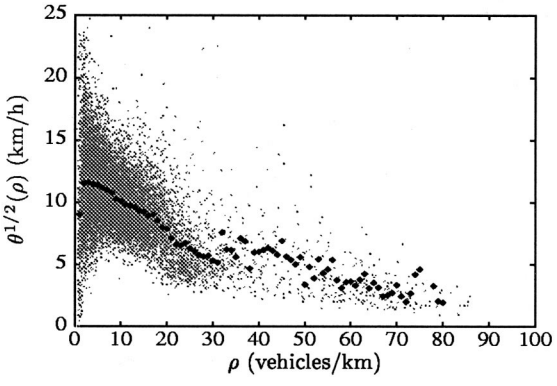

FIG. 14. Density-dependent standard deviation $\sqrt{\theta}$ of vehicle velocities in a single lane of the freeway: Fine dots, 1-minute data; ♦, average values for a given density ρ. The velocity variance θ is more or less monotonically falling with increasing density. The greater scattering above 30 vehicles per kilometer indicates unstable traffic flows. After Helbing, 1997a, 1997b, 1997e.

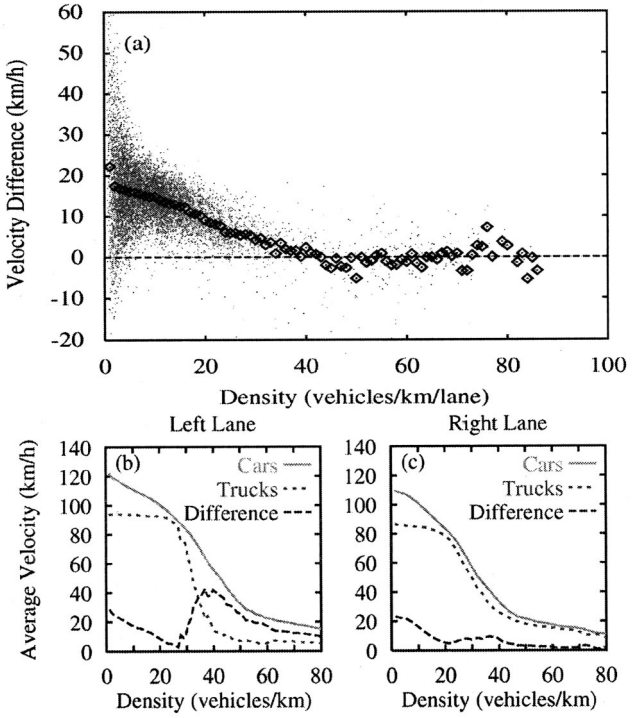

FIG. 15. Difference in average velocities: (a) Difference between the average velocity $V_2(\rho)$ in the left lane and $V_1(\rho)$ in the right lane as a function of the lane-averaged vehicle density ρ. From Helbing *et al.*, 2001b; see also Helbing, 1997a, 1997b; Helbing *et al.*, 2001a. (b),(c) Average velocities of cars and trucks (short and long vehicles) in the left and the right lanes as a function of the density. The difference between these empirical curves shows a minimum around 25 vehicles per kilometer, where cars are almost as slow as trucks. However, at higher densities, cars are faster again, which shows that there must be overtaking maneuvers in the congested density regime. After Helbing and Huberman, 1998; Helbing, Hennecke, *et al.*, 2001b; Helbing, 2001.

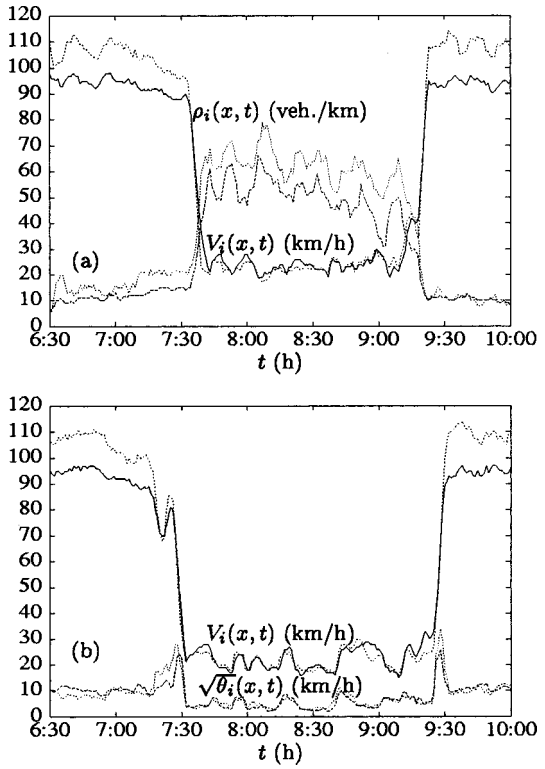

FIG. 16. Comparison of the temporal evolution of different aggregate (macroscopic) traffic variables on neighboring lanes i upstream of a bottleneck: (a) The average velocities $V_i(t)$ synchronize in the congested traffic regime during the rush hours, and the densities $\rho_i(t)$ vary in a correlated manner. Because of the smaller truck fraction in the left lane, in free traffice the speed is higher than in the right lane, while in congested traffic the density is higher. (b) The standard deviations $\sqrt{\theta_i}(t)$ of individual vehicle velocities always show a tendency to be synchronized. If (and only if) the time interval of data averaging is large (here it is 5 min), the variance shows peaks due to sudden changes in the average velocity $V_i(t)$. From Helbing, 1997a, 1997b, 1997e.

E. Congested traffic

1. Jams, stop-and-go waves, and power laws

The phenomenon of stop-and-go waves (start-stop waves) has been empirically studied by many authors, including Edie and Foote (1958), Mika *et al.* (1969), and Koshi *et al.* (1983). The latter have found that the parts of the velocity profile that belong to the fluent stages of stop-and-go waves do not significantly depend on the flow (regarding their height and length), while their oscillation frequency does. Correspondingly, there is no characteristic frequency of stop-and-go traffic, which indicates that we are confronted with nonlinear waves. The average duration of one wave period is normally between 4 and 20 minutes for wide traffic jams (see, for example, Mika *et al.*, 1969; Kühne, 1987; Helbing, 1997a, 1997c, 1997e), and the average wavelength is between 2.5 and 5 km (see, for example, Kerner, 1998a). An analysis of the power spectrum (Mika *et al.*, 1969; Koshi *et al.*, 1983) points to white noise at high wave frequencies ω (Helbing, 1997a, 1997c, 1997e), while a power law $\omega^{-\phi}$ with exponent $\phi=1.4$ is found at low frequencies (Musha and Higuchi, 1976, 1978). The latter has been interpreted as a sign of *self-organized criticality* in the formation of traffic jams (Nagel and Herrmann, 1993; Nagel and Paczuski, 1995). That is, congested traffic would drive itself towards the critical density ρ_{cr}, reflecting that it tries to reestablish the highest vehicle density associated with free flow (see below regarding the segregation between free and congested traffic and Sec. IV.A.5 regarding the constants of traffic flow).

Based on evaluations of aerial photographs, Treiterer and co-workers (1966, 1974) have shown the existence of "phantom traffic jams," i.e., the spontaneous formation of traffic jams with no obvious reason such as an accident or a bottleneck (see Fig. 19). According to Daganzo (1999a), the breakdown of free traffic "can be traced back to a lane change in front of a highly compressed set of cars," which shows that there is actually a reason for jam formation, but its origin can be a rather small disturbance. However, disturbances do not always lead to traffic jams, as del Castillo (1996a) points out. Even under comparable conditions, some perturbations

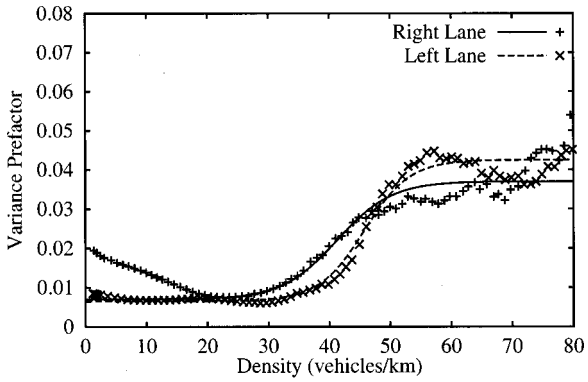

FIG. 17. The density-dependent variance prefactors $A_i(\rho_i) = \theta_i(\rho_i)/[V_i(\rho_i)]^2$ (reflecting something like squared relative individual velocity variations) show significantly increased values in the congested traffic regime, which may be a result of unstable traffic flow (see Figs. 11 and 12). The empirical data can be approximated by fit functions of the form $A_i(\rho_i) = A_{0i} + \Delta A_i/\{1+\exp[-(\rho_i-\rho_{ci})/(0.5\Delta\rho_i)]\}$, where A_{0i} and $A_{0i} + \Delta A_i$ are the variance prefactors for free and congested traffic, respectively, ρ_{ci} is of the order of the critical density for the transition from free to congested traffic, and $\Delta\rho_i$ denotes the width of the transition. From Shvetsov and Helbing, 1999.

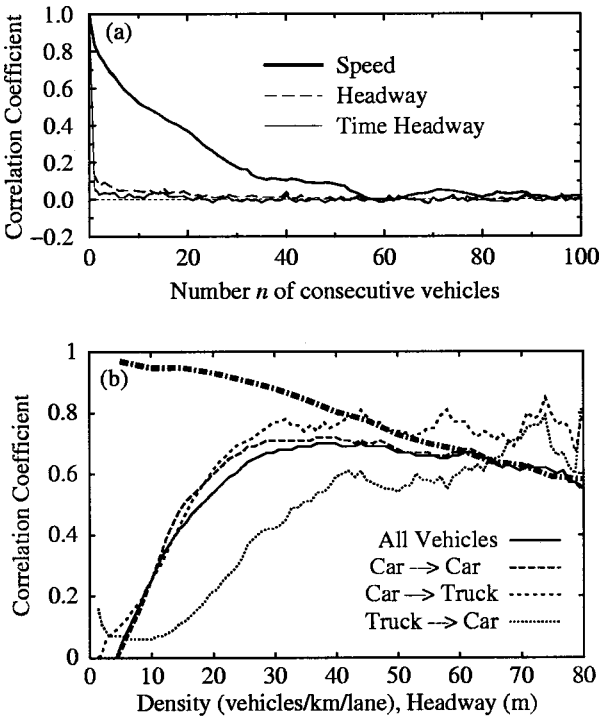

FIG. 18. Observed velocity correlations: (a) Velocity correlation in synchronized flow as a function of the number of consecutive vehicles. The data indicate long-range correlations, which are not observed in free traffic or for traffic variables such as the time headway or headway. After Neubert, Santen *et al.*, 1999. (b) Correlation between the velocities of successive vehicles in the right lane as a function of the density (thin solid, dashed, and dotted lines), determined from single-vehicle data. As expected, the correlation coefficient is about zero at small densities. It reaches a maximum at around 20 to 30 vehicles per kilometer, where the transition from free to congested traffic occurs. Afterwards, it stays at a high level (around 0.65). In the left lane (not displayed), the velocity correlation is a little bit higher, probably because of the smaller fraction of trucks (long vehicles). The correlation coefficient is not sensitive to the type of leading vehicle (car or truck), but to that of the following vehicle, which is reasonable. The heavy-dot-dashed line indicates that, even at small densities of 10 veh./km/lane, the velocity correlation between cars depends strongly on the headway to the next vehicle ahead and becomes almost one for very small headways. This is because different velocities would imply a high danger of accidents. After Helbing, Hennecke, *et al.*, 2001b.

grow and others fade away, which is in accordance with the metastability of traffic mentioned above (Kerner and Konhäuser, 1994; Kerner and Rehborn, 1996b, 1997; Kerner, 1999c).

While small perturbations in free traffic travel downstream (ahead) with a density-dependent velocity $C(\rho) < V$ (Hillegas *et al.*, 1974), large perturbations propagate upstream, i.e., against the direction of the vehicle flow (Edie and Foote, 1958; Mika *et al.*, 1969). Some disturbances have been found to propagate without spreading (Cassidy and Windover, 1995; Windower, 1998; Muñoz and Daganzo, 1999; see also Kerner and Rehborn, 1996a, and the flow and speed data reported by Foster, 1962; Cassidy and Bertini, 1999). The propagation velocity C in congested traffic seems to be roughly comparable with a "natural constant." In each country, it has a typical value in the range $C_0 = 15 \pm 5$ km/h, depending on the accepted safe time clearance and average vehicle length (see, for example, Mika *et al.*, 1969; Kerner and Rehborn, 1996a; Cassidy and Mauch, 2001). Therefore fully developed traffic jams can move in parallel over long time periods and road sections. Their propagation speed is not even influenced by ramps, intersections, or synchronized flow upstream of bottlenecks; see Fig. 20 (Kerner and Rehborn, 1996a; Kerner, 2000a, 2000b).

Wide moving jams are characterized by stable wave profiles and "universal" parameters (Kerner and Rehborn, 1996a). Apart from

(i) the propagation velocity C_0, these are
(ii) the density ρ_{jam} inside of jams,
(iii) the average velocity and flow inside of traffic jams, both of which are approximately zero,
(iv) the outflow Q_{out} from jams (amounting to about 2/3 of the maximum flow reached in free traffic, which probably depends on the sampling interval ΔT),
(v) the density ρ_{out} downstream of jams, if these are propagating through free traffic ("segregation effect" between free and congested traffic). When propagating through synchronized flow, the outflow $Q_{\text{out}}^{\text{sync}}$ of wide moving jams is given by the density $\rho_{\text{out}}^{\text{sync}}$ of the surrounding traffic (Kerner, 1998b).

The concrete values of the characteristic parameters slightly depend on the accepted safe time clearances, average vehicle length, truck fraction, and weather conditions (Kerner and Rehborn, 1998a).

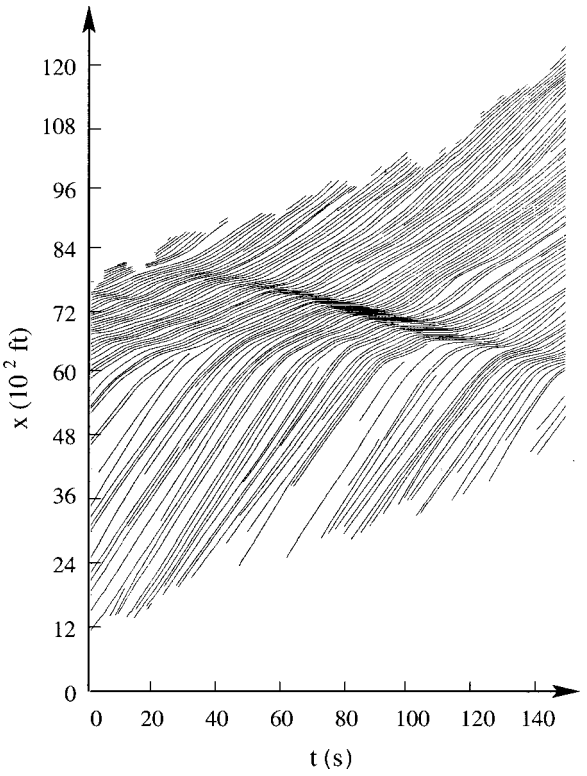

FIG. 19. Emergence of a "phantom traffic jam." The depicted vehicle trajectories were obtained by Treiterer and Myers (1974) by aerial photography (reproduction after Leutzbach, 1988). Broken lines are due to lane changes. While the slopes of the trajectories reflect individual vehicle velocities, their density represents the spatial vehicle density. Correspondingly, the figure shows the formation of a "phantom traffic jam," which stops vehicles temporarily. Note that the downstream jam front propagates upstream with constant velocity.

2. Extended congested traffic

The most common form of congestion is not localized like a wide moving jam, but spatially extended and often persisting over several hours. It is related to a capacity drop. The resulting flow is (at least in the United States) typically 10% or less below the "breakdown flow" of the previous high-flow states.[4] These high-flow states define the theoretically possible capacity. For statistical reasons, it is not fully satisfactory to determine capacity drops from maximum flow values, as these depend on the sampling interval ΔT. In any case, bottleneck flows Q_{bot} after the breakdown of traffic are probably more interesting. Because of Eq. (113), these may be more than 30% below the maximum free flow $Q_{\max}$ [see Fig. 3(b)]. Note that bottleneck flows depend, for example, on ramp flows Q_{rmp} and may therefore vary with location. The congested flow immediately downstream of a

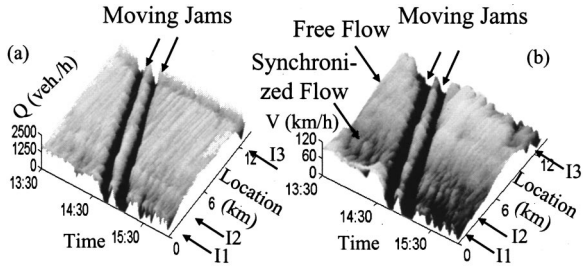

FIG. 20. Example of two wide moving traffic jams propagating in parallel with constant speed through free and congested traffic and across three freeway intersections I1, I2, and I3. From Kerner, 2000a, 2000b; see also Kerner and Rehborn, 1996a; Kerner, 1998b.

bottleneck defines the *discharge flow* $\tilde{Q}_{\mathrm{out}} \geqslant Q_{\mathrm{bot}}$, which appears to be larger than (or equal to) the characteristic outflow Q_{out} from wide jams: $\tilde{Q}_{\mathrm{out}} \geqslant Q_{\mathrm{out}}$.

In extended congested traffic, the velocity drops much more than the flow, but it remains finite. Velocity profiles $V(x,t)$ can differ considerably from one cross section to another (see Fig. 22). In contrast, the temporal profiles of congested traffic flow $Q(x,t)$, when measured at subsequent cross sections x of the road, are often just shifted by some time interval that is varying (see Fig. 21). This may be explained by a linear flow-density relation of the form of Eq. (12) with $dQ_e(\rho)/d\rho = C_0 = -1/(T\rho_{\mathrm{jam}})$ (Hall *et al.*, 1986, 1993; Ozaki, 1993; Dijker *et al.*, 1998; Westland, 1998), together with the continuum equation for the conservation of the vehicle number (see the kinematic wave theory in Sec. III.D.1; Daganzo; 1999a; Smilowitz and Daganzo, 1999; Cassidy and Mauch, 2001). However, a linear flow-density relation in the congested regime is questioned by the "pinch effect" (see Sec. II.E.3 and Fig. 22).

The extended form of congestion is classical and is found mainly upstream of bottlenecks, so that it normally has a spatially fixed ("pinned") downstream front. In contrast, the "upstream front" or rear edge of the congestion is moving back against the flow direction if the (dynamic) capacity Q_{bot} of the bottleneck is exceeded, but downstream (forward) if the traffic volume, i.e., the inflow to the freeway section, is lower than the capacity. Hence this spatially extended form of congestion occurs regularly and reproducibly during rush hours. Note, however, that bottlenecks may have many different origins: on-ramps, reductions in the number of lanes, accidents (even in opposite lanes because of driver curiosity), speed limits, road works, gradients, curves, bad road conditions (possibly due to rain, fog, or ice), bad visibility (for example, because of blinding sun), or divergences [due to "negative" perturbations (see Sec. IV.B), weaving flows by vehicles trying to switch to the slow exit lane, or congestion on the off-ramp; see Daganzo, 1999a; Daganzo *et al.*, 1999; Lawson *et al.*, 1999; Muñoz and Daganzo, 1999]. Moving bottlenecks due to slow vehicles are possible as well (Gazis and Herman, 1992), leading to a forward movement of

[4]See, for example, Banks, 1991a; Kerner and Rehborn, 1996b, 1998b; Persaud *et al.*, 1998; Westland, 1998; Cassidy and Bertini, 1999; see also May, 1964, for an idea on how to exploit this phenomenon with ramp metering; Persaud, 1986; Banks, 1989, 1990; Agyemang-Duah and Hall, 1991; Daganzo, 1996.

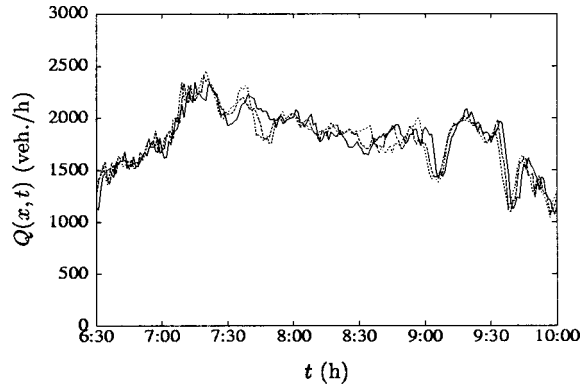

FIG. 21. Example of time-dependent traffic flows at three subsequent cross sections of a 3-km-long freeway section without ramps. (This includes a hardly noticeable breakdown, from free to synchronized congested flow, during the rush hours between 7:30 and 9:30 am; see the corresponding Fig. 16.) The flow profiles at subsequent cross sections are mainly shifted by some time interval, although fluctuations appear in the congested regime. After Helbing, 1997a.

the downstream congestion front. Finally, in cases of two subsequent inhomogeneities of the road, there are forms of congested traffic in which both upstream and downstream fronts are locally fixed (Kerner, 2000a; Lee *et al.*, 2000; Treiber *et al.*, 2000).

While Kerner calls the above extended forms of congested traffic "synchronized flow" because of the synchronization among lanes (see Secs. II.C, II.D), Daganzo (1999b) speaks of "one-pipe flow." Kerner and Rehborn (1997) have pointed out that the transition from free to extended congested traffic is hysteretic in character and looks similar to a first-order phase transition of supersaturated vapor to water ("nucleation effect"). It is often triggered by a small but overcritical peak in the traffic flow (playing the role of a nucleation germ). This perturbation travels downstream in the beginning, but it grows eventually and changes its propagation direction and speed until it travels upstream with velocity C_0. When the perturbation reaches the bottleneck, it triggers a breakdown of traffic flow to the bottleneck flow $Q_{\rm bot}$. In summary, synchronized flow typically starts to form downstream of the bottleneck [cf. Fig. 38(b)].

Kerner (1997, 1998a) has attributed the capacity drop to increased time headways due to delays in acceleration. This is compatible with measurements of stopped vehicles accelerating at a traffic light turning green (Androsch, 1978) or after an incident (Raub and Pfefer, 1998). According to these, the corresponding time-headway distribution has its maximum around 1.8 to 2 seconds, compared to a peak at about 1 s in free flow [cf. Fig. 6(b)]. The reachable saturation flows of accelerating traffic are, therefore, $Q_{\rm out} \approx 1800$ to 2000 vehicles per hour.

Kerner (1998b) points out that the above transition to synchronized congested flow is, in principle, also found on one-lane roads, but then it would no longer be of hysteretic nature or connected with synchronization. Moreover, Kerner and Rehborn (1996b) distinguish three kinds of synchronized flow:

(i) Stationary and homogeneous states in which both the average speed and the flow rate are stationary over a relatively long time interval (see also Hall and Agyemang-Duah, 1991; Persaud *et al.*, 1998; Westland, 1998). I shall call these *homogeneous congested traffic*.
(ii) States in which only the average vehicle speed is stationary, named *homogeneous-in-speed states* (see also Kerner, 1998b; Lee *et al.*, 2000). I interpret this state as "recovering traffic," since it bears several signatures of free traffic (see Secs. II.B and IV.C.2).
(iii) Nonstationary and nonhomogeneous states (see also Kerner, 1998b; Cassidy and Bertini, 1999; Treiber *et al.*, 2000). For these, I shall use the term *oscillating congested traffic*.

Not all of these states are long lived, since there are often spatio-temporal sequences of these different types of synchronized flow, which indicates continuous (second-order) transitions. However, at least states (i) and (iii) are characterized by a wide, two-dimensional scattering of the flow-density data, i.e., an increase in the flow can be related to either an increase or a decrease in the density, in contrast to free flow (see Sec. II.B).

3. The pinch effect

Recently, the spontaneous appearance of stop-and-go traffic has been questioned by Kerner (1998a) and Daganzo *et al.* (1999). In his empirical investigations, Kerner (1998a) finds that jams can be born from extended congested traffic, which presupposes a previous transition from free to synchronized flow. His proposed mechanism for jam formation is as follows (see Fig. 22): Upstream of a section with homogeneous congested traffic close to a bottleneck, there is a *pinch region* characterized by the spontaneous birth of small narrow density clusters, which are growing while they travel further upstream. Wide moving jams are eventually formed by the merging or disappearance of narrow jams, and the mean distance between centers of (narrow) jams (i.e., the average "wavelength") is increasing with the vehicle speed in the synchronized flow. Once formed, the wide jams seem to suppress the occurrence of new narrow jams in between. Similar findings were reported by Koshi *et al.* (1983), who observed that "ripples of speed grow larger in terms of both height and length of the waves as they propagate upstream." Daganzo (1999b) notes as well that "oscillations exist in the one-pipe regime and that these oscillations may grow in amplitude as one moves upstream from an active bottleneck," which he interprets as a pumping effect based on ramp flows. The original interpretation by Koshi *et al.* suggests a nonlinear self-organization phenomenon, assuming a concave, nonlinear shape of the congested flow-density branch (compare also with Sec. IV.B.2). Instead of form-

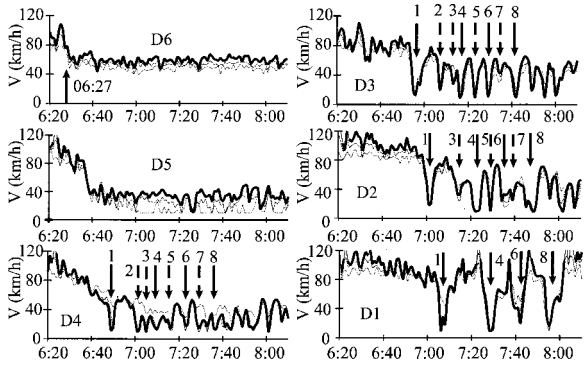

FIG. 22. Examples of time-dependent average velocities in the three lanes of a freeway at subsequent cross sections. After Kerner, 1998a. The figures show a transition from free to synchronized flow at cross section D5, the emergence of narrow jams in the "pinch region" at the upstream cross section D4, and the formation of a few stable wide jams (see further upstream cross section D1). The wide moving jams arise by the merging or disappearance of narrow jams between cross sections D4 and D1.

ing wide jams, narrow jams may coexist when their distance is larger than about 2.5 km (Kerner, 1998a; Treiber *et al.*, 2000).

F. Cars and trucks

Distinguishing vehicles of different lengths (cars and trucks), one finds surprisingly strong variations of the truck fraction; see Fig. 23 (Treiber and Helbing, 1999a). This point may be quite relevant for the explanation of some observed phenomena, as quantities characterizing the behavior of cars and trucks are considerably different. For example, trucks exhibit a different distribution of desired velocities as well as a different distribution of time headways from those of cars (see Fig. 24).

G. Some critical remarks

The collection and evaluation of empirical data is a subject with often underestimated problems. To reach reliable conclusions, in original investigations one should specify

(i) the measurement site and conditions (including applied control measures),
(ii) the sampling interval,
(iii) the aggregation method,
(iv) the statistical properties (variances, frequency distributions, correlations, survival times of traffic states, etc.),
(v) data transformations,
(vi) smoothing procedures,

and the respective dependencies on them.

The measurement conditions include ramps and road sections with their respective inflows and outflows, speed limits, gradients, and curves with the respectively related capacities, in addition to weather conditions,

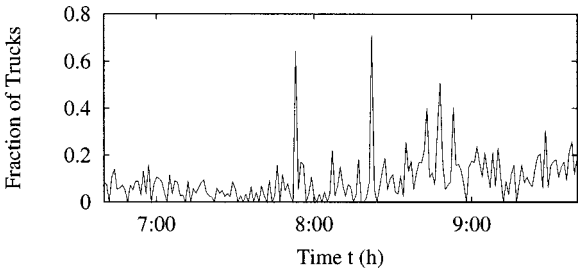

FIG. 23. Variation of the truck fraction with time. As this variation is considerable, it should be taken into account in empirical analyses of traffic flow. From Treiber and Helbing, 1999a.

presence of incidents, and other irregularities. Moreover, one should study the dynamics of the long vehicles separately, which may also have a significant effect (see Sec. II.F).

Particular attention must also be paid to fluctuations of the data, which requires a statistical investigation. For example, it is not obvious whether the scattering of flow-density data in synchronized flow reflects a complex dynamics due to nonlinear interactions or whether it is just because of random fluctuations in the system. In this connection, I remind the reader of the power laws found in the high-frequency variations of macroscopic quantities (see Sec. II.E.1).

Statistical variations of traffic flows imply that all measurements of macroscopic quantities should be complemented by error bars (see, for example, Hall *et al.*, 1986). Due to the relatively small "particle" numbers behind the determination of the macroscopic quantities, the error bars are actually quite large. Hence many temporal variations are within one error bar and are therefore not significant. As a consequence, the empirical determination of the dynamical properties of traffic flows is not a simple task. Fortunately, many hard-to-see effects are in agreement with predictions of plausible traffic models, in particular with deterministic ones (see Secs. IV.B and IV.C.2).

Nevertheless, I would like to call for more refined measurement techniques, which are required for more reliable data. These must take into account correlations between different quantities, as is pointed out by Banks (1995). Tilch and Helbing (2000) have therefore used the following measurement procedures: In order to have comparable sampling sizes, they have averaged over a fixed number ΔN of cars, as suggested by Helbing (1997e). Otherwise the statistical error at small traffic flows (i.e., at low and high densities) would be quite large. This is compensated for by a flexible measurement interval ΔT. It is favorable that ΔT becomes particularly small in the (medium) density range of unstable traffic, so that the method yields a good representation of traffic dynamics. However, choosing small values of ΔN does not make sense, since then the temporal variation of the aggregate values would mainly reflect statistical variations. In order to have a time resolution of about two minutes on each lane, one should select $\Delta N = 50$, while $\Delta N = 100$ can be chosen when averaging over

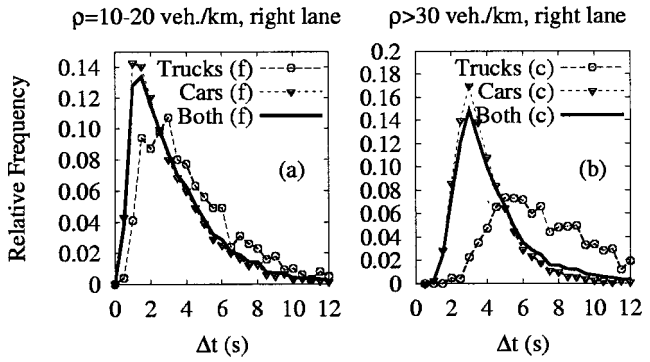

FIG. 24. Separate time-headway distributions for cars and trucks in the right lane for two different density regimes. The time headways in front of trucks (long vehicles) are considerably longer than those of cars, especially in congested traffic. From Tilch and Helbing, 2000.

both lanes. Aggregate values over both lanes for $\Delta N = 50$ are comparable with one-minute averages, but show a smaller statistical scattering at low densities (compare the results in Helbing, 1997a, 1997c with those in Helbing, 1997e).

Based on the passing times t_α^0 of successive vehicles α in the same lane, we are able to calculate the time headways Δt_α. The (measurement) time interval

$$\Delta T = \sum_{\alpha=\alpha_0+1}^{\alpha_0+\Delta N} \Delta t_\alpha \tag{13}$$

for the passing of ΔN vehicles defines the (inverse of the) traffic flow Q via $1/Q = \Delta T/\Delta N = \langle \Delta t_\alpha \rangle$, which is attributed to the time $t = \langle t_\alpha^0 \rangle = \Sigma_\alpha t_\alpha^0/\Delta N$.

Approximating the vehicle headways by $d_\alpha = v_\alpha \Delta t_\alpha$, one obtains

$$\frac{1}{Q} = \langle \Delta t_\alpha \rangle = \left\langle \frac{d_\alpha}{v_\alpha} \right\rangle = \langle d_\alpha \rangle \left\langle \frac{1}{v_\alpha} \right\rangle + \mathrm{cov}\left(d_\alpha, \frac{1}{v_\alpha} \right),$$

where $\mathrm{cov}(d_\alpha, 1/v_\alpha)$ is the covariance between the headways d_α and the inverse velocities $1/v_\alpha$. We expect this covariance to be negative and particularly relevant at large vehicle densities, which is confirmed by the empirical data (see Fig. 25). Defining the density ρ by

$$1/\rho = \langle d_\alpha \rangle \tag{14}$$

and the average velocity V via Eq. (10), we obtain the fluid-dynamic flow relation (46) by the conventional assumption $\mathrm{cov}(d_\alpha, 1/v_\alpha) = 0$. This assumption, however, overestimates the density systematically, since the covariance tends to be negative due to the speed-dependent safety distance of vehicles. In contrast, the common method of determining the density via $Q/\langle v_\alpha \rangle$ systematically underestimates the density (see Fig. 26). Consequently, errors in the measurement of the flow and the density due to a neglect of correlations partly account for the observed scattering of flow-density data in the congested regime.

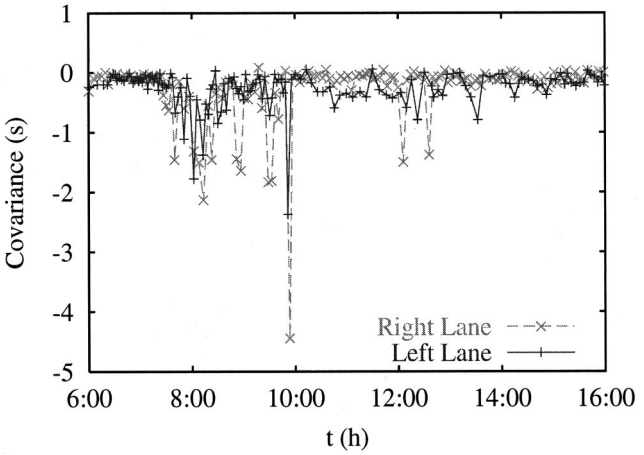

FIG. 25. Covariance between headways d_α and inverse velocities $1/v_\alpha$, which shows significant deviations from zero in congested traffic, while it approximately vanishes in free flow. Even after traffic has recovered, weak correlations seem to remain between headways and vehicle speeds for a considerable time. These probably reflect residual congestion due to platoons that have not fully dissolved. After Tilch, 2001.

III. MODELING APPROACHES FOR VEHICLE TRAFFIC

Since the 1950s, people have simultaneously been thinking about microscopic and macroscopic traffic models, as shown by the development of fluid-dynamic models on the one hand and of car-following (follow-the-leader) models on the other hand. The mesoscopic gas-kinetic (Boltzmann-like) models appeared in the 1960s, while cellular automata and the systematic investigation of the nonlinear dynamics of traffic flow were trends of the 1990s. Recently the availability of better data has stimulated an increasing number of experimental studies and their comparison with traffic models.

Altogether, researchers from engineering, mathematics, operations research, and physics have probably suggested more than 100 different traffic models, which cannot all be covered by this review.[5]

In the following subsections, I can introduce only a few representatives for each modeling approach (selected according to didactical reasons) and try to show the relations among them regarding their instability and other properties (see Secs. IV.A–IV.D).

[5]The following references provide further information: Buckley (1974), Whitham (1974), Gerlough and Huber (1975), Gibson (1981), May (1981), Vumbaco (1981), Hurdle *et al.* (1983), Volmuller and Hamerslag (1984), Gartner and Wilson (1987), Leutzbach (1988), Brannolte (1991), Daganzo (1993), Pave (1993), Snorek *et al.* (1995), Lesort (1996), the Transportation Research Board (1996), Wolf *et al.* (1996), Daganzo (1997a), Gartner *et al.* (1997), Helbing (1997a), Bovy (1998), Rysgaard (1998), Schreckenberg and Wolf (1998), Brilon *et al.* (1999), Ceder (1999), Hall (1999), Helbing, Herrmann, *et al.* (2000), and Helbing, Hennecke, *et al.* (2001a, 2001b). Readers interested in an exhaustive discussion of cellular automata should consult the detailed review by Chowdhury, Santen, and Schadschneider (2000).

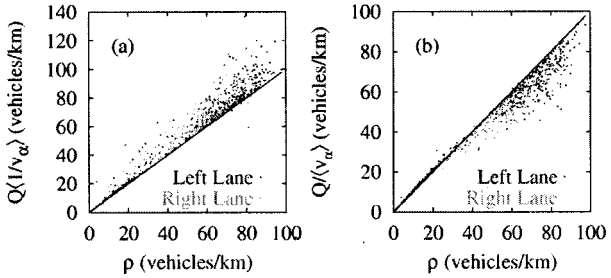

FIG. 26. Fifty-vehicle averages of (a) the density $Q\langle 1/v_\alpha\rangle$ and (b) the conventionally determined density $Q/\langle v_\alpha\rangle$, both as a function of the density ρ according to the proposed definition (14). The usually assumed relations are indicated by solid lines. From Tilch and Helbing, 2000.

Before looking at these models, I should like to formulate some criteria for good traffic models: For reasons of robustness and calibration, such models should contain only a few variables and parameters that have an intuitive meaning. Moreover, these should be easy to measure, and the corresponding values should be realistic. In addition, it is not satisfactory to selectively reproduce subsets of phenomena by different models. Instead, a good traffic model should at least qualitatively reproduce all known features of traffic flows, including the localized and extended forms of congestion. Furthermore, the observed hysteresis effects, complex dynamics, and the existence of the various self-organized constants like the propagation velocity of stop-and-go waves or the outflow from traffic jams should all be reproduced. A good model should also be theoretically consistent and make new predictions allowing us to verify or disprove it. Apart from that, its dynamics should not lead to vehicle collisions or exceed the maximum vehicle density. Finally, the model should allow for a fast numerical simulation.

A. Microscopic follow-the-leader models

Early microscopic traffic models were proposed by Reuschel (1950a, 1950b) and the physicist Pipes (1953). Microscopic traffic models assume that the acceleration of a driver-vehicle unit α is given by the neighboring vehicles. The dominant influence on driving behavior comes from the next vehicle $(\alpha-1)$ ahead, called the *leading vehicle*. Therefore we obtain the following model of driver behavior from Eq. (3):

$$\frac{dv_\alpha(t)}{dt}=\frac{v_\alpha^0+\xi_\alpha(t)-v_\alpha(t)}{\tau_\alpha}+f_{\alpha,(\alpha-1)}(t). \tag{15}$$

Here, $f_{\alpha,(\alpha-1)}(t)\leqslant 0$ describes the normally repulsive effect of vehicle $(\alpha-1)$, which is generally a function of

(i) the relative velocity $\Delta v_\alpha(t)=[v_\alpha(t)-v_{\alpha-1}(t)]$,
(ii) the velocity $v_\alpha(t)$ of vehicle α due to the velocity-dependent safe distance kept to the vehicle in front,
(iii) the headway (brutto distance) $d_\alpha(t)=[x_{\alpha-1}(t)-x_\alpha(t)]$ or the clearance (netto distance) $s_\alpha(t)=[d_\alpha(t)-l_{\alpha-1}]$, with l_α meaning the length of vehicle α.

Consequently, for identically behaving vehicles with $v_\alpha^0=v_0$, $\tau_\alpha=\tau$, and $f_{\alpha,(\alpha-1)}=f$, we would have

$$f_{\alpha,(\alpha-1)}(t)=f(s_\alpha(t),v_\alpha(t),\Delta v_\alpha(t)). \tag{16}$$

If we neglect fluctuations for the time being and introduce the traffic-dependent velocity

$$v^e(s_\alpha,v_\alpha,\Delta v_\alpha)=v_0+\tau f(s_\alpha,v_\alpha,\Delta v_\alpha), \tag{17}$$

to which driver α tries to adapt, we can considerably simplify the generalized (behavioral) force model (15):

$$\frac{dv_\alpha}{dt}=\frac{v^e(s_\alpha,v_\alpha,\Delta v_\alpha)-v_\alpha}{\tau}. \tag{18}$$

1. Noninteger car-following model

Models of the type of Eq. (18) are called *follow-the-leader models*.[6] One of the simplest representatives results from the assumption that the netto distance is given by the velocity-dependent safe distance $s^*(v_\alpha)=s'+Tv_\alpha$, where T has the meaning of the (effective) safe time clearance. This implies $s_\alpha(t)=s^*(v_\alpha(t))$ or, after differentiation with respect to time, $dv_\alpha(t)/dt=[ds_\alpha(t)/dt]/T=[dd_\alpha(t)/dt]/T=[v_{\alpha-1}(t)-v_\alpha(t)]/T$. Unfortunately, this model does not explain the empirically observed density waves (see Sec. II.E.1). Therefore one has to introduce an additional time delay $\Delta t\approx 1.3$ s in adaptation, reflecting the finite reaction time of drivers. This yields the following stimulus-response model:

$$\underbrace{\frac{dv_\alpha(t+\Delta t)}{dt}}_{\text{Response}}=\frac{1}{T}\underbrace{[v_{\alpha-1}(t)-v_\alpha(t)]}_{\text{Stimulus}}. \tag{19}$$

Here, $1/T$ is the sensitivity to the stimulus. This equation belongs to the class of *delay differential equations*, which normally have an unstable solution for sufficiently large delay times Δt. For the above model, Chandler *et al.* (1958) showed that a variation of individual vehicle velocities will be amplified under the instability condition $\Delta t/T>1/2$. The experimental value is $\Delta t/T\approx 0.55$. As a consequence, the nonlinear vehicle dynamics finally gives rise to stop-and-go waves, and also to accidents. In order to cure this, to explain the empirically observed fundamental diagrams, and to unify many other model variants, Gazis *et al.* (1961) introduced a generalized sensitivity factor with two parameters m_1 and m_2:

$$\frac{1}{T}=\frac{1}{T_0}\frac{[v_\alpha(t+\Delta t)]^{m_1}}{[x_{\alpha-1}(t)-x_\alpha(t)]^{m_2}}. \tag{20}$$

The corresponding noninteger car-following model can be rewritten in the form $[dv_\alpha(t+\Delta t)/dt]/[v_\alpha(t+\Delta t)]^{m_1}=(1/T_0)[dd_\alpha(t)/dt]/[d_\alpha(t)]^{m_2}$, which is solved

[6]For examples, see Reuschel, 1950a, 1950b; Pipes, 1953; Chandler *et al.*, 1958; Chow, 1958; Kometani and Sasaki, 1958, 1959, 1961; Gazis *et al.*, 1959; Herman *et al.*, 1959; Gazis *et al.*, 1961; Newell, 1961; Herman and Gardels, 1963; Herman and Rothery, 1963; Fox and Lehmann, 1967; May and Keller, 1967; Hoefs, 1972.

by $f_{m_1}(v_\alpha(t+\Delta t))=c_0+c_1 f_{m_2}(d_\alpha(t))$ with $f_k(z)=z^{1-k}$ if $k\neq 1$ and $\ln z$ otherwise (c_0, c_1 being integration constants). For $m_1\neq 1$ and $m_2\neq 1$ we shall discuss the stationary case related to identical velocities and distances. The vehicle density ρ is then given by the inverse brutto distance $1/d_\alpha$, and the corresponding equilibrium velocity V_e is identical with v_α. Hence we obtain the velocity-density relation $V_e(\rho)=V_0[1-(\rho/\rho_{\max})^{m_2-1}]^{1/(1-m_1)}$ with the free velocity V_0 and the maximum density $\rho_{\max}$. Most of the velocity-density relations under discussion are special cases of the latter formula for different values of the model parameters m_1 and m_2. Realistic fundamental diagrams result, for example, for the noninteger values $m_1\approx 0.8$ and $m_2\approx 2.8$ (May and Keller, 1967; Hoefs, 1972) or $m_1=0.953$ and $m_2=3.05$ (Kühne and Rödiger, 1991; Kühne and Kroen, 1992).

Finally, note that the above noninteger car-following model is used in the traffic simulation package MITSIM and has recently been made more realistic with acceleration-dependent parameters (Yang and Koutsopoulos, 1996; Yang, 1997). However, other car-following models deserve to be mentioned as well (Gipps, 1981; Benekohal and Treiterer, 1988; del Castillo, 1996b; Mason and Woods, 1997). For a historical review see Brackstone and McDonald (2000).

2. The Newell and optimal velocity models

One of the deficiencies of the noninteger car-following models is that it cannot describe the driving behavior of a single vehicle. Without a leading vehicle, i.e., for $d_\alpha\to\infty$, vehicle α would not accelerate at all. Instead, it should approach its desired velocity v_α^0 in free traffic. Therefore other car-following models do not assume an adaptation to the velocity of the leading vehicle, but an adaptation to a distance-dependent velocity $v_e'(d_\alpha)$ which should reflect the safety requirements and is sometimes called the "optimal velocity." While Newell (1961) assumes a delayed adaptation of the form

$$v_\alpha(t+\Delta t)=v_e'(d_\alpha(t))=v_e(s_\alpha(t)), \tag{21}$$

Bando *et al.* (1994) suggest using the relation

$$v_e'(d)=(v_0/2)[\tanh(d-d_c)+\tanh d_c] \tag{22}$$

with constants v_0 and d_c, together with the optimal velocity model

$$\frac{dv_\alpha(t)}{dt}=\frac{v_e'(d_\alpha(t))-v_\alpha(t)}{\tau}, \tag{23}$$

which may be considered as a first-order Taylor approximation $v_\alpha(t+\Delta t)\approx[v_\alpha(t)+\Delta t\, dv_\alpha(t)/dt]$ of Eq. (21) with $\tau=\Delta t$ (see also Bando, Hasebe, Nakayama, *et al.*, 1995; Bando, Hasebe, Nakanishi, *et al.*, 1995). For the optimal velocity model one can show that small perturbations are eventually amplified to traffic jams, if the instability condition

$$\frac{dv_e'(d_\alpha)}{dd_\alpha}=\frac{dv_e(s_\alpha)}{ds_\alpha}>\frac{1}{2\tau} \tag{24}$$

is satisfied (Bando, Hasebe, Nakayama, *et al.*, 1995), i.e., if we have large relaxation times τ or large changes in the velocity $v_e(s_\alpha)$ with the clearance s_α (see Fig. 27). Similar investigations have been carried out for analogous models with an additional explicit delay Δt (Bando *et al.*, 1998; Wang, Wang, *et al.*, 1998).

3. Intelligent driver model

As the optimal velocity model does not contain a driver response to the relative velocity Δv_α with respect to the leading vehicle, it is very sensitive to the concrete choice of the function $v_e'(d_\alpha)$ and produces accidents when fast cars approach standing ones (Helbing and Tilch, 1998). To avoid this, one has to assume particular velocity-distance relations and choose a very small value of τ, which gives unrealistically large accelerations (Manstetten *et al.*, 1997; Bleile, 1999). In reality, however, the acceleration times are about five to ten times larger than the braking times. Moreover, drivers keep a larger safe distance and decelerate earlier when the relative velocity $\Delta v_\alpha(t)$ is high. These aspects have been taken into account, for example, in models by Gipps (1981), Krauß *et al.* (1996, 1997), Helbing (1997a), Manstetten *et al.* (1997), Helbing and Tilch (1998), Bleile (1999), Wolf (1999), and Tomer *et al.* (2000); see also Chang and Lai (1997).

The *intelligent driver model* (Treiber and Helbing, 1999b; Treiber *et al.*, 2000) is a good example of the effort to more closely approximate what drivers do. It is easy to calibrate, robust, accident free, and numerically efficient, yields realistic acceleration and braking behavior, and reproduces the empirically observed phenomena. Moreover, for a certain specification of the model parameters, its fundamental diagram is related to that of the gas-kinetic-based, nonlocal traffic model, which is relevant for the micro-macro link we have in mind (see Sec. III.E). For other specifications, the intelligent driver model shares certain features of the Newell model or the Nagel-Schreckenberg model (see Sec. III.B.1).

The acceleration assumed in the intelligent driver model is a continuous function of the velocity v_α, the clearance $s_\alpha=(d_\alpha-l_{\alpha-1})$, and the velocity difference (approaching rate) Δv_α of vehicle α to the leading vehicle:

$$\frac{dv_\alpha}{dt}=a_\alpha\left[1-\left(\frac{v_\alpha}{v_\alpha^0}\right)^\delta-\left(\frac{s_\alpha^*(v_\alpha,\Delta v_\alpha)}{s_\alpha}\right)^2\right]. \tag{25}$$

This expression is a superposition of the acceleration tendency $a_\alpha[1-(v_\alpha/v_\alpha^0)^\delta]$ on a free road and the deceleration tendency $f_{\alpha,(\alpha-1)}=-a_\alpha[s_\alpha^*(v_\alpha,\Delta v_\alpha)/s_\alpha]^2$ describing interactions with other vehicles. The parameter δ allows us to fit the acceleration behavior. While $\delta=1$ corresponds to an exponential-in-time acceleration on a free road, as assumed by most other models, in the limit $\delta\to\infty$, we can describe a constant acceleration with a_α, until the desired velocity v_α^0 is reached. The deceleration term depends on the ratio between the desired clearance s_α^* and the actual clearance s_α, where the desired clearance

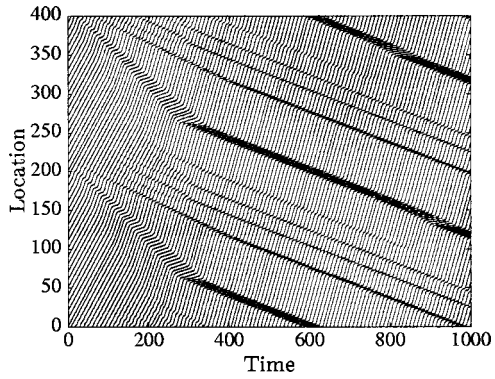

FIG. 27. Trajectories according to the optimal velocity model of Bando, Hasebe, *et al.* (1995) for each fifth vehicle, if the overall density ϱ on a circular road falls into the regime of linearly unstable traffic. As in Fig. 19, small perturbations are amplified and lead to the formation of "phantom traffic jams." From Helbing, 1997a.

$$s_\alpha^*(v_\alpha,\Delta v_\alpha)=s_\alpha'+s_\alpha''\sqrt{\frac{v_\alpha}{v_\alpha^0}}+T_\alpha v_\alpha+\frac{v_\alpha\Delta v_\alpha}{2\sqrt{a_\alpha b_\alpha}} \qquad (26)$$

is dynamically varying with the velocity v_α and the approaching rate Δv_α, reflecting an intelligent driver behavior. The parameters of this model can be chosen individually for each vehicle α, but for the moment we shall drop the index α for readability and assume identical vehicle parameters. These are the desired velocity v_0, the safe time clearance T, the maximum acceleration a, the comfortable deceleration b, the acceleration exponent δ, the jam distances s' and s'', and the vehicle length l, which has no dynamical influence. To reduce the number of parameters, one can assume $\delta=1$, $s''=0$, and $l=0$, which still yields good results.

In equilibrium traffic with $dv_\alpha/dt=0$ and $\Delta v_\alpha=0$, drivers tend to keep a velocity-dependent equilibrium clearance $s_e(v_\alpha)$ to the front vehicle given by $s_e(v)=s^*(v,0)[1-(v/v_0)^\delta]^{-1/2}$. Solving this for the equilibrium velocity $v=v_e$ leads to simple expressions only for $s''=0$ and $\delta=1$, $\delta=2$, or $\delta\to\infty$. In particular, the equilibrium velocity for the special case $\delta=1$ and $s'=s''=0$ is $v_e(s)=\{-1+\sqrt{1+[4T^2(v_0)^2]/s^2}\}s^2/(2v_0T^2)$. From this equation and the micro-macro relation $s=(d-l)=(1/\rho-l)=(1/\rho-1/\rho_{\max})$ between clearance and density follows the corresponding equilibrium traffic flow $Q_e(\rho)=\rho V_e(\rho)$ as a function of the traffic density ρ. The acceleration coefficient δ influences the transition region between the free and congested regimes. For $\delta\to\infty$ and $s''=0$, the fundamental diagram becomes triangular shaped: $Q_e(\rho)=\min(\rho v_0,[1-\rho(l+s')]/T)$. For decreasing δ, it becomes smoother and smoother.

B. Cellular automata

Cellular automaton models are interesting for their speed and their complex dynamic behavior (Wolfram, 1984, 1986, 1994; Stauffer, 1991), including such fascinating phenomena as self-organized criticality (Bak *et al.*, 1987, 1988; Bántay and Jánosi, 1992; Olami *et al.*, 1992), formation of spiral patterns (Markus and Hess, 1990), and oscillatory or chaotic sequences of states (Wolfram, 1984; Markus and Hess, 1990; Nowak and May, 1992). The great speed and efficiency with which they can be computed is a consequence of the following properties, which are ideal preconditions for parallel computing: (i) discretization of space into identical cells (lattice sites) j of size Δx, (ii) a finite number of possible states $g(x)$, (iii) the (parallel) update at times $t=i\Delta t$ with an elementary time step Δt, and (iv) globally applied update rules, based on (v) short-range interactions with a finite (small) number of neighboring sites. Despite these simplifications, cellular automata and related lattice gas automata have a broad range of applications, from realistic simulations of granular media (Peng and Herrmann, 1994) or fluids (including interfacial phenomena and magnetohydrodynamics; Frisch *et al.*, 1986; Chen *et al.*, 1991), to the computation of chemical reactions (Markus and Hess, 1990; Dab *et al.*, 1991) and even the modeling of avalanches (Bantay and Janosi, 1992).

Their application to traffic dynamics has stimulated an enormous amount of research activity, aimed at understanding and controlling traffic instabilities, which are responsible for stop-and-go traffic and congestion, both on freeways and in cities. The first cellular automaton models for freeway traffic go back to Cremer and coworkers (Cremer and Ludwig, 1986; Schütt, 1990) and to Nagel and Schreckenberg (1992). Other early cellular automaton studies were carried out by Biham *et al.* (1992). Since then, there has been an overwhelming number of proposals and publications in this field. Nevertheless, I will keep my discussion short, since the subject has recently been reviewed by Chowdhury, Santen, and Schadschneider (2000). Complementarily, it is worth checking out the Java applets supplied at the Web sites http://www.trafficforum.org/RoadApplet/ and http://www.traffic.uni-duisburg.de/model/index.html, which allow the interested reader to compare the dynamics of various cellular automata.

1. The Nagel-Schreckenberg model and its slow-to-start variant

Cellular automata describe vehicle dynamics in a less detailed manner than follow-the-leader models, but their simplifications favor extremely fast simulation of huge numbers of interacting vehicles. Nagel and Schreckenberg (1992) suggest dividing the street into cells j of length Δx and the time t into intervals i of duration $\Delta t=1$ s. Each cell is either empty or occupied by one vehicle with speed

$$v_i=\hat{v}_i\frac{\Delta x}{\Delta t}, \qquad (27)$$

where $\hat{v}_i\in\{0,1,\ldots,\hat{v}_{\max}\}$. For freeways, one frequently chooses the cell size $\Delta x=7.5$ m and the scaled desired velocity $\hat{v}_{\max}=v_0\Delta t/\Delta x=5$. The car positions are updated in parallel according to the following rules:

(i) *Motion*: Move the vehicle forward by $\hat{v}_i$ cells.

(ii) *Acceleration*: If a vehicle has not yet reached its maximum velocity, increase the velocity to $\hat{v}_i' = (\hat{v}_i + 1)$, corresponding to a constant acceleration $\Delta x/(\Delta t)^2$.

(iii) *Deceleration*: However, if the distance (i.e., the number of cells) to the next vehicle ahead is $\hat{d}_i \leqslant \hat{v}_i'$, the velocity is reduced to $\hat{v}_i'' = (\hat{d}_i - 1)$, otherwise $\hat{v}_i'' = \hat{v}_i'$.

(iv) *Randomization*: With probability p, the velocity is reduced to $\hat{v}_{i+1} = (\hat{v}_i'' - 1)$, if this yields a nonnegative velocity, otherwise $\hat{v}_{i+1} = 0$.

According to steps (ii)–(iv), the updated velocity as a function of the previous velocity $\hat{v}_i$ can be summarized by the formula

$$\hat{v}_{i+1} = \max(0, \min(\hat{v}_{\max}, \hat{d}_i - 1, \hat{v}_i + 1) - \xi_i^{(p)}), \tag{28}$$

where the Boolean random variable $\xi_i^{(p)} = 1$ with probability p and 0 otherwise.

Note that, according to rule (iii), drivers always move below the speed that advances them by the clearance to the car ahead within Δt. Hence the parameter Δt plays, at the same time, the roles of an updating step, of the adaptation time τ, and of the safe time clearance T. Moreover, the discretization length Δx agrees with the minimum space requirement l', i.e., with the inverse jam density. This makes the Nagel-Schreckenberg model extremely compact and elegant.

The model parameter ("slowdown probability") p describes individual velocity fluctuations due to delayed acceleration (imperfect driving). For freeway traffic, Nagel and Schreckenberg have often set $p = 0.5$, which leads to a relatively noisy dynamics (see Fig. 28), while $p = 0.2$ and $\hat{v}_{\max} = 2$ are suitable values for city traffic (Esser and Schreckenberg, 1997).

A variant of this model, the velocity-dependent randomization model (Barlovic *et al.*, 1998), contains a slow-to-start rule. It assumes $p = 0.01$ for finite velocities, while $p_0 = 0.5$ for $\hat{v}_i = 0$. A similar model was proposed by Benjamin *et al.* (1996). The fundamental diagram of the resulting model combines the properties of the Nagel-Schreckenberg model with $p = 0.01$ at low densities with the properties of the one with $p = 0.5$ at high densities. In between, one finds a crossover region in which the solutions of both models can exist, but the high-flow states are metastable. We shall come back to this and other topics later (see Sec. IV.A).

2. Some other cellular automaton models

An interesting variant of the Nagel-Schreckenberg model assumes a *cruise control* (Nagel and Paczuski, 1995), where the fluctuations are turned off for $\hat{v}_i = \hat{v}_{\max}$. Then the lifetime distribution of traffic jams changes from an exponential (Nagel, 1994) to a power-law distribution which implies fractal self-similarity and points to self-organized criticality (Nagel, 1994; Nagel and Rasmussen, 1994).

The cellular automaton model of Brilon and Wu (1999) modifies the Nagel-Schreckenberg model by additionally introducing an acceleration probability and requiring a minimal time clearance for acceleration.

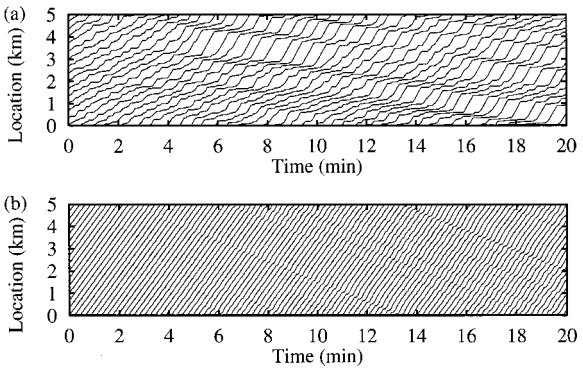

FIG. 28. Trajectories of each tenth vehicle for unstable traffic in the Nagel-Schreckenberg model, if the slowdown probability is (a) $p = 0.5$ and (b) $p = 0.001$. In the limit $p \to 0$, the jam amplitude goes to zero.

Takayasu and Takayasu (1993) were the first to introduce a *slow-to-start rule*. Their model, sometimes referred to as the TT or T2 model, is generalized by Schadschneider and Schreckenberg (1997a); a standing vehicle with velocity $\hat{v}_i = 0$ will accelerate with probability $q = (1 - p)$ if there is exactly one empty cell in front. For $\hat{d}_i > 2$ it will deterministically accelerate to $\hat{v}_{i+1} = 1$.

A model by Nagel and Hermann (1993) can be viewed as a continuum version of the Nagel-Schreckenberg model. Its slightly generalized version by Sauermann and Herrmann (1998) reads

$$\hat{v}_{i+1} = \begin{cases} \max(\hat{d}_i - \hat{\delta}, 0) & \text{for } \hat{v}_i > \hat{d}_i - \hat{\alpha} \\ \min(\hat{v}_i + \hat{a}, \hat{v}_{\max}) & \text{for } \hat{v}_i < \hat{d}_i - \hat{\beta} \\ \hat{v}_i & \text{otherwise.} \end{cases}$$

Here, the acceleration coefficient is determined by $\hat{a} = \hat{a}_{\max} \min(1, \hat{d}_i / \hat{\gamma})$, where $\hat{\alpha}$, $\hat{\beta}$, $\hat{\gamma}$, and $\hat{\delta}$ are the parameters of the model.

Another collision-free continuum-in-space version of the Nagel-Schreckenberg model is related to the model of Gipps (1981) and given by the equation

$$v_\alpha(t+1) = \max[0, \mathrm{rnd}(v_\alpha^{\mathrm{des}}(t) - a\Delta t, v_\alpha^{\mathrm{des}}(t))],$$

where $\mathrm{rnd}(z_1, z_2)$ represents a random number uniformly distributed in the interval $[z_1, z_2)$. The desired velocity is determined by $v_\alpha^{\mathrm{des}}(t) = \min(v_\alpha^{\max}, v_\alpha^{\mathrm{safe}}(t), v + a\Delta t)$, while the safe velocity is calculated via $v_\alpha^{\mathrm{safe}}(t) = v_{\alpha-1}(t) + b[s_\alpha - v_{\alpha-1}(t)\Delta t]/[v_\alpha(t) + b\Delta t]$. This model was developed and investigated in detail by Krauß and co-workers (Krauß *et al.*, 1996, 1997; Krauß, 1998a, 1998b).

A model developed by Ianigro (1994) is based on Petri nets. Yukawa and Kikuchi (1995, 1996) have studied traffic models based on coupled maps (see also Tadaki *et al.*, 1998). Although there are many other cellular automaton models of traffic flow (e.g., Wolf, 1999), I shall mention here only one more, the model of Fukui and Ishibashi (1996a; see also Braude, 1996; Wang, Kwong,

and Hui, 1998a). In it, $\hat{v}_{i+1}=\max[0,\min(\hat{v}_{\max},\hat{d}_i-1)-\xi_i^{(p)}]$ with unlimited acceleration capabilities.

Apart from the slow-to-start models, many cellular automaton models have a principal difference from other models of traffic flow, especially from deterministic approaches like the car-following models described before. They require fluctuations for the explanation of traffic jams. That is, in the limit $p\to 0$, traffic jams will normally disappear (see Fig. 28). This does not disqualify cellular automaton models, since driver behavior is certainly imperfect and traffic flow subject to random influences. However, this raises the following questions: (i) Are fluctuations a dominant or a subordinate effect? (ii) Which kinds of observations require the consideration of noise? (iii) Can cellular automaton models of traffic flow be mathematically connected with other traffic models?

3. The discrete optimal velocity model

To construct a mathematical link between the Nagel-Schreckenberg model and the optimal velocity model, let us discretize the latter: $v_\alpha(t+\Delta t)\approx v_\alpha(t)+[v'_e(d_\alpha(t))-v_\alpha(t)]\Delta t/\tau$. Dropping the vehicle index α and scaling the time by $\Delta t=1$ s, the distances by the cell length Δx (to be specified later), and the velocities by $\Delta x/\Delta t$ results in $\hat{v}_{i+1}=\hat{v}_i+\hat{\lambda}[\hat{v}'_e(\hat{d}_i)-\hat{v}_i]$, where $\hat{\lambda}=\Delta t/\tau$. In order to have integer-valued velocities $\hat{v}$ and locations, we need to introduce a tabular function $h(z)$. Additionally, we shall add some noise for comparison with the Nagel-Schreckenberg model. The resulting discrete and noisy optimal velocity model reads (Helbing and Schreckenberg, 1999)

$$\hat{v}_{i+1}=\max[0,\hat{v}_i+h(\hat{\lambda}[\hat{v}'_e(\hat{d}_i)-\hat{v}_i])-\xi_i^{(p)}]. \tag{29}$$

For the floor function $h(z)=\lfloor z\rfloor$, the argument z is rounded down to the largest natural number $n\leqslant z$. Then the above equation implies $\hat{v}_{i+1}\leqslant\hat{\lambda}\hat{v}'_e(\hat{d}_i)+(1-\hat{\lambda})\hat{v}_i$.

4. Comparison

The above model is practically as efficient and fast as the Nagel-Schreckenberg model, but it allows a fine-grained description of vehicle velocities and locations by selecting small values of Δx. Moreover, it can be specified in such a way that vehicles will normally not jump into the same cell or over each other. However, as in the continuous optimal velocity model itself, the discrete version is sensitive to the choice of the parameter $\hat{\lambda}=\Delta t/\tau$ and the integer-valued velocity-distance function $\hat{v}'_e(\hat{d})$. A value $\hat{\lambda}\approx 0.77$ seems to be optimal. For city traffic, the additional specifications $\hat{v}'_e(\hat{d})=\min(\hat{d}-1,3)$ and $\Delta x=6.25$ m yield realistic results. The most attractive properties of this model are that (i) jam formation is not affected by reducing the fluctuation strength (see Fig. 29), (ii) the characteristic constants of traffic are reproduced (see Secs. II.E.1 and IV.A.5), (iii) the critical densities and the characteristic constants can be calculated, and (iv) a mathematical relation with other cellular automaton models can be constructed.

For example, the Nagel-Schreckenberg model corresponds to the selection $\hat{\lambda}=1$ and $\hat{v}'_e(\hat{d})=\min(\hat{d}-1,\hat{v}_{\max})$. Moreover, $h(z)=\lfloor z\rfloor$, if $z<1$, otherwise $h(z)=1$, which limits acceleration, while deceleration capabilities are unlimited. Nevertheless, these two mathematically related models lead to a different dynamics (compare Figs. 28 and 29), probably because the assumed velocity changes $d\hat{v}'_e(\hat{d})/d\hat{d}$ with the distance assumed in the Nagel-Schreckenberg model are not sufficiently large for a linear instability, and the ratio between acceleration and braking capabilities is too small [see Sec. IV.A.4, Fig. 36(a)].

C. Master equation

Some particle hopping models (see Sec. I.E) simplify the description of transport processes even further than do the above cellular automaton models, in order (i) to identify the minimal requirements for certain phenomena in self-driven many-particle systems, and (ii) to facilitate analytical investigations, although their treatment is not necessarily easier. However, the main difference is that cellular automata are discrete in time rather than continuous, allowing us to specify deterministic processes with transition probability 1.

For a stochastic description, let us consider a system with L states j occupied by n_j particles. The distribution $P(\mathbf{n},t)$ shall denote the probability of finding the system configuration, i.e., the occupation vector

$$\mathbf{n}=(n_1,\ldots,n_j,n_{j+1},\ldots,n_L) \tag{30}$$

at time t. This probability is reduced by transitions to other configurations $\mathbf{n}'$, the frequency of which is proportional to $P(\mathbf{n},t)$. The proportionality factor is the conditional transition probability $P(\mathbf{n}',t+\Delta t|\mathbf{n},t)$ of finding the configuration $\mathbf{n}'$ at time $(t+\Delta t)$, given that we have the configuration $\mathbf{n}$ at time t. Conversely, the probability $P(\mathbf{n},t)$ increases by transitions from configurations $\mathbf{n}'$ to $\mathbf{n}$, which are proportional to the occurrence probability $P(\mathbf{n}',t)$ of $\mathbf{n}'$ and to the transition probability $P(\mathbf{n},t+\Delta t|\mathbf{n}',t)$. Considering the normalization $\Sigma_{\mathbf{n}'}P(\mathbf{n}',t+\Delta t|\mathbf{n},t)=1$, the resulting balance equation governing the dynamics of so-called Markov chains reads

$$P(\mathbf{n},t+\Delta t)=\sum_{\mathbf{n}'}P(\mathbf{n},t+\Delta t|\mathbf{n}',t)P(\mathbf{n}',t), \tag{31}$$

or, in the continuous limit $\Delta t\to 0$,

$$\frac{dP(\mathbf{n},t)}{dt}=\sum_{\mathbf{n}'(\neq\mathbf{n})}W(\mathbf{n}|\mathbf{n}';t)P(\mathbf{n}',t) - \sum_{\mathbf{n}'(\neq\mathbf{n})}W(\mathbf{n}'|\mathbf{n};t)P(\mathbf{n},t), \tag{32}$$

where we have introduced the transition rates

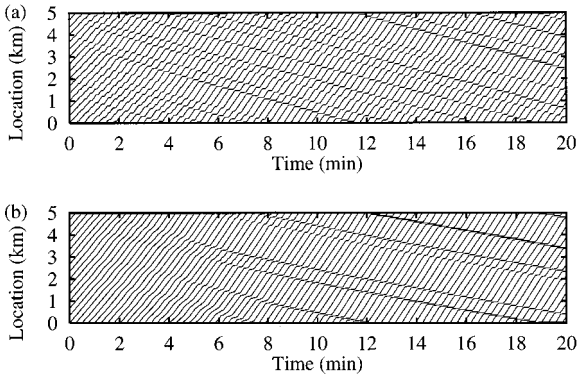

FIG. 29. Trajectories of each tenth vehicle in the congested regime according to the discrete version of the optimal velocity model for slowdown probability (a) $p=0.5$ and (b) $p=0.001$. Jam formation does not disappear for small values of p. These just reduce the average distance between traffic jams, while their amplitude remains constant (see Helbing and Schreckenberg, 1999).

$$W(\mathbf{n}|\mathbf{n}';t)=\lim_{\Delta t\to 0}\frac{P(\mathbf{n},t+\Delta t|\mathbf{n}',t)}{\Delta t}\quad(\mathbf{n}'\neq\mathbf{n}).$$

Note that the master equation (32) assumes the conditional probabilities $P(\mathbf{n},t+\Delta t|\mathbf{n}',t)$ to depend on t and Δt only, but not on previous time steps.

For the totally asymmetric simple exclusion process (TASEP; see Sec. I.E), we have

$$P(\mathbf{n}',t+\Delta t|\mathbf{n},t)=\begin{cases}qn_j(1-n_{j+1}) & \text{if } \mathbf{n}'=\mathbf{n}_{j,(j+1)}\\ 0 & \text{otherwise,}\end{cases}\tag{33}$$

where

$$\mathbf{n}_{jj'}=(n_1,\ldots,n_j-1,\ldots,n_{j'}+1,\ldots,n_L).$$

In the continuous limit, we assume $\lim_{\Delta t\to 0}q/\Delta t=\nu$.

1. Solution methods, mapping to spin chains, and the matrix product ansatz

Since the master equation is linear, many solution methods are available for it (cf. the books and reviews by Feller, 1967; Haken, 1977; van Kampen, 1981; Gardiner, 1985; Haus and Kehr, 1987; Weiss, 1994; Helbing, 1995a; Schütz, 2000a; see also Helbing and Molini, 1995). For example, one can map the TASEP to a spin system by identifying empty sites with down spins and occupied ones with up spins. Following Doi (1976; see also Sandow and Trimper, 1993b; Kaulke and Trimper, 1995), the probability distribution $P(\mathbf{n},t)$ can be related to a state vector $|P(t)\rangle$ in Fock space, and with respect to its orthonormal basis $\{|\mathbf{n}_k\rangle\}$ we have the relation $|P(t)\rangle=\Sigma_k P(\mathbf{n}_k,t)|\mathbf{n}_k\rangle$. The linear master equation becomes $\partial|P(t)\rangle/\partial t=\mathcal{L}|P(t)\rangle$, where the linear operator $\mathcal{L}$ can, as in a second quantization, be expressed in terms of creation and annihilation operators usually satisfying Bose commutation rules (Doi, 1976; Grassberger and Scheunert, 1980; Peliti, 1985; Sandow and Trimper, 1993a). When the occupation numbers per lattice site are limited to a maximum value, one has to take into account the exclusion principle, leading to commutation rules of Pauli operators or similar ones (Gwa and Spohn, 1992; Rudavets, 1993; Sandow and Trimper, 1993b; Alcaraz *et al.*, 1994; Schütz and Sandow, 1994).

Alternatively, one may rewrite the master equation as a Schrödinger equation in imaginary time by setting $\mathcal{H}=-\mathcal{L}$ (Felderhof and Suzuki, 1971; Siggia, 1977; Alexander and Holstein, 1978; Schütz, 2000a). The stochastic Hamiltonian $\mathcal{H}$ is defined by its matrix elements $\langle\mathbf{n}_k|\mathcal{H}|\mathbf{n}_k\rangle=\Sigma_{l(\neq k)}W(\mathbf{n}_l|\mathbf{n}_k)$, and $\langle\mathbf{n}_k|\mathcal{H}|\mathbf{n}_l\rangle=-W(\mathbf{n}_k|\mathbf{n}_l)$. The stationary state corresponds to the eigenvector of $\mathcal{H}$ or $\mathcal{L}$ with eigenvalue 0, i.e., it can be interpreted as the ground state. For discrete time dynamics, the corresponding equation (31) can be analogously rewritten as $|P(t+\Delta t)\rangle=\mathcal{T}|P(t)\rangle$. Here the stationary state is the eigenvector of the transfer matrix $\mathcal{T}$ with eigenvalue 1. It can be determined by the matrix product ansatz (Derrida *et al.*, 1993; Hinrichsen, 1996; Derrida and Evans, 1997; Rajewsky and Schreckenberg, 1997; Rajewsky *et al.*, 1998; Karimipour, 1999c; Klauck and Schadschneider, 1999; see also Krebs and Sandow, 1997, for an existence theorem). The stationary solution is

$$P_{\rm st}(\mathbf{n})=\frac{1}{Z_L}\left\langle W\left|\prod_{j=1}^{L}[n_j\mathcal{D}+(1-n_j)\mathcal{E}]\right|V\right\rangle,\tag{34}$$

where $|V\rangle$ and $|W\rangle$ are vectors characterizing the boundary conditions, $\mathcal{D}$ and $\mathcal{E}$ are suitable matrices, and $Z_L=\langle W|(\mathcal{D}+\mathcal{E})^L|V\rangle$ is a normalization constant. More general formulas are available for dynamic solutions, using Bethe ansatz equations (Stinchcombe and Schütz, 1995a, 1995b; Sasamoto and Wadati, 1997; Schütz, 1998).

2. The mean-field approach and the Boltzmann equation

It is often useful to consider the mean-value equations for the expected values $\langle n_j\rangle=\Sigma_{\mathbf{n}}n_jP(\mathbf{n},t)$, which we obtain by multiplying Eq. (32) with n_j, summing over $\mathbf{n}$, and suitably interchanging $\mathbf{n}$ and $\mathbf{n}'$:

$$\frac{d\langle n_j\rangle}{dt}=\sum_{\mathbf{n}}n_j\frac{dP(\mathbf{n},t)}{dt}=\langle m_j(\mathbf{n},t)\rangle.\tag{35}$$

Here we have introduced the first jump moments,

$$m_j(\mathbf{n},t)=\sum_{\mathbf{n}'}(n_j'-n_j)W(\mathbf{n}'|\mathbf{n};t).\tag{36}$$

Let us assume spontaneous transitions with individual transition rates $w(j'|j)$ from state j to j' and pair interactions changing the states from j and k to j' and k' with transition rates $w_2(j',k'|j,k)$. Defining

$$\mathbf{n}_{jj'}^{kk'}=(\ldots,n_j-1,\ldots,n_{j'}+1,\ldots,n_k-1,\ldots,n_{k'}+1,\ldots),$$

we find that the corresponding configurational transition rates are given by

$$W(\mathbf{n}'|\mathbf{n})=\begin{cases}w(j'|j)n_j & \text{if } \mathbf{n}'=\mathbf{n}_{jj'}\\ w_2(j',k'|j,k)n_jn_k & \text{if } \mathbf{n}'=\mathbf{n}_{jj'}^{kk'}\\ 0 & \text{otherwise.}\end{cases}\tag{37}$$

That is, the total rate of spontaneous transitions is proportional to the number n_j of particles that may change their state j independently of each other, while the total rate of pair interactions is proportional to the number $n_j n_k$ of possible interactions between particles in states j and k. Inserting Eq. (37) into Eq. (36) eventually leads to

$$m_j(\mathbf{n}) = \sum_{j'} \left[w(j|j') + \sum_{k,k'} w_2(j,k|j',k') n_{k'} \right] n_{j'} - \sum_{j'} \left[w(j'|j) + \sum_{k,k'} w_2(j',k'|j,k) n_k \right] n_j \quad (38)$$

(see, for example, Helbing, 1992a, 1995a). The mean-field approach assumes

$$\langle m_j(\mathbf{n}) \rangle \approx m_j(\langle \mathbf{n} \rangle), \quad (39)$$

i.e., that the system dynamics is determined by the mean value $\langle \mathbf{n} \rangle$, which is true for a sharply peaked, unimodal distribution $P(\mathbf{n},t)$. This leads to the generalized Boltzmann equation

$$\frac{d\rho(j,t)}{dt} = \sum_{j'} \left[w(j|j') + \sum_{k,k'} \hat{w}_2(j,k|j',k') \rho(k',t) \right] \rho(j',t) - \sum_{j'} \left[w(j'|j) + \sum_{k,k'} \hat{w}_2(j',k'|j,k) \rho(k,t) \right] \rho(j,t), \quad (40)$$

where we have introduced $\hat{w}_2(j',k'|j,k) = w_2(j',k'|j,k)\Delta x$ and the densities $\rho(j,t) = \langle n_j \rangle / \Delta x$. Note that this Boltzmann equation neglects the covariances

$$\sigma_{jk}(t) = \langle (n_j - \langle n_j \rangle)(n_k - \langle n_k \rangle) \rangle = (\langle n_j n_k \rangle - \langle n_j \rangle \langle n_k \rangle)$$

and the corresponding correlations $r_{jk}(t) = \sigma_{jk} / \sqrt{\sigma_{jj}\sigma_{kk}}$.

3. The totally asymmetric simple exclusion process and the Nagel-Schreckenberg model

For a TASEP with the transition rates of Eq. (33), the mean-field approach of Eq. (40) yields

$$\frac{d\langle n_j \rangle}{dt} = Q_{j-1}(t) - Q_j(t) \quad (41)$$

with the particle flow

$$Q_j(t) = \nu \langle n_j (1 - n_{j+1}) \rangle \approx \nu \langle n_j \rangle (1 - \langle n_j \rangle). \quad (42)$$

While in open systems exact calculations are difficult due to correlations, this relation becomes exact for the stationary state of periodic systems (Spohn, 1991; Schadschneider and Schreckenberg, 1993; Schreckenberg *et al.*, 1995; Liggett, 1999). A spatially continuous approximation of Eq. (41) results in the Burgers equation (53) or, in lowest-order approximation, in the Lighthill-Whitham equation (49).

However, replacing the random sequential update of the TASEP by a parallel update, we end up with the traffic model of Nagel and Schreckenberg with $\hat{v}_{\max} = 1$ and $p = (1 - q)$ (see Sec. III.B.1). For a parallel update, the state changes of many particles are coupled, leading to significant correlations. Consequently we have to take into account higher-order interactions in the respective transition rates $W(\mathbf{n}'|\mathbf{n})$. It turns out that the above result for the TASEP corresponds to the *site-oriented mean-field theory* for the Nagel-Schreckenberg model with $\hat{v}_{\max} = 1$, which underestimates the flows by neglecting the correlations (Nagel and Schreckenberg, 1992; Schreckenberg *et al.*, 1995). This can be corrected for by eliminating so-called paradisical or Garden of Eden states (Moore, 1962) that cannot be reached dynamically when a parallel update is applied (Schadschneider and Schreckenberg, 1998). Alternatively, one can develop a *car-oriented mean-field theory*, which calculates the probabilities $P_n(t)$ of finding n empty sites in front of a vehicle (Schadschneider and Schreckenberg, 1997b). A superior method (Schadschneider, 1999) is a *site-oriented cluster-theoretic approach* (Schadschneider and Schreckenberg, 1993; Schreckenberg *et al.*, 1995), calculating occurrence probabilities of states composed of n successive sites (Kikuchi, 1966; Gutowitz *et al.*, 1987; ben-Avraham and Köhler, 1992; Crisanti *et al.*, 1993). Instead of Eq. (39), a two-cluster approximation gives

$$\langle n_{j-1}(t) n_j(t) n_{j+1}(t) n_{j+2}(t) \rangle \approx \frac{\langle n_{j-1}(t) n_j(t) \rangle \langle n_j(t) n_{j+1}(t) \rangle \langle n_{j+1}(t) n_{j+2}(t) \rangle}{\langle n_j(t) \rangle \langle n_{j+1}(t) \rangle}.$$

This allows us to calculate the time-dependent average flow $Q(t) = q \langle \langle n_j(t)[1 - n_{j+1}(t)] \rangle \rangle / \Delta t = \hat{Q}(t)/\Delta t$ (Wang and Hui, 1997), if we take into account that the occupation numbers change according to

$$n_j(t+1) = [1 - \xi_{j-1}^{(1-p)}(t)] n_{j-1}(t)[1 - n_j(t)] + n_j(t) n_{j+1}(t) + \xi_j^{(p)}(t) n_j(t)[1 - n_{j+1}(t)].$$

In the above formulas, $\langle \langle n_j \rangle \rangle = \varrho \Delta x$ indicates an average over all lattice sites j. For the stationary case, one can finally derive the correct stationary flow-density relation

$$\hat{Q} = \frac{1}{2} \{ 1 - [1 - 4q \langle \langle n_j \rangle \rangle (1 - \langle \langle n_j \rangle \rangle)]^{1/2} \} \quad (43)$$

(Yaguchi, 1986; Schadschneider and Schreckenberg, 1993, 1997b, 1998; Schreckenberg *et al.*, 1995). The above results can be gained using $\langle \xi_j^{(p)}(t) \rangle = p$, $\xi_j^{(p)}(t) \xi_j^{(1-p)}(t) = 0$, $[\xi_j^{(p)}(t)]^2 = \xi_j^{(p)}(t)$, as well as the statistical independence of $\xi_j^{(p)}(t)$, $\xi_{j+1}^{(p)}(t)$, and $\xi_j^{(p)}(t+1)$ (Wang and Hui, 1997). The dynamics and correlation functions are also different from the TASEP (Schadschneider, 1999).

4. Nucleation and jamming transition

A master equation model for the jamming transition on a circular road[7] of length L has been developed by Mahnke and Pieret (1997). It assumes that congested regions eventually merge to form one big "megajam." If the spatial dynamics of the N cars is neglected, we need only one single occupation number n to count the number of cars in the traffic jam. Moreover, the model assumes that cars leave a standing traffic jam with the constant rate $w(n-1|n)=1/T$. They join the queue with the rate $w(n+1|n)=v_e(s(n))/s(n)$ given by the vehicle speed $v_e(s)=v_0 s^2/[(s_0)^2+s^2]$, divided by the average clearance $s(n)=(L-Nl)/(N-n)$ of freely moving vehicles (s_0 being some constant). Mahnke and Kaupužs (1999) derive the stationary distribution $P_{\rm st}(n)$ of the queue length n and show a transition from free to congested traffic at a certain critical vehicle density. While the maximum of the probability distribution $P_{\rm st}(n)$ is located at $n=1$ in free traffic, in congested traffic it is located at some finite value $n>1$, which is growing with the vehicle density.

Mahnke and Kaupužs compare the nucleation, growth, and condensation of car clusters with the formation of liquid droplets in a supersaturated vapor (Schweitzer *et al.*, 1988; Ebeling *et al.*, 1990). Moreover, they recognize that, for fixed scaled parameters and fixed vehicle length l, the fundamental flow-density diagram of their model is dependent on the road length L. This, however, results from the fact that they relate the flow to the overall vehicle density $\varrho=N/L$ rather than to the local density $\rho=1/[l+s(n)]$.

5. Fokker-Planck equation

Kühne and Anstett (1999) have obtained results similar to those of Mahnke and co-workers, and they have managed to derive the distribution $P_{\rm st}(n)$ and the location of its maximum as well. Their calculations are based on the related Fokker-Planck equation

$$\frac{\partial \hat{P}(y,t)}{\partial t} = -\frac{\partial}{\partial y}[\hat{m}(y,t)\hat{P}(y,t)] + \frac{1}{2}\frac{\partial^2}{\partial y^2}[\hat{m}_2(y,t)\hat{P}(y,t)] \tag{44}$$

for the scaled, quasicontinuous variable $y=n/N$. This Fokker-Planck equation can be viewed as a second-order Taylor approximation of the master equation, after this has been rewritten in the form $d\hat{P}(y,t)/dt = \Sigma_{y'}[\hat{W}(y',y-y')\hat{P}(y-y',t)-\hat{W}(y',y)\hat{P}(y,t)]$ with $\hat{W}(y',y)=W((y+y')N|yN)=W(n+y'N|n)$. Correspondingly, the first jump moment, which has the meaning of a drift coefficient, is $\hat{m}(y,t)=\Sigma_{y'}y'\hat{W}(y',y)$, while the second jump moment, which can be interpreted as a diffusion coefficient, is given by $\hat{m}_2(y,t)=\Sigma_{y'}(y')^2\hat{W}(y',y)$. Details regarding the Fokker-Planck equation and its solution can be found in the books by van Kampen (1981), Horsthemke and Lefever (1984), Gardiner (1985), and Risken (1989).

D. Macroscopic traffic models

As we shall see in Sec. IV.A.4, the above findings of Mahnke, Kühne, and co-workers regarding the fundamental diagram and the nucleation effect are quite compatible with those for macroscopic traffic models. In contrast to microscopic traffic models, macroscopic ones are restricted to the description of the collective vehicle dynamics in terms of the spatial vehicle density $\rho(x,t)$ per lane and the average velocity $V(x,t)$ as a function of the freeway location x and time t. Macroscopic models have often been preferred to car-following models for numerical efficiency, but in terms of computation speed they cannot compete with cellular automata. However, some favorable properties are (i) their good agreement with empirical data (see Sec. IV.B.1), (ii) their suitability for analytical investigations (see Sec. IV), (iii) the simple treatment of inflows from ramps (see Sec. IV.B), and (iv) the possibility of simulating the traffic dynamics in several lanes by effective one-lane models considering a certain probability of overtaking (see Sec. III.E).

1. The Lighthill-Whitham model

The oldest and still the most popular macroscopic traffic model goes back to Lighthill and Whitham (1955). It appears that Richards (1956) developed the same model independently of them. Their fluid-dynamic model is based on the fact that, away from on- or off-ramps, no vehicles are entering or leaving the freeway (at least if we neglect accidents). This conservation of the vehicle number leads to the continuity equation

$$\frac{\partial \rho(x,t)}{dt} + \frac{\partial Q(x,t)}{\partial x} = 0. \tag{45}$$

Here,

$$Q(x,t)=\rho(x,t)V(x,t) \tag{46}$$

is the traffic flow per lane, which is the product of the density and the average velocity (see Sec. III.E).

We may apply the so-called total or substantial derivative

$$\frac{d_v}{dt}=\frac{\partial}{\partial t}+V\frac{\partial}{\partial x},$$

describing temporal changes in a coordinate system moving with velocity $V(x,t)$, i.e., with "the substance" (the vehicles). With this, we can rewrite Eq. (45) in the form $d_v\rho(x,t)/dt=-\rho(x,t)\partial V(x,t)/\partial x$, from which we conclude that the vehicle density increases in time

[7]For the theoretical study of a spatially homogeneous system, one often simulates a periodically closed, circular ring road without on- and off-ramps. This allows the identification of the properties of a closed system without impurities and without the particular knowledge of measured boundary conditions. However, the scenario of a ring road is not very characteristic or relevant for real systems, as the study of inhomogeneous roads with bottlenecks has shown (see Sec. IV.B).

$(d_v\rho/dt>0)$, where the velocity decreases in the course of the road $(\partial V/\partial x<0)$, and vice versa. Moreover, the density can never become negative, since $\rho(x,t)=0$ implies $d_v\rho(x,t)/dt=0$.

Equation (45) is naturally part of any macroscopic traffic model. The difficulty is to specify the traffic flow $Q(x,t)$. Lighthill and Whitham assume that the flow is simply a function of the density:

$$Q(x,t)=Q_e(\rho(x,t))=\rho V_e(\rho(x,t))\geqslant 0. \tag{47}$$

Here, the fundamental (flow-density) diagram $Q_e(\rho)$ and the equilibrium velocity-density relation $V_e(\rho)$ are thought to be suitable fit functions of empirical data, for which there are many proposals (see, for example, Sec. III.A). The first measurements by Greenshields (1935) had suggested a linear relation of the form

$$V_e(\rho)=V_0(1-\rho/\rho_{\text{jam}}), \tag{48}$$

which is still sometimes used for analytical investigations.

Inserting Eq. (47) into the continuity equation (45), we obtain

$$\frac{\partial\rho}{\partial t}+C(\rho)\frac{\partial\rho}{\partial x}=0. \tag{49}$$

This is a nonlinear wave equation (Whitham, 1974, 1979), which describes the propagation of kinematic waves with velocity

$$C(\rho)=\frac{dQ_e}{d\rho}=V_e(\rho)+\rho\frac{dV_e}{d\rho}. \tag{50}$$

Because of $dV_e(\rho)/d\rho\leqslant 0$, we have $C(\rho)\leqslant V_e(\rho)$. Hence the kinematic waves always propagate backwards with respect to the average velocity $V_e(\rho)$ of motion, namely, with the speed $c(\rho)=[C(\rho)-V_e(\rho)]=\rho\, dV_e(\rho)/d\rho\leqslant 0$.

Note that $C(\rho)$ is the speed of the characteristic lines (i.e., of local information propagation), which is density dependent. In contrast to linear waves, the characteristic lines intersect, because their speed in congested areas is lower. This gives rise to changes of the wave profile, that is, to the formation of shock fronts, while the amplitude of kinematic waves does not change significantly (see Fig. 30). A shock front is characterized by the upstream value ρ_- and the downstream value ρ_+ of the density (see Fig. 31). The difference in the flow Q_- upstream and the flow Q_+ downstream causes a density jump $(\rho_+-\rho_-)$ moving with speed S. Because of vehicle conservation, we have $(Q_+-Q_-)=(\rho_+-\rho_-)S$. Consequently, with Eq. (47), the speed of shock propagation is

$$S(\rho_+,\rho_-)=[Q_e(\rho_+)-Q_e(\rho_-)]/(\rho_+-\rho_-) \tag{51}$$

(see Fig. 31).

Based on this information, we can understand the phase diagram for the TASEP (see Fig. 32 and Secs. I.E, III.C, and III.C.3). Stimulated by a study by Krug (1991), the corresponding results were obtained by Schütz and Domany (1993) and Derrida *et al.* (1993). A detailed overview is given by Schütz (2000a). For a system with open boundary conditions with average occupation numbers $\langle n_0\rangle$ at the upstream end and $\langle n_{L+1}\rangle$ at the downstream end, they found the lower density to dominate within the system if $\langle n_0\rangle=q_0/q<1/2$ and $\langle n_0\rangle=q_0/q<q_{L+1}/q=(1-\langle n_{L+1}\rangle)$, while the higher density dominated in the system if $\langle n_0\rangle=q_0/q>q_{L+1}/q=(1-\langle n_{L+1}\rangle)$ and $(1-\langle n_{L+1}\rangle)=q_{L+1}/q<1/2$. This is a consequence of downstream shock propagation in the first case, while shocks propagate upstream in the second case. When the line $\langle n_0\rangle=q_0/q=q_{L+1}/q=(1-\langle n_{L+1}\rangle)$ is crossed, a phase transition from a low-density state to a high-density state occurs. Finally, under the condition $\langle n_0\rangle=q_0/q>1/2$ and $q_{L+1}/q>1/2$, i.e., $\langle n_{L+1}\rangle<1/2$, the system takes on a maximum flow state. For a more detailed analysis see the review by Schütz (2000a). Related studies have been also carried out by Nagatani (1995c).

2. The Burgers equation

The Lighthill-Whitham model is very instructive and is the basis of an elaborate shock-wave theory (Haight, 1963; Gazis, 1974; Whitham, 1974; Hida, 1979; Newell, 1993; Daganzo, 1999b), but the development of shock waves results in serious difficulties for solving the Lighthill-Whitham model numerically. A suitable integration method is the *Godunov scheme* (Godunov, 1959; Ansorge, 1990; Bui *et al.*, 1992; LeVeque, 1992; Lebaque, 1995). As an alternative, Newell (1993), Daganzo (1994, 1995a, 1995b), and Lebacque (1997) have recently developed variants of the Lighthill-Whitham model.

To avoid the development of shock fronts, one often adds a small diffusion term to the Lighthill-Whitham model to smooth the wave fronts. Whitham himself (1974) suggested generalizing Eq. (47) according to $Q=[Q_e(\rho)-D\,\partial\rho/\partial x]$ or

$$V(x,t)=V_e(\rho(x,t))-\frac{D}{\rho(x,t)}\frac{\partial\rho(x,t)}{\partial x}. \tag{52}$$

The resulting equation reads

$$\frac{\partial\rho}{\partial t}+\left[V_e(\rho)+\rho\frac{dV_e}{d\rho}\right]\frac{\partial\rho}{\partial x}=\frac{\partial}{\partial x}\left(D\frac{\partial\rho}{\partial x}\right). \tag{53}$$

The last term is a diffusion term. For a diffusion constant $D>0$, it yields a significant contribution only when the curvature $\partial^2\rho/\partial x^2$ of the density is great. In case of a density maximum, the curvature is negative, which results in a reduction of the density. A density minimum is smoothed out for analogous reasons.

For analytical considerations, we shall assume the linear velocity-density relation of Eq. (48). With the resulting propagation speed $C(x,t)=V_0[1-2\rho(x,t)/\rho_{\text{jam}}]$ of kinematic waves, we can then transform Eq. (53) into

$$\frac{\partial C(x,t)}{\partial t}+C(x,t)\frac{\partial C(x,t)}{\partial x}=D\frac{\partial^2 C(x,t)}{\partial x^2}. \tag{54}$$

This equation, known as the *Burgers equation*, is the simplest equation containing nonlinear propagation and

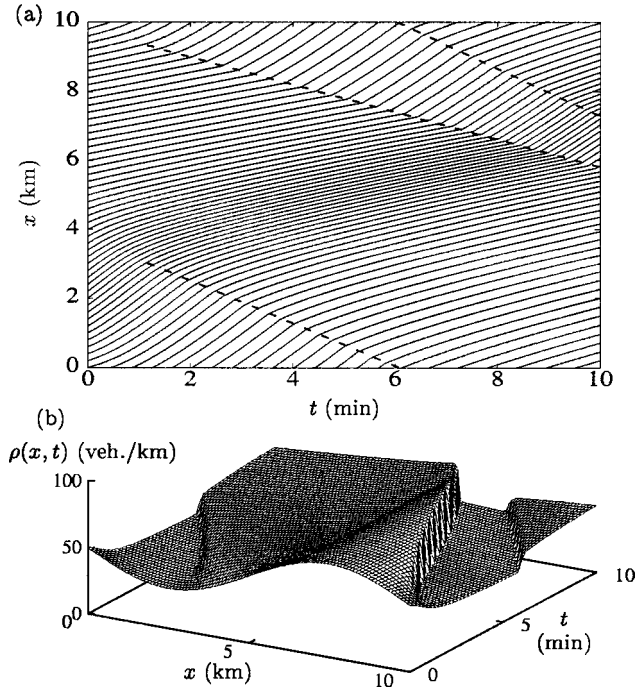

FIG. 30. Formation of shock fronts: (a) Trajectories of each tenth vehicle and (b) corresponding spatio-temporal density plot illustrating the formation of a shock wave on a circular road according to the Lighthill-Whitham model. Although the initial condition is a smooth sinusoidal wave, the upstream and downstream fronts grow steeper and steeper, eventually producing discontinuous jumps in the density profile, which propagate with constant speeds. The wave amplitude remains approximately unchanged. From Helbing, 1997a.

diffusion. Surprisingly, it can be solved exactly, because it is related to the linear heat equation

$$\frac{\partial \Psi(x,t)}{\partial t} = D \frac{\partial^2 \Psi(x,t)}{\partial x^2} \tag{55}$$

by means of the Cole-Hopf transformation $C(x,t) = -[2D/\Psi(x,t)]\partial\Psi(x,t)/\partial x$ (Whitham, 1974).

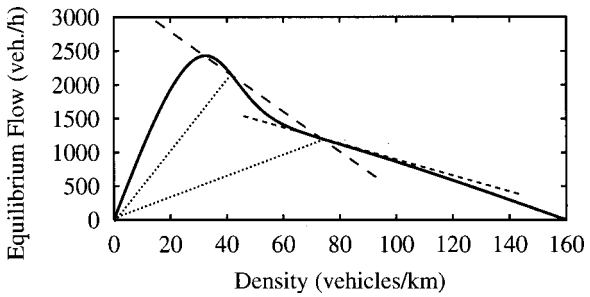

FIG. 31. Illustration of the geometrical relations between the fundamental diagram $Q_e(\rho)$ (solid line) and other quantities characterizing traffic flow. Dotted lines, the vehicle velocity $V_e(\rho)$ corresponding to the slope of the line connecting the origin (0,0) and the point $(\rho, Q_e(\rho))$. Short dashed line, propagation speed $C(\rho)$ of density waves corresponding to the slope of the tangent $dQ_e(\rho)/d\rho$. Long dashed line, speed S of shock waves corresponding to the slope of the connecting line between $(\rho_-, Q_e(\rho_-))$ and $(\rho_+, Q_e(\rho_+))$.

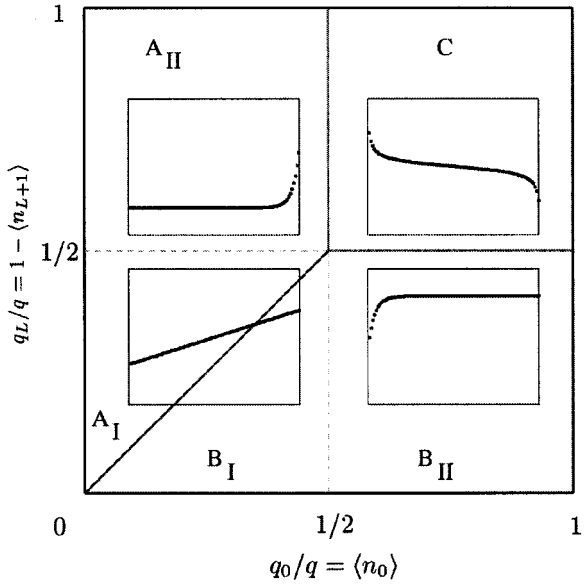

FIG. 32. Phase diagram of the totally asymmetric simple exclusion process (TASEP) with open boundaries and of other models that can be macroscopically described by the Lighthill-Whitham or Burgers equation, with representative density profiles (see insets). The diagonal line separates the areas $A_{\rm I}$ and $A_{\rm II}$ of downstream shock propagation from the areas $B_{\rm I}$ and $B_{\rm II}$ of upstream shock propagation with corresponding changes in the density profile. Consequently crossing this line is related to a transition between a low-density phase controlled by the upstream boundary and a high-density phase controlled by the downstream boundary. Area C is characterized by the maximum possible flow. After Schütz and Domany, 1993; Schütz, 2000a.

The Burgers equation overcomes the problem of shock waves, but it cannot explain the self-organization of phantom traffic jams or stop-and-go waves (see Fig. 33). Recently, most research has focused on the noisy Burgers equation containing an additional fluctuation term (Forster *et al.*, 1977; Musha and Higuchi, 1978; Nagel, 1995, 1996).

3. Payne's model and its variants

Payne (1971, 1979a) complemented the continuity equation (45) by a dynamic velocity equation, which he derived from Newell's car-following model (21) by means of a Taylor approximation. Recently, related approaches have been pursued by Helbing (1998a), Nelson (2000), and Berg *et al.* (2000).

Payne identified microscopic and macroscopic velocities according to $v_\alpha(t+\Delta t) = V(x+V\Delta t, t+\Delta t) \approx [V(x,t) + V\Delta t \partial V(x,t)/\partial x + \Delta t \partial V(x,t)/\partial t]$. Moreover, he replaced the inverse of the headway d_α to the car in front by the density ρ at the place $x + d_\alpha(t)/2$ in the middle between the leading and the following vehicle:

$$\begin{aligned} 1/d_\alpha(t) &= \rho(x + d_\alpha(t)/2, t) \\ &= \rho(x + 1/(2\rho), t) \\ &\approx [\rho(x,t) + 1/(2\rho)\partial\rho(x,t)/\partial x]. \end{aligned}$$

This yields

$$v_e'(d_\alpha(t)) = V_e(1/d_\alpha(t)) \approx \{V_e(\rho(x,t)) + 1/[2\rho(x,t)] \times [dV_e(\rho)/d\rho]\partial\rho(x,t)/\partial x\}.$$

From the previous equations we can obtain Payne's velocity equation,

$$\frac{\partial V}{\partial t} + V\frac{\partial V}{\partial x} = \frac{1}{\Delta t}\left[V_e(\rho) - \frac{D(\rho)}{\rho}\frac{\partial \rho}{\partial x} - V\right], \tag{56}$$

where we have introduced the density-dependent diffusion $D(\rho) = -0.5 dV_e(\rho)/\partial\rho = 0.5|dV_e(\rho)/d\rho| \geq 0$. The single terms of Eq. (56) have the following interpretation:

(i) As in hydrodynamics, the term $V\partial V/\partial x$ is called the *transport or convection term*. It describes a motion of the velocity profile with the vehicles.

(ii) The term $-[D(\rho)/(\rho\Delta t)]\partial\rho/\partial x$ is called the *anticipation term*, since it reflects the reaction of identical drivers to the traffic situation in their surrounding, particularly in front of them.

(iii) The *relaxation term* $[V_e(\rho) - V]/\Delta t$ describes the adaptation of the average velocity $V(x,t)$ to the density-dependent equilibrium velocity $V_e(\rho)$. This adaptation is exponential in time with relaxation time Δt.

The linear instability condition of Payne's model agrees exactly with that of the optimal velocity model, if we set $\tau = \Delta t$ (see Secs. III.A.2 and IV.A.1). In the limit $\Delta t \to 0$, one can derive the stable model (52) as an adiabatic approximation of Eq. (56). Inserting this into the continuity equation, we obtain Eq. (53) with Payne's density-dependent diffusion function.

For numerical robustness, Payne (1979a, 1979b) used a special discretization modifying his original model by numerical viscosity terms. His model was taken up by many people, for example, Papageorgiou (1983). Cremer and co-workers multiplied the anticipation term by a factor of $\rho/(\rho+\rho_0)$ with some constant $\rho_0 > 0$ to get a more realistic behavior at small vehicle densities $\rho \approx 0$ (Cremer, 1979; Cremer and Papageorgiou, 1981; Cremer and May, 1986; Cremer and Meißner, 1993). A discrete version of this model is used in the simulation package SIMONE (Meißner and Böker, 1996). Smulders (1986, 1987, 1989) introduced additional fluctuation terms in the continuity and velocity equations to reflect the observed variations of the macroscopic traffic quantities. Further modifications of Payne's freeway simulation package FREFLO (Payne, 1979b) were suggested by Rathi *et al.* (1987).

4. The models of Prigogine and Phillips

An alternative model was proposed by Phillips (1979a, 1979b), who derived it from a modified version of Prigogine's Boltzmann-like traffic model (see Sec. III.E.1). Like Prigogine and Herman (1971), he obtained the continuity equation (45) and the velocity equation

$$\frac{\partial V}{\partial t} + V\frac{\partial V}{\partial x} = -\frac{1}{\rho}\frac{\partial P}{\partial x} + \frac{1}{\tau(\rho)}[V_e(\rho) - V], \tag{57}$$

but with another density-dependent relaxation time $\tau(\rho)$. The quantity $P(x,t) = \rho(x,t)\,\theta(x,t)$ denotes the *traffic pressure*, where $\theta(x,t)$ is the velocity variance of differently driving vehicles. For this variance, one can either derive an approximate dynamic equation or assume a variance-density relation such as $\theta(x,t) = \theta_0[1 - \rho(x,t)/\rho_{\rm jam}] \geq 0$ (Phillips, 1979a, 1979b). According to this, the variance decreases with increasing density and vanishes together with the equilibrium velocity $V_e(\rho)$ at the jam density $\rho_{\rm jam}$, as expected.

Like the Payne model, the model by Phillips is unstable in a certain density range. Hence it could explain emergent stop-and-go waves, but it is not numerically robust. In particular, at high densities ρ the traffic pressure decreases with ρ, so that vehicles would accelerate into congested regions, which is unrealistic.

5. The models of Whitham, Kühne, Kerner, Konhäuser, and Lee *et al.*

With Eq. (47), the Lighthill-Whitham model assumes that the traffic flow is always in equilibrium $Q_e(\rho)$. This is at least very questionable for medium densities (Kerner and Rehborn, 1996b; Kerner *et al.*, 1997), where there is no unique empirical relation between flow and density (see Secs. II.B and IV.A.3). Although some researchers believe that the Lighthill-Whitham theory is correct, implying that there would be no unstable traffic in which disturbances are amplified, Daganzo (1999a) recently noted that "large oscillations in flow, speed and cumulative count increase in amplitude across the detectors spanning a long freeway queue and its intervening on-ramps" (cf. Figs. 22 and 41). Moreover, Cassidy and Bertini (1999) state that "the discharge flows in active bottlenecks exhibit near-stationary patterns that (slowly) alternate about a constant rate . . . . The onset of upstream queueing was always accompanied by an especially low discharge flow followed by a recovery rate and these are the effects of driver behavior we do not yet understand" [cf. Figs. 3(b) and 38(d)].

Whitham himself (1974) suggested a generalization of the Lighthill-Whitham theory, which is related to Phillips' model, but without the mentioned problem of decreasing traffic pressure. He obtained it from the continuity equation together with the assumption that the adaptation to the velocity (52) can be delayed by some relaxation time τ: $d_v V/dt = [V_e(\rho) - (D/\rho)\partial\rho/\partial x - V]/\tau$. Therefore Whitham's velocity equation reads $\partial V/\partial t + V\partial V/\partial x = -(\theta_0/\rho)\partial\rho/\partial x + [V_e(\rho) - V]/\tau$ with suitable constants $\theta_0 = D > 0$ and $\tau > 0$.

Unfortunately, this model shows the same problems with numerical robustness as the models of Payne and Phillips, since it eventually produces shocklike waves. Therefore Kühne (1984a, 1984b, 1987) added a viscosity term $\nu\partial^2 V/\partial x^2$, which has an effect similar to that of the

diffusion term in the Burgers equation and resolves the problem (cf. Fig. 33). In analogy with the Navier-Stokes equation for compressible fluids, Kerner and Konhäuser (1993) preferred a viscosity term of the form $(\eta/\rho)\partial^2 V/\partial x^2$, leading to the velocity equation

$$\frac{\partial V}{\partial t}+V\frac{\partial V}{\partial x}=-\frac{\theta_0}{\rho}\frac{\partial \rho}{\partial x}+\frac{\eta}{\rho}\frac{\partial^2 V}{\partial x^2}+\frac{V_e(\rho)-V}{\tau}. \quad (58)$$

A stochastic version of this Kerner-Konhäuser model has been developed by Kerner *et al.* (1995b) to consider fluctuations in vehicle acceleration (Kühne, 1987).

It turns out that the above Kerner-Konhäuser model is rather sensitive to the choice of parameters and the velocity-density relation. This is probably for reasons similar to those for the optimal velocity model, as both have no dependence on the relative velocity between cars. The probably best parameter set was specified by Lee *et al.* (1998).

6. The Weidlich-Hilliges model

The basic version of the model by Weidlich and Hilliges (Weidlich, 1992; Hilliges, Reiner, and Weidlich, 1993; Hilliges and Weidlich, 1995) is discrete and related to Daganzo's cell transmission model (Daganzo, 1994, 1995a): The freeway is divided into cells j of equal length Δx, reminiscent of cellular automaton models. Moreover, the density $\hat{\rho}(j,t)=\rho(j\Delta x,t)$ is governed by the spatially discretized continuity equation

$$\frac{\partial \hat{\rho}(j,t)}{\partial t}+\frac{\hat{Q}(j,t)-\hat{Q}(j-1,t)}{\Delta x}=0. \quad (59)$$

However, Weidlich and Hilliges assume for the flow the phenomenologically motivated relation

$$\hat{Q}(j,t)=\hat{\rho}(j,t)\hat{V}(j+1,t), \quad (60)$$

according to which the drivers in cell j adapt their speed to the velocity in the next cell $(j+1)$. This looks like a generalization of the mean value equations of the totally asymmetric simple exclusion process (see Sec. III.C.3) and reflects an anticipatory behavior of the drivers. The choice $\Delta x\approx 100\,\mathrm{m}$ of the cell length is therefore determined by driver behavior. Under the assumption $\hat{V}(j,t)=V_e(\hat{\rho}(j,t))$, the model cannot describe emergent stop-and-go waves, since the continuous version of the Weidlich-Hilliges model corresponds to Eq. (53) with the diffusion function $D(\rho)=[V_e(\rho)-\rho dV_e/d\rho]\Delta x/2 \geqslant 0$, as is shown by a Taylor expansion of $\rho((j-1)\Delta x,t)$ and $V((j+1)\Delta x,t)$. For the linear velocity-density relation (48), we have simply a diffusion constant $D=V_0\Delta x/2$, which implies an equivalence to the Burgers equation (54).

To model self-organized stop-and-go waves, Hilliges and Weidlich (1995) have supplemented Eqs. (59) and (60) by the dynamic velocity equation

$$\frac{\partial \hat{V}(j,t)}{\partial t}+\hat{V}(j,t)\frac{\hat{V}(j+1,t)-\hat{V}(j-1,t)}{2\Delta x}=\frac{V_e(\hat{\rho}(j,t))-\hat{V}(j,t)}{\tau}, \quad (61)$$

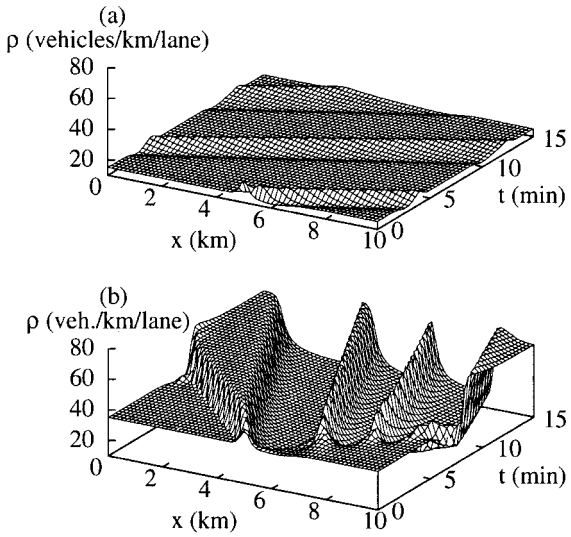

FIG. 33. Illustration of the typical traffic dynamics according to macroscopic models with a dynamic velocity equation. The simulations were carried out with the nonlocal gas-kinetic-based traffic model introduced in Sec. III.E.4 and show the spatio-temporal evolution of the traffic density $\rho(x,t)$ on a circular road of circumference 10 km, starting with homogeneous traffic, to which a localized initial perturbation (108) of amplitude $\Delta\rho=10$ vehicles/km/lane was added. (a) Free and stable traffic at low vehicle density. (b) Formation of stop-and-go waves in the range of linearly unstable traffic at medium vehicle density. From Treiber *et al.*, 1999; Helbing, Hennecke, *et al.*, 2001a, 2001b.

with $\tau\approx 5$ s. In the continuous limit $\Delta x\to 0$, the terms on the left-hand side correspond to the substantial time derivative $d_v V/dt=\partial V/\partial t+V\partial V/\partial x$.

Moreover, Hilliges and Weidlich (1995) have shown that $\partial\hat{\rho}(j,t)/\partial t\geqslant 0$ if $\hat{\rho}(j,t)=0$, and $\partial\hat{V}(j,t)/\partial t\geqslant 0$ if $\hat{V}(j,t)=0$. This guarantees the required non-negativity of the density and the average velocity. In addition, they have developed simple rules for the treatment of junctions, which allow the simulation of large freeway networks.

7. Common structure of macroscopic traffic models

The previous models are closely related to each other (Helbing, 1997a, 1997e), as they can all be viewed as special cases of the density equation

$$\frac{\partial \rho}{\partial t}+V\frac{\partial \rho}{\partial x}=-\rho\frac{\partial V}{\partial x}+D(\rho)\frac{\partial^2 \rho}{\partial x^2}+\xi_1(x,t) \quad (62)$$

and the velocity equation

$$\frac{\partial V}{\partial t}+V\frac{\partial V}{\partial x}=-\frac{1}{\rho}\frac{dP}{d\rho}\frac{\partial \rho}{\partial x}+\nu\frac{\partial^2 V}{\partial x^2}+\frac{1}{\tau}(V_e-V)+\xi_2(x,t). \quad (63)$$

The differences are in the specification of the diffusion $D(\rho)$, the fluctuations $\xi_1(x,t),\xi_2(x,t)$, the traffic pressure $P(\rho)$, the viscositylike quantity $\nu(\rho)$, the relaxation time $\tau(\rho)$, and the equilibrium velocity $V_e(\rho)$. The

Lighthill-Whitham model, for example, results in the limit $\tau \to 0$. Payne's model is satisfied with $\tau = \Delta t$ and $P(\rho) = [V_0 - V_e(\rho)]/(2\Delta t)$, while $P(\rho) = \rho\theta_0$ in the Kerner-Konhäuser model (58). Clearly, some parameters must be set to zero.

Section III.E will show how to derive macroscopic from microscopic traffic models. We shall see that D and ξ_1 should be nonvanishing only in first-order models restricting themselves to a density equation. In second-order models with a dynamic velocity equation, the pressure P consists of a contribution $\rho\theta$, if there is a variation of individual velocities due to fluctuations or different driver-vehicle types, and other contributions that are due to the nonlocality of vehicle interactions (Helbing, 1996b, 1997a, 1998a, 1998c; see also Secs. III.E.5 and III.D.3). Daganzo (1995c) has criticized second-order macroscopic traffic models as fundamentally unsound, but his arguments have been invalidated (Whitham, 1974; Paveri-Fontana, 1975; Helbing, 1995b, 1996a, 1996b, 1997a; Helbing and Treiber, 1999; Treiber *et al.*, 1999; Aw and Rascle, 2000; Zhang, 2000).

E. Gas-kinetic traffic models and the micro-macro link

In the following paragraphs, I shall show how the car-following models of Sec. III.A can be connected with macroscopic traffic models via a mesoscopic level of description.

1. Prigogine's Boltzmann-like model

Starting in 1960, Prigogine and co-workers proposed, improved, and investigated a simple gas-kinetic model (Prigogine and Andrews, 1960; Prigogine, 1961). The results are summarized in the book by Prigogine and Herman (1971), to which I refer in the following.

Gas-kinetic theories are based on an equation for the phase-space density,

$$\tilde{\rho}(x,v,t) = \rho(x,t)\tilde{P}(v;x,t), \tag{64}$$

which is the product of the vehicle density $\rho(x,t)$ and the distribution $\tilde{P}(v;x,t)$ of vehicle speeds v at location x and time t. Because of vehicle conservation, we find again a kind of continuity equation for the phase-space density:

$$\frac{d_v\tilde{\rho}}{dt} = \frac{\partial\tilde{\rho}}{\partial t} + v\frac{\partial\tilde{\rho}}{\partial x} = \left(\frac{d\tilde{\rho}}{dt}\right)_{\text{acc}} + \left(\frac{d\tilde{\rho}}{dt}\right)_{\text{int}}. \tag{65}$$

However, compared to Eq. (45), this conservation equation is not zero on the right-hand side, because of velocity changes. In a coordinate system moving with speed v, the temporal change of the phase-space density is given by the acceleration behavior and interactions of the vehicles.

Prigogine suggested that the acceleration behavior can be described by a relaxation of the velocity distribution $\tilde{P}(v;x,t)$ to some desired distribution $\tilde{P}_0(v)$:

$$\left(\frac{d\tilde{\rho}}{dt}\right)_{\text{acc}} = \frac{\rho(x,t)}{\tau(\rho(x,t))}[\tilde{P}_0(v) - \tilde{P}(v;x,t)]. \tag{66}$$

The quantity $\tau(\rho)$ again denotes a density-dependent relaxation time. In this model, $\tilde{P}_0(v)$ reflects the variation of the desired velocities among drivers, causing the scattering of the actual vehicle velocities v. The distribution $\tilde{P}_0(v)$ can be obtained by measuring the velocity distribution of vehicles with large clearances (Tilch, 2001).

Interactions among the vehicles are modeled by the Boltzmann-like term

$$\left(\frac{d\tilde{\rho}}{dt}\right)_{\text{int}} = \int_{w>v} dw[1-\hat{p}(\rho)]|w-v|\tilde{\rho}(x,w,t)\tilde{\rho}(x,v,t) - \int_{w<v} dw[1-\hat{p}(\rho)]|v-w|\tilde{\rho}(x,v,t)\tilde{\rho}(x,w,t). \tag{67}$$

This assumes that fast vehicles with velocity w interact with slower ones with velocity $v<w$ at a rate $|w-v|\tilde{\rho}(x,w,t)\tilde{\rho}(x,v,t)$, which is proportional to the relative velocity $|w-v|$ and to the product of the phase-space densities of the interacting vehicles, describing how often vehicles with velocities w and v meet at place x. Given that the faster vehicle can overtake with some density-dependent probability $\hat{p}(\rho)$, it will have to decelerate to the velocity v of the slower vehicle with probability $[1-\hat{p}(\rho)]$, increasing the phase-space density $\tilde{\rho}(x,v,t)$ accordingly. However, the phase-space density is decreased when vehicles of velocity v meet slower vehicles with velocity $w<v$. This is reflected by the last term of Eq. (67).

The interaction term (67) can be simplified to

$$\left(\frac{d\tilde{\rho}}{dt}\right)_{\text{int}} = [1-\hat{p}(\rho(x,t))]\rho(x,t)[V(x,t)-v]\tilde{\rho}(x,v,t) \tag{68}$$

by introducing the average velocity

$$V(x,t) = \int dv\, v\tilde{P}(v;x,t) = \int dv\, v\frac{\tilde{\rho}(x,v,t)}{\rho(x,t)}. \tag{69}$$

Additionally, we define the velocity variance

$$\theta(x,t) = \int dv[v-V(x,t)]^2\tilde{P}(v;x,t) \tag{70}$$

and the average desired velocity $V_0 = \int dv\tilde{P}_0(v)$. To derive macroscopic density and velocity equations, we multiply the kinetic equation given by Eqs. (65), (66), and (68) by 1 or v and integrate over v, taking into account that the vehicle density is given by

$$\rho(x,t) = \int dv\tilde{\rho}(x,v,t). \tag{71}$$

We obtain Eqs. (62) and (63) with $D(\rho) = 0 = \nu(\rho)$, $\xi_1(t) = 0 = \xi_2(t)$, the traffic pressure

$$P(\rho,\theta) = \rho\theta, \tag{72}$$

and the equilibrium velocity

$$V_e(\rho,\theta) = V_0 - \tau(\rho)[1-\hat{p}(\rho)]\rho\theta. \tag{73}$$

That is, gas-kinetic approach allowed Prigogine and his co-workers to derive mathematical relations for the

model functions P and V_e, which other researchers previously had to guess by phenomenological considerations. Unfortunately, the above relations are valid only for small densities, but theories for higher densities are also available (see Secs. III.E.3 and III.E.4).

Analyzing the Boltzmann-like traffic model, Prigogine (1961) found a transition from free to congested traffic above a certain critical density, which he compared to the phase transition from a gaseous to a fluid phase (see also Prigogine and Herman, 1971). This congested state is characterized by the appearance of a second maximum of the velocity distribution at $v=0$. That is, some of the vehicles move, while others are completely at rest. This bimodal equilibrium distribution is also found in modern variants of Prigogine's model (Nelson, 1995; Nelson *et al.*, 1997), as a consequence of the special acceleration term (66).

To obtain a better agreement with empirical data, Phillips (1977, 1979a, 1979b) modified Prigogine's relations for the overtaking probability $\hat{p}(\rho)$ and the relaxation time $\tau(\rho)$. Moreover, he assumed that the distribution of desired velocities $\tilde{P}_0(v)$ depends on the density ρ and the average velocity V. Finally, he made several proposals for the velocity variance θ. Prigogine's model has also been improved by Andrews (1970a, 1970b, 1973a, 1973b), Paveri-Fontana (1975), Phillips (1977, 1979a), Nelson (1995), Helbing (1995c, 1995d, 1996a, 1996b, 1997a, 1997d, 1998a), Klar *et al.* (1996), Nagatani (1996a, 1996b, 1996c, 1997a, 1997b), Wagner *et al.* (1996), Wegener and Klar (1996), Wagner (1997a, 1997b, 1997c, 1998b), Klar and Wegener (1997, 1999a, 1999b), Shvetsov and Helbing (1999). They modified the acceleration term, introduced velocity correlations among successive vehicles, investigated interactions among neighboring lanes, and/or considered space requirements.

2. Paveri-Fontana's model

Paveri-Fontana (1975) carried out a very detailed investigation of Prigogine's gas-kinetic traffic model and recognized some strange features. He criticized the fact that the acceleration term (66) would describe discontinuous velocity jumps occurring with a rate proportional to $1/\tau(\rho)$. Moreover, the desired velocities of vehicles were a property of the road and not the drivers, while there are actually different driver personalities—aggressive ones, driving fast, and timid ones, driving slowly (Daganzo, 1995c).

Paveri-Fontana resolved these problems by distinguishing different driver-vehicle types. These were characterized by individual desired velocities v_0. As a consequence, he introduced an extended phase-space density $\rho_*(x,v,v_0,t)$ and the corresponding gas-kinetic equation. By integration over v_0, one can regain Eq. (65). While Paveri-Fontata specified the interaction term analogously to Prigogine's, a different approach was chosen for the acceleration term. It corresponds to the microscopic acceleration law

$$dv/dt=(v_0-v)/\tau(\rho), \tag{74}$$

finally resulting in the formula

$$\left(\frac{d\tilde{\rho}}{dt}\right)_{\text{acc}}=-\frac{\partial}{\partial v}\left[\tilde{\rho}(x,v,t)\,\frac{\tilde{V}_0(v;x,t)-v}{\tau(\rho(x,t))}\right] \tag{75}$$

(Helbing, 1995d, 1996a; Wagner *et al.*, 1996). Here, the quantity $\tilde{V}_0(v;x,t)=\int dv_0 v_0 \rho_*(x,v,v_0,t)/\tilde{\rho}(x,v,t) \approx V_0(x,t)+[v-V(x,t)]C'(x,t)/\theta(x,t)$ denotes the average desired velocity of vehicles moving with velocity v, which is greater for fast vehicles. While $V_0(x,t)=\int dv_0 \int dv\, v_0 \rho_*(x,v,v_0,t)/\rho(x,t)$ represents the average desired velocity at place x and time t, $C'(x,t)=\int dv_0 \int dv\,(v-V)(v_0-V_0)\rho_*(x,v,v_0,t)/\rho(x,t)$ represents the covariance between the actual and desired velocities. In spite of these differences, the macroscopic equations for the density and the average velocity agree exactly with those of Prigogine. However, the equations for the velocity variance, the covariance, the average desired velocity, and so on are different.

The construction and properties of solutions to the Paveri-Fontana equation have been carefully studied (Barone, 1981; Semenzato, 1981a, 1981b). In addition, it should be noted that there are further alternatives to the specification (75) of the acceleration term. For example, Alberti and Belli (1978) assume a density-dependent driver behavior. In contrast, Nelson (1995) and others (Wegener and Klar, 1996; Klar and Wegener, 1997) have proposed an acceleration interaction leading to mathematical expressions similar to Prigogine's interaction term.

3. Construction of a micro-macro link

For the derivation of macroscopic equations from microscopic ones, one may start with the master equation (32) together with the transition rates (37), if the state j is replaced by the state vector (x,v) and the sums are replaced by integrals due to the continuity of the phase space. The spontaneous state changes are described by the transition rate

$$\begin{aligned} w(x',v'|x,v)=&\lim_{\Delta t\to 0}\frac{1}{\Delta t}\,\delta(x'-(x+v\Delta t)) \\ &\times\int d\xi\,\frac{1}{\sqrt{2\pi\tilde{D}\Delta t}}\,e^{-(\xi\Delta t/\tau)^2/(2\tilde{D}\Delta t)} \\ &\times\delta\left[v'-\left(v+\frac{v_0+\xi-v}{\tau}\Delta t\right)\right], \end{aligned} \tag{76}$$

reflecting the motion and acceleration of identical vehicles with Gaussian-distributed velocity fluctuations. Inserting this into Eq. (40) and reformulating the respective terms as a Fokker-Planck equation (see Sec. III.C.5) gives, together with $\tilde{\rho}(x,v,t)=\langle n_{(x,v)}\rangle/\Delta x$, the following kinetic equation:

$$\frac{\partial\tilde{\rho}}{dt}+\frac{\partial(\tilde{\rho}v)}{\partial x}+\frac{\partial}{\partial v}\left(\tilde{\rho}\frac{v_0-v}{\tau}\right)=\frac{1}{2}\,\frac{\partial^2(\tilde{\rho}\tilde{D})}{\partial v^2}+\left(\frac{\partial\tilde{\rho}}{\partial t}\right)_{\text{int}}. \tag{77}$$

Here the quantity $\tilde{D}$ represents a velocity diffusion coefficient, and

$$\left(\frac{\partial\tilde{\rho}}{\partial t}\right)_{\text{int}} = \int dx' \int dv' \int dy \int dw \int dy' \int dw' \times[\hat{w}_2(x,v,y,w|x',v',y',w')\tilde{\rho}_2(x',v',y',w',t) - \hat{w}_2(x',v',y',w'|x,v,y,w)\tilde{\rho}_2(x,v,y,w,t)] \tag{78}$$

is the interaction term, where we have introduced the pair-distribution function $\tilde{\rho}_2(x,v,y,w,t)=\langle n_{(x,v)}n_{(y,w)}\rangle/(\Delta x)^2$. The transition rates $\hat{w}_2(x',v',y',w'|x,v,y,w)$ are proportional to the relative velocity $|v-w|$ and proportional to the probability of transitions from the states (x,v) and (y,w) of two interacting vehicles to the states (x',v') and (y',w'). During the interactions, the car locations do not change significantly, only the velocities. Therefore we have

$$\begin{aligned}\hat{w}_2(x',v',y',w'|x,v,y,w) &= \lim_{\Delta t\to 0}\frac{1}{\Delta t}[1-\hat{p}(\rho)]|v-w| \\ &\times\delta(v'-[v+f(x,v,y,w)\Delta t])\delta(x'-x) \\ &\times\delta(w'-[w+f(y,w,x,v)\Delta t])\delta(y'-y)\end{aligned} \tag{79}$$

(Helbing, 1997a). Here the force f is specified in agreement with Eq. (16). The location and velocity of the interaction partner are represented by y and w, respectively. Quantities without and with a prime ($'$) represent the respective values before and after the interaction. To simplify the equations, we shall assume hard-core interactions corresponding to abrupt braking maneuvers, when neighboring particles approach each other and have a distance d^*, i.e., $y=(x\pm d^*)$. Moreover, let us assume the relations $(v'-w')=-\varepsilon(1-\mu)(v-w)$ and $(v'+w')=(1-\mu)v+(1+\mu)w$ corresponding to

$$\begin{aligned}v' &= \frac{1-\mu-\varepsilon(1-\mu)}{2}v+\frac{1+\mu+\varepsilon(1-\mu)}{2}w, \\ w' &= \frac{1-\mu+\varepsilon(1-\mu)}{2}v+\frac{1+\mu-\varepsilon(1-\mu)}{2}w.\end{aligned} \tag{80}$$

By variation of the single parameter μ reflecting the asymmetry of interactions, we are able to switch between vehicle interactions for $\mu=1$ (velocity adaptation) and granular interactions for $\mu=0$ (conservation of momentum, see Foerster *et al.*, 1994). In addition, the parameter ε allows us to control the degree of energy dissipation in granular interactions, where $\varepsilon(1-\mu)=1$ corresponds to the elastic case with energy conservation relevant for idealized fluids.

Prigogine's Boltzmann-like interaction term is obtained for $\mu=1$, $d^*=0$ (pointlike vehicles), and the so-called *vehicular chaos approximation* $\tilde{\rho}_2(x,v,y,w,t)\approx\tilde{\rho}(x,v,t)\tilde{\rho}(y,w,t)$, which assumes statistical independence of the vehicle velocities v and w. This is justified only in free traffic. At higher densities, we must take into account the increase in the interaction rate by a density-dependent factor $\hat{\chi}\geqslant 1$ (Chapman and Cowling, 1939; Lun *et al.*, 1984; Jenkins and Richman, 1985), since the proportion $1/\hat{\chi}\geqslant 0$ of free space is reduced by the vehicular space requirements (Helbing, 1995b, 1995d, 1996a, 1996b; Wagner *et al.*, 1996; Klar and Wegener, 1997). For simplicity, we shall assume that the overtaking probability is given by just this proportion of free space, i.e.,

$$\hat{p}=1/\hat{\chi} \tag{81}$$

(Treiber *et al.*, 1999). At high vehicle densities, the velocities of successive cars will additionally be correlated. This is particularly clear for vehicle platoons (Islam and Consul, 1991), in which the variation of vehicle velocities is considerably reduced (see Sec. II.D). There have been several suggestions for the treatment of vehicle platoons (Andrews, 1970a, 1970b, 1973a, 1973b; Beylich, 1979, 1981). One possibility, related to an approach by Lampis (1978) and others (Poethke, 1982; see Leutzbach, 1988; Hoogendoorn, 1999; Hoogendoorn and Bovy, 1999a, 1999b), is to distinguish a fraction $\hat{c}(\rho)$ of free vehicles and a fraction $[1-\hat{c}(\rho)]$ of bound (i.e., obstructed) vehicles, for which separate but coupled equations can be derived (Helbing, 1997a, 1997d). The most realistic description of vehicle platoons, however, is to set up equations for vehicle clusters of different sizes (Beylich, 1979, 1981). Unfortunately, this produces a very complex hierarchy of spatio-temporal equations, from which useful macroscopic equations have not yet been successfully derived. Instead, we may simply assume a correlation r of successive vehicle velocities, which increases from zero to positive values when the density changes from low to high; see Fig. 18(b). Taking also into account the fact that vehicle velocities are more or less Gaussian distributed (see Figs. 13 and 34; Pampel, 1955; Gerlough and Huber, 1975; May, 1990; cf. also Alvarez *et al.*, 1990), one may approximate the two-vehicle velocity distribution function by a bivariate Gaussian function,

$$\tilde{P}_2(v,w)=\frac{\sqrt{\det R}}{2\pi}e^{-R(v,w)/2} \tag{82}$$

with the quadratic form $R(v,w)=[(v-V)^2/\theta-2r(v-V)(w-V_+)/\sqrt{\theta\theta_+}+(w-V_+)^2/\theta_+]/(1-r^2)$ and its determinant $\det R=1/[\theta\theta'(1-r^2)]$ (Shvetsov and Helbing, 1999). Here, V denotes the average velocity and θ the velocity variance of vehicles at location x and time t, whereas the variables with the subscript "+" refer to the location $x_+=[x+d^*(V)]$ of the interaction point. Often one chooses the interaction distance

$$d^*(V)=\gamma\left(\frac{1}{\rho_{\max}}+TV\right), \tag{83}$$

where $\gamma\geqslant 1$ is an anticipation factor. I should mention that an exact analytical solution of the gas-kinetic equations is not available, even for the stationary case, but formula (82) seems to be a good approximation of numerical results; see Fig. 34 (Wagner, 1997a). The bi-

variate Gaussian distribution is also favorable for the evaluation of the interaction integrals, and it makes sense for $3\sqrt{\theta} \leqslant V$, so that negative velocities are negligible.

Summarizing the above considerations, a good approximation for the pair distribution function $\tilde{\rho}_2$ at high vehicle densities is given by

$$\tilde{\rho}_2(x,v,x_+,w,t) = \hat{\chi}_+ \rho(x,t)\rho(x_+,t)\tilde{P}_2(v,w;x,x_+,t), \tag{84}$$

and the resulting Enskog-like gas-kinetic traffic equation reads

$$\frac{\partial \tilde{\rho}}{\partial t} = -\frac{\partial(\tilde{\rho}v)}{\partial x} - \frac{\partial}{\partial v}\left(\tilde{\rho}\frac{V_0 - v}{\tau}\right) + \frac{\partial^2}{\partial v^2}(\tilde{\rho}\tilde{D}) + (1-\hat{p}_+)\hat{\chi}_+\rho\rho_+\left[\int_{w>v} dw(w-v)\tilde{P}_2(w,v) - \int_{w<v} dw(v-w)\tilde{P}_2(v,w)\right]. \tag{85}$$

4. The nonlocal, gas-kinetic-based traffic model

A realistic and consistent macroscopic traffic model is obtained by multiplying Eq. (77) with v^k $(k \in \{0,1,2\})$ and subsequent integration over v. The corresponding calculations are more or less straightforward, but very cumbersome, so the results took some time to achieve (Helbing, 1995d, 1996a, 1996b, 1997a, 1998a; Helbing and Treiber, 1998a; Shvetsov and Helbing, 1999). They can be cast into the general form of the continuity equation (62) and the velocity equation (63), but instead of V_e we have a nonlocal expression,

$$V^e = V_0 - \underbrace{\tau[1-\hat{p}(\rho_+)]\hat{\chi}(\rho_+)\rho_+ B(\Delta V, \theta_\Delta)}_{\text{Braking interaction term}}. \tag{86}$$

This nonlocality has some effects that other macroscopic models produce by their pressure and viscosity (or diffusion) terms. Related to this is the higher numerical efficiency of the nonlocal gas-kinetic-based traffic model used in the simulation package MASTER (Helbing and Treiber, 1999). The dependence of the braking interaction on the effective dimensionless velocity difference $\Delta V = (V - V_+)/\sqrt{\theta_\Delta}$ between the actual position x and the interaction point x_+ takes into account effects of the velocity variances θ, θ_+ and the correlation r among successive cars [see Fig. 18(b)]: $\theta_\Delta = (\theta - 2r\sqrt{\theta\theta_+} + \theta_+)$. The Boltzmann factor

$$B(\Delta V, \theta_\Delta) = \theta_\Delta\{\Delta V \Phi(\Delta V) + [1+(\Delta V)^2]E(\Delta V)\} \tag{87}$$

in the braking term is monotonically increasing with ΔV and contains the normal distribution $\Phi(z) = e^{-z^2/2}/\sqrt{2\pi}$ and the Gaussian error function $E(z) = \int_{-\infty}^{z} dz' \Phi(z')$.

To close the system of equations, we specify the velocity correlation r as a function of the density according to empirical observations [see Fig. 18(b)]. Moreover, for a description of the presently known properties of traffic flows it seems sufficient to describe the variance by the equilibrium relation $\theta = \tilde{D}\tau$ of the dynamical variance equation (Helbing, 1996b, 1997a), which also determines the traffic pressure via $P = \rho\theta$ or, more exactly, Eq. (119). Empirical data (Helbing, 1996b, 1997a, 1997c; Treiber *et al.*, 1999) suggest that the variance is a density-dependent fraction $A(\rho)$ of the squared average velocity:

$$\theta = A(\rho)V^2. \tag{88}$$

This guarantees that the velocity variance will vanish if the average velocity goes to zero, as required, but it will be finite otherwise. The variance prefactor A is higher in congested traffic than in free traffic (see Fig. 17).

Finally, the average time clearance of vehicles should correspond to the safe time clearance T, if the vehicle density is high. Hence, in dense and homogeneous traffic situations with $V_+ = V$ and $\theta_+ = \theta$, we should have $V = (1/\rho - 1/\rho_{\max})/T$. This is to be identified with the equilibrium velocity

$$V_e(\rho) = \frac{\tilde{V}^2}{2V_0}\left(-1 + \sqrt{1 + \frac{4V_0^2}{\tilde{V}^2}}\right), \tag{89}$$

where $\tilde{V}^2 = V_0/[\tau\rho A(\rho)(1-\hat{p})\hat{\chi}]$. For the effective cross section, therefore, we obtain

$$[1-\hat{p}(\rho)]\hat{\chi}(\rho) = \frac{V_0\rho T^2}{\tau A(\rho_{\max})(1-\rho/\rho_{\max})^2}, \tag{90}$$

which also makes sense in the low-density limit $\rho \to 0$, since it implies $\hat{\chi} \to 1$ and $\hat{p} \to 1$.

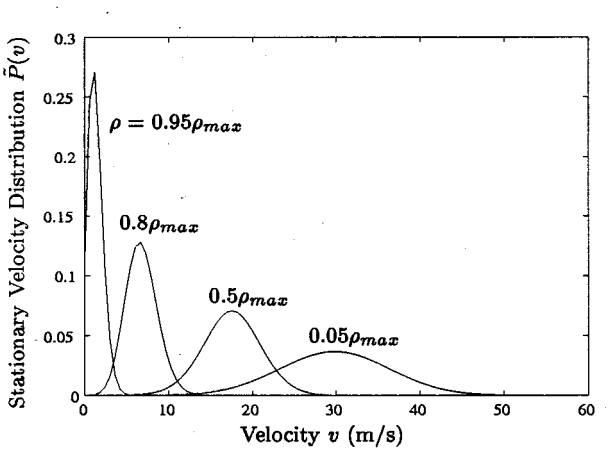

FIG. 34. Stationary velocity distributions at different vehicle densities obtained by numerical solution of a gas-kinetic traffic model. After Wagner, 1997a.

5. Navier-Stokes-like traffic equations

The above derivation of macroscopic traffic equations was carried out up to Euler order only, based on the

(zeroth-order) approximation of local equilibrium. This assumes that the form $\tilde{\rho}_0(x,v,t)$ of the phase-space density in equilibrium remains unchanged in dynamic situations, but it is given by the local values of the density $\rho(x,t)$ and possibly other macroscopic variables; see, for example, Eq. (93). For fluids and granular media, however, it is known that the phase-space density also depends on their gradients, which is a consequence of the finite adaptation time T_0 needed to reach local equilibrium (Huang, 1987). The related correction terms lead to Navier-Stokes equations, which have also been derived for gas-kinetic traffic models (Helbing, 1996b, 1998c; Wagner, 1997b; Klar and Wegener, 1999a, 1999b). For ordinary gases, the Navier-Stokes terms (transport terms) are calculated from the kinetic equation by means of the Chapman-Enskog method (Enskog, 1917; Chapman and Cowling, 1939; Liboff, 1990). Here I shall sketch the more intuitive relaxation-time approximation (Huang, 1987; for details see Helbing and Treiber, 1998c). This assumes that

(i) the deviation $\delta\tilde{\rho}(x,v,t)=[\tilde{\rho}(x,v,t)-\tilde{\rho}_0(x,v,t)]$ is small compared to $\tilde{\rho}_0(x,v,t)$, so that

$$\frac{d_v\tilde{\rho}}{dt}+\frac{\partial}{\partial v}\left(\tilde{\rho}\frac{v_0-v}{\tau}\right)-\frac{1}{2}\frac{\partial^2(\tilde{\rho}\tilde{D})}{\partial v^2}-\left(\frac{\partial\tilde{\rho}}{\partial t}\right)_{\rm int}$$
$$\approx\frac{d_v\tilde{\rho}_0}{dt}+\frac{\partial}{\partial v}\left(\tilde{\rho}_0\frac{v_0-v}{\tau}\right)-\frac{\theta}{2\tau}\frac{\partial^2\tilde{\rho}_0}{\partial v^2}$$
$$-\left(\frac{\partial\tilde{\rho}_0}{\partial t}\right)_{\rm int}-\mathcal{L}(\delta\tilde{\rho}) \qquad (91)$$

with $d_v/dt\equiv\partial/\partial t+v\,\partial/\partial x=\partial/\partial t+V_e\partial/\partial x+\delta v\,\partial/\partial x$ and $\delta v(x,t)=[v-V_e(x,t)]$,

(ii) the effect of the linear interaction operator $\mathcal{L}$ can be characterized by its slowest eigenvalue $-1/T_0<0$ (which depends on the density and velocity variance):

$$\mathcal{L}(\delta\tilde{\rho})\approx-\frac{\delta\tilde{\rho}(x,v,t)}{T_0}. \qquad (92)$$

In order to reach a time-scale separation, the equilibrium distribution is usually expressed in terms of the macroscopic variables with the slowest dynamics related to the conserved quantities. In fluids, these are the particle number, momentum, and kinetic energy, while in traffic, this is the particle number only. Between the dynamics of the velocity moments $\langle v^k\rangle$ and $\langle v^{k+1}\rangle$ with $k\geqslant 1$, there is no clear separation of time scales. Therefore one should express the equilibrium phase-space density as a function of the vehicle density $\rho(x,t)$ only:

$$\tilde{\rho}_0(x,v,t)=\frac{\rho}{[2\pi\theta_e(\rho)]^{1/2}}\exp\left\{-\frac{[v-V_e(\rho)]^2}{2\theta_e(\rho)}\right\}, \qquad (93)$$

where $\theta_e(\rho)=A(\rho)[V_e(\rho)]^2$. The same is done with the pair distribution function $\tilde{P}_2(v,w)$. This allows us to determine

$$\frac{d_v\tilde{\rho}_0}{dt}=\frac{d\tilde{\rho}_0}{d\rho}\frac{d_v\rho}{dt}=\frac{d\tilde{\rho}_0}{d\rho}\left(\frac{\partial\rho}{\partial t}+V_e\frac{\partial\rho}{\partial x}+\delta v\frac{\partial\rho}{\partial x}\right). \qquad (94)$$

The relation $d\tilde{\rho}_0/d\rho$ can be simply obtained by differentiation of $\tilde{\rho}_0$, whereas $\partial\rho/\partial t+V_e\partial\rho/\partial x=-\rho\partial V_e/\partial x$ follows from the continuity equation (45) in the Euler approximation. Inserting Eqs. (92)–(94) into Eq. (91) finally yields

$$\delta\tilde{\rho}(x,v,t)=-T_0\Bigg\{\tilde{\rho}_0\Bigg[\frac{1}{\rho}+\frac{\delta v}{\theta_e}\frac{dV_e}{d\rho}+\frac{1}{2\theta_e}\left(\frac{\delta v^2}{\theta}-1\right)\frac{d\theta_e}{d\rho}\Bigg]\left(-\rho\frac{\partial V_e}{\partial x}+\delta v\frac{\partial\rho}{\partial x}\right)$$
$$+\frac{\tilde{\rho}_0}{\tau}\left(-\frac{v_0-V_e}{\theta_e}\delta v+\frac{\delta v^2}{\theta_e}-1\right)$$
$$-\frac{\tilde{\rho}_0}{2\tau}\left(\frac{\delta v^2}{\theta_e}-1\right)-\left(\frac{\partial\tilde{\rho}_0}{dt}\right)_{\rm int}\Bigg\}.$$

Integrating this over v gives exactly zero, i.e., there are no corrections to the vehicle density. However, multiplying this by δv and afterwards integrating over δv yields corrections $\delta V(x,t)=[V(x,t)-V_e(\rho(x,t))]$ to the equilibrium velocity according to

$$\rho\,\delta V=-T_0\rho\Bigg[\frac{\theta_e}{\rho}\frac{\partial\rho}{\partial x}+\frac{d\theta_e}{d\rho}\frac{\partial\rho}{\partial x}-\frac{dV_e}{d\rho}\rho\frac{\partial V_e}{\partial x}+\frac{V_e-v_0}{\tau}$$
$$+(1-p_+)\chi_+\rho_+B\Bigg]$$
$$=T_0\left[-\frac{\partial(\rho\theta_e)}{\partial x}+\left(\rho\frac{dV_e}{d\rho}\right)^2\frac{\partial\rho}{\partial x}+\frac{\rho}{\tau}(V^e-V_e)\right], \qquad (95)$$

where B is again the Boltzmann factor (87). Interestingly enough, this Navier-Stokes correction contains all terms and therefore captures all effects of the dynamic velocity equation (63) in the Euler approximation, which makes the success of the Euler-like gas-kinetic-based traffic model understandable. Considering $V_+=V_e(\rho_+)=V_e(\rho(x+d,t))\approx[V_e(\rho(x,t))+d(dV_e/d\rho)\partial\rho/\partial x]$ and $\theta_+\approx[\theta_e(\rho(x,t))+d(d\theta_e/d\rho)\partial\rho/\partial x]$, we can carry out the linear Taylor approximation

$$\frac{\rho}{\tau}(V^e-V_e)\approx\frac{\rho d}{\tau}\left(\frac{\partial V^e}{\partial\rho_+}+\frac{\partial V^e}{\partial V_+}\frac{dV_e}{d\rho}+\frac{\partial V^e}{\partial\theta_+}\frac{d\theta_e}{d\rho}\right)\frac{\partial\rho}{\partial x}$$
$$=\left(\frac{\partial(\rho\theta_e)}{\partial\rho}-\frac{\partial P_{\rm eff}}{\partial\rho}\right)\frac{\partial\rho}{\partial x} \qquad (96)$$

for the purpose of linear stability analysis. This defines the effective traffic pressure $P_{\rm eff}$ which, apart from the kinematic dispersion effect $\rho\theta$, contains additional terms arising from vehicle interactions, as in Payne's model and in Sec. III.E.6. It can be shown that, in contrast to $d(\rho\theta_e)/d\rho$, $dP_{\rm eff}/d\rho$ is non-negative for reasonably chosen parameter values and thereby resolves the problem of vehicle acceleration into congested areas (see Helbing, 1996b, 1997a; Helbing and Greiner, 1997). Inserting Eqs. (95) and (96) into the continuity equation (45) results in an equation of type (53) with the diffusion function

$$D(\rho)=T_0\left[\frac{dP_{\rm eff}}{d\rho}-\left(\rho\frac{dV_e}{d\rho}\right)^2\right]. \quad (97)$$

This diffusion function in the Navier-Stokes-like traffic model without a dynamic velocity equation becomes negative exactly when the Euler-like traffic model *with* a dynamic velocity equation becomes linearly unstable. Unfortunately, the resulting equation is even more difficult to solve numerically than the Lighthill-Whitham model. This problem can, however, be resolved by taking into account higher-order terms suppressing high-frequency oscillations.

6. Simultaneous microsimulation and macrosimulation

We shall now discuss a way of obtaining macroscopic from microscopic traffic models that is different from the gas-kinetic approach (see Hennecke *et al.*, 2000; Helbing *et al.*, 2001b). For this, we define an average velocity by, for example, linear interpolation between the velocities of neighboring vehicles:

$$V(x,t)=\frac{v_\alpha(t)[x_{\alpha-1}(t)-x]+v_{\alpha-1}(t)[x-x_\alpha(t)]}{x_{\alpha-1}(t)-x_\alpha(t)} \quad (98)$$

where $(x_{\alpha-1}\geqslant x\geqslant x_\alpha)$. While the derivative with respect to x gives us $\partial V/\partial x=[v_{\alpha-1}(t)-v_\alpha(t)]/[x_{\alpha-1}(t)-x_\alpha(t)]$, the derivative with respect to t gives us the exact equation

$$\left(\frac{\partial}{\partial t}+V\frac{\partial}{\partial x}\right)V=A(x,t), \quad (99)$$

where

$$A(x,t)=\frac{a'_\alpha(t)[x_{\alpha-1}(t)-x]+a'_{\alpha-1}(t)[x-x_\alpha(t)]}{x_{\alpha-1}(t)-x_\alpha(t)} \quad (100)$$

is the linear interpolation of the vehicle accelerations $a'_\alpha=dv_\alpha/dt$ characterizing the microscopic model. For most car-following models, the acceleration function can be written in the form $a'_\alpha=a'(s_\alpha,v_\alpha,\Delta v_\alpha)$, where $s_\alpha=(x_{\alpha-1}-x_\alpha-l_{\alpha-1})$ is the netto distance to the vehicle in front and $\Delta v_\alpha=(v_\alpha-v_{\alpha-1})$ the approaching rate. In order to obtain a macroscopic system of partial differential equations for the average velocity and density, the arguments v_α, Δv_α, and s_α of the vehicle acceleration have to be expressed in terms of macroscopic fields, in particular the local vehicle density $\rho(x,t)$ defined by

$$\frac{1}{\rho(x,t)}=\frac{1}{\rho_{\max}}+\frac{s_\alpha(t)[x_{\alpha-1}(t)-x]+s_{\alpha-1}(t)[x-x_\alpha(t)]}{x_{\alpha-1}(t)-x_\alpha(t)}. \quad (101)$$

Specifically, we make the following approximations: $A(x,t)\approx a'(S(x,t),V(x,t),\Delta V(x,t))$, with $S(x,t)=1/2[\rho^{-1}(x,t)+\rho_+^{-1}(x,t)]-\rho_{\max}^{-1}$, $\Delta V(x,t)=[V(x,t)-V_+(x,t)]$, and the nonlocality given by $g_+(x,t)=g(x+1/\rho(x,t),t)$ with $g\in\{\rho,V\}$. In this way, we obtain a nonlocal macroscopic velocity equation, which supplements the continuity equation (45) for the vehicle density and defines, for a given microscopic traffic model, a complementary macroscopic model. Note that it does not contain a pressure term $(1/\rho)\partial P/\partial x$ with $P=\rho\theta$, in contrast to the gas-kinetic-based traffic model described above, since we have assumed identical vehicles and a deterministic dynamics corresponding to $\theta=0$. For heterogeneous traffic, we expect the additional term $-(1/\rho)\partial(\rho\theta_e)/\partial x$, where $\theta_e(\rho)$ reflects the resulting, density-dependent velocity variance of the vehicles. For the intelligent driver model (see Sec. III.A.3), the above procedure leads to a remarkable agreement, at least for identical vehicles. It is even possible to carry out simultaneous microsimulations and macrosimulations of neighboring freeway sections without any significant changes in the density and velocity profiles or their propagation speed. This has been shown for downstream propagating perturbations, for traffic jams propagating upstream, and for complex spatio-temporal traffic patterns (Hennecke *et al.*, 2000; Helbing *et al.*, 2001b).

7. Mesoscopic traffic models

For the sake of completeness, I also mention some "mesoscopic" traffic models, which describe the microscopic vehicle dynamics as a function of macroscopic fields. Examples are the model by Wiedemann and Schwerdtfeger (1987) applied in the simulation tool DYNEMO (Schwerdtfeger, 1987) and the model of Kates *et al.* (1998) used in the simulation tool ANIMAL.

IV. PROPERTIES OF TRAFFIC MODELS

In order to see which model ingredients are required to reproduce certain observations, we shall start with simple one-lane models for identical vehicles and add more and more aspects throughout the next sections.

A. Identical vehicles on homogeneous freeways

1. "Phantom traffic jams" and stop-and-go traffic

For a long time, traffic research has aimed at reproducing the fundamental diagram and the kind of phantom traffic jams observed by Treiterer and others (see Sec. II.E.1). In the past, the fundamental diagram was normally fitted by calibration of the parameters in the equilibrium flow-density relation of the model under consideration. This procedure, however, makes sense only in the density regime(s) of stable traffic, as we shall see that unstable traffic does not just oscillate around the fundamental diagram.

Most traffic models have the following mechanism of traffic instability in common:

(i) *Overreaction* of drivers, which is either reflected by a positive slowdown probability p or a delayed reaction (relaxation time τ or reaction time Δt).

(ii) *Chain reaction* of followers: Before a decelerated vehicle manages to return to its previous speed,

the next car approaches and has to brake as well (Nagel and Paczuski, 1995). Overreacting followers are getting slower and slower, until traffic comes to a standstill, although everyone likes to drive fast.

The instability condition for the cellular automaton model of Nagel and Schreckenberg with small slowdown probability $p \approx 0$ follows directly from (ii). Starting with equally distributed vehicles on a circular road, a vehicle reaches the leader in one time step Δt, if the average clearance $(L-N\Delta x)/N=(L/N-\Delta x)$ becomes smaller than the average distance moved with the free velocity $(\hat{v}_{\max}-p)\Delta x/\Delta t$. Hence the average vehicle density $\varrho = N/L$ above which jams are formed is $\varrho \approx 1/[(\hat{v}_{\max}+1)\Delta x]$ (Nagel and Herrmann, 1993; Eisenblätter *et al.*, 1998; Lübeck *et al.*, 1998). A formula for finite slowdown probabilities $p>0$, which takes into account that fluctuations may add up and initiate jam formation, has recently been derived by Gerwinski and Krug (1999). They calculated the resolution speed $C_0(p) = \hat{C}_0(p)\Delta x/\Delta t$ of the downstream front of a "megajam" and obtained

$$\varrho = \frac{\hat{C}_0(p)}{[\hat{v}_{\max}-p+\hat{C}_0(p)]\Delta x} \tag{102}$$

with $\hat{C}_0(p) \leqslant (1-p)$.

For most traffic models, however, the instability of traffic flow is investigated by means of a linear stability analysis. This will be sketched below.

For microscopic models of the form

$$\frac{dv_\alpha(t+\Delta t)}{dt} = \frac{v^e(s_\alpha(t), v_\alpha(t), \Delta v_\alpha(t)) - v_\alpha(t)}{\tau},$$

often with the simple specification $v^e(s,v,\Delta v)=v_e(s)$, we start our analysis by assuming a circular road of length L with homogeneous traffic flow of density ϱ. Homogeneity implies that all $N=\varrho L$ vehicles α are separated by identical distances $d=(s+l)=1/\varrho$, and the relative velocity Δv_α is zero. Hence the situation is similar to a lattice of coupled particles in solid-state physics, with the difference that

(i) the particles move with identical velocity $v = v_e(s)$ along the trajectories $x_0(0)-\alpha(s+l)+vt = x_0(0)-\alpha d+vt$,
(ii) the interactions are repulsive and anisotropic, and
(iii) there is a driving force counteracting the repulsion.

The dynamics of this spatially homogeneous equilibrium state in the presence of disturbances is therefore not obvious, but as usual we can carry out a stability analysis of the linearized model equations:

$$\frac{d\delta v_\alpha(t)}{dt} + \Delta t \frac{d^2\delta v_\alpha(t)}{dt^2} = \frac{1}{\tau}\left\{ \frac{\partial v^e}{\partial s}[\delta x_{\alpha-1}(t) - \delta x_\alpha(t)] + \frac{\partial v^e}{\partial v}\delta v_\alpha(t) + \frac{\partial v^e}{\partial \Delta v}[\delta v_\alpha(t) - \delta v_{\alpha-1}(t)] - \delta v_\alpha(t) \right\}.$$

Due to linearization, this equation is valid only for small disturbances $\delta v_\alpha(t) = d\delta x_\alpha(t)/dt = [v_\alpha(t)-v] \ll v$ and $\delta x_\alpha(t) = x_\alpha(t) - [x_0(0)-\alpha d+vt] \ll d$. Its general solution has the form of a Fourier series:

$$\delta x_\alpha(t) = \frac{1}{N}\sum_{k=0}^{N-1} c_k \exp\left(2\pi i \frac{\alpha k}{N} + (\lambda_k - i\omega_k)t \right),$$

where c_k are the amplitudes of oscillations with wavelength L/k, frequency ω_k, and exponential growth parameter λ_k ($k \in \{1,2,\ldots,N\}$). Inserting this into the linearized model equations gives consistency relations for $(\lambda_k - i\omega_k)$, which have the form of characteristic polynomials. These determine the possible eigenvalues $(\lambda_k - i\omega_k)$. The homogeneous solution is stable with respect to small perturbations only if $\lambda_k < 0$ for all $k \in \{1,2,\ldots,N\}$. Otherwise it is potentially unstable with respect to fluctuations $\xi_\alpha(t)$. Specific analyses for different car-following models yield the instability conditions presented in Sec. III.A. For details see Herman *et al.* (1959) or Bando, Hasebe, Nakayama, *et al.* (1995). Typically one finds that traffic becomes unstable if the reaction time Δt or the relaxation time τ exceed a certain critical value.

For macroscopic traffic models, we proceed similarly. Let us assume spatially homogeneous traffic of average density ϱ and velocity $V_e(\varrho)$, which is slightly disturbed according to $\delta\rho(x,t) = [\rho(x,t)-\varrho] \ll \varrho$ and $\delta V(x,t) = [V(x,t) - V_e(\varrho)] \ll V_e(\varrho)$. The linearized density equation (62) reads, apart from fluctuations,

$$\frac{\partial \delta\rho}{\partial t} + V_e(\varrho)\frac{\partial \delta\rho}{\partial x} = -\varrho\frac{\partial \delta V}{\partial x} + D(\varrho)\frac{\partial^2 \delta\rho}{\partial x^2}, \tag{103}$$

while the linearized velocity equation (63) is

$$\frac{\partial \delta V}{\partial t} + V_e(\varrho)\frac{\partial \delta V}{\partial x} = -\frac{1}{\varrho}\frac{dP(\varrho)}{d\rho}\frac{\partial \delta\rho}{\partial x} + \nu(\varrho)\frac{\partial^2 \delta V}{\partial x^2} + \frac{1}{\tau(\varrho)}\left[\frac{dV_e(\varrho)}{d\rho}\delta\rho(x,t) - \delta V(x,t) \right]. \tag{104}$$

The general solution of Eq. (104) is given by Fourier series of $\delta\rho(x,t)$ and $\delta V(x,t)$:

$$\delta\rho(x,t) = \sum_l \int dk \rho_k^l \exp\{ikx + [\lambda_k^l(\varrho) - i\omega_k^l(\varrho)]t\},$$

$$\delta V(x,t) = \sum_l \int dk V_k^l \exp\{ikx + [\lambda_k^l(\varrho) - i\omega_k^l(\varrho)]t\},$$

where ρ_k^l and V_k^l are amplitudes. The possible values of $(\lambda_k^l - i\omega_k^l)$ are given by the eigenvalues $\tilde{\lambda}_k^l = [\lambda_k^l - i(\omega_k^l - kV_e(\varrho))]$ of the matrix

$$\begin{pmatrix} -D(\varrho)k^2 - \tilde{\lambda}_k^l & -ik\varrho \\ -\frac{ik}{\varrho}\frac{dP(\varrho)}{d\rho} + \frac{1}{\tau(\varrho)}\frac{dV_e}{d\rho} & -\nu(\varrho)k^2 - \frac{1}{\tau(\varrho)} - \tilde{\lambda}_k^l \end{pmatrix}.$$

Stability requires the real values $\lambda_k^l(\varrho)$ of the solutions of the corresponding characteristic polynomial to be negative for all wave numbers k. This leads to the stability condition

$$\varrho\sqrt{\tau(\varrho)}\left|\frac{dV_e(\varrho)}{d\rho}\right| \leqslant \left[\tau(\varrho)\frac{dP(\varrho)}{d\rho} + D(\varrho)\right]^{1/2}, \quad (105)$$

where equality yields the critical densities ρ_{c2} and ρ_{c3} determining the range of linear instability. For details see Kühne and Rödiger (1991) and Helbing (1997a). As a consequence, traffic flow in the Lighthill-Whitham model with $D(\varrho)=0$ and $\tau\to 0$ is marginally stable, while Eq. (53) and the related Burgers equation (54) are always stable, if $D(\varrho)>0$. Payne's model with $D(\varrho)=0$ and $dP(\varrho)/d\rho = |dV_e(\varrho)/d\rho|/(2\tau)$ becomes unstable on the condition $\varrho|dV_e(\varrho)/d\rho| > 1/(2\varrho\tau)$. This agrees with the instability condition (24) of the optimal velocity model, if we consider that $dv_e'/dd = (dV_e/d\rho)/(dd/d\rho) = -\rho^2(dV_e/d\rho)$. According to this, stability can be improved by decreasing the relaxation time τ (i.e., by higher acceleration). The instability condition for the models of Kühne, Kerner, and Konhäuser with $D(\varrho)=0$ and $dP(\varrho)/d\rho = \theta_0$ is $\varrho|dV_e(\varrho)/d\rho| > \sqrt{\theta_0}$, if the road is long (Kühne and Rödiger, 1991; Kerner and Konhäuser, 1993). Hence traffic flow becomes unstable if the velocity-density relation $V_e(\rho)$ falls too rapidly with increasing density, so that drivers cannot compensate for changes in the traffic situation sufficiently fast.

2. (Auto)Solitons, the Korteweg–de Vries equation, and the Ginzburg-Landau equation

Instead of using the original equations, in nonlinear science it is common to investigate spatio-temporal patterns appearing in the vicinity of an instability threshold by means of approximate model equations based on series expansions (Cross and Hohenberg, 1993; Haken, 1977). In this way, the original equations can sometimes be replaced by the Korteweg–de Vries equation

$$\frac{\partial\tilde{V}}{\partial\tilde{t}} + (1+\tilde{V})\frac{\partial\tilde{V}}{\partial\tilde{x}} + \tilde{\nu}\frac{\partial^3\tilde{V}}{\partial\tilde{x}^3} = 0, \quad (106)$$

where the tilde ($\tilde{}$) indicates a scaling of the variables, or by the Ginzburg-Landau equation (Cross and Hohenberg, 1993). Kühne (1984b) was the first to apply this approach to the study of traffic dynamics (see also Sick, 1989). Moreover, Kurtze and Hong (1995) were able to derive a perturbed (modified) Korteweg–de Vries equation and solitonlike solutions from the Kerner-Konhäuser model for densities immediately above the critical density ρ_{cr}. A similar result was obtained by Komatsu and Sasa (1995) for the microscopic optimal velocity model (see also Whitham, 1990; Igarashi *et al.*, 1999).

A valid derivation of such model equations requires that the solutions of the original equations in the vicinity of the instability threshold be of small amplitude and stable, otherwise the approximate equations can be completely misleading (Cross and Hohenberg, 1993). Therefore the application of approximate model equations to traffic is restricted to the practically irrelevant case with $\rho_{c1} \approx \rho_{c2} \approx \rho_{c3} \approx \rho_{c4}$, where instability barely exists. In the optimal velocity model, this condition would be fulfilled, if the inverse density and relaxation time were close to the critical point $(d_{cr}, 1/\tau_{cr}) = (d_c, 2dv_e'(d_c)/d\,d)$, where d_c is the turning point of the velocity-distance relation (22) with $d^2v_e'(d_c)/d\,d^2 = 0$. For that case, Nagatani (1998b, 1998c; see also Muramatsu and Nagatani, 1999) derived the time-dependent Ginzburg-Landau equation

$$\frac{\partial S'}{\partial t} = -\left(\frac{\partial}{\partial x'} - \frac{1}{2}\frac{\partial^2}{\partial x'^2}\right)\frac{\delta\Phi'(S')}{\delta S'}, \quad (107)$$

with $x' = \alpha + 2t\tau[dv_e'(d_c)/d\,d]^2$, $S' = (d - d_c)$,

$$\Phi'(S') = \int dx'\left[\frac{1}{48}\frac{dv_e'(d_c)}{d\,d}\left(\frac{\partial S'}{\partial x'}\right)^2 + \phi'(S')\right],$$

and the thermodynamic potential

$$\phi'(S') = -\frac{dv_e'(d_c)}{d\,d}\left(\tau\frac{dv_e'(d_c)}{d\,d} - \frac{1}{2}\right)S'^2 + \frac{1}{24}\left|\frac{d^3v_e'(d_c)}{d\,d^3}\right|S'^4.$$

Moreover, Nagatani (1998b, 1998c) calculated the uniform and kink solutions, the coexistence curve defined by $\partial\phi'/\partial S' = 0$, and the spinodal line given by $\partial^2\phi'/\partial S'^2 = 0$ (see also Komatsu and Sasa, 1995). In his formalism, the inverse relaxation time $1/\tau$ plays the role of the temperature in a conventional phase transition, and the headways d corresponds to the order parameter. See also the study by Reiss *et al.* (1986) for an earlier application of thermodynamic ideas to traffic.

Approximate equations for nonlinear solutions at large amplitudes have been developed by Kerner *et al.* (1997), based on the theory of *autosolitons* (Kerner and Osipov, 1994). Moreover, the features of wide moving jams have been compared with autosolitons in physical systems (Kerner, 1995). They are reminiscent of properties found in some reaction-diffusion systems (Mikhailov, 1991a, 1991b; Meron, 1992; Kapral and Showalter, 1995; Woesler *et al.*, 1996).

3. Jam formation: Local breakdown and cluster effects, segregation, and self-organized criticality

Wave formation in traffic has some particular features. It turns out that the traffic equations are so highly nonlinear that a linear approximation is only of very limited

use. For example, the wave number k^* associated with the largest growth rate $\lambda^l_{k^*}(\varrho)$ at a given average density ϱ does not at all determine the finally resulting wavelength via $2\pi/k^*$. Moreover, the forming waves are typically not periodic. Even when starting with a small sinusoidal perturbation, the wave amplitude will not just grow linearly. Instead, the extended perturbation will drastically change its shape until it eventually becomes localized. Kerner and Konhäuser (1994) call this the *local breakdown effect*. The resulting perturbation has a characteristic form that can be approximated by the function

$$\rho(x,t_0)=\varrho+\Delta\rho\left[\cosh^{-2}\left(\frac{x-x_0}{w_+}\right)-\frac{w_+}{w_-}\cosh^{-2}\left(\frac{x-x_0-(w_++w_-)}{w_-}\right)\right], \quad (108)$$

with suitable parameters t_0, x_0, w_+, and w_- determining its location and width; see Fig. 35(a). When this shape has been reached, the perturbation grows more and more, playing the role of a nucleus for jam formation (Kerner and Konhäuser, 1994). While small-amplitude perturbations flow with the traffic, the propagation speed becomes slower with increasing perturbation amplitude and eventually becomes negative. The final result is a wide traffic jam of characteristic form, which propagates upstream. This is because vehicles are leaving the standing jam at the front, while new ones are joining the traffic jam at its end. The traffic jam is localized, which is known as the *local cluster effect* (Kerner and Konhäuser, 1994; Herrmann and Kerner, 1998). Moreover, it is normally surrounded by free traffic flow. Hence one could say that there is a *phase separation (segregation)* between free and congested traffic (Kerner and Konhäuser, 1994; Kerner and Rehborn, 1996a). The result of this noise-induced ordering process (Helbing and Platkowski, 2000) is similar to an equilibrium between two different phases (a freely moving, "gaseous" state and a jammed, "condensed" state). In other words, traffic jams absorb as many cars as necessary to have free traffic in the rest of the system. The resulting state of the system is not a partial congestion with all vehicles moving slowly, as the velocity-density relation $V_e(\rho)$ would suggest.

After a traffic jam has developed a stationary shape, it moves with constant velocity $C<0$ upstream along the road. Therefore we have the relations $\rho(x,t)=\rho(x-Ct,0)$ and $Q(x,t)=Q(x-Ct,0)$. Inserting this into the continuity equation (45) gives $-C\partial\rho(x_*,0)/\partial x_*+\partial Q(x_*,0)/\partial x_*=0$ with $x_*=(x-Ct)$, which is solved by

$$Q(x_*,0)=Q_0+C\rho(x_*,0)=J(\rho(x_*,0)) \quad (109)$$

with a suitable constant Q_0 (Kerner and Konhäuser, 1994). Hence the flow-density relation of a fully developed traffic jam is a linear curve with negative slope $C<0$, the so-called *jam line* $J(\rho)$. While first-order macroscopic traffic models like the Lighthill-Whitham model have to assume this linear relation for congested traffic, in second-order models with a dynamic velocity equation the linear jam line is normally the result of self-organization and often differs significantly from the fundamental diagram $Q_e(\rho)$ (Kerner and Konhäuser, 1994; Kerner and Rehborn, 1996a). Therefore the fundamental diagram should be fitted only in the range of stable traffic flow, while congested traffic flow does not necessarily relate to the fundamental diagram.

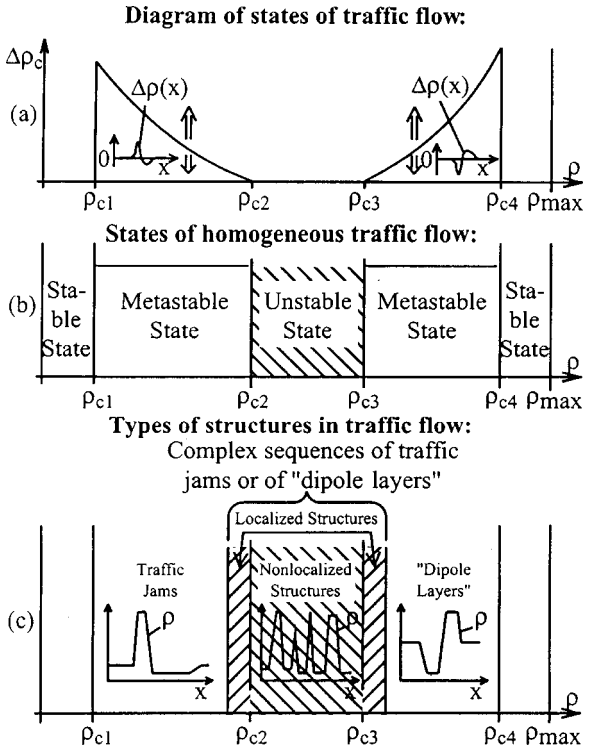

FIG. 35. States and structures in traffic flow: (a) The chosen localized perturbation and the density-dependent perturbation amplitudes $\Delta\rho_c$ required for jam formation in the metastable density regime. (b) Instability diagram of homogeneous (and slightly inhomogeneous) traffic flow. (c) Finally resulting traffic patterns as a function of density regime. Simplified diagram after Kerner *et al.*, 1995a, 1996; see also Kerner and Konhäuser, 1994.

Finally, note that the above-described mechanism of jam formation and the existence of the jam line $J(\rho)$ seems to apply to all models with a deterministic instability mechanism, i.e., to models with a linearly unstable density regime (Bando, Hasebe, Nakanishi, *et al.*, 1995; Herrmann and Kerner, 1998; Helbing and Schreckenberg, 1999; Treiber *et al.*, 1999, 2000). Many cellular automaton traffic models and other probabilistic models have a different mechanism of jamming, but show a tendency for phase segregation between free and congested traffic as well (Nagel, 1994, 1996; see also Schreckenberg *et al.*, 1995; Chowdhury, Ghosh, *et al.*, 1997; Lübeck *et al.*, 1998; Roters *et al.*, 1999). In a strict sense, phase segregation is found in slow-to-start models, while it is restricted in the Nagel-Schreckenberg model. Interestingly enough, the "cruise control" variant of the latter and a few other cellular automaton models display power-law behavior in the density variations (Choi and Lee, 1995; Csányi and Kertész, 1995; Nagatani, 1995b,

1998a; Yukawa and Kikuchi, 1995; Zhang and Hu, 1995). Therefore Nagel and Herrmann (1993) as well as Nagel and Paczuski (1995) have interpreted jam formation as a self-organized critical phenomenon (Bak *et al.*, 1987), which is related to fractal self-similarity (Nagel and Rasmussen, 1994).

4. Instability diagram, stop-and-go waves, metastability, and hysteresis

Phase diagrams are a very powerful method for characterizing the parameter dependence of the possible states of a system. They are of great importance in thermodynamics, with various applications in metallurgy, chemistry, etc. Moreover, they allow us to compare very different kinds of systems like equilibrium and nonequilibrium ones, or microscopic and macroscopic ones, whose equivalence cannot simply be shown by transformation to normal forms (Kuramoto, 1989; Manneville, 1990; Eckmann *et al.*, 1993). Defining universality classes by mathematically equivalent phase diagrams, one can even compare systems as different as physical, chemical, biological, and social ones, which is done in *general systems theory* (Buckley, 1967; von Bertalanffy, 1968; Rapoport, 1986).

The phase diagram for the different traffic states on a homogeneous, circular one-lane road as a function of the density ϱ is usually called the *instability diagram*. Most traffic models predict a stable traffic flow at small vehicle densities and unstable traffic flow above a certain critical density $\rho_{\rm cr}$. At very high densities, many models with a deterministic instability mechanism become stable again, corresponding to creeping traffic, while the Nagel-Schreckenberg model and other cellular automaton models predict unstable traffic. Based on the calculation of limiting cases, a more detailed picture has been suggested by Kühne (1991a). He distinguishes supercritical and subcritical regimes, solitary waves, and shock fronts with either increasing or decreasing densities in the downstream direction.

Simplifying matters a little, based on a numerical analysis of their macroscopic traffic model, Kerner and Konhäuser found the following picture (see Fig. 35): Below some density $\rho_{\rm c1}$, any kind of disturbance eventually disappears. Between the densities $\rho_{\rm c1}$ and $\rho_{\rm c2}$, one wide traffic jam builds up, given a large enough perturbation. A series of traffic jams appears in a density range between $\rho_{\rm c2}$ and some density $\rho_{\rm c3}$. An "anticluster" or "dipole layer" can be triggered if the density ϱ is between $\rho_{\rm c3}$ and $\rho_{\rm c4}$, while any disturbance disappears in stable traffic above some density $\rho_{\rm c4}$. The critical densities ρ_{ck} depend mainly on the choice of the pressure function, the relaxation time, and the velocity-density relation.

The interpretation of these findings is as follows (Kerner and Konhäuser, 1994): Traffic is linearly unstable between the densities $\rho_{\rm c2}$ and $\rho_{\rm c3}$. Therefore the slightest inhomogeneity can cause a traffic jam. Such an inhomogeneity can even be the transition region between a traffic jam and the surrounding traffic. Hence an existing traffic jam will produce a new traffic jam (downstream of it), which generates another traffic jam, and so on, until there are not enough vehicles left to form another jam. Such an irregular series of traffic jams is called *stop-and-go traffic*. Kühne's (1991a) interpretation of this irregularity was based on chaotic dynamics, motivated by an approximate mapping of his traffic model on the Lorenz equation (Kühne and Beckschulte, 1993). However, numerical investigations indicate that the largest Lyapunov exponent stays close to zero (Koch, 1996).

Stop-and-go waves have been compared with waves in shallow water (Kühne, 1984b; Hwang and Chang, 1987), as well as with the clogging of sand falling through a vertical pipe (Schick and Verveen, 1974; Baxter *et al.*, 1989; Lee, 1994; Pöschel, 1994; Peng and Herrmann, 1995) and of lead spheres falling through a fluid column (Horikawa *et al.*, 1996; Nakahara and Isoda, 1997), although the propagation direction is mostly opposite.

Kerner and Konhäuser (1994) have shown that, in the density ranges $[\rho_{\rm c1},\rho_{\rm c2}]$ and $[\rho_{\rm c3},\rho_{\rm c4}]$, an existing traffic jam does not trigger any further jams, because traffic flow is no longer linearly unstable. In these density regimes, they found *metastable traffic*, which is characterized by a critical amplitude $\Delta\rho_c(\varrho)$ for the formation of traffic jams. This amplitude is zero for $\varrho=\rho_{\rm c2}$ and $\varrho=\rho_{\rm c3}$, while it grows towards the stable regimes and is expected to diverge at $\varrho=\rho_{\rm c1}$ and $\varrho=\rho_{\rm c4}$ (see Fig. 35). Perturbations with subcritical amplitudes $\Delta\rho<\Delta\rho_c$ are eventually damped out (analogous to the stable density ranges), while perturbations with supercritical amplitudes $\Delta\rho>\Delta\rho_c$ grow and form traffic jams (similar to the linearly unstable density ranges). The situation in metastable traffic is, therefore, similar to that in supersaturated vapor (Kerner and Konhäuser, 1994), where an overcritical nucleus is required for condensation ("nucleation effect").

Interestingly, there are also traffic models without the phenomenon of metastability. Investigations by Krauß (1998a, 1998b) for a Gipps-like family of traffic models (Gipps, 1981; see also McDonald *et al.*, 1998) suggest the following general outline (see Fig. 36):

(i) Models with a high ratio between maximum acceleration a and maximum deceleration b never show any structure formation, since traffic flow is always stable.
(ii) Models with a relatively high maximum deceleration b display a jamming transition, which is not hysteretic. As a consequence, there are no metastable high-flow states and the outflow from jams is maximal.
(iii) A hysteretic jamming transition with metastable high-flow states and a characteristic, reduced outflow $Q_{\rm out}$ from traffic jams (see Sec. IV.A.5) is found for relatively small accelerations and medium decelerations.

The existence of high-flow states requires the flow $Q_{\rm out}=Q_e(\rho_{\rm out})$ to be smaller than the flow $Q_{\rm cr}=Q_e(\rho_{\rm cr})$ at which traffic becomes linearly unstable, so that there is a density range of metastable traffic. By

variation of model parameters, it is also possible to have the case $Q_{cr}<Q_{out}$, where traffic breaks down before it can reach high-flow states. This corresponds to case (ii) of the above classification by Krauß (1998a, 1998b), in which traffic flow never exceeds the jam line $J(\rho)$ (see Fig. 36). The Nagel-Schreckenberg model belongs to class (ii). Based on an analysis of its correlation function (Eisenblätter *et al.*, 1998; Neubert, Lee, and Schreckenberg, 1999; Schadschneider, 1999) and other methods, it has been shown that the jamming transition in the Nagel-Schreckenberg model is not hysteretic in nature, but continuous for $p=0$. For $0<p<1$, there is strong evidence for a crossover (Sasvari and Kertész, 1997; Eisenblätter *et al.*, 1998; Neubert, Lee, and Schreckenberg, 1999; Schadschneider, 1999; Chowdhury, Kertész, *et al.*, 2000), although some people believe in critical behavior (Roters *et al.*, 1999, 2000).

Note that cellular automaton models with metastable high-flow states do exist, basically all slow-to-start models (Takayasu and Takayasu, 1993; Benjamin *et al.*, 1996; Barlovic *et al.*, 1998). However, it remains to be seen whether this metastability is of the same type as described above, since in probabilistic models the transition from high-flow states to jamming is due to the unfortunate adding up of fluctuations. One would have to check whether perturbations of the form of Eq. (108) tend to fade away when they are smaller than a certain critical amplitude $\Delta\rho_c$, but always grow when they are overcritical. Alternatively, one could determine the phase diagram of traffic states in the presence of bottlenecks (see Sec. IV.B.1).

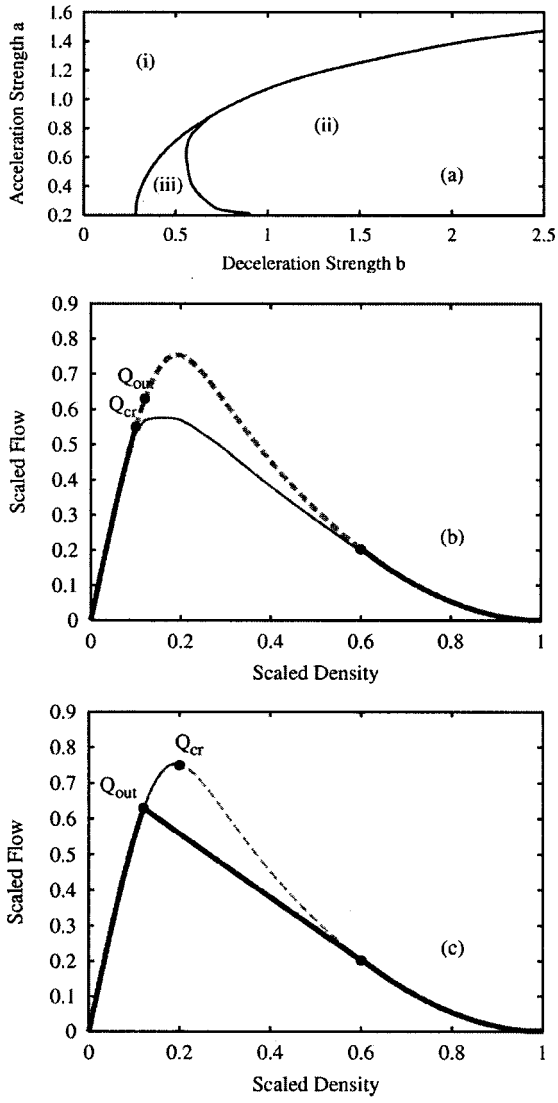

FIG. 36. Comparison of traffic models by their dynamical properties: (a) Schematic phase diagram of model classes as a function of the acceleration strength a and the deceleration strength b. (b) Models belonging to phase (i) have no critical density ρ_{cr} and display stable traffic in accordance with the fundamental diagram (heavy solid and dashed lines), while models belonging to phase (ii) show a nonhysteretic jamming transition with a resulting flow-density relation represented by solid lines. (c) A hysteretic phase transition with metastable high-flow states is found for models belonging to phase (iii). The model behavior is determined by the relative magnitude of the outflow Q_{out} from congested traffic compared to the flow $Q_{cr}=Q_e(\rho_{cr})$ at which traffic becomes linearly unstable with respect to small perturbations. After Krauß, 1998a.

5. Self-organized, "natural" constants of traffic flow

If the fundamental diagram $Q_e(\rho)$ is not linear in the congested regime, the jam line $J(\rho)$ could, in principle, be a function of the average density ϱ throughout the system. The same applies to the propagation velocity C of the jam, which is given by the slope of the jam line. However, in some traffic models, the jam line $J(\rho)$ and the propagation velocity C are independent of the average density ϱ, the initial conditions, and other factors (Kerner, 1999b), which is very surprising. This was first shown by analytical investigations for wide jams in the limit of small viscosity (Kerner and Konhäuser, 1994; Kerner *et al.*, 1997), based on the theory of autosolitons (Kerner and Osipov, 1994). Since then, empirical evidence has been found for this independence (Kerner and Rehborn, 1996a).

Note that the characteristic jam line $J(\rho)$ defines some other constants as well: The intersection point (ρ_{out}, Q_{out}) with the free branch of the fundamental diagram $Q_e(\rho)$ determines, because of the phase segregation between jammed and free traffic, the density ρ_{out} downstream of traffic jams. The quantity ρ_{out} is a characteristic density between ρ_{c1} and ρ_{c2}, which depends on the choice of the traffic model and the specification of the model parameters. Moreover, the value Q_{out} characterizes the outflow from traffic jams. Finally, the density ρ_{jam} at which the jam line $J(\rho)$ becomes zero agrees with the density inside of standing traffic jams.

In summary, we have the following characteristic constants of wide traffic jams: the density ρ_{out} downstream of the jam (if it is not traveling through "synchronized" congested traffic; see Kerner, 1998b), the outflow $Q_{out}=Q_e(\rho_{out})$ from the jam, the density ρ_{jam} of traffic inside the jam, for which $J(\rho_{jam})=0$, and the propagation velocity $C_0=Q_e(\rho_{out})/(\rho_{out}-\rho_{jam})$ of the jam. Note that

these "natural constants" of traffic have not been implemented into the models described above. They are rather a result of self-organization of traffic, i.e., dynamical invariants. These are related to an attractor of the system dynamics, determining the form of the wave fronts. In nonlinear systems, however, the size and shape of an attractor would usually change with the control parameter, in this case the density. The attractor in the congested traffic regime can only be independent of the density if the transition is hysteretic and associated with phase segregation between free and jammed traffic.

Not all traffic models display this independence. For example, although the microscopic optimal velocity model produces a similar dynamics to that of the Kerner-Konhäuser model (58) (Berg *et al.*, 2000), for certain velocity-distance functions $v_e'(d)$ its propagation velocity depends on the average density ϱ (Herrmann and Kerner, 1998). This happens if the jam density ρ_{jam} varies with the vehicle velocity when approaching a jam and, therefore, with the average density ϱ and the initial conditions. The density dependence can, however, be suppressed by suitable discretizations of the optimal velocity model (Helbing and Schreckenberg, 1999) or by models in which the approaching process depends on the relative velocity, for example the gas kinetic-based traffic model or the intelligent driver model (Treiber *et al.*, 1999, 2000). It is also suppressed by particular velocity-distance functions such as the simplified relation $v_e(d)=v_0\Theta'(d-d_0)$, where $\Theta'(z)$ denotes the Heaviside function, which is 1 for $z>0$ and otherwise 0. For this choice, the optimal velocity model can be exactly solved. Sugiyama and Yamada (1997) find that the dynamics of fully developed jams can be represented by a hysteresis loop in the speed-over-distance plane rather than the above Heaviside function (see Fig. 37). Moreover, the characteristic constants of traffic flow are related through the equation $1/\rho_{\text{out}}=1/\rho_{\text{jam}}+v_0T'$, where $T'=(t_\alpha-t_{\alpha-1})$ is the characteristic time interval between the moments t_α, when successive cars α have a distance d_0 to the respective leading car $(\alpha-1)$ and start accelerating in order to leave the downstream jam front. The densities ρ_{out} and ρ_{jam} of free and jammed traffic, respectively, follow from $1/\rho_{\text{out}}=d_0+v_0T'/2$. Moreover, the resolution velocity of jam fronts can be determined as $C_0=[x_\alpha(t_\alpha)-x_{\alpha-1}(t_{\alpha-1})]/(t_\alpha-t_{\alpha-1})=-1/\rho_{\text{jam}}T'=-1/\rho_{\text{jam}}T$. Finally, the time interval $T'=T$ between accelerating vehicles is given by $T'/\tau=2(1-e^{-T'/\tau})$.

Summarizing the above results, one finds characteristic traffic constants if the jam density ρ_{jam} developing at the *upstream* end of traffic jams is independent of the surrounding traffic. In contrast to ρ_{jam}, the time interval T' between accelerating vehicles is determined by the dynamics at the *downstream* jam front. It results from the fact that the initial conditions for accelerating vehicles at jam fronts are more or less identical: The cars have equal headways $d_{\text{jam}}\approx 1/\rho_{\text{jam}}$ to the respective leading vehicle and start with the same velocity $v\approx 0$. The calculation of the characteristic constants is nevertheless a difficult task. For some models, analytical results have been obtained by Kerner *et al.* (1997), Helbing and Schreckenberg (1999), and Gerwinski and Krug (1999).

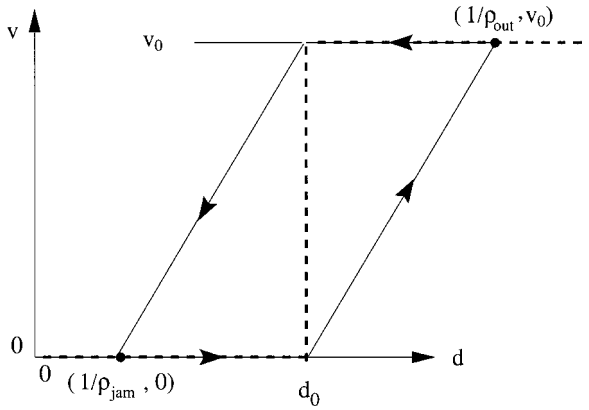

FIG. 37. Hysteresis loop of fully developed traffic jams (solid lines with arrows), emerging in the optimal velocity model (23) with the equilibrium speed-distance relation $v_e(d)=v_0\Theta'(d-d_0)$ (dashed line). After Sugiyama and Yamada, 1997.

6. Kerner's hypotheses

It appears that the above theoretical results cover many of the observations summarized in Sec. II.E. However, Kerner (1998a, 1998b, 1999a, 1999b, 2000a, 2000b, 2000c) was surprised by the following aspects and has, therefore, questioned previously developed traffic models:

(i) Synchronized flows of types (i) and (ii) (see Sec. II.E.2) can exist for a long time (Kerner and Rehborn, 1996b), i.e., they can be stable, at least with respect to fluctuations of small amplitude (see also the discussion of stable congested flow by Westland, 1998).

(ii) Wide jams and stop-and-go traffic are rarely formed spontaneously (Kerner and Rehborn, 1997; Kerner, 1999c, 2000c), but occur reproducibly at the same freeway sections during rush hours. Instead of a transition from free traffic to stop-and-go traffic, one normally observes two successive transitions: a hysteretic one from free flow to synchronized flow (Kerner and Rehborn, 1997) and another one from synchronized flow to stop-and-go waves (Kerner, 1998a; see Sec. II.E.3).

In conclusion, the transition to synchronized flow appears more frequently than the transition to stop-and-go traffic. To explain this, Kerner (1998a, 1998b, 1999a, 1999c, 2000a, 2000b) has developed a set of hypotheses for his three-phase traffic theory (see Secs. II.B and II.E), which can be outlined as follows:

(i) The whole multitude of hypothetical homogeneous and stationary (steady) states of synchronized flow is related to a two-dimensional region in the flow-density plane. This region is the same for a multilane road and for a one-lane road.

(ii) All hypothetical homogeneous and stationary (steady) states of free flow and synchronized flow are stable with respect to infinitesimal perturbations.
(iii) There are two qualitatively different kinds of nucleation effects and the related first-order phase transitions in the homogeneous states of traffic flow:
—the nucleation effect responsible for jam formation, and
—the nucleation effect responsible for the phase transition from free to synchronized flow.
(iv) At each given density in homogeneous states of free flow, the critical amplitude of a local density perturbation and/or velocity perturbation, which is needed for a phase transition from free flow to synchronized flow, is considerably lower than the critical amplitude of a local perturbation needed for jam formation in free flow. In other words, the probability of a phase transition from free flow to synchronized flow is considerably higher than the probability of jam emergence in free flow.
(v) The jam line $J(\rho)$ (see Sec. IV.A.3) determines the threshold for jam formation. All (i.e., an infinite number of) states of traffic flow related to the line J are threshold states with respect to jam formation: Traffic states below the jam line $J(\rho)$ would always be stable, while states above it would be metastable. At the same distance above the line $J(\rho)$, the critical amplitude of local perturbations triggering jam formation is higher in free flow than in synchronized flow. Therefore a transition to a wide moving jam occurs much more frequently from synchronized than from free flow.
(vi) The transition from free to synchronized flow is due to an avalanche self-decrease in the mean probability of overtaking, since it is associated with a synchronization among lanes.
(vii) The hysteretic transition to wide jams is related to an avalanchelike growth of a critical perturbation of the density, average velocity, or traffic flow; see the nucleation effect described in Sec. IV.A.4.

Simulation models reflecting these hypotheses could certainly be constructed, but further empirical evidence for them is still to be found.

B. Transition to congested traffic at bottlenecks and ramps

The effects of changes in the number of lanes and ramps have been simulated since the early days of applied traffic simulations (see, for example, Munjal *et al.*, 1971; Phillips, 1977; Cremer, 1979; Makigami *et al.*, 1983), but no systematic study of the observed phenomena, their properties, mechanisms, and preconditions was carried out. More recently, various theoretically motivated studies have been carried out by physicists as well. These assume, for example, local "defects," "impurities," or bottlenecks with reduced "permeability," which are mostly associated with a locally decreased velocity. Typical results for one single defect are

(i) a drop in the freeway capacity to a value $Q_{\rm bot}$ at the impurity,
(ii) segregation into one area of free and and one area of congested traffic,
(iii) localization of the downstream front of congested traffic at the bottleneck,
(iv) shocklike propagation of the upstream congestion front in agreement with the Lighthill-Whitham theory, particularly Eq. (51) with $Q_+ = Q_{\rm bot}$,
(v) a stationary length of the congested area on circular roads, since the inflow Q_- is determined by the outflow $Q_{\rm bot}$ from the bottleneck.

Investigations of this kind have been carried out for particle hopping models like the TASEP with random sequential update (Janowky and Lebowitz, 1992, 1994) and for traffic models with parallel update (Chung and Hui, 1994; Csahók and Vicsek, 1994; Emmerich and Rank, 1995). One is certainly tempted to compare the congested traffic appearing in these models with the observed "synchronized" congested flow discussed earlier, but several elements seem to be missing:

(i) the hysteretic nature of the transition, characterized by the nucleation effect, i.e., the requirement of an overcritical perturbation,
(ii) the typical dynamics leading to the formation of synchronized congested flow (see Sec. II.E.2), and
(iii) the wide scattering of flow-density data.

In other simulations with inhomogeneities, researchers have recognized wavelike forms of congested traffic behind bottlenecks (Csahók and Vicsek, 1994; Hilliges, 1995; Klar *et al.*, 1996; Nagatani, 1997c; Lee *et al.*, 1998). One can even find period-doubling scenarios upstream of stationary bottlenecks (Nagatani, 1997c) or due to time-dependent local perturbations (Nicolas *et al.*, 1994, 1996; Koch, 1996), which are analytically understandable. Moreover, Kerner *et al.* (1995a) have simulated slightly inhomogeneous traffic on a circular freeway with on- and off-ramps, for which inflows and outflows were chosen identically. They found the interesting phenomenon of a localized stationary cluster along the on-ramp, which triggered a traffic jam when the on-ramp flow was reduced. However, these and other simulations with the Kerner-Konhäuser model (58) were not fully consistent with the above-outlined phenomena, so that Kerner developed the set of hypotheses sketched in Sec. IV.A.6. I believe the reason for the discrepancy between observations and simulations may have been the assumptions of periodic boundary conditions and uniform traffic, i.e., identical driver-vehicle units (see below and Sec. IV.C.2). This is, however, still a controversial topic, which certainly requires more detailed investigations in the future.

In 1998, Lee *et al.* tried to reproduce the hysteretic phase transition to synchronized congested flow by simulation of a circular road with the Kerner-Konhäuser

model, including on- and off-ramps, but with different parameters and a modified velocity-density function $V_e(\rho)$. By a temporary peak in the on-ramp flow, they managed to trigger a form of stop-and-go traffic that was propagating upstream, but its downstream front was pinned at the location of the ramp. They called it the "recurring hump" state and compared it to autocatalytic oscillators. Free traffic would correspond to a point attractor and the oscillating traffic state to a stable limit cycle. In terms of nonlinear dynamics, the transition corresponds to a *Hopf bifurcation*, but a subcritical one, since the critical ramp flow depends on the size of the perturbation (from Helbing and Treiber, 1998b).

Lee *et al.* have pointed out that free traffic survives a pulse-type perturbation of finite amplitude if the ramp flow is below a certain critical value. However, once a recurring hump state has formed, it is self-maintained until the ramp flow falls below another critical value, which is smaller than the one for the transition from free traffic to the recurring hump state. This proves the hysteretic nature of the transition. Moreover, Lee *et al.* have shown a gradual spatial transition from the recurring hump state to free flow downstream of the ramp. They have also demonstrated a synchronization among neighboring freeway lanes as a result of lane changes. Therefore they have suggested that their model can describe the empirically observed first-order phase transition to synchronized flow, where the two-dimensional scattering of synchronized congested traffic is understood as a result of the fact that the amplitude of the oscillating traffic state depends on the ramp flow. The similarity to empirical data, however, was rather loose. Moreover the central question, how to explain homogeneous and stationary congested traffic (see Secs. IV.A.6 and II.E.2) remained unanswered.

Independently of Lee *et al.*, Helbing and Treiber (1998a) submitted another study two weeks later. Based on the nonlocal, gas-kinetic-based traffic model, they simulated a freeway section with open boundary conditions and one on-ramp, since the transition to synchronized congested flow had been mostly observed close to ramps. Ramps were modeled by means of a source term in the continuity equation:

$$\frac{\partial\rho(x,t)}{\partial t}+\frac{\partial}{\partial x}[\rho(x,t)V(x,t)]=\frac{Q_{\mathrm{rmp}}(t)}{IL}. \tag{110}$$

Here $Q_{\mathrm{rmp}}(t)$ represents the ramp flow entering the I-lane freeway over a ramp section of effective length L. The simulation scenario assumed that the sum

$$Q_{\mathrm{down}}=Q_{\mathrm{up}}+Q_{\mathrm{rmp}}(t)/I \tag{111}$$

of the flow Q_{up} upstream of the ramp and the ramp flow $Q_{\mathrm{rmp}}(t)/I$ per freeway lane had reached the regime of metastable traffic flow with $Q_e(\rho_{c1})<Q_{\mathrm{down}}<Q_e(\rho_{c2})$ downstream of the ramp. Hence, without any perturbation, there was free traffic flow. However, a short overcritical peak in the ramp flow $Q_{\mathrm{rmp}}(t)$ triggered a growing perturbation, which traveled downstream in the beginning but changed its propagation speed and direction as it grew larger. Consequently, it returned to the ramp ("boomerang effect") and initiated a continuously growing region of extended congested traffic when it arrived there (see Fig. 38). The reason for this is basically the dynamical reduction of the freeway capacity to the outflow $\tilde{Q}_{\mathrm{out}}$ from congested traffic (see Secs. II.E and IV.A.5). This allows us to understand what Daganzo *et al.* (1999) call the "activation" of a bottleneck. Note that the outflow $\tilde{Q}_{\mathrm{out}}$ depends on the ramp length L (Helbing and Treiber, 1998a; Treiber *et al.*, 2000), but in some traffic models and in reality it is also a function of the ramp flow Q_{rmp}, the average speed V_{bot} in the congested area, and possibly other variables (such as the delay time owing to congestion, since drivers may change their behavior). We expect the relations $\partial\tilde{Q}_{\mathrm{out}}/\partial L\geqslant 0$, $\partial\tilde{Q}_{\mathrm{out}}/\partial Q_{\mathrm{rmp}}\leqslant 0$, $\partial\tilde{Q}_{\mathrm{out}}/\partial V_{\mathrm{bot}}\geqslant 0$, and

$$\lim_{Q_{\mathrm{rmp}}\to 0}\ \lim_{V_{\mathrm{bot}}\to 0}\ \lim_{L\to\infty}\tilde{Q}_{\mathrm{out}}(Q_{\mathrm{rmp}}/I,V_{\mathrm{bot}},L)=Q_{\mathrm{out}}. \tag{112}$$

Note that both $\tilde{Q}_{\mathrm{out}}$ and Q_{out} are also functions of the model parameters V_0, T, etc. (and of their spatial changes along the road).

The (congested) bottleneck flow

$$Q_{\mathrm{bot}}=\tilde{Q}_{\mathrm{out}}-Q_{\mathrm{rmp}}/I=\tilde{Q}_{\mathrm{out}}-\Delta Q \tag{113}$$

immediately upstream of the ramp is given by the outflow $\tilde{Q}_{\mathrm{out}}$ minus the ramp flow Q_{rmp}/I per lane defining the *bottleneck strength* ΔQ.[8] Let $\rho_{\mathrm{bot}}>\rho_{c2}$ be the associated density according to the congested branch of the fundamental diagram, i.e., $Q_{\mathrm{bot}}=Q_e(\rho_{\mathrm{bot}})$. Then the congested traffic flow upstream of the bottleneck is homogeneous if ρ_{bot} falls in the stable or metastable range; otherwise one observes different forms of congestion (see Sec. IV.B.1). Hence the above hysteretic transition to *homogeneous congested traffic* can explain the occurrence of homogeneous and stationary (steady) congested traffic states. The scattering of synchronized congested flow can be accounted for by a mixture of different vehicles types such as cars and trucks (Treiber and Helbing, 1999a; see Sec. IV.C.2). However, apart from a heterogeneity in the time headways (Banks, 1999), there are also other proposals for this scattering, which are more difficult to verify or disprove empirically: complex dynamics with forward- and backward-propagating shock waves (Kerner and Rehborn, 1996a; Kerner, 1998b, 2000a, 2000b), changes in the behavior of "frustrated" drivers (Krauß, 1998a), anticipation effects (Wagner, 1998a; Knospe *et al.*, 2000a, 2000b), nonunique equilibrium solutions (Nelson and Sopasakis, 1998; Nelson, 2000), or multiple metastable oscillating states

[8]At particularly long on-ramps (e.g., at freeway intersections), some part $\alpha' Q_{\mathrm{rmp}}$ (with $0<\alpha'<1$) of the ramp flow may enter the freeway downstream of the congestion front as if it would enter over an additional downstream on-ramp. In such cases, the formula (113) for the bottleneck flow must be replaced by $Q_{\mathrm{bot}}=\tilde{Q}_{\mathrm{out}}-(1-\alpha')Q_{\mathrm{rmp}}/I$, and the resulting downstream flow is given by $\tilde{Q}_{\mathrm{out}}+\alpha' Q_{\mathrm{rmp}}/I$.

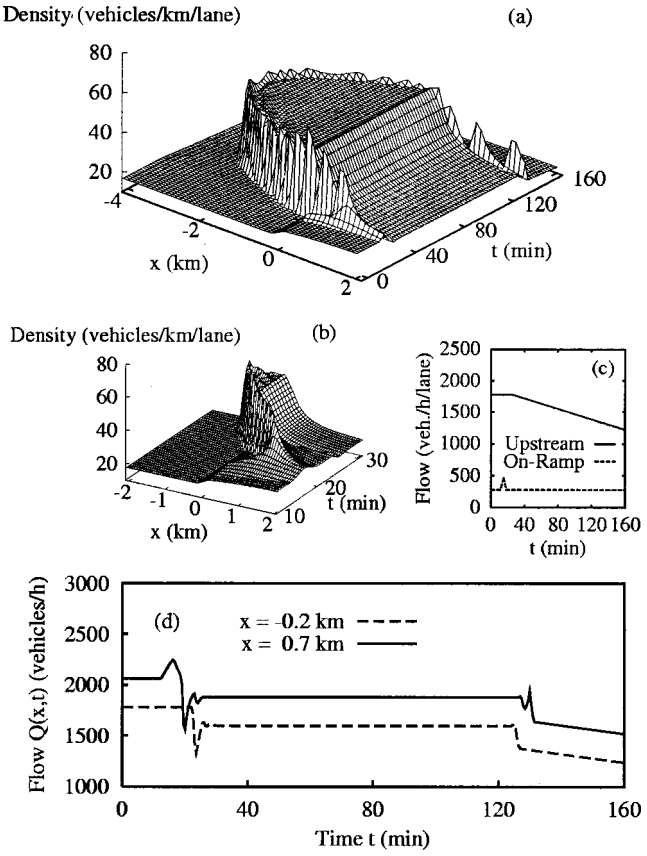

FIG. 38. Spatio-temporal evolution of the density after a small peak in the inflow from the on-ramp. The on-ramp merges with the main road at $x=0$ km. Traffic flows from left to right. In (a), the parabolically shaped region of high density corresponds to the resulting synchronized congested flow. Plot (b) illustrates in greater detail that the congestion starts to build up downstream of the bottleneck (see Sec. II.E.2). (c) The time-dependent inflows $Q_{\rm up}$ at the upstream boundary and $Q_{\rm rmp}/I$ at the on-ramp. (d) Simulated traffic flows at two cross sections showing the temporary drop below the finally resulting bottleneck flow (dashed line) and discharge flow (solid line) observed in real traffic; cf. Fig. 3(b). After Helbing and Treiber, 1998a; Helbing, Hennecke, *et al.*, 2001a, 2001b.

(Tomer *et al.*, 2000). Nonunique solutions are also expected for the noninteger car-following model (19), where the vehicle acceleration dv/dt is always zero when the relative velocity Δv becomes zero, no matter how small the distance is. However, most of these states are not stable with respect to fluctuations, if no discontinuous driver reaction is introduced.

Let us now explain why the downstream front of extended congested traffic is located at the bottleneck and stationary: If it were located downstream of the ramp for some reason, its downstream front would travel upstream as in traffic jams. So the question is why it does not continue to move upstream when the downstream front has reached the bottleneck. When it would pass the on-ramp, it would continue to emit the flow $\tilde{Q}_{\rm out}$, leading to an increased flow $(\tilde{Q}_{\rm out}+Q_{\rm rmp}/I)>(Q_{\rm up}+Q_{\rm rmp}/I)$ at the ramp, which would again queue up. The spatial extension of the congested area is reduced only when the traffic flow $Q_{\rm up}$ falls below the bottleneck flow $Q_{\rm bot}$. This is usually the case after the rush hour.

Finally, I should mention that congested traffic can also be triggered by a perturbation in the traffic flow $Q_{\rm up}(t)$ entering the upstream freeway section. It can even be caused by a supercritical "negative" perturbation with a reduction of the vehicle density and flow as, for example, at an off-ramp (Helbing, 2001). This is because vehicles will accelerate into the region of reduced density, followed by a successive deceleration. Therefore a negative density perturbation is rapidly transformed into the characteristic perturbation that triggers congested traffic (see Sec. IV.A.3).

1. Phase diagram of traffic states at inhomogeneities (bottlenecks)

Theoretical investigations of traffic dynamics have long been carried out mainly for circular roads. The corresponding results were, in fact, misleading, since it is usually not possible to enter the linearly unstable region $\varrho>\rho_{c2}$ of congested traffic on a homogeneous road. High densities were produced by means of the initial condition, but they normally cannot be reached by natural inflows into a homogeneous freeway with open boundaries, no matter how high the inflow is. Consequently, spontaneously forming traffic jams are rather unlikely, apart from temporary ones caused by sufficiently large perturbations. However, the situation changes drastically for inhomogeneous roads with ramps or other bottlenecks.

Helbing *et al.* (1999) have systematically explored the resulting traffic states at inhomogeneities, triggered by a fully developed perturbation (jam), as a function of the ramp flow $Q_{\rm rmp}/I$ per freeway lane and the upstream traffic flow $Q_{\rm up}$. In this way, they found a variety of congested traffic states and their relation to each other (see Fig. 39). Free traffic was, of course, observed if the total downstream traffic flow $Q_{\rm down}=(Q_{\rm up}+Q_{\rm rmp}/I)$ was stable with respect to large perturbations, i.e., if $Q_{\rm down}<Q_e(\rho_{c1})$. As expected, extended congested traffic states were found when the traffic flow $(Q_{\rm up}+Q_{\rm rmp}/I)$ exceeded the maximum flow $Q_{\rm max}=\max_\rho Q_e(\rho)$, i.e., the theoretical freeway capacity for homogeneous traffic. However, congested traffic occurred even for smaller traffic flows $(Q_{\rm up}+Q_{\rm rmp}/I)<Q_{\rm max}$ triggered by perturbations. Consequently, it could be avoided by suppressing perturbations with suitable technical measures (see Sec. IV.G.).

The classical form of extended congested traffic is *homogeneous congested traffic* [see Fig. 40(a)], which is formed if the density $\rho_{\rm bot}$ in the congested region falls into the (meta)stable regime. Decreasing the ramp flow $Q_{\rm rmp}$ will increase the flow $Q_{\rm bot}=(\tilde{Q}_{\rm out}-Q_{\rm rmp}/I)$ in the congested region and decrease the related density $\rho_{\rm bot}$. When it falls into the unstable regime, i.e., when we have $\rho_{\rm bot}<\rho_{c3}$ or $Q_{\rm bot}>Q_e(\rho_{c3})$, we can expect *oscillating congested traffic* [see Fig. 40(b)]. However, in deterministic models and without any additional perturbations, homogeneous congested traffic extends up to

$Q_{\rm bot} > Q_e(\rho_{\rm cv})$ with a smaller density $\rho_{\rm cv} < \rho_{\rm c3}$. The reason is that, above a density of $\rho_{\rm cv}$, traffic flow is *convectively stable* (Helbing *et al.*, 1999), i.e., perturbations are convected away from the location of the disturbance (Manneville, 1990; Cross and Hohenberg, 1993). While the transition from free traffic to congested traffic is hysteretic (see Sec. IV.B), the transition from the homogeneous congested traffic state to the oscillating congested traffic state is continuous. A suitable order parameter for characterizing this transition is the oscillation amplitude.

Let us assume that we further reduce the ramp flow, so that congestion is expected to become less serious. Then, at some characteristic ramp flow $Q^0_{\rm rmp}$, the oscillation amplitude becomes so large that the time-dependent flow-density curve reaches the free branch of the fundamental diagram $Q_e(\rho)$. For $Q_{\rm rmp} < Q^0_{\rm rmp}$ we therefore speak of *triggered stop-and-go traffic* [see Fig. 40(c)]. A suitable order parameter would be the average distance between locations of maximum congestion. Drivers far upstream of a bottleneck will be very much puzzled by the alternation of jams and free traffic, since these jams seem to appear without any plausible reason, analogous to phantom traffic jams. The triggering mechanism of repeated jam formation is as follows: When the upstream traveling perturbation reaches the bottleneck, it triggers another small perturbation, which travels downstream. As described in Secs. II.E and IV.A.3, this perturbation changes its propagation speed and direction while growing. As a consequence, the emerging jam returns like a boomerang and triggers another small perturbation when reaching the bottleneck. This process repeats time and again, thereby causing the triggered stop-and-go state.

If the traffic flow $Q_{\rm down}$ downstream of the inhomogeneity is not linearly unstable, the triggered small perturbation cannot grow, and we will have only a single localized cluster, which normally passes the inhomogeneity and moves upstream. The condition for this *moving localized cluster* or wide moving jam is obviously $(Q_{\rm up} + Q_{\rm rmp}/I) < Q_e(\rho_{\rm c2})$. However, if $Q_{\rm up} < Q_e(\rho_{\rm c1})$, i.e., when the flow upstream of the bottleneck is stable, a congested state cannot survive upstream of the inhomogeneity. In that case, we find a *standing* or *pinned localized cluster* at the location of the bottleneck [see Fig. 40(d)]. Oscillatory forms of pinned localized clusters are possible as well (Lee *et al.*, 1999; Treiber *et al.*, 2000). The transition between localized clusters and extended forms of congested traffic is given by the condition $(Q_{\rm up} + Q_{\rm rmp}/I) > \tilde{Q}_{\rm out}$, requiring that the overall traffic flow $(Q_{\rm up} + Q_{\rm rmp}/I)$ exceeds the outflow $\tilde{Q}_{\rm out}$ from congested traffic.

Finally, I would like to repeat that the transition between free and congested traffic is of first order (i.e., hysteretic), while the transitions between extended forms of congested traffic (homogeneous, oscillating, and triggered stop-and-go traffic) seem to be continuous. As a consequence of the former, one can have direct transitions from free traffic to homogeneous or oscillating congested traffic without crossing localized cluster states or triggered stop-and-go waves. Normally the traffic flows $Q_{\rm up}(t)$ and $Q_{\rm rmp}(t)$ increase so drastically during the rush hour that a phase point belonging to the area of extended congested traffic is reached before free traffic flow breaks down. The theory predicts that this will happen on weekdays characterized by high traffic flows, while at the same freeway section localized cluster or triggered stop-and-go states should appear on days with less pronounced rush hours.

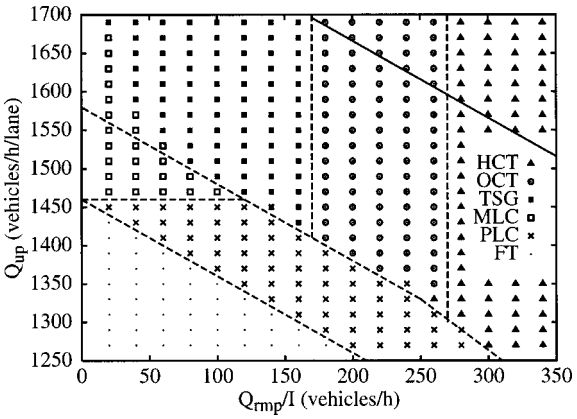

FIG. 39. Numerically determined phase diagram of the traffic states forming in the vicinity of an on-ramp as a function of the inflows $Q_{\rm up}$ and $Q_{\rm rmp}/I$ per freeway lane on the main road and the on-ramp: HCT, homogeneous congested traffic; OCT, oscillatory congested traffic; TSG, triggered stop-and-go traffic; MLC, moving localized clusters; PLC, pinned localized clusters; FT, free traffic. These states are triggered by a fully developed localized cluster traveling upstream and passing the ramp (cf. Fig. 40). Dashed lines indicate the theoretical phase boundaries. The lowest diagonal line $(Q_{\rm up} + Q_{\rm rmp}/I) = Q_e(\rho_{c1})$ separates free traffic from wide jams, while the central diagonal line $(Q_{\rm up} + Q_{\rm rmp}/I) = \tilde{Q}_{\rm out} \approx Q_e(\rho_{c2})$ separates localized from extended forms of congested traffic. The localized cluster states between these two diagonals require metastable downstream traffic. Finally, the highest (solid) diagonal line represents the condition $(Q_{\rm up} + Q_{\rm rmp}/I) = Q_{\rm max}$ limiting the region in which a breakdown of traffic flow is caused by exceeding the theoretically possible freeway capacity $Q_{\rm max}$ (upper right corner). All congested traffic states below this line are caused by perturbations and are therefore avoidable by technical control measures. After Helbing, Hennecke, and Treiber, 1999; Helbing, Hennecke, *et al.*, 2001a.

It should be stressed that the above analytical relations for the transitions between free traffic and the five different forms of congested traffic are in good agreement with numerical results (see Fig. 39). Moreover, according to the quantities appearing in these analytical relations, the transitions are basically a consequence of the instability diagram, combined with the fundamental diagram and the jam line. Therefore we expect the above phase diagram to be universal for all microscopic and macroscopic traffic models having the same instability diagram. This prediction has been confirmed for several models. Lee *et al.* (1999) have found analogous transitions for the Kerner-Konhäuser model (58), but recognized a region of tristability, where it is a matter of

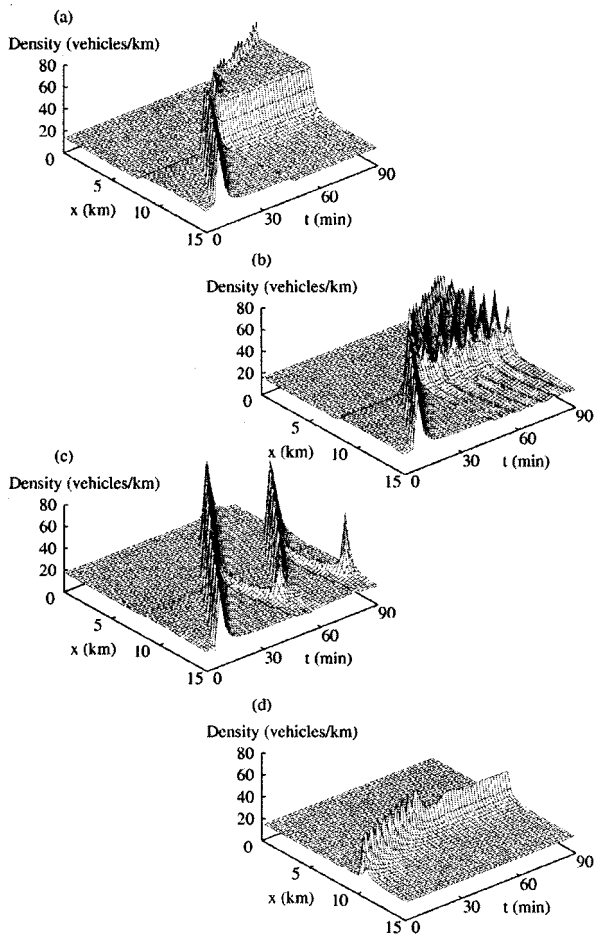

FIG. 40. Spatio-temporal dynamics of typical representatives of congested states that are triggered at an on-ramp by a fully developed perturbation traveling upstream. The center of the on-ramp is located at $x=8.0$ km. The displayed states are (a) homogeneous congested traffic, (b) oscillatory congested traffic, (c) triggered stop-and-go traffic, and (d) a pinned localized cluster. From Helbing, Hennecke, *et al.*, 2001a, 2001b; after Helbing, Hennecke, and Treiber, 1999.

history whether one ends up with free traffic, a pinned localized cluster, or oscillating congested traffic. This tristability is probably the result of a dynamical variation of $\tilde{Q}_{\rm out}$, as pointed out by Treiber *et al.* (2000), who have also reproduced the phase diagram for the intelligent driver model (see Sec. III.A.3). Moreover, they have presented empirical data confirming the existence of all five congested traffic states. These were successfully reproduced in simulation scenarios with the intelligent driver model using the measured boundary conditions. Only one parameter, the safe time clearance T, was varied to calibrate both the capacity of the different freeway sections and their bottlenecks. It was also demonstrated that different kinds of bottlenecks have qualitatively the same effects. This requires a generalized definition of bottleneck strength ΔQ,

$$\Delta Q = Q_{\rm rmp}/I + \tilde{Q}_{\rm out} - \tilde{Q}'_{\rm out}, \tag{114}$$

where $\tilde{Q}_{\rm out}$ denotes the outflow from congested traffic at the freeway section with the largest capacity and $\tilde{Q}'_{\rm out}$ the outflow at the bottleneck. Spatial changes in the number $I(x)$ of lanes can be reflected by virtual ramp flows (Shvetsov and Helbing, 1999):

$$\frac{Q_{\rm rmp}}{IL} = -\frac{\rho V}{I}\frac{\partial I(x)}{\partial x}. \tag{115}$$

This follows from the continuity equation $\partial(I\rho)/\partial t + \partial(I\rho V)/\partial x = 0$.

Recently Lee *et al.* (2000) presented an empirical phase diagram, for which the corresponding freeway stretch contains several capacity changes, which complicate matters. Such freeway sections often show congestion with a stationary (pinned) upstream end. It can also happen that a jam travels through a short section of stable traffic, because there is a finite *penetration depth* (Treiber *et al.*, 2000). Finally, I would like to mention a number of other simulation studies with open boundaries that have recently been carried out (Bengrine *et al.*, 1999; Mitarai and Nakanishi, 1999, 2000; Popkov and Schütz, 1999; Popkov *et al.*, 2000; Cheybani *et al.*, 2001a, 2001b).

To summarize, a comparison between numerical simulations and empirical data suggests the following: Homogeneous congested traffic seems to be the same as synchronized traffic flow of type (i) (see Sec. II.E.2), while oscillating congested traffic seems to be related to synchronized flow of type (iii). Homogeneous-in-speed states, which are also called synchronized flow of type (ii), are found where congested traffic relaxes towards free traffic [see Figs. 42(b) and 5; Tilch and Helbing, 2000, Fig. 3, right]. Moreover, the term "recurring hump state" (see Lee *et al.*, 1998, 1999) summarizes all oscillating forms of congested traffic, while "nonhomogeneous congested traffic" was used for all forms of unstable traffic (Tomer *et al.*, 2000).

Let us now ask what the above theory predicts for models with different instability diagrams. If the model is stable over the whole density range, as is the Burgers equation or the TASEP, we expect just two states: free traffic and homogeneous congested traffic, in agreement with numerical results (Janowsky and Lebowitz, 1992, 1994) and exact analytical ones (Schütz, 1993). If the model displays stable traffic at low densities and unstable traffic at high densities, we expect free traffic and oscillating traffic, including the possibility of triggered stop-and-go waves. This was, for example, observed by Emmerich and Rank (1995) for the Nagel-Schreckenberg model (see also Diedrich *et al.*, 2000; Cheybani *et al.*, 2001b). For the case of stable traffic at low and high densities, but unstable traffic at medium densities (without metastable density ranges), one should find free traffic, oscillating traffic states (including triggered stop-and-go waves), and homogeneous congested traffic. This could possibly be tested with the Weidlich-Hilliges model. The existence of moving and pinned localized clusters would normally require a metastable state between free traffic and linearly unstable traffic.

Finally, assume models with stable traffic at low densities and metastable traffic above a certain critical den-

sity ρ_{c1}, but no range of linearly unstable traffic, as suggested by Kerner (see Sec. IV.A.6). In such kinds of models, which would probably have to assume discontinuous switches between different driver behaviors (strategies) (see Sec. IV.F), oscillatory congested traffic and triggered stop-and-go waves should not exist. Identifying localized cluster states, both moving and pinned ones, with wide moving jams, but homogeneous congested traffic with synchronized flow, would give a similar picture to the three-phase traffic theory proposed by Kerner (see Secs. II.B. and IV.A.6): The possible traffic states would be free traffic, wide jams, and synchronized flow. Transitions to synchronized flow would occur when the traffic flow $(Q_{up}+Q_{rmp}/I)$ exceeded the maximum capacity Q_{max}. This would tend to happen at bottlenecks, where the metastable density regime is entered first. The transition would cause a queueing of vehicles and a capacity drop due to the increased time headways of accelerating vehicles at downstream congestion fronts. In contrast, transitions to wide moving jams would always have to be triggered by supercritical perturbations. This would most frequently happen in congested areas upstream of bottlenecks ("pinch effect"; see Sec. II.E.3), as metastable traffic is rather unlikely on homogeneous stretches of a freeway. Moreover, the scattering of flow-density data in synchronized congested traffic could be explained by some source of fluctuations, e.g., heterogeneous driver-vehicle behavior (see Sec. IV.C.2).

The above considerations demonstrate how powerful the method of the phase diagram is. Based on a few characteristic quantities (the critical flows), one can predict the dynamical states of a given model as well as the phase boundaries. Moreover, one can classify traffic models into a few universality classes. It does not matter whether the model is of microscopic or macroscopic, of deterministic or probabilistic nature.

2. Spatial coexistence of states and the pinch effect

In simulations with the intelligent driver model, Treiber and Helbing (1999b) have simulated a scenario that is reminiscent of the pinch effect reported by Kerner (1998a) and similar observations by Koshi *et al.* (1983). This scenario is characterized by the spatial coexistence of different kinds of congested traffic, which can occur upstream of bottlenecks even on rampless road sections, as the transitions between the concerned congested states are continuous (see Sec. IV.B.1). Starting with homogeneous congested traffic at a bottleneck, Treiber and Helbing found oscillating congested traffic upstream of it, but stop-and-go traffic even further upstream (see also Helbing, Hennecke, *et al.*, 2001b). For comparison, upstream of a bottleneck Kerner has observed transitions from synchronized flow to a "pinch region" characterized by narrow clusters, which eventually merged to form wide moving jams (see Fig. 41 and Sec. II.E.3). Personally, I consider this phenomenon as strong evidence for the existence of linearly unstable traffic.

According to the model of Treiber and Helbing (1999b), the conditions for this spatial coexistence of congested traffic states are the following. The density ρ_{bot} in the congested region immediately upstream of the bottleneck should be in the linearly unstable, but convectively stable, range $[\rho_{cv},\rho_{c3}]$, where perturbations are convected away in the upstream direction (Manneville, 1990; Cross and Hohenberg, 1993). In this case, traffic flow will appear stationary and homogeneous close to the bottleneck, but small perturbations will grow as they propagate upstream in the congested region starting at the bottleneck. If the perturbations propagate faster than the congested region expands, they will reach the area of free traffic upstream of the bottleneck. During rush hours, it is quite likely that this free flow is in the metastable range between ρ_{c1} and ρ_{c2}. Consequently, sufficiently large perturbations can trigger the formation of jams, which continue traveling upstream, while small perturbations are absorbed. Note that this phenomenon should be widespread, since the range $[\rho_{cv},\rho_{c3}]$ of convectively stable traffic can be quite large, so it is likely to appear when the freeway flow Q_{up} exceeds the critical flow $Q_e(\rho_{c1})$.

C. Heterogeneous traffic

In reality, driver-vehicle units are not identical, but behave differently, which may be reflected by individual parameter sets. This is easy to do in microscopic traffic models, while gas-kinetic and macroscopic models require generalizations. Such generalized models have been developed for a continuous distribution of desired velocities (Paveri-Fontana, 1975; Helbing, 1995c, 1995d, 1996a, 1997a; Wagner *et al.*, 1996; Wagner, 1997a, 1997b, 1997c). However, if several driver-vehicle parameters are varied, it is more practical to distinguish several classes of vehicles, such as aggressive drivers ("rabbits") and timid ones ("slugs") (Daganzo, 1995c, 1999a) or cars and trucks (short and long vehicles; see, for example, Helbing, 1996d, 1997a, 1997d; Hoogendoorn, 1999; Hoogendoorn and Bovy, 1999a, 1999b, 2000b; Shvetsov and Helbing, 1999). New phenomena arising from the heterogeneity of driver-vehicle units are platoon formation and scattering of flow-density data, as is outlined below.

1. Power-law platoon formation and quenched disorder

The simplest models for heterogeneity are particle hopping models with quenched disorder. For example, Evans (1996), Krug and Ferrari (1996), Karimipour (1999a, 1999b), and Seppäläinen and Krug (1999) study a simplified version of a model by Benjamini *et al.* (1996). It corresponds to the one-dimensional driven lattice gas known as TASEP, but with particle-specific, constant jump rates q_α. Since overtaking is not allowed in this model, Krug and Ferrari found a sharp phase transition between the low-density regime, where all particles are queueing behind the slowest particle, and the high-density regime, where the particles are equally distributed. While at low densities the slow particles "feel free traffic" until the critical density is reached [cf. the

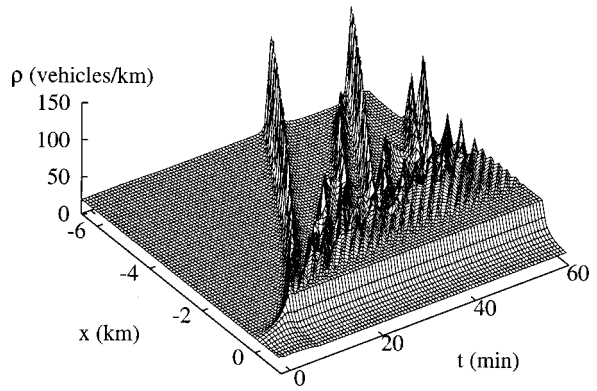

FIG. 41. Illustration of the spatial coexistence of homogeneous congested traffic, oscillatory congested traffic, and triggered stop-and-go waves in a simulation with the intelligent driver model for an inhomogeneous freeway without ramps. Traffic flows in the positive x direction. The spatio-temporal density plot shows the breakdown to homogeneous congested traffic near the inhomogeneity and stop-and-go waves emanating from this region. The inhomogeneity corresponds to an increased safe time clearance $T'>T$ between $x=0$ km and $x=0.3$ km, reflecting more careful driving. Downstream of the inhomogeneity, vehicles accelerate into free traffic. From Treiber and Helbing, 1999b; Helbing, Hennecke, *et al.*, 2001b.

truck curve in Figs. 15(b), 15(c), and 43(a)], the growth of particle clusters ("platoons") is characterized by a power-law coarsening. If particles move ballistically with individual velocities v_α and form a platoon when a faster particle reaches a slower one, the platoon size $n_{\rm pl}(t)$ grows according to

$$n_{\rm pl}(t)\sim t^{(m'+1)/(m'+2)}, \tag{116}$$

where the exponent m' characterizes the distribution $P_0(v)\sim(v-v_{\min})^{m'}$ of free velocities in the neighborhood of the minimal desired velocity $v_{\min}$ (Ben-Naim *et al.*, 1994; Nagatani, 1996c; Ben-Naim and Krapivsky, 1997, 1998, 1999; see also Nagatani, 1995a; Nagatani *et al.*, 1998; for spatial inhomogeneities see the results of Krug, 2000). Above the critical density, the differences among fast and slow particles become irrelevant, because there is so little space that all particles have to move slower than preferred. The formation of platoons has been compared with *Bose-Einstein condensation*, where the steady-state velocity of the particles is analogous to the fugacity of the ideal Bose gas (Evans, 1996; Krug and Ferrari, 1996; Chowdhury, Santen, and Schadschneider, 2000).

Platoon formation and power-law coarsening has also been found in microscopic models with parallel update (Ben-Naim *et al.*, 1994; Nagatani, 1996c; Ben-Naim and Krapivsky, 1997, 1998, 1999; Nagatani *et al.*, 1998; see also Fukui and Ishibashi, 1996a; Nagatani, 2000). An example is the Nagel-Schreckenberg model with quenched disorder, i.e., vehicle-specific slowdown probabilities p_α (Ktitarev *et al.*, 1997; Knospe *et al.*, 1999).

In real traffic, platoons remain limited in size (see Sec. II.D). This is probably because of occasional possibilities for lane changes on multilane roads. A model for platoon size distributions has been developed by Islam and Consul (1991).

2. Scattering

In order to model the observed scattering of congested flow-density data, Helbing *et al.* have simulated traffic with different driver-vehicle units. In contrast to the models discussed in Sec. IV.C.1, they used traffic models with a linearly unstable density regime, namely, the gas-kinetic-based model (Treiber and Helbing, 1999a), the discrete optimal velocity model (Helbing and Schreckenberg, 1999), and the intelligent driver model (Treiber *et al.*, 2000). Since they could determine the time-dependent variation of the percentage of long vehicles in their empirical data, they distinguished two vehicle classes, cars and trucks (short and long vehicles). These were characterized by two different sets of parameters, i.e., two different fundamental diagrams. Consequently, the effective fundamental diagram was a function of the measured proportion of long vehicles. Performing simulations with the empirically obtained boundary conditions and truck proportions (see Fig. 23), they managed to reproduce the observed transition from free to synchronized congested flow semi-quantitatively; see Fig. 42 (Treiber and Helbing, 1999a).

In particular, the spatial dependence of the flow-density data on the respective freeway cross section was well reproduced, including the relaxation to free traffic downstream of the bottleneck, which leads to homogeneous-in-speed states, i.e., synchronized flow of type (ii). Moreover, the flow-density data had a one-dimensional dependence in the regime of free traffic, while they were widely scattered in the congested regime. The most important requirement for this was a considerable difference in the safe time clearance T_α of cars and trucks. This is certainly in agreement with the facts (see Fig. 24), and it is also compatible with the explanation of the randomly sloped flow-density changes suggested by Banks (see Sec. II.B). If this interpretation of the scattering of flow-density data is correct, one should observe a smaller variation of flow-density data on days when truck traffic is reduced or prohibited. However, some scattering is always expected due to the wide distribution of time headways (see Figs. 6 and 24).

D. Multilane traffic and synchronization

1. Gas-kinetic and macroscopic models

Traffic models have also been developed for multilane traffic (Gazis *et al.*, 1962; Munjal *et al.*, 1971; Munjal and Pipes, 1971; Makigami *et al.*, 1983; Daganzo, 1997b; Daganzo *et al.*, 1997; Holland and Woods, 1997). In gas-kinetic and macroscopic traffic models, this is reflected by additional lane-changing terms (Rørbech, 1976; Michalopoulos *et al.*, 1984; Helbing, 1996d, 1997a, 1997d; Helbing and Greiner, 1997; Hoogendoorn, 1999; Hoogendoorn and Bovy, 1999a, 1999b; Klar and Wegener, 1999a, 1999b; Shvetsov and Helbing, 1999). Representing the vehicle density in lane i by $\rho_i(x,t)$ and the

lane-specific average velocity by $V_i(x,t)$, the lane-specific density equations of the form of Eq. (110) are complemented by the additional contributions

$$+\frac{\rho_{i-1}}{\tau_{i-1}^{+}}-\frac{\rho_i}{\tau_i^{+}}+\frac{\rho_{i+1}}{\tau_{i+1}^{-}}-\frac{\rho_i}{\tau_i^{-}}. \tag{117}$$

Here, $1/\tau_i^{+}$ is the density-dependent lane-changing rate from lane i to lane $(i+1)$, while $1/\tau_i^{-}$ describes analogous changes to lane $(i-1)$. Empirical measurements of lane-specific data and lane-changing rates are rare (Sparman, 1978; Hall and Lam, 1988; Chang and Kao, 1991; McDonald *et al.*, 1994; Brackstone and McDonald, 1996; Brackstone *et al.*, 1998). Based on his data, Sparman (1978) proposed the relation $1/\tau_i^{\pm}=c_i^{\pm}\rho_i(\rho_{\max}-\rho_{i\pm1})$ with suitable lane-dependent constants $c_i^{\pm}$.

The additional terms in the velocity equations include

$$+\frac{\rho_{i-1}}{\tau_{i-1}^{+}}(V_{i-1}-V_i)+\frac{\rho_{i+1}}{\tau_{i+1}^{-}}(V_{i+1}-V_i). \tag{118}$$

These terms lead to a velocity adaptation in neighboring lanes, which is responsible for the synchronization among lanes in congested traffic (Lee *et al.*, 1998) and allows the treatment of multilane traffic by effective one-lane models (Shvetsov and Helbing, 1999). Similar adaptation terms are obtained for the variances. More detailed calculations yield further terms reflecting that overtaking vehicles transfer their higher speed to the neighboring lane (Helbing, 1997a, 1997d).

The lane-specific traffic equations allow us to derive simplified equations for the whole freeway cross section. It turns out that, compared to the effective one-lane model used earlier, one has to correct the expression for the traffic pressure at small densities, where the average velocities in the neighboring lanes are not synchronized (Helbing, 1997a, 1997d):

$$P(x,t)\approx\rho(x,t)[\,\theta(x,t)+\langle(V_i-V)^2\rangle]. \tag{119}$$

The density-dependent contribution $\langle(V_i-V)^2\rangle$ reflects the difference in the lane-specific speeds V_i, which also contributes to the overall velocity variance of vehicles [see Fig. 15(a)]. In contrast, the interaction frequency among vehicles, which enters the braking interaction term in Eq. (86) and V^e, depends on the lane-specific variance θ.

2. Microscopic models and cellular automata

A microscopic modeling of lane changes (Fox and Lehmann, 1967; Levin, 1976; Daganzo, 1981; Mahamassani and Sheffi, 1981; Ahmed *et al.*, 1996) turns out to be an intricate problem for several reasons:

(i) Because of legal regulations, lane changing is not symmetric, at least in Europe.
(ii) Drivers accept smaller gaps than usual in response to lane closures, i.e., they behave differently.
(iii) The minimum gaps required for lane changing depend on the velocity and the speed differences between neighboring vehicles in the adjacent lane(s).
(iv) Without assuming fluctuations or heterogeneous vehicles, it is hard to reproduce the high numbers of lane changes that drivers can make by means of tricky maneuvers.

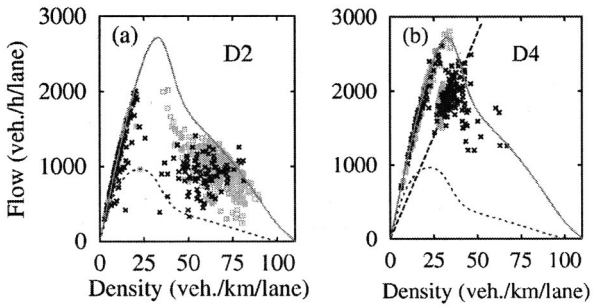

FIG. 42. Empirical one-minute data (dark crosses) in flow-density space and related simulation results (gray boxes) at two different cross sections of the freeway. (a) Synchronized congested flow in the section upstream of a bottleneck. (b) Homogeneous-in-speed states in the nearby section downstream of the bottleneck. The simulations manage to reproduce both the one-dimensional flow-density relation at small densities and the scattering over a two-dimensional region in the congested regime. For comparison, we have displayed the equilibrium flow-density relations for traffic consisting of 100% cars (solid line) and 100% trucks (dashed line). The respective model parameters were weighted with the measured, time-dependent truck fraction; see Fig. 23. After Treiber and Helbing, 1999a; Helbing *et al.*, 2001a, 2001b.

As a consequence, classical gap acceptance models do not work very well (Gipps, 1986; Yang and Koutsopoulos, 1996). Benz (1993) and Helbing (1997a) have, therefore, suggested a flexible lane-changing criterion. Lane-changing rules for cellular automata have been developed, as well (Nagatani, 1993, 1994a, 1994b, 1996a; Zhang and Hu, 1995; Rickert *et al.*, 1996; Chowdhury, Ghosh, *et al.*, 1997; Wagner *et al.*, 1997; Awazu, 1998; Nagel *et al.*, 1998; Brilon and Wu, 1999).

In modern lane-changing models, the lane is changed if both an *incentive criterion* and a *safety criterion* are fulfilled (Nagel *et al.*, 1998). The incentive criterion checks whether the considered driver α could go faster on (one of) the neighboring lane(s). The preferred lane is that for which the absolute value $|f_{\alpha\beta}|$ of the repulsive interaction force with the respective leading vehicle β is smallest. It is, however, reasonable to introduce a certain threshold value for lane changing. The safety criterion is fulfilled if the anticipated repulsive interaction forces with respect to neighboring vehicles in the adjacent lane stay below a certain critical value that depends on the friendliness of driver α. The intelligent driver model and other models considering velocity differences take into account that the gap required for lane changing must be greater if the new following vehicle approaches rapidly, i.e., if its relative velocity with respect to the lane-changing vehicle is large.

To obtain reasonable lane-changing rates, one has either to work with a probabilistic model or to distinguish different vehicle types like cars and trucks or to introduce tricky driver strategies. In a low density range around 25 vehicles per kilometer and lane, simulations by Helbing and Huberman (1998) indicated a transition to a *coherent movement* of cars and trucks, which they could confirm empirically [compare Fig. 43(a) with Figs. 15(b) and 15(c)]. In this state, fast and slow vehicles drive with the same speed, i.e., they are moving like a solid block. This is caused by a breakdown of the lane-changing rate [see Fig. 43(b)] when the freeway becomes crowded, so that drivers no longer find sufficiently large gaps for overtaking [see Fig. 43(c)]. However, the coherent state is destroyed when traffic flow becomes unstable. Then vehicle gaps are again widely scattered [see Fig. 43(d)], and lane changing is sometimes possible.

The properties of multilane traffic have recently been the subject of considerable interest, as is documented by further studies (Chowdhury, Wolf, and Schreckenberg, 1997; Belitsky *et al.*, 2001; see also Goldbach *et al.*, 2000; Lubashevsky and Mahnke, 2000).

E. Bidirectional and city traffic

Traffic models have also been developed for bidirectional traffic (Dutkiewicz *et al.*, 1995; Lee *et al.*, 1997; Simon and Gutowitz, 1998; Fouladvand and Lee, 1999) and city traffic.[9] Interested readers should consult the reviews by Papageorgiou (1999), Chowdhury, Santen, and Schadschneider (2000), and the corresponding chapters in *Traffic and Granular Flow '97, '99* (Schreckenberg and Wolf, 1998; Helbing, Herrmann, *et al.*, 2000). Here I shall be very brief.

Traffic dynamics in cities is quite different from that on freeways, since it is to a large extent determined by the intersections. The first model for city traffic in the physics literature goes back to Biham, Middleton, and Levine (1992). It is based on a two-dimensional square lattice with periodic boundary conditions, in which each site represents a crossing of northbound and eastbound traffic. The sites can be either empty or occupied by a northbound or eastbound vehicle. Eastbound vehicles are synchronously updated every odd time step, while northbound vehicles are updated every even time step, reflecting synchronized and periodic traffic signals at the crossings. During the parallel updates, a vehicle moves ahead by one site, if this is empty; otherwise it has to wait. Biham *et al.* (1992) observed a first-order transition from free traffic to jammed traffic with zero velocity throughout the system, which appears at a finite density due to a gridlock of northbound and eastbound traffic along diagonal lines (see also Fukui and Ishibashi, 1996b). This first-order transition is also characteristic for most other models of city traffic. For a detailled discussion of the related literature see the review by Chowdhury, Santen, and Schadschneider (2000).

F. Effects beyond physics

There are some effects that are not at all or only partly represented by the physical traffic models described in Sec. III:

(i) the anticipation behavior of drivers (Ozaki, 1993; Wagner, 1998a; Lenz *et al.*, 1999; Knospe *et al.*, 2000a, 2000b);
(ii) the reaction to blinkers,
(iii) the avoidance of driving side by side,
(iv) the adaptation of velocity to surrounding traffic (Herman *et al.*, 1973),
(v) the tolerance of small time clearances for a limited time (Treiterer and Myers, 1974);
(vi) the reduction of gaps to avoid vehicles' cutting in (Daganzo, 1999a),
(vii) the avoidance of the truck lane, even if it is underutilized [Brackstone and McDonald, 1996; Daganzo, 1997c, 1999a (the "Los Gatos effect"); Helbing, 1997a, 1997b; Helbing and Huberman, 1998],
(viii) motivations for lane changing (Redelmeier and Tibshirani, 1999),
(ix) effects of attention (Michaels and Cozan, 1962; Todosiev, 1963; Todosiev and Barbosa, 1963/64; Michaels, 1965),
(x) changes of driver strategies (Migowsky *et al.*, 1994),
(xi) effects of road conditions, visibility, etc.

Certainly such effects can be also modeled in a mathematical way, and this has partly been done in submicroscopic models of vehicle dynamics (Wiedemann, 1974) and vehicle simulators such as VISSIM (Fellendorf, 1996) or PELOPS (Ludmann *et al.*, 1997). However, most of the above effects are hard to test empirically and difficult to verify or disprove. Therefore we are leaving the realm of physics here and eventually entering the realm of driver psychology (Daganzo, 1999a).

G. Traffic control and optimization

Traffic control and optimization is an old and large field (see, for example, Cremer, 1978; Cremer and May, 1985; Smulders, 1989; Kühne, 1993; Dougherty, 1995; Kühne *et al.*, 1995, 1997; Taale and Middelham, 1995; Schweitzer, Ebeling, *et al.*, 1998), too extensive to be discussed in detail here. Overviews of optimization approaches by physicists can be found in the *Proceedings of the Workshops on Traffic and Granular Flow* (Wolf *et al.*, 1996; Schreckenberg and Wolf, 1998; Helbing,

[9]See, for example, the following articles and simulation programs: TRANSYT by Robertson, 1969a, 1969b; Schmidt-Schmiedebach, 1973; Herman and Prigogine, 1979; SCOOT by Hunt *et al.*, 1982; Cremer and Ludwig, 1986; Williams *et al.*, 1987; Mahmassani *et al.*, 1990; MAKSIMOS by Putensen, 1994; MIXSIM by Hoque and McDonald, 1995; PADSIM by Peytchev and Bargiela, 1995.

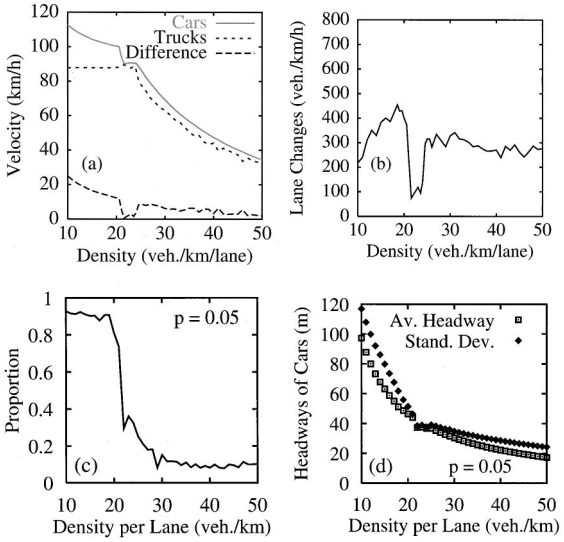

FIG. 43. Lane changing as a function of traffic density: (a) transition to coherent vehicle traffic; (b) breakdown of the lane-changing rate at densities above 20 vehicles per kilometer and lane; (c) rapid decay of the proportion of successful lane changes (i.e., the quotient between actual and desired lane changes). (d) Opportunities for lane changing rapidly diminish as gaps corresponding to about twice the safe headway required for lane changing cease to exist, i.e., when the quotient of the standard deviation of vehicle headways to their mean value is small. The breakdown of the lane-changing rate seems to imply a decoupling of the lanes, i.e., an effective one-lane behavior. However, this is already the result of a self-organization process based on two-lane interactions, since any significant perturbation of the coherent state (like different velocities in the neighboring lanes) will cause frequent lane changes (Shvetsov and Helbing, 1999). By filling large gaps, the gap distribution is considerably modified. This eventually reduces the possibilities for lane changes so that the coherent state is restored. After Helbing and Huberman, 1998; see also Helbing, 2001.

Herrmann, *et al.*, 2000; see also Claus *et al.*, 1999), while readers interested in the engineering literature are referred to the books and review articles of Pagageorgiou (1995, 1999) and Lapierre and Steierwald (1987). These also discuss the available software packages for the simulation and optimization of street networks and/or traffic lights such as TRANSYT (Robertson, 1969a, 1969b), SCOOT (Hunt *et al.*, 1982), OPAC (Gartner, 1983), PRODYN (Farges *et al.*, 1984), CRONOS (Boillot *et al.*, 1992), and many others. I should also mention the cellular-automata-based projects OLSIM (Kaumann *et al.*, 2000; see http://www.traffic.uni-duisburg.de/OLSIM/) and TRANSIMS (Nagel and Barrett, 1997; Rickert and Nagel, 1997; Simon and Nagel, 1998; see http://www-transims.tsasa.lanl.gov). A complementary list of microsimulation tools can be found at http://www.its.leeds.ac.uk/smartest/links.html.

While optimization of city traffic is based on a synchronization of traffic lights, most optimization approaches for freeways are based on a homogenization of vehicle traffic, as stop-and-go traffic, jams, and congested traffic are associated with reduced efficiency due to a capacity drop (see, for example, Huberman and Helbing, 1999), often triggered by perturbations in the flow (see Sec. IV.B). Perturbations should, therefore, be suppressed by technical measures such as intelligent speed limits, adaptive on-ramp controls, traffic-dependent rerouting, and driver assistance systems (see, for example, Treiber and Helbing, 2001).

V. PEDESTRIAN TRAFFIC

Pedestrian crowds have been empirically studied for more than four decades now (Hankin and Wright, 1958; Oeding, 1963; Hoel, 1968; Older, 1968; Navin and Wheeler, 1969; Carstens and Ring, 1970; O'Flaherty and Parkinson, 1972; Weidmann, 1993). The evaluation methods applied have been based on direct observation, photographs, and time-lapse films. Apart from behavioral investigations (Hill, 1984; Batty, 1997), the main goal of these studies was to develop a level-of-service concept (Fruin, 1971; Polus *et al.*, 1983; Mōri and Tsukaguchi, 1987), design elements of pedestrian facilities (Schubert, 1967; Boeminghaus, 1982; Pauls, 1984; Whyte, 1988; Helbing, 1997a; Helbing, Molnár, *et al.*, 2001), or planning guidelines (Kirsch, 1964; Predtetschenski and Milinski, 1971; Transportation Research Board, 1985; Davis and Braaksma, 1988; Brilon *et al.*, 1993). The guidelines usually have the form of regression relations which are, however, not very well suited for the prediction of pedestrian flows in pedestrian zones and buildings with an unusual architecture, or for extreme conditions such as evacuation (see Sec. V.D). Therefore a number of simulation models have been proposed, e.g., queueing models (Yuhaski and Macgregor Smith, 1989; Roy, 1992; Løvås, 1994; Hamacher and Tjandra, 2001), transition matrix models (Garbrecht, 1973), and stochastic models (Mayne, 1954; Ashford *et al.*, 1976), which are partly related to each other. In addition, there are models for the route choice behavior of pedestrians (Borgers and Timmermans, 1986a, 1986b; Helbing, 1992a; Timmermans *et al.*, 1992; Hoogendoorn *et al.*, 2001).

None of these concepts adequately takes into account the self-organization effects occurring in pedestrian crowds, effects which may, however, lead to unexpected obstructions due to mutual disturbances of pedestrian flows. More promising in this regard is the approach taken by Henderson. He conjectured that pedestrian crowds behave similarly to gases or fluids (Henderson, 1971, 1974; Henderson and Lyons, 1972; Henderson and Jenkins, 1973; see also AlGadhi and Mahmassani, 1990; Hughes, 2000, 2001; AlGadhi *et al.*, 2001). This could be partially confirmed (see Sec. V.A). However, a realistic gas-kinetic or fluid-dynamic theory for pedestrians must contain corrections due to their particular interactions (i.e., avoidance and deceleration maneuvers), which, of course, do not conserve momentum and energy. Although such a theory can actually be formulated (Helbing, 1992a, 1992b; Hoogendoorn and Bovy, 2000a), for practical applications a direct simulation of individual

pedestrian motion is preferable, since this is more flexible. As a consequence, current research focuses on the microsimulation of pedestrian crowds, which also allows one to consider the breakdown of coordination by excluded-volume effects related to the discrete, "granular" structure of pedestrian flows. In this connection, a social (behavioral) force model of individual pedestrian dynamics has been developed (Helbing, 1991, 1996d, 1997a, 1998b; Helbing *et al.*, 1994; Helbing and Molnár, 1995, 1997; Molnár, 1996a, 1996b; Helbing and Vicsek, 1999; Helbing *et al.*, 2000a, 2000b; see Secs. I.C and V.B). A discrete and simple forerunner of this model was proposed by Gipps and Marksjö (1985). There have been many other recent models of pedestrian traffic dynamics. These include microsimulation models (Kayatz, 2000; Hoogendoorn *et al.*, 2001; Sugiyama *et al.*, 2001); cellular automaton models (Blue and Adler, 1998, 1999, 2001a, 2001b; Bolay, 1998; Fukui and Ishibashi, 1999a, 1999b; Muramatsu *et al.*, 1999; Klüpfel *et al.*, 2000; Muramatsu and Nagatani, 2000a, 2000b; Burstedde, Kirchner, *et al.*, 2001; Burstedde, Klauck, *et al.*, 2001; Dijkstra *et al.*, 2001; Keßel *et al.*, 2001; Schadschneider, 2001), emergency and evacuation models (Drager *et al.*, 1992; Ebihara *et al.*, 1992; Ketchell *et al.*, 1993; Okazaki and Matsushita, 1993; Still, 1993, 2000; Thomson and Marchant, 1993; Løvås, 1998; Klüpfel *et al.*, 2000; Hamacher and Tjandra, 2001), and artificial-intelligence-based models (Gopal and Smith, 1990; Reynolds, 1994, 1999; Schelhorn *et al.*, 1999; Dijkstra *et al.*, 2001).

A. Observations

Together with my collaborators I have investigated pedestrian motion for several years and have evaluated a number of video films. Despite the sometimes chaotic appearance of individual pedestrian behavior, one can find patterns, some of which become best visible in time-lapse films like those produced by Arns (1993). In describing these, I also summarize results of other pedestrian studies and observations (the following summary is based on Helbing, 1997a, 1998b; Helbing, Molnár, *et al.*, 2001c):

(i) Pedestrians feel a strong aversion to taking detours or moving opposite to their desired walking direction, even if the direct way is crowded. However, there is also some evidence that pedestrians normally choose the *fastest* route to their next destination, but not the *shortest* one (Ganem, 1998). In general, pedestrians take into account detours as well as the comfort of walking, thereby minimizing the effort to reach their destination (Helbing, Keltsch, and Molnár, 1997; Helbing, Schweitzer, *et al.*, 1997). Their paths can be approximated by polygons.

(ii) Pedestrians prefer to walk with an individual desired speed, which corresponds to the most comfortable (i.e., least energy-consuming) walking speed (see Weidmann, 1993) as long as it is not necessary to go faster in order to reach the destination in time. The desired speeds within pedestrian crowds are Gaussian distributed with a mean value of approximately 1.34 m/s and a standard deviation of about 0.26 m/s (Henderson, 1971). However, the average speed depends on the situation (Predtetschenski and Milinski, 1971), sex and age, time of day, purpose of the trip, surroundings, etc. (see Weidmann, 1993).

(iii) Pedestrians keep a certain distance from other pedestrians and borders (of streets, walls, and obstacles; see the Transportation Research Board, 1985; Brilon *et al.*, 1993). This distance is smaller the more hurried a pedestrian is, and it decreases with growing pedestrian density. Resting individuals (waiting on a railway platform for a train, sitting in a dining hall, or lying at a beach) are uniformly distributed over the available area if there are no acquaintances among the individuals. Pedestrian density increases (i.e., interpersonal distances lessen) around particularly attractive places. It decreases with growing velocity variance (for example, on a dance floor; see Helbing, 1992b, 1997a). Individuals who know each other may form groups which are entities behaving similarly to single pedestrians. Group sizes are Poisson distributed (Coleman and James, 1961; Coleman, 1964; Goodman, 1964).

(iv) In situations of escape panic (Helbing, Farkas, and Vicsek, 2000b), individuals are often nervous, and sometimes they move irrationally. Moreover, people move or try to move considerably faster than normal (Predtetschenski and Milinski, 1971). Individuals start pushing, and interactions among people become physical in nature. Moving and, in particular, passing of a bottleneck becomes uncoordinated (Mintz, 1951). At exits, arching and clogging are observed (Predtetschenski and Milinski, 1971), and jams build up (Mintz, 1951). The physical interactions in the jammed crowd add up and cause dangerous pressures up to 4500 Newtons per meter (Elliott and Smith, 1993; Smith and Dickie, 1993), which can bend steel barriers or tear down brick walls. Escape is further slowed by fallen or injured people turning into "obstacles." Finally, people tend to show herding behavior, i.e., to do what other people do (Quarantelli, 1957; Keating, 1982). As a consequence, alternative exits are often overlooked or not efficiently used in escape situations (Keating, 1982; Elliott and Smith, 1993).

(v) At medium and high pedestrian densities, the motion of pedestrian crowds shows some striking analogies with the motion of gases, fluids, and granular flows. For example, I found that footprints of pedestrians in snow look similar to streamlines of fluids (Helbing, 1992a). At borderlines between opposite directions of walking one can observe "viscous fingering" (Kadanoff, 1985; Stanley and Ostrowsky, 1986). The emergence of pedestrian streams through standing crowds

(Arns, 1993; Helbing, 1997a, Fig. 2.6; 1998b, Fig. 1; Helbing, Molnár, *et al.*, 2001, Fig. 1) appears analogous to the formation of river beds (Stølum, 1996; Rodríguez-Iturbe and Rinaldo, 1997; Caldarelli, 2001). Moreover, in a manner similar to segregation or stratification phenomena in granular media (Santra *et al.*, 1996; Makse *et al.*, 1997), pedestrians spontaneously organize into lanes of uniform walking direction, if the pedestrian density is high enough (Oeding, 1963; Helbing, 1991, 1997a, Fig. 2.5; 1998b, Fig. 2; Helbing, Molnár, *et al.*, 2001, Fig. 2). At bottlenecks (e.g., corridors, staircases, or doors), the passing direction of pedestrians oscillates (Helbing *et al.*, 1994; Helbing and Molnár, 1995). This may be compared to the "saline oscillator" (Yoshikawa *et al.*, 1991) or the granular "ticking hour glass" (Wu *et al.*, 1993; Pennec *et al.*, 1996). Finally, one can find the propagation of shock waves in dense pedestrian crowds pushing forward (see also Virkler and Elayadath, 1994). The arching and clogging in panicking crowds (Helbing *et al.*, 2000b) is similar to the outflow of rough granular media through small openings (Ristow and Herrmann, 1994; Wolf and Grassberger, 1997).

B. Social (behavioral) force model of pedestrian dynamics

For reliable simulations of pedestrian crowds we do not need to know whether a certain pedestrian, say, turns to the right at the next intersection. It is sufficient to have a good estimate of what percentage of pedestrians turns to the right. This can be either empirically measured or calculated by means of a route choice model like that of Borgers and Timmermans (1986a, 1986b). In some sense, the uncertainty about individual behaviors is averaged out at the macroscopic level of description, as in fluid dynamics.

Nevertheless, I shall now focus on a more flexible microscopic simulation approach based on the social (behavioral) force concept outlined in Sec. I.C. Particular advantages of this approach are the consideration of (i) excluded-volume effects due to the granular structure of a pedestrian crowd and (ii) the flexible usage of space by pedestrians, requiring a (quasi)continuous treatment of motion. It turns out that these points are essential to reproduce the above-mentioned phenomena in a natural way.

As outlined in Sec. I.C, we describe the different motivations of and influences on a pedestrian α by separate force terms. First of all, the decisions and intentions of where and how fast to go are reflected by the driving term $v_\alpha^0(t)\mathbf{e}_\alpha^0(t)/\tau_\alpha$, in which $v_\alpha^0(t)$ is the desired velocity and $\mathbf{e}_\alpha^0(t)$ the desired direction of motion. The interactions among pedestrians are described by forces

$$\mathbf{f}_{\alpha\beta}(t)=\mathbf{f}_{\alpha\beta}^{\mathrm{soc}}(t)+\mathbf{f}_{\alpha\beta}^{\mathrm{ph}}(t), \tag{120}$$

which consist of a socio-psychological contribution $\mathbf{f}_{\alpha\beta}^{\mathrm{soc}}(t)$ and physical interactions $\mathbf{f}_{\alpha\beta}^{\mathrm{ph}}(t)$, if pedestrians come too close to each other. The socio-psychological component reflects the tendency of pedestrians to keep a certain distance from other pedestrians and may be described by a force of the form

$$\mathbf{f}_{\alpha\beta}^{\mathrm{soc}}(t)=A_\alpha \exp[(r_{\alpha\beta}-d_{\alpha\beta})/B_\alpha]\mathbf{n}_{\alpha\beta} \times\left(\lambda_\alpha+(1-\lambda_\alpha)\frac{1+\cos(\varphi_{\alpha\beta})}{2}\right). \tag{121}$$

Here, A_α denotes the interaction strength and B_α the range of the repulsive interaction, which are individual parameters and partly dependent on cultural conventions. $d_{\alpha\beta}(t)=\|\mathbf{x}_\alpha(t)-\mathbf{x}_\beta(t)\|$ is the distance between the centers of mass of pedestrians α and β, $r_{\alpha\beta}=(r_\alpha+r_\beta)$ the sum of their radii r_α and r_β, and

$$\mathbf{n}_{\alpha\beta}(t)=(n_{\alpha\beta}^1(t),n_{\alpha\beta}^2(t))=\frac{\mathbf{x}_\alpha(t)-\mathbf{x}_\beta(t)}{d_{\alpha\beta}(t)}$$

the normalized vector pointing from pedestrian β to α. Finally, with the choice $\lambda_\alpha<1$, we can take into account the anisotropic character of pedestrian interactions, as the situation in front of a pedestrian has a larger impact on his or her behavior than things happening behind. The angle $\varphi_{\alpha\beta}(t)$ denotes the angle between the direction $\mathbf{e}_\alpha(t)=\mathbf{v}_\alpha(t)/\|\mathbf{v}_\alpha(t)\|$ of motion and the direction $-\mathbf{n}_{\alpha\beta}(t)$ of the object exerting the repulsive force, i.e., $\cos\varphi_{\alpha\beta}(t)=-\mathbf{n}_{\alpha\beta}(t)\cdot\mathbf{e}_\alpha(t)$. One may, of course, take into account other details such as a velocity dependence of the forces and noncircular-shaped pedestrian bodies, but this has no qualitative effect on the dynamics of the simulations. In fact, most observed self-organization phenomena are quite insensitive to the specification of the interaction forces, as different studies have shown (Helbing and Molnár, 1995; Molnár, 1996a; Helbing and Vicsek, 1999; Helbing *et al.*, 2000a, 2000b).

The physical interaction $\mathbf{f}_{\alpha\beta}^{\mathrm{ph}}$ plays a role only when pedestrians have physical contact with each other, i.e., if $r_{\alpha\beta}\geqslant d_{\alpha\beta}$. In this case, we assume two additional forces inspired by granular interactions (Ristow and Herrmann, 1994; Wolf and Grassberger, 1997): First, a *body force* $k(r_{\alpha\beta}-d_{\alpha\beta})\mathbf{n}_{\alpha\beta}$ counteracting body compression and second a *sliding friction force* $\kappa(r_{\alpha\beta}-d_{\alpha\beta})\Delta v_{\beta\alpha}^t\mathbf{t}_{\alpha\beta}$ impeding relative tangential motion:

$$\mathbf{f}_{\alpha\beta}^{\mathrm{ph}}(t)=k\Theta(r_{\alpha\beta}-d_{\alpha\beta})\mathbf{n}_{\alpha\beta}+\kappa\Theta(r_{\alpha\beta}-d_{\alpha\beta})\Delta v_{\beta\alpha}^t\mathbf{t}_{\alpha\beta}, \tag{122}$$

where the function $\Theta(z)$ is equal to its argument z, if $z>0$, otherwise 0. Moreover, $\mathbf{t}_{\alpha\beta}=(-n_{\alpha\beta}^2,n_{\alpha\beta}^1)$ is the tangential direction and $\Delta v_{\beta\alpha}^t=(\mathbf{v}_\beta-\mathbf{v}_\alpha)\cdot\mathbf{t}_{\alpha\beta}$ the tangential velocity difference, while k and κ represent large constants. Strictly speaking, friction effects already set in before pedestrians touch each other, because of the socio-psychological tendency not to pass other individuals with a high relative velocity when the distance is small. This is, however, not important for the effects we discuss below.

The interaction with boundaries like walls and other obstacles is treated analogously to pedestrian interactions, i.e., if $d_{\alpha b}(t)$ is the distance to boundary b, $\mathbf{n}_{\alpha b}(t)$ denotes the direction perpendicular to it, and $\mathbf{t}_{\alpha b}(t)$ the

direction tangential to it, the corresponding interaction force with the boundary reads

$$\mathbf{f}_{\alpha b}=\{A_\alpha \exp[(r_\alpha-d_{\alpha b})/B_\alpha]+k\Theta(r_\alpha-d_{\alpha b})\}\mathbf{n}_{\alpha b} - \kappa\Theta(r_\alpha-d_{\alpha b})(\mathbf{v}_\alpha\cdot\mathbf{t}_{\alpha b})\mathbf{t}_{\alpha b}\,. \quad (123)$$

Moreover, we may also take into account time-dependent attractive interactions towards window displays, sights, or special attractions i by social forces of the type of Eq. (121). However, in comparison with repulsive interactions, the corresponding interaction range $B_{\alpha i}$ is usually larger and the strength parameter $A_{\alpha i}(t)$ typically smaller, negative, and time dependent. Additionally, the joining behavior (Dewdney, 1987) of families, friends, or tourist groups can be reflected by forces of the type $\mathbf{f}^{\rm att}_{\alpha\beta}(t)=-C_{\alpha\beta}\mathbf{n}_{\alpha\beta}(t)$, which guarantee that acquainted individuals rejoin, after they have accidentally been separated by other pedestrians. Finally, we can take into account unsystematic variations of individual behavior and voluntary deviations from the assumed behavioral laws by a fluctuation term $\boldsymbol{\xi}_\alpha(t)$. Therefore the resulting pedestrian model corresponds to Eq. (3), but the sum of interaction forces $\Sigma_{\beta(\neq\alpha)}\mathbf{f}_{\alpha\beta}(t)$ is replaced by the sum of all the above-mentioned attractive and repulsive interaction and boundary forces. The resulting expression looks rather complicated, but in the following, we shall drop attraction effects and assume $\lambda_\alpha=0$ for simplicity, so that the interaction forces become isotropic and conform with Newton's third law. Moreover, the physical interactions are relevant mainly in panic situations, so we normally have just repulsive social and boundary interactions: $\Sigma_{\beta(\neq\alpha)}\mathbf{f}^{\rm soc}_{\alpha\beta}(t)+\Sigma_b\mathbf{f}_{\alpha b}(t)$.

C. Self-organization phenomena and noise-induced ordering

Despite its simplifications, the behavioral force model of pedestrian dynamics describes a large number of observed phenomena quite realistically. In particular, it allows one to explain various self-organized spatio-temporal patterns that are not externally planned, prescribed, or organized, e.g., by traffic signs, laws, or behavioral conventions. Instead, the spatio-temporal patterns discussed below emerge due to the nonlinear interactions of pedestrians even without assuming strategic considerations, communication, or imitative behavior of pedestrians. All these collective patterns of motion are symmetry-breaking phenomena, although the model was formulated as completely symmetric with respect to the right-hand and the left-hand sides (Helbing, 1997a, 1998b; Helbing and Molnár, 1997; Helbing, Molnár, *et al.*, 2001). Several of the self-organization phenomena discussed below could in the meantime be reproduced with other simulation models as well (see, for example, Kayatz, 2000; Still, 2000; Blue and Adler, 2001a, 2001b; Burstedde, Kirchner, *et al.*, 2001; Burstedde, Klauck, *et al.*, 2001; Hoogendoorn *et al.*, 2001; Schreckenberg and Sharma, 2001).

1. Segregation

The microsimulations reproduce the empirically observed formation of lanes consisting of pedestrians with the same desired walking direction; see Fig. 44 (Helbing *et al.*, 1994; Helbing and Molnár, 1995, 1997; Helbing, 1996d, 1997a; Molnár, 1996a, 1996b; Helbing and Vicsek, 1999; Helbing, Molnár, *et al.*, 2001). For open boundary conditions, these lanes are dynamically varying. Their number depends on the width of the street (Helbing and Molnár, 1995; Helbing, 1997a), on pedestrian density, and on the noise level. Interestingly, one finds a noise-induced ordering (Helbing and Vicsek, 1999; Helbing and Platkowski, 2000): Compared to low noise amplitudes, medium ones result in a more pronounced segregation (i.e., a smaller number of lanes), while high noise amplitudes lead to a "freezing by heating" effect (see Sec. V.D.1).

The conventional interpretation of lane formation is as follows: Pedestrians tend to walk on the side prescribed in vehicular traffic. However, the above model can explain lane formation even without assuming a preference for any side (Helbing and Vicsek, 1999; Helbing, Farkas, and Vicsek, 2000a). The most relevant point is the higher relative velocity of pedestrians walking in opposite directions. As a consequence, they have more frequent interactions until they have segregated into separate lanes. The resulting collective pattern of motion minimizes avoidance maneuvers, if fluctuations are weak. Assuming identical desired velocities $v^0_\alpha=v_0$, the most stable configuration corresponds to a state with minimal interaction strength,

$$-\frac{1}{N}\sum_{\alpha\neq\beta}\tau\mathbf{f}_{\alpha\beta}\cdot\mathbf{e}^0_\alpha\approx\frac{1}{N}\sum_\alpha(v_0-\mathbf{v}_\alpha\cdot\mathbf{e}^0_\alpha)=v_0(1-E).$$

It is related to a maximum *efficiency of motion*,

$$E=\frac{1}{N}\sum_\alpha\frac{\mathbf{v}_\alpha\cdot\mathbf{e}_\alpha}{v_0} \quad (124)$$

(Helbing and Vicsek, 1999). The efficiency E with $0\leqslant E\leqslant 1$ (where $N=\Sigma_\alpha 1$ is the number of pedestrians α) describes the average fraction of the desired speed v_0 with which pedestrians actually approach their destinations. That is, lane formation "globally" maximizes the average velocity into the desired direction of motion, although the model does not even assume that pedestrians would try to optimize their behavior locally. This is a consequence of the symmetrical interactions among pedestrians with opposite walking directions. One can even show that a large class of driven many-particle systems, if they self-organize at all, tend to globally optimize their state (Helbing and Vicsek, 1999). This "optimal self-organization" was also observed in the formation of coherent motion in a system of cars and trucks, which was related with a minimization of the lane-changing rate (see Sec. IV.D.2). Another example is the emergence of optimal path systems by bundling of trails (see Fig. 1).

2. Oscillations

In simulations of bottlenecks like doors, oscillatory changes (alternation) of the passing direction are observed if people do not panic; see Fig. 45 (Helbing, Molnár, and Schweitzer, 1994; Helbing and Molnár, 1995, 1997; Helbing, 1996d, 1997a; Molnár, 1996a, 1996b; Helbing, Molnár, *et al.*, 2001).

The mechanism leading to alternating flows is the following: Once a pedestrian is able to pass the narrowing, pedestrians with the same walking direction can easily follow. Hence the number and "pressure" of waiting and pushing pedestrians becomes less than on the other side of the narrowing where, consequently, the chance to occupy the passage grows. This leads to a deadlock situation that is followed by a change in the passing direction. Getting through the bottleneck is easier if it is broad and short so that the passing direction changes more frequently. Note that two adjacent separate doors in a wall are more efficient than one single door with double width. By self-organization, each door is then used by one walking direction for a long time; see Fig. 46 (Molnár, 1996a, 1996b; Helbing, 1997a, 1998b; Helbing and Molnár, 1997; Helbing, Molnár, *et al.*, 2001). The reason is that pedestrians who pass a door clear the way for their successors, in a manner similar to lane formation.

3. Rotation

At intersections one is confronted with various alternating collective patterns of motion which are very short-lived and unstable. For example, phases during which the intersection is crossed in "vertical" or "horizontal" direction alternate with phases of temporary roundabout traffic; see Fig. 47 (Helbing *et al.*, 1994; Helbing, 1996d, 1997a; Molnár, 1996a, 1996b; Helbing and Molnár, 1997; Helbing, Molnár, *et al.*, 2001). This self-organized roundabout traffic is similar to the emergent rotation found for self-driven particles (Duparcmeur *et al.*, 1995). It is connected with small detours but decreases the frequency of necessary deceleration, stopping, and avoidance maneuvers considerably, so that pedestrian motion becomes more efficient on average. The efficiency of pedestrian flow can be increased by putting an obstacle in the center of the intersection, since this favors smooth roundabout traffic compared with competing, inefficient patterns of motion (Molnár, 1996a; Helbing, 1997a).

D. Collective phenomena in panic situations

The behavior of pedestrians in panic situations (e.g., in some cases of emergency evacuation) displays certain characteristic features:

(i) People get nervous, resulting in a higher level of fluctuations.
(ii) They try to escape from the cause of panic, which can be reflected by a significantly higher desired velocity.

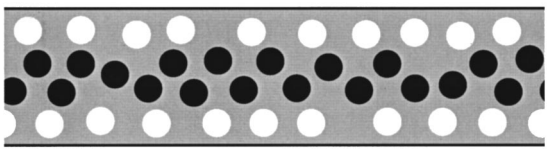

FIG. 44. Formation of lanes in initially disordered pedestrian crowds with opposite walking directions: white circles, pedestrians moving from left to right; black circles, pedestrians moving in the opposite direction. Lane formation does not require the periodic boundary conditions applied above; see the Java applet http://www.helbing.org/Pedestrians/Corridor.html. After Helbing, Farkas, and Vicsek, 2000a; Helbing, 2001; see also Helbing, Molnár, and Schweitzer, 1994; Helbing and Molnár, 1995.

(iii) Individuals in complex situations who do not know what is the right thing to do orient themselves by the actions of their neighbors, i.e., they tend to do what other people do. We shall describe this as an additional herding interaction, but attractive interactions probably have a similar effect.

Let us now discuss the fundamental collective effects of fluctuations, increased desired velocities, and herding behavior. In contrast to other approaches, we do not assume or imply that individuals in panic or emergency situations would behave in a relentless or asocial manner, although they sometimes do.

1. "Freezing by heating"

The effect of getting nervous has been investigated by Helbing, Farkas, and Vicsek (2000a). Let us assume that the individual level of fluctuations is given by

$$\eta_\alpha = (1 - n'_\alpha)\,\eta_0 + n'_\alpha \eta_{\max}, \tag{125}$$

where n'_α with $0 \leqslant n'_\alpha \leqslant 1$ measures the nervousness of pedestrian α. The parameter η_0 is the normal and $\eta_{\max}$ the maximum fluctuation strength. It turned out that, at sufficiently high pedestrian densities, lanes were destroyed by increasing the fluctuation strength (which is analogous to the temperature). However, instead of the expected transition from the "fluid" lane state to a disordered, "gaseous" state, Helbing *et al.* found the formation of a solid state. It was characterized by a blocked situation with a regular (i.e., "crystallized" or "frozen") structure so that this paradoxial transition was called *freezing by heating* (see Fig. 48). Remarkably, the blocked state had a *higher* degree of order, although the internal energy was increased and the resulting state was metastable with respect to structural perturbations such as the exchange of oppositely moving particles. Therefore "freezing by heating" is just the opposite of what one would expect for equilibrium systems and different from fluctuation-driven ordering phenomena in metallic glasses and some granular systems (Rosato *et al.*, 1987; Gallas *et al.*, 1992; Umbanhowar *et al.*, 1996), where fluctuations lead from a disordered metastable state to

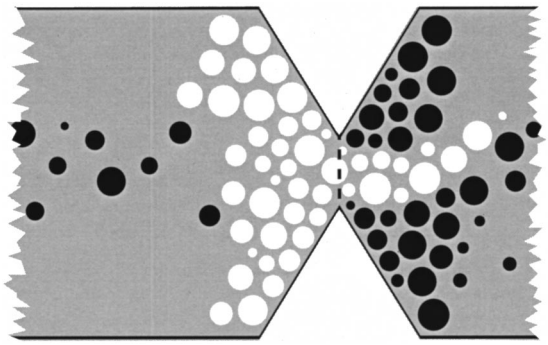

FIG. 45. Oscillations of the passing direction at a bottleneck. After Helbing, 2001; see also Helbing, Molnár, and Schweitzer, 1994; Helbing and Molnár, 1995. Dynamic simulations are available at http://www.helbing.org/Pedestrians/Door.html.

an ordered stable state. A model for related noise-induced ordering processes has been developed by Helbing and Platkowski (2000).

The preconditions for the unusual freezing-by-heating transition are the additional driving term and dissipative friction. Inhomogeneities in the channel diameter or other impurities that temporarily slow down pedestrians can further this transition at the places in question. Finally note that a transition from fluid to blocked pedestrian counterflows is also observed when a critical particle density is exceeded (Muramatsu *et al.*, 1999; Helbing, Farkas, and Vicsek, 2000a).

2. "Faster-is-slower effect"

The effect of increasing the desired velocity was studied by Helbing, Farkas, and Vicsek (2000b). They found that the simulated outflow from a room is well coordinated and regular if the desired velocities $v_\alpha^0 = v_0$ are normal. However, for desired velocities above 1.5 m/s, i.e., for people in a rush (as in many panic situations), one observes an irregular succession of archlike blockings of the exit and avalanchelike bunches of leaving pedestrians when the arches break up (see Fig. 49). This phenomenon is compatible with the empirical observations mentioned above and comparable to intermittent clogging found in granular flows through funnels or hoppers (Ristow and Herrmann, 1994; Wolf and Grassberger, 1997).

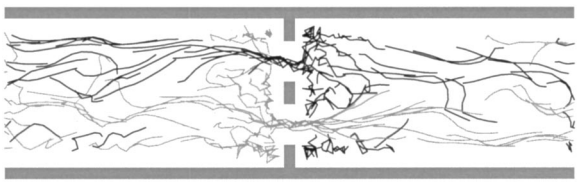

FIG. 46. Pedestrians with opposite walking directions using different doors as a result of self-organization when two alternative passageways are available. After Molnár, 1996a, 1996b; Helbing and Molnár, 1997; Helbing, 1997a, 1998b; Helbing, Molnár, *et al.*, 2001.

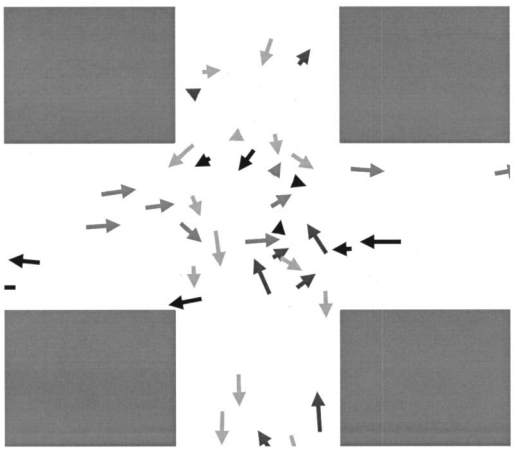

FIG. 47. Self-organized, short-lived roundabout traffic in intersecting pedestrian streams. From Helbing, 1996d, 1997a; Helbing and Molnár, 1997; Helbing, Molnár, *et al.*, 2001; see also Helbing, Molnár, and Schweitzer, 1994; Molnár, 1996a, 1996b.

Because clogging is connected with delays, trying to move faster (i.e., increasing v_α^0) can cause a smaller average speed of leaving, if the friction parameter κ is large (Helbing, Farkas, and Vicsek, 2000b). This "faster-is-slower effect" is particularly tragic in the presence of fires, where fleeing people sometimes reduce their own chances of survival. As a consequence, models for everyday pedestrian streams are not very suitable for realistic simulations of emergency situations, which require at least modified parameter sets corresponding to less efficient pedestrian behavior. Related fatalities can be estimated by the number of pedestrians reached by the fire front (see http://angel.elte.hu/~panic/ or http://www.panics.org).

Since interpersonal friction is assumed to have, on average, no deceleration effect in a crowd if the boundaries are sufficiently remote, the arching underlying the clogging effect requires a combination of several effects: First, slowing down due to a bottleneck such as a door, and second, strong interpersonal friction, which becomes an important factor only when pedestrians get too close to each other. It is, however, noteworthy that the faster-is-slower effect also occurs when the sliding friction force changes continuously with the distance rather than being "switched on" at a certain distance r_β as in the model above.

The danger of clogging can be minimized by avoiding bottlenecks in the construction of stadia and public buildings. Notice, however, that jamming can also occur at widenings of escape routes. This comes from disturbances due to pedestrians who expand into the wide area because of their repulsive interactions or try to overtake each other. These squeeze into the main stream again at the end of the widening, which acts like a bottleneck and leads to jamming. Significantly improved outflows in panic situations can be achieved by columns placed asymmetrically in front of the exits, which reduce the pressure at the door and thereby also reduce injuries (see http://angel.elte.hu/~panic/ or http://www.panics.org).

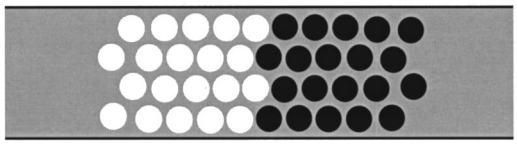

FIG. 48. Noise-induced formation of a crystallized, "frozen" state in a periodic corridor used by oppositely moving pedestrians. After Helbing, Farkas, and Vicsek, 2000a; Helbing, 2001.

3. "Phantom panics"

Sometimes, panics have occurred without any comprehensible reason such as a fire or another threatening event. Due to the "faster-is-slower effect," panics can be triggered by small pedestrian counterflows (Elliott and Smith, 1993), which cause delays to the crowd intending to leave. Stopped pedestrians in the back, who do not see the reason for the temporary slowdown, become impatient and pushy. In accordance with observations (Helbing, 1991, 1997a), one may describe this by an increase in the desired velocity, for example, by the formula

$$v_\alpha^0(t)=[1-n'_\alpha(t)]v_\alpha^0(0)+n'_\alpha(t)v_\alpha^{\max}. \tag{126}$$

Here, $v_\alpha^{\max}$ is the maximum desired velocity and $v_\alpha^0(0)$ the initial one, corresponding to the expected velocity of leaving. The time-dependent parameter

$$n'_\alpha(t)=1-\frac{\overline{v}_\alpha(t)}{v_\alpha^0(0)} \tag{127}$$

reflects the nervousness of pedestrian α, where $\overline{v}_\alpha(t)$ denotes the average speed in the desired direction of motion. Altogether, long waiting times increase the desired velocity, which can produce inefficient outflow. This further increases the waiting times, and so on, so that this tragic feedback can eventually trigger such high pressures that people are crushed or fall and are trampled. It is therefore imperative to have sufficiently wide exits and to prevent counterflows when large crowds want to leave (Helbing, Farkas, and Vicsek, 2000b).

4. Herding behavior

Let us now discuss a situation in which pedestrians are trying to leave a room with heavy smoke, but first have to find one of the hidden exits (see Fig. 50). Each pedestrian α may either select an individual direction $\mathbf{e}_\alpha^*$ or follow the average direction $\langle \mathbf{e}_\beta(t)\rangle_\alpha$ of his neighbors β within a certain radius R_α (Vicsek *et al.*, 1995), or try a mixture of both. We assume that both options are again weighted with the parameter n'_α of nervousness:

$$\mathbf{e}_\alpha^0(t)=\mathrm{Norm}[(1-n'_\alpha)\mathbf{e}_\alpha^*+n'_\alpha\langle \mathbf{e}_\beta(t)\rangle_\alpha], \tag{128}$$

where $\mathrm{Norm}(\mathbf{z})=\mathbf{z}/\|\mathbf{z}\|$ denotes normalization of a vector $\mathbf{z}$ to unit length. As a consequence, we have individualistic behavior if n'_α is low, but herding behavior if n'_α is high. Therefore n'_α reflects the degree of panic of individual α.

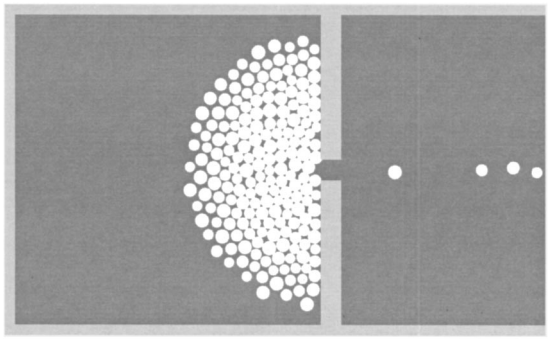

FIG. 49. Panicking pedestrians often come so close to each other that their physical contacts lead to the buildup of pressure and obstructing friction effects. This results in temporary arching and clogging related to inefficient and irregular outflows. After Helbing, Farkas, and Vicsek, 2000b; Helbing, 2001.

Our model indicates that neither individualistic nor herding behavior performs well. Pure individualistic behavior means that a few pedestrians will find an exit accidentally, while the others will not leave the room in time before being poisoned by smoke. Herding may, in some cases, guide the mass in the right directions, but this requires that there be someone who knows a suitable way out, e.g., trained personnel. However, in new and complex crisis situations, herding behavior normally implies that the complete crowd is eventually moving in the same and probably wrong or jammed direction, so that available exits are not efficiently used (see Fig. 50), in agreement with observations. According to simulation results by Helbing, Farkas, and Vicsek (2000b), optimal chances of survival are expected for a certain mixture of individualistic and herding behavior, where individualism allows some people to detect the exits and herding guarantees that successful behavior is imitated by small groups of pedestrians.

VI. FLOCKING AND SPIN SYSTEMS, HERDING, AND OSCILLATIONS AT STOCK MARKETS

Models for herding behavior have already been developed in order to understand the flocking of birds (Reynolds, 1987), the formation of fish schools, or the herding of sheep based on a nonequilibrium analog of ferromagnetic models (Vicsek *et al.*, 1995). More or less related models of swarm formation have been developed, as well.[10]

[10]See, for example, Stevens (1992), Miramontes *et al.* (1993), Hemmingsson (1995), Rauch *et al.* (1995), Toner and Tu (1995), Albano (1996), Bussemaker *et al.* (1997), Schweitzer (1997b), Stevens and Schweitzer (1997), and Mikhailov and Zanette (1999); see also Sec. I.F.

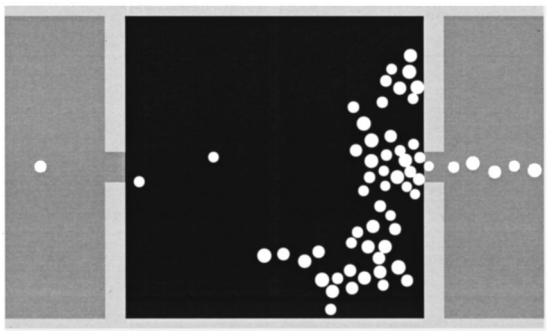

FIG. 50. Herding behavior of panicking pedestrians in a smoky room (black), leading to an inefficient use of available escape routes. From Helbing, Farkas, and Vicsek, 2000b.

Possibly the simplest model for the behavior of birds is as follows. Let us assume all birds α are moving with a certain finite speed $\|\mathbf{v}_\alpha(t)\|=v_\alpha^0=v_0$. To make flock formation less trivial, we set $\mathbf{f}_{\alpha\beta}=\mathbf{0}$ and do without the assumption of long-range attractive and short-range repulsive interactions among birds. Equation (4) can then be simplified to $\mathbf{e}_\alpha(t)=[\mathbf{e}_\alpha^0(t)+\boldsymbol{\chi}_\alpha(t)]$, which is solved together with

$$\frac{d\mathbf{x}_\alpha}{dt}\approx\frac{[\mathbf{x}_\alpha(t+\Delta t)-\mathbf{x}_\alpha(t)]}{\Delta t}=v_0\mathbf{e}_\alpha(t). \tag{129}$$

We are now assuming that a bird α orients itself at the mean direction of motion $\mathrm{Norm}(\langle\mathbf{e}_\beta(t-\Delta t)\rangle_\alpha)=\mathrm{Norm}(\langle\mathbf{v}_\beta(t-\Delta t)\rangle_\alpha)$ of those birds β that are nearby within a radius R_α at time $(t-\Delta t)$. As a consequence, the direction of motion $\mathbf{e}_\alpha^0$ is adapted to the average one in the immediate environment with a reaction time of Δt: $\mathbf{e}_\alpha^0(t)=\mathrm{Norm}(\langle\mathbf{e}_\beta(t-\Delta t)\rangle_\alpha)$. In order not to have velocity changes, we assume that the fluctuations $\boldsymbol{\chi}_\alpha(t)$ influence only the directions $\mathbf{e}_\alpha(t)$, but have a stronger influence, the greater the fluctuation level η is. The vector $[\mathbf{e}_\alpha^0(t)+\boldsymbol{\chi}_\alpha(t)]$ is therefore also normalized. Consequently, the above *self-propelled particle model* can be summarized by Eq. (129) and

$$\mathbf{e}_\alpha(t+\Delta t)=\mathrm{Norm}(\mathrm{Norm}\langle\mathbf{e}_\beta(t)\rangle_\alpha+\boldsymbol{\chi}'_\alpha(t)), \tag{130}$$

where the fluctuations $\boldsymbol{\chi}'_\alpha(t)$ are uniformly distributed in a sphere of radius η.

The computer simulations start with a uniform distribution of particles and mostly use periodic boundary conditions. Figure 51 shows two representative snapshots of the two-dimensional model variant for $v_0=0$ and $v_0\neq0$. An exploration of the model behavior in three dimensions yields a phase diagram with an ordered phase and a disordered one (see Fig. 52). For $v_0\neq0$, no matter how small the average particle density ϱ is, there is always a critical fluctuation strength $\eta_c(\varrho)$, below which the directions $\mathbf{e}_\alpha(t)$ of motion are aligned and particle clusters are formed, even without attractive interactions (Czirók, Vicsek, and Vicsek, 1999). In other words, birds flock only if the fluctuation strength is small enough. Otherwise, they fly around in a disordered way. At a given fluctuation strength η, flocking is more likely if their density ϱ is high, which is in agreement with observations. Moreover, the model reproduces that birds keep a certain (R_α-dependent) distance from each other, although no repulsive interactions have been assumed.

While the critical fluctuation strength $\eta_c(\varrho)$ separating ordered and disordered behavior seems to be independent of the concrete velocity $v_0>0$, the behavior of an equilibrium system with $v_0=0$ is considerably different. It corresponds to the behavior of a *Heisenberg spin system* with homogeneous particle density ϱ, in which the spins $\mathbf{e}_\alpha$ align parallel as in a ferromagnet if the temperature (which is proportional to the fluctuation strength η) is below some critical temperature. However, this ferromagnetic ordering takes place only if the particle density ϱ exceeds a certain *percolation value* $\varrho_c\approx0.75$ (see Fig. 52). Surprisingly enough, the behavior for $v_0=0$ and $v_0\neq0$ is, therefore, fundamentally different.

In conclusion, nonequilibrium systems can differ considerably from equilibrium ones. The motion of the particles in a self-driven nonequilibrium system seems to have an effect similar to that of a long-range interaction, since it is mainly a matter of time until the particles meet and interact with each other. As a consequence, one can find a transition to an ordered phase even in an analogous one-dimensional nonequilibrium system (Czirók, Barabási, and Vicsek, 1999), while the related equilibrium system with $v_0=0$ is always disordered in the presence of fluctuations (Mermin and Wagner, 1966).

Allow me to become a little bit philosophical towards the end of this review. As is reflected in bubbles and crashes in stock exchange markets, the reinforcement of buying and selling decisions sometimes also exhibits features of herding behavior (see, for example, Farmer, 1998; Youssefmir *et al.*, 1998; Lux and Marchesi, 1999). Remember that herding behavior is frequently found in complex situations where individuals do not know the right thing to do. Everyone then counts on collective intelligence, believing that a crowd is following someone who has identified the right action. However, as has been shown for panicking pedestrians seeking an exit, such mass behavior can have undesirable results, since alternatives are not efficiently utilized.

The corresponding herding model in Sec. V.D.4 could be viewed as a paradigm for problem-solving behavior in science, economics, and politics, where new solutions to complex problems have to be found in a way comparable to finding the exit from a smoky room. From simulation results, we may conclude that people will not manage to cope with a sequence of challenging situations if everyone sticks to his own idea egocentrically, but they will also fail if everyone follows the same idea because the possible spectrum of solutions is not adequately explored. Therefore the best strategy appears to be pluralism, with a reasonable degree of readiness to follow good ideas of others, while a totalitarian regime would probably not survive a series of crises. This fits well with experimental data on the efficiency of group problem solving (Anderson, 1961; Kelley and Thibaut,

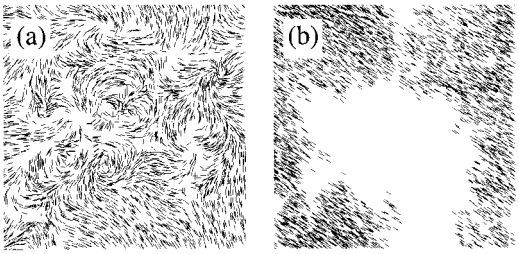

FIG. 51. Typical simulation results for the two-dimensional, self-propelled particle model given by Eqs. (129) and (130). (a) Ferromagnetic ordering for $v_0=0$. (b) Flocking of particles moving in the same direction for $v_0>0$. After Vicsek *et al.*, 1995.

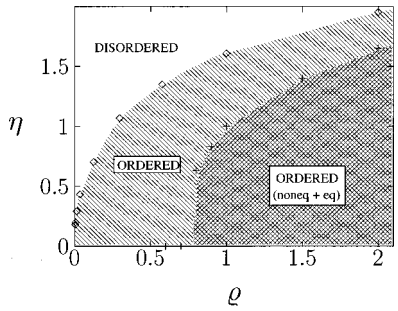

FIG. 52. Phase diagram of the three-dimensional self-propelled particle model and the corresponding ferromagnetic system. The nonequilibrium self-propelled particle system becomes ordered in the whole region below the curve $\eta_c(\varrho)$ connecting the diamonds. In the static equilibrium case with $v_0=0$, the ordered region extends only up to a finite "percolation" density; see the beginning of the area given by the curve connecting the plus signs. After Czirók, Vicsek, and Vicsek, 1999.

1969; Laughlin *et al.*, 1975), according to which groups normally perform better than individuals, but masses are inefficient in finding new solutions to complex problems.

Considering the phase diagram in Fig. 52, we may also conjecture that, in the presence of a given level η of fluctuations, there is a certain critical density above which people tend to show mass behavior and below which they behave individualistically. In fact, the tendency towards mass behavior is higher in dense populations than in dilute ones. In summary, findings for self-driven many-particle systems reach far into the realm of the social, economic, and psychological sciences.

Another example is the analogy between irregular oscillations of prices in the stock market and of pedestrian flows at bottlenecks (see Sec. V.C.2). The idea is as follows: Traffic is a prime example of individuals competing for limited resources (namely, space). In the stock market, we have a competition for money by two different groups: optimistic traders ("bulls") and pessimistic ones ("bears"). The optimists count on rising stock prices and increase the price by their orders. In contrast, pessimists speculate on a decrease in the price and reduce it by their selling of stocks. Hence traders belonging to the same group enforce each others' (buying or selling) actions, while optimists and pessimists push (the price) in opposite directions. Consequently there is an analogy with opposing pedestrian streams pushing at a bottleneck, which is reflected in a roughly similar dynamics (Helbing, 2001).

VII. SUMMARY AND OUTLOOK

In this review, I have shown that many aspects of traffic flow and other living systems can be reflected by models of self-driven many-particle systems. This implies that interactions within these systems dominate socio-psychological effects. Although there are still many interesting open questions and controversies, calling for intensified research activities, one can already state that traffic theory is a prime example of a mathematically advanced, semiquantitative description of human behavior. Meanwhile, it appears feasible to reproduce the observed complex transitions between different traffic states (see Sec. II.E) by simulation models adapted to the measurement site by variation of one parameter value only and working with the empirically measured boundary conditions (see Sec. IV.B.1). One could even say there are some natural laws governing the behavior of drivers and pedestrians. This includes the self-organized, characteristic constants of traffic flow (see Secs. II.E.1 and IV.A.5), the collective patterns of motion observed in pedestrian crowds (see Secs. V.C and V.D), and the trail formation behavior of humans (see Sec. I.F.5).

Self-driven many-particle systems display a surprisingly rich spectrum of spatio-temporal pattern formation phenomena. They were described by Newton's equation of motion (in which Newton's third law *actio=reactio* was sometimes relaxed), complemented by driving forces and frictional dissipation. Based on small modifications, we often found considerably different behavior compared to analogous systems from classical or equilibrium statistical mechanics, but there were also various analogies with driven fluids or granular media (see Secs. III.E.3, IV.A.4, and V.A). Important factors for the finally resulting patterns were (i) the specification of the desired velocities and directions of motion in the driving term, (ii) inhomogeneities and other boundary effects, (iii) the heterogeneity among particles, and (iv) the degree of fluctuations. Many of the systems are characterized by nonlinear feedback mechanisms, so that small perturbations can have strong effects like "phantom traffic jams" (see Secs. II.E.1 and IV.A.1) or "phantom panics" (see Sec. V.D.3). These effects are often counterintuitive, such as "freezing by heating" (see Sec. V.D.1) or the "faster-is-slower effect" (see Sec. V.D.2). From classical many-particle systems with attractive interactions, we are used to the idea that increasing temperature breaks up structures and destroys patterns, i.e., fluid structures are replaced by gaseous ones, not by solid ones. By contrast, in the considered self-driven dissipative many-particle systems with repulsive interactions, one can find all sorts of breakdown and structure formation phenomena when the "temperature" (i.e., the

fluctuation strength) is increased. Nevertheless, the combination of repulsive interactions with a driving term and dissipation also gives rise to phenomena typical for attractive interactions, e.g., the segregation effects observed in the formation of traffic jams (see Sec. IV.A.3) and pedestrian lanes (see Sec. V.C.1), or the emergence of the coherent moving state in a system of cars and trucks (see Sec. IV.D.2).

The description of the phenomena in self-driven many-particle systems uses and generalizes almost the complete spectrum of methods developed in nonequilibrium statistical physics and nonlinear dynamics. It has close relations with kinetic gas theory and fluid dynamics, soft matter, solid-state physics, and even quantum mechanics (see Sec. III.C.1), while the corresponding nonequilibrium thermodynamics is still to be developed. However, there are aspects of universality found in traffic, as is exemplified by the power-law behavior of traffic flows (see Secs. II.E.1 and IV.A.3) and the phase diagrams of traffic dynamics and model characteristics (see Figs. 35, 36, and 39). In the spirit of general systems theory (Buckley, 1967; von Bertalanffy, 1968; Rapoport, 1986), one could even go one step further: Many phenomena found in traffic systems, where drivers or pedestrians compete for limited space, may have implications for other biological and socio-economic systems in which individuals compete for limited resources. In fact, jamming and herding phenomena are found in various living systems, from animal colonies, markets, administrations, or societies to science, economics, and politics. Therefore traffic is a good and especially concrete example for studying certain aspects of socio-psychological phenomena in an experimental setup. Possibly this could help us to gain a better understanding of more complex human behavior in the future.

Self-driven many-particle systems are also interesting from a practical point of view. They are related to aspects of collective intelligence (see, for example, the work carried out at the Santa Fe Institute, http://www.santafe.edu/sfi/research/indexResearchAreas.html, by scientists like Botee and Bonabeau, 1998; Wolpert and Tumer, 1999; Kube and Bonabeau, 2000). Based on suitable interactions, many-particle and many-agent systems can organize themselves and reach an optimal state (Helbing and Vicsek, 1999). Such a distributed strategy based on local optimization is more efficient and robust than classical, centralized control strategies. In particular, the outcome on large scales is relatively insensitive to the local failure of control.

ACKNOWLEDGMENTS

I would like to thank the German Research Foundation (DFG) and the Federal Ministry for Education and Science (BMBF) for financial support through the grants He 2789/1-1, He 2789/2-1, and the project SANDY, grant no. 13N7092. Many thanks also for the warm hospitality I experienced at the Tel Aviv University, the Weizmann Institute of Science, the Xerox Palo Alto Research Center (Xerox PARC), the Eötvös University, and the Collegium Budapest—Institute for Advanced Study. Furthermore, I am grateful for fruitful collaborations with and/or comments by James Banks, Eshel Ben-Jacob, Kai Bolay, András Czirók, Illés Farkas, Isaac Goldhirsch, Ansgar Hennecke, Bernardo Huberman, Boris Kerner, Joachim Krug, Péter Molnár, David Mukamel, Joachim Peinke, Andreas Schadschneider, Michael Schreckenberg, Gunter Schütz, Rudolf Sollacher, Benno Tilch, Martin Treiber, Tamás Vicsek, and others, who have also supplied various figures. Finally, I am obliged to the Dutch Ministry of Transport, Public Works and Water Management, the Bosch GmbH, Stuttgart, the Autobahndirektion Südbayern, and the Hessisches Landesamt für Straßen und Verkehrswesen for providing traffic data. Tilo Grigat, Daniel Kern, Martina Seifert, Benno Tilch, Martin Treiber, and Torsten Werner have provided a great deal of help with the references and corrections.

REFERENCES

Note: For an extended list of references with titles and final pages, see http://www.trafficforum.org.

Agyemang-Duah, K., and F. L. Hall, 1991, in *Highway Capacity and Level of Service*, edited by U. Brannolte (Balkema, Rotterdam), p. 1.

Ahmed, K. I., M. E. Ben-Akiva, H. N. Koutsopoulos, and R. B. Mishalani, 1996, in *Transportation and Traffic Theory: Proceedings of the 13th International Symposium on Transportation and Traffic Theory*, edited by J. B. Lesort (Pergamon-Elsevier, Tarrytown, NY), p. 501.

Albano, E. V., 1996, Phys. Rev. Lett. **77**, 2129.

Alberti, E., and G. Belli, 1978, Transp. Res. **12**, 33.

Alcaraz, F. C., M. Droz, M. Henkel, and V. Rittenberg, 1994, Ann. Phys. (N.Y.) **230**, 250.

Alexander, S., and T. Holstein, 1978, Phys. Rev. B **18**, 301.

AlGadhi, S. A. H., and H. S. Mahmassani, 1990, in *Proceedings of the 11th International Symposium on Transportation and Traffic Theory*, edited by M. Koshi (Elsevier, New York), p. 59.

AlGadhi, S. A. H, H. S. Mahmassani, and R. Herman, 2001, in *Pedestrian and Evacuation Dynamics*, edited by M. Schreckenberg and S. D. Sharma (Springer, Berlin), p. 3.

Alon, U., M. R. Evans, H. Hinrichsen, and D. Mukamel, 1996, Phys. Rev. Lett. **76**, 2746.

Alvarez, A., J. J. Brey, and J. M. Casado, 1990, Transp. Res., Part B: Methodol. **24B**, 193.

Anderson, N. H., 1961, J. Soc. Psychol. **55**, 67.

Andrews, F. C., 1970a, Transp. Res. **4**, 359.

Andrews, F. C., 1970b, Transp. Res. **4**, 367.

Andrews, F. C., 1973a, Transp. Res. **7**, 223.

Andrews, F. C., 1973b, Transp. Res. **7**, 233.

Androsch, W., 1978, Ph.D. thesis (Technische Hochschule, Darmstadt).

Ansorge, R., 1990, Transp. Res., Part B: Methodol. **24B**, 133.

Arns, T., 1993, *Video films of pedestrian crowds* (available from Thomas Arns, Wannenstr. 22, 70199 Stuttgart, Germany).

Ashford, N., M. O'Leary, and P. D. McGinity, 1976, Traffic Eng. Control **17**, 207.

Astumian, R. D., 1997, Science **276**, 917.
Aw, A., and M. Rascle, 2000, SIAM (Soc. Ind. Appl. Math.) J. Appl. Math. **60**, 916.
Awazu, A., 1998, J. Phys. Soc. Jpn. **67**, 1071.
Baeck, T., 1996, *Evolutionary Algorithms in Theory and Practice* (Oxford University, New York).
Bak, P., 1996, *How Nature Works: The Science of Self-Organized Criticality* (Copernicus, New York).
Bak, P., C. Tang, and K. Wiesenfeld, 1987, Phys. Rev. Lett. **59**, 381.
Bak, P., C. Tang, and K. Wiesenfeld, 1988, Phys. Rev. A **38**, 364.
Bando, M., K. Hasebe, K. Nakanishi, and A. Nakayama, 1998, Phys. Rev. E **58**, 5429.
Bando, M., K. Hasebe, K. Nakanishi, A. Nakayama, A. Shibata, and Y. Sugiyama, 1995, J. Phys. I **5**, 1389.
Bando, M., K. Hasebe, A. Nakayama, A. Shibata, and Y. Sugiyama, 1994, Jpn. J. Ind. Appl. Math. **11**, 203.
Bando, M., K. Hasebe, A. Nakayama, A. Shibata, and Y. Sugiyama, 1995, Phys. Rev. E **51**, 1035.
Banks, J. H., 1989, Transp. Res. Rec. **1225**, 53.
Banks, J. H., 1990, Transp. Res. Rec. **1287**, 20.
Banks, J. H., 1991a, Transp. Res. Rec. **1320**, 83.
Banks, J. H., 1991b, Transp. Res. Rec. **1320**, 234.
Banks, J. H., 1995, Transp. Res. Rec. **1510**, 1.
Banks, J. H., 1999, Transp. Res. Rec. **1678**, 128.
Bántay, P., and I. M. Jánosi, 1992, Phys. Rev. Lett. **68**, 2058.
Barabási, A.-L., and H. E. Stanley, 1995, *Fractal Concepts in Surface Growth* (Cambridge University, Cambridge, England).
Barlovic, R., L. Santen, A. Schadschneider, and M. Schreckenberg, 1998, Eur. Phys. J. B **5**, 793.
Barone, E., 1981, Transp. Theory Stat. Phys. **9**, 59.
Batty, M., 1997, Nature (London) **388**, 19.
Baxter, G. W., R. P. Behringer, T. Fagert, and G. A. Johnson, 1989, Phys. Rev. Lett. **62**, 2825.
Belitsky, V., J. Krug, E. J. Neves, and G. M. Schütz, 2001, J. Stat. Phys. **103**, 945.
ben-Avraham, D., and J. Köhler, 1992, Phys. Rev. A **45**, 8358.
Benekohal, R. F., and J. Treiterer, 1988, Transp. Res. Rec. **1194**, 99.
Bengrine, M., A. Benyoussef, H. Ez-Zahraouy, J. Krug, M. Loulidi, and F. Mhirech, 1999, J. Phys. A **32**, 2527.
Ben-Jacob, E., 1993, Contemp. Phys. **34**, 247.
Ben-Jacob, E., 1997, Contemp. Phys. **38**, 205.
Ben-Jacob, E., I. Cohen, and H. Levine, 2000, Adv. Phys. **49**, 395.
Ben-Jacob, E., O. Shochet, A. Tenenbaum, I. Cohen, A. Czirók, and T. Vicsek, 1994, Nature (London) **368**, 46.
Benjamin, S. C., N. F. Johnson, and P. M. Hui, 1996, J. Phys. A **29**, 3119.
Benjamini, I., P. A. Ferrari, and C. Landim, 1996, Stochastic Proc. Appl. **61**, 181.
Ben-Naim, E., and P. L. Krapivsky, 1997, Phys. Rev. E **56**, 6680.
Ben-Naim, E., and P. L. Krapivsky, 1998, J. Phys. A **31**, 8073.
Ben-Naim, E., and P. L. Krapivsky, 1999, Phys. Rev. E **59**, 88.
Ben-Naim, E., P. L. Krapivsky, and S. Redner, 1994, Phys. Rev. E **50**, 822.
Benz, T., 1993, in *Modelling and Simulation 1993*, edited by A. Pave (Society for Computer Simulation Intenational, Ghent), p. 486.
Berg, P., A. Mason, and A. Woods, 2000, Phys. Rev. E **61**, 1056.
Beylich, A. E., 1979, in *Rarefied Gas Dynamics*, edited by R. Campargue (Commissariat à l'Energie Atomique, Paris), Vol. 1, p. 129.
Beylich, A. E., 1981, in *Neue Wege in der Mechanik*, edited by G. Adomeit and H.-J. Frieske (VDI-Verlag, Düsseldorf), p. 171.
Biham, O., A. A. Middleton, and D. Levine, 1992, Phys. Rev. A **46**, R6124.
Bleile, T., 1997, in *Proceedings of the 4th World Congress on Intelligent Transport Systems*, October 1997, Berlin (ITS Congress Association, Brussels), CD Rom, paper No. 00022.
Bleile, T., 1999, Ph.D. thesis (University of Stuttgart).
Blue, V. J., and J. L. Adler, 1998, Transp. Res. Rec. **1644**, 29.
Blue, V. J., and J. L. Adler, 1999, in *Proceedings of the 14th International Symposium on Transportation and Traffic Theory*, edited by A. Ceder (Pergamon, New York), p. 235.
Blue, V. J., and J. L. Adler, 2001a, Transp. Res., Part B: Methodol. **35B**, 293.
Blue, V. J., and J. L. Adler, 2001b, in *Pedestrian and Evacuation Dynamics*, edited by M. Schreckenberg and S. D. Sharma (Springer, Berlin), p. 115.
Boeminghaus, D., 1982, *Fußgängerbereiche+Gestaltungselemente/Pedestrian Areas and Design Elements/Zones pour Piétons+Elements de Conception* (Krämer, Stuttgart).
Boillot, F., J. M. Blosseville, J. B. Lesort, V. Motyka, M. Papageorgiou, and S. Sellam, 1992, in *Proceedings of the 6th IEE International Conference on Road Traffic Monitoring and Control* (Institution of Electrical Engineers, London), p. 75.
Bolay, K., 1998, Master's thesis (University of Stuttgart).
Bolterauer, H., and M. Opper, 1981, Z. Phys. B: Condens. Matter **55**, 155.
Boltzmann, L., 1964, *Lectures on Gas Theory* (University of California, Berkeley).
Bonabeau, E., 1996, J. Phys. I **6**, 309.
Borgers, A., and H. Timmermans, 1986a, Geograph. Anal. **18**, 115.
Borgers, A., and H. Timmermans, 1986b, Socio-Econ. Plan. Sci. **20**, 25.
Botee, H. M., and E. Bonabeau, 1998, Adv. Compl. Syst. **1**, 149.
Bottom, J., M. Ben-Akiva, M. Bierlaire, I. Chabini, H. Koutsopoulos, and Q. Yang, 1999, in *Proceedings of the 14th International Symposium on Transportation and Traffic Theory*, edited by A. Ceder (Pergamon, New York), p. 577.
Bourzutschky, M., and J. Miller, 1995, Phys. Rev. Lett. **74**, 2216.
Bovy, P. H. L., 1998, Ed., *Motorway Traffic Flow Analysis. New Methodologies and Recent Empirical Findings* (Delft University of Technology, Delft).
Brackstone, M., and M. McDonald, 1996, in *Traffic and Granular Flow*, edited by D. E. Wolf, M. Schreckenberg, and A. Bachem (World Scientific, Singapore), p. 151.
Brackstone, M., and M. McDonald, 2000, Transp. Res. F **2**, 181.
Brackstone, M., M. McDonald, and J. Wu, 1998, in *Proceedings of the 9th International Conference on Road Transport Information and Control* (Institute of Electrical Engineers, London), p. 160.
Brannolte, U., 1991, Ed., *Highway Capacity and Level of Service* (Balkema, Rotterdam).
Braude, V., 1996, Master's thesis (Weizmann Institute of Science).
Brilon, W., M. Großmann, and H. Blanke, 1993, *Verfahren für die Berechnung der Leistungsfähigkeit und Qualität des Ver-*

kehrsablaufes auf Straßen (Bundesministerium für Verkehr, Abt. Straßenbau, Bonn-Bad Godesberg).
Brilon, W., F. Huber, M. Schreckenberg, and H. Wallentowitz, 1999, Eds., *Traffic and Mobility: Simulation—Economics—Environment* (Springer, Heidelberg).
Brilon, W., and M. Ponzlet, 1996, in *Traffic and Granular Flow*, edited by D. E. Wolf, M. Schreckenberg, and A. Bachem (World Scientific, Singapore), p. 23.
Brilon, W., and N. Wu, 1999, in *Traffic and Mobility: Simulation—Economics—Environment*, edited by W. Brilon, F. Huber, M. Schreckenberg, and H. Wallentowitz (Springer, Heidelberg), p. 163.
Buchholtz, V., and T. Pöschel, 1993, Int. J. Mod. Phys. C **4**, 1049.
Buckley, D., 1974, Ed., *Proceedings of the 6th International Symposium on Transportation and Traffic Theory* (Reed, London).
Buckley, W., 1967, *Sociology and Modern Systems Theory* (Prentice-Hall, Englewood Cliffs, NJ).
Bui, D. D., P. Nelson, and S. L. Narasimhan, 1992, "Computational Realizations of the Entropy Condition in Modeling Congested Traffic Flow" (Texas Transportation Institute, Texas A&M University System), Report No. FHWA/TX-92/1232-7.
Burstedde, C., A. Kirchner, K. Klauck, A. Schadschneider, and J. Zittartz, 2001, in *Pedestrian and Evacuation Dynamics*, edited by M. Schreckenberg and S. D. Sharma (Springer, Berlin), p. 87.
Burstedde, C., K. Klauck, A. Schadschneider, and J. Zittartz, 2001, Physica A **295**, 507.
Bussemaker, H. J., A. Deutsch, and E. Geigant, 1997, Phys. Rev. Lett. **78**, 5018.
Caldarelli, G., 2001, Phys. Rev. E **63**, 021118.
Carstens, R. L., and S. L. Ring, 1970, Traffic Eng. **41**, 38.
Cassidy, M. J., and R. L. Bertini, 1999, Transp. Res., Part B: Methodol. **33B**, 25.
Cassidy, M. J., and M. Mauch, 2001, Transp. Res., Part A: Policy Pract. **35A**, 143.
Cassidy, M. J., and J. R. Windover, 1995, Transp. Res. Rec. **1484**, 73.
Ceder, A., 1999, Ed., *Proceedings of the 14th International Symposium on Transportation and Traffic Theory* (Pergamon, New York).
Ceder, A., and A. D. May, 1976, Transp. Res. Rec. **567**, 1.
Cercignani, C., and M. Lampis, 1988, J. Stat. Phys. **53**, 655.
Chandler, R. E., R. Herman, and E. W. Montroll, 1958, Oper. Res. **6**, 165.
Chang, G.-L., and Y.-M. Kao, 1991, Transp. Res., Part A **25A**, 375.
Chang, T., and I. Lai, 1997, Transp. Res., Part C: Emerg. Technol. **5**, 333.
Chapman, S., and T. G. Cowling, 1939, *The Mathematical Theory of Nonuniform Gases* (Cambridge University, Cambridge, England).
Chen, S., H. Chen, D. Martínez, and W. Matthaeus, 1991, Phys. Rev. Lett. **67**, 3776.
Chen, Y., 1997, Phys. Rev. Lett. **79**, 3117.
Cheybani, S., J. Kertész, and M. Schreckenberg, 2001a, Phys. Rev. E **63**, 016107.
Cheybani, S., J. Kertész, and M. Schreckenberg, 2001b, Phys. Rev. E **63**, 016108.
Choi, M. Y., and H. Y. Lee, 1995, Phys. Rev. E **52**, 5979.
Chow, T.-S., 1958, Oper. Res. **6**, 827.
Chowdhury, D., K. Ghosh, A. Majumdar, S. Sinha, and R. B. Stinchcombe, 1997, Physica A **246**, 471.
Chowdhury, D., J. Kertész, K. Nagel, L. Santen, and A. Schadschneider, 2000, Phys. Rev. E **61**, 3270.
Chowdhury, D., L. Santen, and A. Schadschneider, 2000, Phys. Rep. **329**, 199.
Chowdhury, D., L. Santen, A. Schadschneider, S. Sinha, and A. Pasupathy, 1999, J. Phys. A **32**, 3229.
Chowdhury, D., D. E. Wolf, and M. Schreckenberg, 1997, Physica A **235**, 417.
Chung, K. H., and P. M. Hui, 1994, J. Phys. Soc. Jpn. **63**, 4338.
Cladis, P. E., and P. Palffy-Muhoray, 1995, Eds., *Spatio-Temporal Patterns in Nonequilibrium Complex Systems* (Addison-Wesley, Reading, MA).
Claus, V., D. Helbing, and H. J. Herrmann, 1999, Eds., *Proceedings of the Workshop "Verkehrsplanung und -simulation"* (Informatik Verbund Stuttgart, University of Stuttgart).
Cohen, E. G. D., 1968, in *Fundamental Problems in Statistical Mechanics II*, edited by E. G. D. Cohen (Wiley, New York), p. 228.
Cohen, E. G. D., 1969, in *Transport Phenomena in Fluids*, edited by H. J. M. Hanley (Dekker, New York), p. 119.
Coleman, J. S., 1964, *Introduction to Mathematical Sociology* (Free, New York), p. 361.
Coleman, J. S., and J. James, 1961, Sociometry **24**, 36.
Cremer, M., 1978, Oper. Res. **15**, 1575.
Cremer, M., 1979, *Der Verkehrsfluß auf Schnellstraßen* (Springer, Berling).
Cremer, M., and J. Ludwig, 1986, Math. Comput. Simul. **28**, 297.
Cremer, M., and A. D. May, 1985, *An Extended Traffic Model for Freeway Control*, Technical Report UCB-ITS-RR-85-7 (Institute of Transportation Studies, University of California, Berkeley).
Cremer, M., and A. D. May, 1986, *An Extended Traffic Flow Model for Inner Urban Freeways* (Arbeitsbereich Automatisierungstechnik, Technische Universität Hamburg-Harburg).
Cremer, M., and F. Meißner, 1993, in *Modelling and Simulation 1993*, edited by A. Pave (Society for Computer Simulation International, Ghent), p. 515.
Cremer, M., and M. Papageorgiou, 1981, Automatica **17**, 837.
Crisanti, A., G. Paladin, and A. Vulpiani, 1993, *Products of Random Matrices in Statistical Physics* (Springer, Berlin).
Cross, M. C., and P. C. Hohenberg, 1993, Rev. Mod. Phys. **65**, 851.
Csahók, Z., and T. Vicsek, 1994, J. Phys. A **27**, L591.
Csányi, G., and J. Kertész, 1995, J. Phys. A **28**, L427.
Czirók, A., A. Barabási, and T. Vicsek, 1999, Phys. Rev. Lett. **82**, 209.
Czirók, A., M. Vicsek, and T. Vicsek, 1999, Physica A **264**, 299.
Dab, D., J.-P. Boon, and Y.-X. Li, 1991, Phys. Rev. Lett. **66**, 2535.
Daganzo, C. F., 1981, Transp. Res., Part B: Methodol. **15B**, 1.
Daganzo, C. F., 1993, Ed., *Proceedings of the 12th International Symposium on the Theory of Traffic Flow and Transportation* (Elsevier, Amsterdam).
Daganzo, C. F., 1994, Transp. Res., Part B: Methodol. **28B**, 269.
Daganzo, C. F., 1995a, Transp. Res., Part B: Methodol. **29B**, 79.
Daganzo, C. F., 1995b, Transp. Res., Part B: Methodol. **29B**, 261.
Daganzo, C. F., 1995c, Transp. Res., Part B: Methodol. **29B**, 277.

Daganzo, C. F., 1996, in *Transportation and Traffic Theory: Proceedings of the 13th International Symposium on Transportation and Traffic Theory*, edited by J. B. Lesort (Pergamon-Elsevier, Tarrytown, NY), p. 629.
Daganzo, C. F., 1997a, *Fundamentals of Transportation and Traffic Operations* (Pergamon-Elsevier, Oxford, England).
Daganzo, C. F., 1997b, Transp. Res., Part B: Methodol. **31B**, 83.
Daganzo, C. F., 1997c, Working Paper UCB-ITS-WP-97-4 (Institute of Transportation Studies, University of California, Berkeley, CA).
Daganzo, C. F., 1999a, *A Behavioral Theory of Multi-lane Traffic Flow. I: Long Homogeneous Freeway Sections*. Research Report UCB-ITS-RR-99-5 (Institute of Transportation Studies, University of California, Berkeley, CA).
Daganzo, C. F., 1999b, *A Behavioral Theory of Multi-lane Traffic Flow. II: Merges and the Onset of Congestion*. Research Report UCB-ITS-RR-99-6 (Institute of Transportation Studies, University of California, Berkeley, CA).
Daganzo, C. F., M. J. Cassidy, and R. L. Bertini, 1999, Transp. Res., Part A **33A**, 365.
Daganzo, C. F., W.-H. Lin, and J. M. Del Castillo, 1997, Transp. Res., Part B: Methodol. **31B**, 105.
Davis, D. G., and J. P. Braaksma, 1988, Transp. Res., Part A **22A**, 375.
DeAngelis, D. L., and L. J. Gross, 1992, Eds., *Individual-Based Models and Approaches in Ecology: Populations, Communities, and Ecosystems* (Chapman and Hall, New York).
del Castillo, J. M., 1996a, in *Traffic and Granular Flow '97*, edited by M. Schreckenberg and D. E. Wolf (Springer, Singapore), p. 381.
del Castillo, J. M., 1996b, in *Transportation and Traffic Theory: Proceedings of the 13th International Symposium on Transportation and Traffic Theory*, edited by J. B. Lesort (Pergamon-Elsevier, Tarrytown, N.Y.), p. 517.
Deneubourg, J. L., S. Goss, N. Franks, and J. M. Pasteels, 1989, J. Insect Behav. **2**, 719.
Derrida, B., E. Domany, and D. Mukamel, 1992, J. Stat. Phys. **69**, 667.
Derrida, B., and M. R. Evans, 1997, in *Nonequilibrium Statistical Mechanics in One Dimension*, edited by V. Privman (Cambridge University, Cambridge, England), p. 277.
Derrida, B., M. R. Evans, V. Hakim, and V. Pasquier, 1993, J. Phys. A **26**, 1493.
Dewdney, A. K., 1987, Sci. Am. **257**, 104.
Diedrich, G., L. Santen, A. Schadschneider, and J. Zittartz, 2000, Int. J. Mod. Phys. C **11**, 335.
Dijker, T., P. H. L. Bovy, and R. G. M. M. Vermijs, 1998, in *Motorway Traffic Flow Analysis, New Methodologies and Recent Empirical Findings*, edited by P. H. L. Bovy (Delft University of Technology, Delft), p. 49.
Dijkstra, J., J. Jessurun, and H. Timmermans, 2001, in *Pedestrian and Evacuation Dynamics*, edited by M. Schreckenberg and S. D. Sharma (Springer, Berlin), p. 173.
Dillon, D. S., and F. L. Hall, 1987, Transp. Res. Rec. **1132**, 66.
Doi, J., 1976, J. Phys. A **9**, 1465.
Domany, E., and W. Kinzel, 1984, Phys. Rev. Lett. **53**, 311.
Domb, C., and M. S. Green, 1972–1976, Eds., *Phase Transitions and Critical Phenomena* (Academic, New York), Vols. 1–6.
Domb, C., and J. L. Lebowitz, 1983–2000, Eds., *Phase Transitions and Critical Phenomena* (Academic, New York), Vols. 7–19.
Dougherty, M., 1995, Transp. Res., Part C: Emerg. Technol. **3**, 247.
Drager, K. H., G. Løvås, J. Wiklund, H. Soma, D. Duong, A. Violas, and V. Lanèrès, 1992, in *Proceedings of the 1992 Emergency Management and Engineering Conference*, edited by K. H. Drager (Society for Computer Simulation, Orlando, FL), p. 101.
Drazin, P. G., and W. H. Reid, 1981, *Hydrodynamic Stability* (Cambridge University, Cambridge, England).
Du, Y., H. Li, and L. P. Kadanoff, 1995, Phys. Rev. Lett. **74**, 1268.
Dufty, J. W., A. Santos, and J. J. Brey, 1996, Phys. Rev. Lett. **77**, 1270.
Dunkel, J., W. Ebeling, U. Erdmann, and V. A. Makarov, 2001, Int. J. Bifurcation Chaos Appl. Sci. Eng. (in press).
Duparcmeur, Y. L., H. Herrmann, and J. P. Troadec, 1995, J. Phys. I **5**, 1119.
Dutkiewicz, J., J. Suda, and J. Okulewicz, 1995, in *Modelling and Simulation ESM 1995*, edited by M. Snorek, M. Sujansky, and A. Verbraeck (Society for Computer Simulation International, Istanbul), p. 347.
Ebeling, W., U. Erdmann, J. Dunkel, and M. Jenssen, 2000, J. Stat. Phys. **101**, 443.
Ebeling, W., and M. Jenssen, 1992, Physica A **188**, 350.
Ebeling, W., and M. Jenssen, 1999, Proc. SPIE **3726**, 112.
Ebeling, W., L. Schimansky-Geier, and F. Schweitzer, 1990, Z. Phys. Chem. Neue Folge **169**, 1.
Ebeling, W., F. Schweitzer, and B. Tilch, 1999, BioSystems **49**, 17.
Ebihara, M., A. Ohtsuki, and H. Iwaki, 1992, Microcomput. Civ. Eng. **7**, 63.
Eckmann, J.-P., H. Epstein, and C. E. Wayne, 1993, Ann. I.H.P. Phys. Theor. **58**, 287.
Edie, L. C., 1961, Oper. Res. **9**, 66.
Edie, L. C., and R. S. Foote, 1958, Highw. Res. Board, Proc. Annu. Meet. **37**, 334.
Ehrichs, E. E., H. M. Jaeger, G. S. Karczmar, J. B. Knight, V. Y. Kuperman, and S. R. Nagel, 1995, Science **267**, 1632.
Eigen, M., 1971, Naturwissenschaften **58**, 465.
Eigen, M., and P. Schuster, 1979, *The Hypercycle* (Springer, Berlin).
Eisenblätter, B., L. Santen, A. Schadschneider, and M. Schreckenberg, 1998, Phys. Rev. E **57**, 1309.
Elefteriadou, L., R. Roess, and W. McShane, 1995, Transp. Res. Rec. **1484**, 80.
Elliott, D., and D. Smith, 1993, Ind. Env. Crisis Q. **7**, 205.
Emmerich, H., and E. Rank, 1995, Physica A **216**, 435.
Enskog, D., 1917, Ph.D. thesis (University of Uppsala).
Esser, J., and M. Schreckenberg, 1997, Int. J. Mod. Phys. C **8**, 1025.
Evans, M. R., 1996, Europhys. Lett. **36**, 13.
Evans, M. R., D. P. Foster, C. Godréche, and D. Mukamel, 1995, Phys. Rev. Lett. **74**, 208.
Evans, M. R., Y. Kafri, H. M. Koduvely, and D. Mukamel, 1998, Phys. Rev. Lett. **80**, 425.
Family, F., and T. Vicsek, 1991, Eds., *Dynamics of Fractal Surfaces* (World Scientific, Singapore).
Farges, J.-L., J.-J. Henry, and J. Tufal, 1984, in *Control in Transportation Systems: Proceedings of the 4th IFAC/IFIP/IFORS Conference*, edited by D. Klamt and R. Lauber (Pergamon, Oxford), p. 307.
Farmer, J. D., 1998, e-print adap-org/9812005.
Farmer, J. D., 2000, Int. J. Theor. Appl. Finance **3**, 425.

Feistel, R., and W. Ebeling, 1989, *Evolution of Complex Systems. Self-Organization, Entropy and Development* (Kluwer, Dordrecht).
Felderhof, B. V., and M. Suzuki, 1971, Physica (Amsterdam) **56**, 43.
Fellendorf, M., 1996, in *Traffic Technology International '96* (UK & International, Dorking, England), p. 190.
Feller, W., 1967, *An Introduction to Probability Theory and Its Applications*, 3rd ed. (Wiley, New York).
Ferrari, P. A., 1994, in *Probability and Phase Transition*, edited by G. Grimmett (Kluwer Academic, Dordrecht), p. 35.
Fisher, R. A., 1930, *The Genetical Theory of Natural Selection* (Oxford University, Oxford).
Foerster, S. F., M. Y. Louge, H. Chang, and K. Allia, 1994, Phys. Fluids **6**, 1108.
Forbes, T. W., J. J. Mullin, and M. E. Simpson, 1967, in *Proceedings of the 3rd International Symposium on the Theory of Traffic Flow*, edited by L. C. Edie (Elsevier, New York), p. 97.
Forster, D., D. R. Nelson, and M. J. Stephen, 1977, Phys. Rev. A **16**, 732.
Foster, J., 1962, in *Proceedings of the 1st Conference of the Australian Road Research Board* (Australian Road Research Board, Victoria, Australia), p. 229.
Fouladvand, M. E., and H.-W. Lee, 1999, Phys. Rev. E **60**, 6465.
Fox, P., and F. G. Lehman, 1967, Highw. Res. Rec. **199**, 33.
Frisch, U., B. Hasslacher, and Y. Pomeau, 1986, Phys. Rev. Lett. **56**, 1505.
Fruin, J. J., 1971, Highw. Res. Rec. **355**, 1.
Fukui, M., and Y. Ishibashi, 1996a, J. Phys. Soc. Jpn. **65**, 1868.
Fukui, M., and Y. Ishibashi, 1996b, J. Phys. Soc. Jpn. **65**, 1871.
Fukui, M., and Y. Ishibashi, 1999a, J. Phys. Soc. Jpn. **68**, 2861.
Fukui, M., and Y. Ishibashi, 1999b, J. Phys. Soc. Jpn. **68**, 3738.
Gallas, J., H. J. Herrmann, and S. Sokołowski, 1992, Phys. Rev. Lett. **69**, 1371.
Ganem, J., 1998, Phys. Teach. **36**, 76.
Garbrecht, D., 1973, Traffic Q. **27**, 89.
Gardiner, C. W., 1985, *Handbook of Stochastic Methods*, 2nd ed. (Springer, Berlin).
Gartner, N. H., 1983, Transp. Res. Rec. **906**, 75.
Gartner, N., C. Messer, and A. Rathi, 1997, Eds., *Traffic Flow Theory* (Federal Highway Administration, Washington, DC).
Gartner, N. H., and N. H. M. Wilson, 1987, Eds., *Proceedings of the 10th International Symposium on Transportation and Traffic Theory* (Elsevier, New York).
Gazis, D. C., 1974, *Traffic Science* (Wiley, New York).
Gazis, D. C., and R. Herman, 1992, Transp. Sci. **26**, 223.
Gazis, D. C., R. Herman, and R. B. Potts, 1959, Oper. Res. **7**, 499.
Gazis, D. C., R. Herman, and R. W. Rothery, 1961, Oper. Res. **9**, 545.
Gazis, D. C., R. Herman, and G. H. Weiss, 1962, Oper. Res. **10**, 658.
Gazis, D. C., and C. H. Knapp, 1971, Transp. Sci. **5**, 283.
Gebhardt, T., and S. Grossmann, 1994, Phys. Rev. E **50**, 3705.
Gerlough, D. L., and M. J. Huber, 1975, *Traffic Flow Theory*. Special Report 165 (Transportation Research Board, Washington, DC).
Gerwinski, M., and J. Krug, 1999, Phys. Rev. E **60**, 188.
Gibson, D. R. P., 1981, in *Special Report 194*, edited by B. J. Vumbaco (National Academy of Sciences, Washington, DC), p. 12.
Gilchrist, R. S., and F. L. Hall, 1989, Transp. Res. Rec. **1225**, 99.
Gipps, P. G., 1981, Transp. Res., Part B: Methodol. **15B**, 105.
Gipps, P. G., 1986, Transp. Res., Part B: Methodol. **20B**, 403.
Gipps, P. G., and B. Marksjö, 1985, Math. Comput. Simul. **27**, 95.
Godunov, S. K., 1959, Mat. Sb. **47**, 271.
Goldbach, M., A. Eidmann, and A. Kittel, 2000, Phys. Rev. E **61**, 1239.
Goldhirsch, I., 1995, Science **267**, 116.
Goldhirsch, I., M.-L. Tan, and G. Zanetti, 1993, J. Sci. Comput. **8**, 1.
Golding, I., Y. Kozlovsky, I. Cohen, and E. Ben-Jacob, 1998, Physica A **260**, 510.
Goodman, L. A., 1964, Am. J. Sociol. **70**, 170.
Gopal, S., and T. R. Smith, 1990, in *Spatial Choices and Processes*, edited by M. M. Fischer, P. Nijkamp, and Y. Y. Papageorgiou (North-Holland, Amsterdam), p. 169.
Grassberger, P., and M. Scheunert, 1980, Fortschr. Phys. **28**, 547.
Greenberg, H., 1959, Oper. Res. **7**, 79.
Greenshields, B. D., 1935, in *Proceedings of the Highway Research Board* (Highway Research Board, Washington, D.C.), Vol. 14, p. 448.
Greiner, A., 1996, Master's thesis (University of Stuttgart).
Großmann, S., 2000, Rev. Mod. Phys. **72**, 603.
Gutowitz, H. A., J. D. Victor, and B. W. Knight, 1987, Physica D **28**, 18.
Gwa, L.-H., and H. Spohn, 1992, Phys. Rev. Lett. **68**, 725.
Hänggi, P., and R. Bartussek, 1996, in *Nonlinear Physics of Complex Systems—Current Status and Future Trends*, edited by J. Parisi, S. C. Müller, and W. Zimmermann (Springer, Berlin), p. 294.
Haff, P. K., 1983, J. Fluid Mech. **134**, 401.
Haight, F. A., 1963, *Mathematical Theories of Traffic Flow* (Academic, New York).
Haken, H., 1977, *Synergetics* (Springer, Berlin).
Haken, H., 1983, *Advanced Synergetics* (Springer, Berlin).
Haken, H., 1988, *Information and Self-Organization* (Springer, Berlin).
Hall, F. L., 1987, Transp. Res., Part A **21A**, 191.
Hall, F. L., and K. Agyemang-Duah, 1991, Transp. Res. Rec. **1320**, 91.
Hall, F. L., B. L. Allen, and M. A. Gunter, 1986, Transp. Res., Part A **20A**, 197.
Hall, F. L., V. F. Hurdle, and J. H. Banks, 1992, Transp. Res. Rec. **1365**, 12.
Hall, F. L., and T. N. Lam, 1988, Transp. Res., Part A **22**, 45.
Hall, F. L., A. Pushkar, and Y. Shi, 1993, Transp. Res. Rec. **1510**, 24.
Hall, R. W., 1999, *Handbook of Transportation Science* (Kluwer Academic, Boston).
Hamacher, H. W., and S. A. Tjandra, 2001a, in *Pedestrian and Evacuation Dynamics*, edited by M. Schreckenberg and S. D. Sharma (Springer, Berlin), p. 227.
Hamacher, H. W., and S. A. Tjandra, 2001b, in *Pedestrian and Evacuation Dynamics*, edited by M. Schreckenberg and S. D. Sharma (Springer, Berlin), p. 267.
Hankin, B. D., and R. A. Wright, 1958, Oper. Res. Q. **9**, 81.
Haus, J. W., and K. W. Kehr, 1987, Phys. Rep. **150**, 263.
Hayakawa, H., S. Yue, and D. C. Hong, 1995, Phys. Rev. Lett. **75**, 2328.

Helbing, D., 1990, Master's thesis (Georg-August University, Göttingen).
Helbing, D., 1991, Behav. Sci. **36**, 298.
Helbing, D., 1992a, *Stochastische Methoden, nichtlineare Dynamik und quantitative Modelle sozialer Prozesse*, Ph.D. thesis (University of Stuttgart); published by Shaker, Aachen, 1993.
Helbing, D., 1992b, Complex Syst. **6**, 391.
Helbing, D., 1992c, in *Economic Evolution and Demographic Change. Formal Models in Social Sciences*, edited by G. Haag, U. Mueller, and K. G. Troitzsch (Springer, Berlin), p. 330.
Helbing, D., 1993a, Physica A **193**, 241.
Helbing, D., 1993b, Physica A **196**, 546.
Helbing, D., 1994, J. Math. Sociol. **19**, 189.
Helbing, D., 1995a, *Quantitative Sociodynamics. Stochastic Methods and Models of Social Interaction Processes* (Kluwer Academic, Dordrecht).
Helbing, D., 1995b, Phys. Rev. E **51**, 3164.
Helbing, D., 1995c, Physica A **219**, 375.
Helbing, D., 1995d, Physica A **219**, 391.
Helbing, D., 1996a, Phys. Rev. E **53**, 2366.
Helbing, D., 1996b, Physica A **233**, 253.
Helbing, D., 1996c, Theory Dec. **40**, 149.
Helbing, D., 1996d, in *Traffic and Granular Flow*, edited by D. E. Wolf, M. Schreckenberg, and A. Bachem (World Scientific, Singapore), p. 87.
Helbing, D., 1997a, *Verkehrsdynamik* (Springer, Berlin).
Helbing, D., 1997b, Phys. Rev. E **55**, R25.
Helbing, D., 1997c, Phys. Rev. E **55**, 3735.
Helbing, D., 1997d, Physica A **242**, 175.
Helbing, D., 1997e, in *Transportation Systems*, edited by M. Papageorgiou and A. Pouliezos (IFAC, Technical University of Crete, Chania), Vol. 2, p. 809.
Helbing, D., 1998a, in *A Perspective Look at Nonlinear Media. From Physics to Biology and Social Sciences*, edited by J. Parisi, S. C. Müller, and W. Zimmermann (Springer, Berlin), p. 122.
Helbing, D., 1998b, in *Traffic and Granular Flow '97*, edited by M. Schreckenberg and D. E. Wolf (Springer, Singapore), p. 21.
Helbing, D., 1998c, Phys. Rev. E **57**, 6176.
Helbing, D., 2001, Phys. Bl. **57**, 27.
Helbing, D., I. J. Farkas, and T. Vicsek, 2000a, Phys. Rev. Lett. **84**, 1240.
Helbing, D., I. J. Farkas, and T. Vicsek, 2000b, Nature (London) **407**, 487.
Helbing, D., and A. Greiner, 1997, Phys. Rev. E **55**, 5498.
Helbing, D., A. Hennecke, V. Shvetsov, and M. Treiber, 2001a, Transp. Res., Part B: Methodol. **35B**, 183.
Helbing, D., A. Hennecke, V. Shvetsov, and M. Treiber, 2001b, Math. Comput. Model (in press).
Helbing, D., A. Hennecke, and M. Treiber, 1999, Phys. Rev. Lett. **82**, 4360.
Helbing, D., H. J. Herrmann, M. Schreckenberg, and D. E. Wolf, 2000, Eds., *Traffic and Granular Flow '99: Social, Traffic, and Granular Dynamics* (Springer, Berlin).
Helbing, D., and B. A. Huberman, 1998, Nature (London) **396**, 738.
Helbing, D., J. Keltsch, and P. Molnár, 1997, Nature (London) **388**, 47.
Helbing, D., and R. Molini, 1995, Phys. Lett. A **212**, 130.
Helbing, D., and P. Molnár, 1995, Phys. Rev. E **51**, 4282.
Helbing, D., and P. Molnár, 1997, in *Self-Organization of Complex Structures: From Individual to Collective Dynamics*, edited by F. Schweitzer (Gordon and Breach, London), p. 569.
Helbing, D., P. Molnár, I. Farkas, and K. Bolay, 2001, Environ. Plan. B **28**, 361.
Helbing, D., P. Molnár, and F. Schweitzer, 1994, in *Evolution of Natural Structures* (Sonderforschungsbereich 230, Stuttgart), p. 229.
Helbing, D., D. Mukamel, and G. M. Schütz, 1999, Phys. Rev. Lett. **82**, 10.
Helbing, D., and T. Platkowski, 2000, Int. J. Chaos Theor. Appl. **5**, 25.
Helbing, D., and M. Schreckenberg, 1999, Phys. Rev. E **59**, R2505.
Helbing, D., F. Schweitzer, J. Keltsch, and P. Molnár, 1997, Phys. Rev. E **56**, 2527.
Helbing, D., and B. Tilch, 1998, Phys. Rev. E **58**, 133.
Helbing, D., and M. Treiber, 1998a, Phys. Rev. Lett. **81**, 3042.
Helbing, D., and M. Treiber, 1998b, Science **282**, 2001.
Helbing, D., and M. Treiber, 1998c, Granular Matter **1**, 21.
Helbing, D., and M. Treiber, 1999, Comput. Sci. Eng. **1**, 89.
Helbing, D., and T. Vicsek, 1999, New J. Phys. **1**, 13.1.
Hemmingsson, J., 1995, J. Phys. A **28**, 4245.
Henderson, L. F., 1971, Nature (London) **229**, 381.
Henderson, L. F., 1974, Transp. Res. **8**, 509.
Henderson, L. F., and D. M. Jenkins, 1973, Transp. Res. **8**, 71.
Henderson, L. F., and D. J. Lyons, 1972, Nature (London) **240**, 353.
Hennecke, A., M. Treiber, and D. Helbing, 2000, in *Traffic and Granular Flow '99: Social, Traffic, and Granular Dynamics*, edited by D. Helbing, H. J. Herrmann, M. Schreckenberg, and D. E. Wolf (Springer, Berlin), p. 383.
Herkner, W. H., 1975, Z. Klin. Psychol. Psychol. **4**, 50.
Herman, R., and K. Gardels, 1963, Sci. Am. **209**, 35.
Herman, R., T. Lam, and I. Prigogine, 1973, Science **179**, 918.
Herman, R., E. W. Montroll, R. B. Potts, and R. W. Rothery, 1959, Oper. Res. **7**, 86.
Herman, R., and I. Prigogine, 1979, Science **204**, 148.
Herman, R., and R. Rothery, 1963, J. Oper. Res. Soc. Jpn. **5**, 74.
Herrmann, M., and B. S. Kerner, 1998, Physica A **255**, 163.
Hida, K., 1979, in *Theoretical and Applied Mechanics, Vol. 27* (University of Tokyo, Tokyo), p. 451.
Hill, M. R., 1984, *Walking, Crossing Streets, and Choosing Pedestrian Routes* (University of Nebraska, Lincoln).
Hillegas, B. D., D. G. Houghton, and P. J. Athol, 1974, Transp. Res. Rec. **495**, 53.
Hilliges, M., 1995, *Ein phänomenologisches Modell des dynamischen Verkehrsflusses in Schnellstraßennetzen* (Shaker, Aachen).
Hilliges, M., R. Reiner, and W. Weidlich, 1993, in *Modelling and Simulation 1993*, edited by A. Pave (Society for Computer Simulation International, Ghent), p. 505.
Hilliges, M., and W. Weidlich, 1995, Transp. Res., Part B: Methodol. **29B**, 407.
Hinrichsen, H., 1996, J. Phys. A **29**, 3659.
Hinrichsen, H., R. Livi, D. Mukamel, and A. Politi, 1997, Phys. Rev. Lett. **79**, 2710.
Hirshfeld, D., Y. Radzyner, and D. C. Rapaport, 1997, Phys. Rev. E **56**, 4404.
Hoefs, D. H., 1972, *Untersuchung des Fahrverhaltens in Fahrzeugkolonnen* (Bundesministerium für Verkehr, Abt. Straßenbau, Bonn-Bad Godesberg).

Hoel, L. A., 1968, Traffic Eng. Control **38**, 10.
Hohenberg, P. C., and B. I. Halperin, 1977, Rev. Mod. Phys. **49**, 435.
Holland, E. N., and A. W. Woods, 1997, Transp. Res., Part B: Methodol. **31B**, 473.
Hoogendoorn, S., 1999, *Multiclass Continuum Modelling of Multilane Traffic Flow* (Delft University of Technology, Delft).
Hoogendoorn, S., and P. H. L. Bovy, 1998, in *Motorway Traffic Flow Analysis. New Methodologies and Recent Empirical Findings*, edited by P. H. L. Bovy (Delft University of Technology, Delft), p. 71.
Hoogendoorn, S., and P. H. L. Bovy, 1999a, Transp. Res. Rec. **1678**, 150.
Hoogendoorn, S., and P. H. L. Bovy, 1999b, in *Proceedings of the 14th International Symposium of Transportation and Traffic Theory* (Pergamon, New York), p. 27.
Hoogendoorn, S. P., and P. H. L. Bovy, 2000a, Transp. Res. Rec. **1710**, 28.
Hoogendoorn, S. P., and P. H. L. Bovy, 2000b, Transp. Res., Part B: Methodol. **34B**, 123.
Hoogendoorn, S. P., P. H. L. Bovy, and W. Daamen, 2001, in *Pedestrian and Evacuation Dynamics*, edited by M. Schreckenberg and S. D. Sharma (Springer, Berlin), p. 123.
Hoover, W. G., 1986, *Molecular Dynamics* (Springer, Berlin).
Hoque, S., and M. McDonald, 1995, in *Modelling and Simulation ESM 1995*, edited by M. Snorek, M. Sujansky, and A. Verbraeck (Society for Computer Simulation International, Istanbul), p. 321.
Horikawa, S., T. Isoda, T. Nakayama, A. Nakahara, and M. Matsushita, 1996, Physica A **233**, 699.
Horsthemke, W., and R. Lefever, 1984, *Noise-Induced Transitions* (Springer, Berlin).
Huang, K., 1987, *Statistical Mechanics*, 2nd ed. (Wiley, New York).
Huberman, B. A., and N. S. Glance, 1993, Proc. Natl. Acad. Sci. U.S.A. **90**, 7716.
Huberman, B. A., and D. Helbing, 1999, Europhys. Lett. **47**, 196.
Hughes, R. L., 2000, Math. Comput. Simul. **53**, 367.
Hughes, R. L., 2001, Transp. Res., Part B: Methodol. (in press).
Hunt, P. B., D. I. Robertson, and R. D. Bretherton, 1982, Traffic Eng. Control **23**, 190.
Hurdle, V. F., E. Hauer, and G. N. Stewart, 1983, Eds., *Proceedings of the 8th International Symposium on Transportation and Traffic Flow Theory* (University of Toronto, Toronto, Ontario).
Hwang, S.-H., and H.-C. Chang, 1987, Phys. Fluids **30**, 1259.
Ianigro, S., 1994, Ph.D. thesis (Universität der Bundeswehr, Hamburg).
Igarashi, Y., K. Itoh, K. Nakanishi, K. Ogura, and K. Yokokawa, 1999, Phys. Rev. Lett. **83**, 718.
Islam, M. N., and P. C. Consul, 1991, Transp. Res., Part B: Methodol. **25B**, 365.
Janowsky, S. A., and J. L. Lebowitz, 1992, Phys. Rev. A **45**, 618.
Janowsky, S. A., and J. L. Lebowitz, 1994, J. Stat. Phys. **77**, 35.
Jenkins, J. T., and M. W. Richman, 1985, Phys. Fluids **28**, 3485.
Jenssen, M., 1991, Phys. Lett. A **159**, 6.
Johnson, N. R., 1987, Social Probl. **34**, 362.
Joseph, D. D., 1976, *Stability of Fluid Motions I and II* (Springer, Berlin).
Jülicher, F., A. Ajdari, and J. Prost, 1997, Rev. Mod. Phys. **69**, 1269.
Kadanoff, L. P., 1985, J. Stat. Phys. **39**, 267.
Kai, S., 1992, Ed., *Pattern Formation in Complex Dissipative Systems* (World Scientific, Singapore).
Kapral, R., and K. Showalter, 1995, Eds., *Chemical Waves and Patterns* (Kluwer, Dordrecht).
Karimipour, V., 1999a, Phys. Rev. E **59**, 205.
Karimipour, V., 1999b, Europhys. Lett. **47**, 304.
Karimipour, V., 1999c, Europhys. Lett. **47**, 501.
Kates, R., K. Bogenberger, and M. Hoops, 1998, in *Traffic and Granular Flow '97*, edited by M. Schreckenberg and D. E. Wolf (Springer, Singapore), p. 453.
Katz, S., J. L. Lebowitz, and H. Spohn, 1984, J. Stat. Phys. **34**, 497.
Kaulke, M., and S. Trimper, 1995, J. Phys. A **28**, 5445.
Kaumann, O., K. Froese, R. Chrobok, J. Wahle, L. Neubert, and M. Schreckenberg, 2000, in *Traffic and Granular Flow '99: Social, Traffic, and Granular Dynamics*, edited by D. Helbing, H. J. Herrmann, M. Schreckenberg, and D. E. Wolf (Springer, Berlin), p. 351.
Kayatz, C., 2000, e-print n.ethz.ch/student/floo/pedestrians/ped.html.
Keating, J. P., 1982, Fire J. **57**, 61.
Keizer, J., 1987, *Statistical Thermodynamics of Nonequilibrium Processes* (Springer, New York).
Kelley, H. H., and J. W. Thibaut, 1969, in *The Handbook of Social Psychology*, edited by G. Lindzey and E. Aronson (Addison-Wesley, Reading, MA), Vol. 4.
Kerner, B. S., 1995, in *Chaotic, Fractal, and Nonlinear Signal Processing*, edited by R. A. Katz (AIP, New York), p. 777.
Kerner, B. S., 1997, in *Transportation Systems 1997*, edited by M. Papageorgiou and A. Pouliezos (Elsevier, London), p. 765.
Kerner, B. S., 1998a, Phys. Rev. Lett. **81**, 3797.
Kerner, B. S., 1998b, in *Proceedings of the 3rd International Symposium on Highway Capacity* edited by R. Rysgaard (Road Directorate, Denmark), Vol. 2, p. 621.
Kerner, B. S., 1998c, in *Traffic and Granular Flow '97*, edited by M. Schreckenberg and D. E. Wolf (Springer, New York), p. 239.
Kerner, B. S., 1999a, Transp. Res. Rec. **1678**, 160.
Kerner, B. S., 1999b, Phys. World **12** (8), 25.
Kerner, B. S., 1999c, in *Proceedings of the 14th International Symposium on Transportation and Traffic Theory*, edited by A. Ceder (Pergamon, New York), p. 147.
Kerner, B. S., 2000a, in *Traffic and Granular Flow '99: Social, Traffic, and Granular Dynamics*, edited by D. Helbing, H. J. Herrmann, M. Schreckenberg, and D. E. Wolf (Springer, Berlin), p. 253.
Kerner, B. S., 2000b, Transp. Res. Rec. **1710**, 136.
Kerner, B. S., 2000c, J. Phys. A **33**, L221.
Kerner, B. S., S. L. Klenov, and P. Konhäuser, 1997, Phys. Rev. E **56**, 4200.
Kerner, B. S., and P. Konhäuser, 1993, Phys. Rev. E **48**, R2335.
Kerner, B. S., and P. Konhäuser, 1994, Phys. Rev. E **50**, 54.
Kerner, B. S., P. Konhäuser, and M. Schilke, 1995a, Phys. Rev. E **51**, R6243.
Kerner, B. S., P. Konhäuser, and M. Schilke, 1995b, in *Proceedings of the 7th World Conference on Transport Research*, edited by D. Hensher, J. King, and T. H. Oum (Pergamon, Oxford), Vol. 2, p. 167.

Kerner, B. S., P. Konhäuser, and M. Schilke, 1996, Phys. Lett. A **215**, 45.
Kerner, B. S., and V. V. Osipov, 1994, *Autosolitons: A New Approach to Problems of Self-Organization and Turbulence* (Kluwer, Dordrecht).
Kerner, B. S., and H. Rehborn, 1996a, Phys. Rev. E **53**, R1297.
Kerner, B. S., and H. Rehborn, 1996b, Phys. Rev. E **53**, R4275.
Kerner, B. S., and H. Rehborn, 1997, Phys. Rev. Lett. **79**, 4030.
Kerner, B. S., and H. Rehborn, 1998a, Int. Verkehrswesen **50**, 196.
Kerner, B. S., and H. Rehborn, 1998b, Int. Verkehrswesen **50**, 347.
Keßel, A., H. Klüpfel, J. Wahle, and M. Schreckenberg, 2001, in *Pedestrian and Evacuation Dynamics*, edited by M. Schreckenberg and S. D. Sharma (Springer, Berlin), p. 193
Ketchell, N., S. Cole, D. M. Webber, C. A. Marriott, P. J. Stephens, I. R. Brearley, J. Fraser, J. Doheny, and J. Smart, 1993, in *Engineering for Crowd Safety*, edited by R. A. Smith and J. F. Dickie (Elsevier, Amsterdam), p. 361.
Kikuchi, R., 1966, Suppl. Prog. Theor. Phys. **35**, 1.
Kirsch, H., 1964, *Leistungsfähigkeit und Dimensionierung von Fußgängerwegen*. Reihe *Straßenbau and Straßenverkehrstechnik*, Heft 33 (Bundesministerium für Verkehr, Abt. Straßenbau, Bonn).
Klar, A., R. D. Kühne, and R. Wegener, 1996, Surv. Math. Ind. **6**, 215.
Klar, A., and R. Wegener, 1997, J. Stat. Phys. **87**, 91.
Klar, A., and R. Wegener, 1999a, SIAM (Soc. Ind. Appl. Math.) J. Appl. Math. **59**, 983.
Klar, A., and R. Wegener, 1999b, SIAM (Soc. Ind. Appl. Math.) J. Appl. Math. **59**, 1002.
Klauck, K., and A. Schadschneider, 1999, Physica A **271**, 102.
Klimontovich, Y. L., 1986, *Statistical Physics* (Harwood Academic, Chur, Switzerland).
Klockgether, J., and H.-P. Schwefel, 1970, in *Proceedings of the Eleventh Symposium on Engineering Aspects of Magnetohydrodynamics*, edited by D. G. Elliott (California Institute of Technology, Pasadena, CA), p. 141.
Klüpfel, H., M. Meyer-König, J. Wahle, and M. Schreckenberg, 2000, in *Theoretical and Practical Issues on Cellular Automata, Proceedings of the 4th International Conference on Cellular Automata for Research and Industry*, edited by S. Bandini and T. Worsch (Springer, London), p. 63.
Knospe, W., L. Santen, A. Schadschneider, and M. Schreckenberg, 1999, Physica A **265**, 614.
Knospe, W., L. Santen, A. Schadschneider, and M. Schreckenberg, 2000a, in *Traffic and Granular Flow '99: Social, Traffic, and Granular Dynamics*, edited by D. Helbing, H. J. Herrmann, M. Schreckenberg, and D. E. Wolf (Springer, Berlin), p. 431.
Knospe, W., L. Santen, A. Schadschneider, and M. Schreckenberg, 2000b, J. Phys. A **33**, L477.
Kobryn, A. E., V. G. Morozov, I. P. Omelyan, and M. V. Tokarchuk, 1996, Physica A **230**, 189.
Koch, N., 1996, Ph.D. thesis (University of Stuttgart).
Kolomeisky, A. B., G. M. Schütz, E. B. Kolomeisky, and J. P. Straley, 1998, J. Phys. A **31**, 6911.
Komatsu, T. S., and S.-i. Sasa, 1995, Phys. Rev. E **52**, 5574.
Kometani, E., and T. Sasaki, 1958, J. Oper. Res. Soc. Jpn. **2**, 11.
Kometani, E., and T. Sasaki, 1959, Oper. Res. **7**, 704.
Kometani, E., and T. Sasaki, 1961, in *Theory of Traffic Flow*, edited by R. Herman (Elsevier, Amsterdam), p. 105.
Koshi, M., M. Iwasaki, and I. Ohkura, 1983, in *Proceedings of the 8th International Symposium on Transportation and Traffic Flow Theory* (University of Toronto, Toronto), p. 403.
Krauß, S., 1998a, *Microscopic Modeling of Traffic Flow: Investigation of Collision Free Vehicle Dynamics*. Report No. 98-08 (DLR-Deutsches Zentrum für Luft- und Raumfahrt e.V., Cologne).
Krauß, S., 1998b, in *Traffic and Granular Flow '97*, edited by M. Schreckenberg and D. E. Wolf (Springer, New York), p. 269.
Krauß, S., P. Wagner, and C. Gawron, 1996, Phys. Rev. E **54**, 3707.
Krauß, S., P. Wagner, and C. Gawron, 1997, Phys. Rev. E **55**, 5597.
Krebs, K., and S. Sandow, 1997, J. Phys. A **30**, 3165.
Krug, J., 1991, Phys. Rev. Lett. **67**, 1882.
Krug, J., 2000, Braz. J. Phys. **30**, 97.
Krug, J., and P. A. Ferrari, 1996, J. Phys. A **29**, L465.
Ktitarev, D., D. Chowdhury, and D. E. Wolf, 1997, J. Phys. A **30**, L221.
Kube, C. R., and E. Bonabeau, 2000, Rob. Auton. Syst. **30**, 85.
Kühne, R. D., 1984a, in *Proceedings of the 9th International Symposium on Transportation and Traffic Theory*, edited by I. Volmuller and R. Hamerslag (VNU Science, Utrecht), p. 21.
Kühne, R., 1984b, Phys. Unserer Zeit **3**, 84.
Kühne, R. D., 1987, in *Proceedings of the 10th International Symposium on Transportation and Traffic Theory*, edited by N. H. Gartner and N. H. M. Wilson (Elsevier, New York), p. 119.
Kühne, R., 1991a, in *Highway Capacity and Level of Service*, Proceedings of the International Symposium on Highway Capacity, edited by U. Brannolte (Balkema, Rotterdam), p. 211.
Kühne, R., 1991b, Phys. Bl. **47**, 201.
Kühne, R. D., 1993, in *21st Summer Annual Meeting on Traffic Management and Road Safety* (Institute of Science and Technology, University of Manchester, England), p. 153.
Kühne, R., and N. Anstett, 1999, in *Proceedings of the 14th International Symposium on Transportation and Traffic Theory*, edited by A. Ceder (Pergamon, New York), p. S177.
Kühne, R. D., and R. Beckschulte, 1993, in *Proceedings of the 12th International Symposium on the Theory of Traffic Flow and Transportation*, edited by C. F. Daganzo (Elsevier, Amsterdam), p. 367.
Kühne, R. D., and A. Kroen, 1992, in *International Conference on Artificial Intelligence Applications in Transportation Engineering*, June 20–24, 1992 (San Buenaventura, CA), p. 173.
Kühne, R. D., K. Langbein-Euchner, M. Hilliges, and N. Koch, 1995, in *Proceedings of the 6th International Conference on Computing in Civil and Building Engineering* (Balkema, Rotterdam), p. 1431.
Kühne, R. D., K. Langbein-Euchner, M. Hilliges, and N. Koch, 1997, Transp. Res. Rec. **1554**, 153.
Kühne, R. D., and M. B. Rödiger, 1991, in *Proceedings of the 1991 Winter Simulation Conference*, edited by B. L. Nelson, W. D. Kelton, and G. M. Clark (Society for Computer Simulation International, Phoenix, AZ), p. 762.
Kuramoto, Y., 1989, Prog. Theor. Phys. Suppl. **99**, 244.
Kurtze, D. A., and D. C. Hong, 1995, Phys. Rev. E **52**, 218.
Lampis, M., 1978, Transp. Sci. **12**, 16.
Landau, L. D., and E. M. Lifshits, 1980, *Course of Theoretical Physics* (Pergamon, Oxford), Vol. 5.
Landau, L. D., and E. M. Lifshits, 1987, *Course of Theoretical Physics* (Pergamon, Oxford), Vol. 6.

Lapierre, R., and G. Steierwald, 1987, *Verkehrsleittechnik für den Straßenverkehr, Band I: Grundlagen and Technologien der Verkehrsleittechnik* (Springer, Berlin).
Laughlin, P. R., N. L. Kerr, J. H. Davis, H. M. Halff, and K. A. Marciniak, 1975, J. Pers. Soc. Psychol. **31**, 522.
Lawson, T., W. H. Lin, and M. Cassidy, 1999, *Validation of the Incremental Transfer Model*. PATH Working Paper (Institute of Transportation Studies, University of California, Berkeley, CA).
Lebacque, J. P., 1995, *The Godunov Scheme and What it Means for First Order Traffic Flow Models* (Centre d'Enseignement et de Recherche en Mathématique, Informatique et Calcul Scientifique, NOISY-LE-GRAND Cedex).
Lebacque, J. P., 1997, in *Transportation Systems*, edited by M. Papageorigiou and A. Pouliezos (IFAC, Technical University of Crete, Chania), Vol. 2, p. 815.
Lee, J., 1994, Phys. Rev. E **49**, 281.
Lee, H. W., V. Popkov, and D. Kim, 1997, J. Phys. A **30**, 8497.
Lee, H. Y., H.-W. Lee, and D. Kim, 1998, Phys. Rev. Lett. **81**, 1130.
Lee, H. Y., H.-W. Lee, and D. Kim, 1999, Phys. Rev. E **59**, 5101.
Lee, H. Y., H.-W. Lee, and D. Kim, 2000, Phys. Rev. E **62**, 4737.
Lenz, H., C. K. Wagner, and R. Sollacher, 1999, Eur. Phys. J. B **7**, 331.
Leong, H. J. W., 1968, in *Proceedings of the Australian Road Research Board* (Road Research Board, Victoria, Australia), Vol. 4, p. 791.
Lesort, J. B., 1996, Ed., *Transportation and Traffic Theory: Proceedings of the 13th International Symposium on Transportation and Traffic Theory* (Pergamon-Elsevier, Tarrytown, NY).
Leutzbach, W., 1988, *Introduction to the Theory of Traffic Flow* (Springer, Berlin).
LeVeque, R. J., 1992, *Numerical Methods for Conservation Laws* (Birkhäuser, Basel).
Levin, M., 1976, Transp. Res. Rec. **596**, 30.
Lewin, K., 1951, *Field Theory in Social Science* (Harper, New York).
Liboff, R. L., 1990, *Kinetic Theory* (Prentice-Hall, London).
Liggett, T. M., 1975, Trans. Am. Math. Soc. **179**, 433.
Liggett, T. M., 1985, *Interacting Particle Systems* (Springer, New York).
Liggett, T. M., 1999, *Stochastic Interacting Systems: Contact, Voter and Exclusion Processes* (Springer, Berlin).
Lighthill, M. J., and G. B. Whitham, 1955, Proc. R. Soc. London, Ser. A **229**, 317.
Løvås, G. G., 1993, in *Modelling and Simulation 1993*, edited by A. Pave (Society for Computer Simulation, Ghent), p. 469.
Løvås, G. G., 1994, Transp. Res., Part B: Methodol. **28B**, 429.
Løvås, G. G., 1998, IEEE Trans. Eng. Manage. **45**, 181.
Lubashevsky, I., and R. Mahnke, 2000, Phys. Rev. E **62**, 6082.
Lübeck, S., M. Schreckenberg, and K. D. Usadel, 1998, Phys. Rev. E **57**, 1171.
Ludmann, J., D. Neunzig, and M. Weilkes, 1997, Veh. Syst. Dyn. **27**, 491.
Lun, C. K. K., S. B. Savage, D. J. Jeffrey, and N. Chepurniy, 1984, J. Fluid Mech. **140**, 223.
Lutsko, J. F., 1997, Phys. Rev. Lett. **78**, 243.
Lux, T., and M. Marchesi, 1999, Nature (London) **397**, 498.
Ma, S.-K., 1976, *Modern Theory of Critical Phenomena* (Benjamin, New York).
Ma, S.-K., 1985, *Statistical Mechanics* (World Scientific, Singapore).
Mahmassani, H. S., R. Jayakrishnan, and R. Herman, 1990, Transp. Res., Part A **24A**, 149.
Mahmassani, H., and Y. Sheffi, 1981, Transp. Res., Part B: Methodol. **15B**, 143.
Mahnke, R., and J. Kaupužs, 1999, Phys. Rev. E **59**, 117.
Mahnke, R., and N. Pieret, 1997, Phys. Rev. E **56**, 2666.
Makigami, Y., T. Nakanishi, M. Toyama, and R. Mizote, 1983, in *Proceedings of the 8th International Symposium on Transportation and Traffic Flow Theory*, edited by V. F. Hurdle, E. Hauer, and G. N. Stewart (University of Toronto, Toronto), p. 427.
Makse, H. A., S. Havlin, P. R. King, and H. E. Stanley, 1997, Nature (London) **386**, 379.
Mandelbrot, B. B., 1983, *The Fractal Geometry of Nature* (Freeman, New York).
Manneville, P., 1990, *Dissipative Structures and Weak Turbulence* (Academic, New York).
Manstetten, D., W. Krautter, and T. Schwab, 1997, in *Proceedings of the 4th World Congress on Intelligent Transport Systems*, October 1997, Berlin (ITS Congress Association, Brussels), CD Rom, Paper No. 00648.
Markus, M., and B. Hess, 1990, Nature (London) **347**, 56.
Mason, A. D., and A. W. Woods, 1997, Phys. Rev. E **55**, 2203.
May, A. D., 1964, High. Res. Rec. **59**, 9.
May, A. D., 1981, in *Special Report 194*, edited by B. J. Vumbaco (National Academy of Sciences, Washington, DC), p. 23.
May, A. D., 1990, *Traffic Flow Fundamentals* (Prentice Hall, Englewood Cliffs, NJ).
May, A. D., Jr., and H. E. M. Keller, 1967, Highw. Res. Rec. **199**, 19.
Mayne, A. J., 1954, Biometrika **41**, 375.
McDonald, M., M. Brackstone, and D. Jeffery, 1994, in *Proceedings of the 27th ISATA Conference*, Aachen, November 1994 (Automotive Automation, Croyden, England), p. 365.
McDonald, M., M. Brackstone, and B. Sultan, 1998, in *Proceedings of the 3rd International Symposium on Highway Capacity*, edited by R. Rysgaard (Road Directorate, Denmark), p. 757.
McNamara, S., and W. R. Young, 1992, Phys. Fluids A **4**, 496.
Meißner, F., and G. Böker, 1996, *Bedienungsanleitung für das Simulationspaket SIMONE* (Technische Universität Hamburg-Harburg, Hamburg).
Melo, F., P. B. Umbanhowar, and H. L. Swinney, 1995, Phys. Rev. Lett. **75**, 3838.
Mermin, N. D., and H. Wagner, 1966, Phys. Rev. Lett. **17**, 1133.
Meron, E., 1992, Phys. Rep. **218**, 1.
Michaels, R. M., 1965, in *Proceedings of the 2nd International Symposium on the Theory of Traffic Flow 1963* (OECD, Paris), p. 44.
Michaels, R. M., and L. W. Cozan, 1962, Highw. Res. Rec. **25**, 1.
Michalopoulos, P. G., D. E. Beskos, and Y. Yamauchi, 1984, Transp. Res., Part B: Methodol. **18B**, 377.
Migowsky, S., T. Wanschura, and P. Ruján, 1994, Z. Phys. B: Condens. Matter **95**, 407.
Mika, H. S., J. B. Kreer, and L. S. Yuan, 1969, Highw. Res. Rec. **279**, 1.
Mikhailov, A. S., 1991a, *Foundations of Synergetics I* (Springer, Berlin).

Mikhailov, A. S., 1991b, *Foundations of Synergetics II* (Springer, Berlin).
Mikhailov, A. S., and D. H. Zanette, 1999, Phys. Rev. E **60**, 4571.
Miller, N. E., 1944, in *Personality and the Behavior Disorders*, edited by J. McV. Hunt (Ronald, New York), Vol. 1.
Miller, N. E., 1959, in *Psychology: A Study of Science*, edited by S. Koch (McGraw Hill, New York), Vol. 2.
Mintz, A., 1951, J. Abnorm. Soc. Psychol. **46**, 150.
Miramontes, O., R. V. Solé, and B. C. Goodwin, 1993, Physica D **63**, 145.
Mitarai, N., and H. Nakanishi, 1999, J. Phys. Soc. Jpn. **68**, 2475.
Mitarai, N., and H. Nakanishi, 2000, Phys. Rev. Lett. **85**, 1766.
Molnár, P., 1996a, *Modellierung und Simulation der Dynamik von Fußgängerströmen* (Shaker, Aachen).
Molnár, P., 1996b, in *Social Science Microsimulation*, edited by J. Doran, N. Gilbert, U. Mueller, and K. Troitzsch (Springer, Berlin), p. 155.
Moore, E. F., 1962, Proc. Symb. Appl. Math. **14**, 17.
Mōri, M., and H. Tsukaguchi, 1987, Transp. Res., Part A **21A**, 223.
Munjal, P. K., Y.-S. Hsu, and R. L. Lawrence, 1971, Transp. Res. **5**, 257.
Munjal, P. K., and L. A. Pipes, 1971, Transp. Res. **5**, 241.
Muñoz, J. C., and C. F. Daganzo, 1999, PATH Working Paper.
Muramatsu, M., T. Irie, and T. Nagatani, 1999, Physica A **267**, 487.
Muramatsu, M., and T. Nagatani, 1999, Phys. Rev. E **60**, 180.
Muramatsu, M., and T. Nagatani, 2000a, Physica A **275**, 281.
Muramatsu, M., and T. Nagatani, 2000b, Physica A **286**, 377.
Musha, T., and H. Higuchi, 1976, Jpn. J. Appl. Phys. **15**, 1271.
Musha, T., and H. Higuchi, 1978, Jpn. J. Appl. Phys. **17**, 811.
Nagatani, T., 1993, J. Phys. A **26**, L781.
Nagatani, T., 1994a, Physica A **202**, 449.
Nagatani, T., 1994b, J. Phys. Soc. Jpn. **63**, 52.
Nagatani, T., 1995a, Phys. Rev. E **51**, 922.
Nagatani, T., 1995b, J. Phys. A **28**, L119.
Nagatani, T., 1995c, J. Phys. A **28**, 7079.
Nagatani, T., 1996a, J. Phys. A **29**, 6531.
Nagatani, T., 1996b, J. Phys. Soc. Jpn. **65**, 3150.
Nagatani, T., 1996c, J. Phys. Soc. Jpn. **65**, 3386.
Nagatani, T., 1997a, Physica A **237**, 67.
Nagatani, T., 1997b, J. Phys. Soc. Jpn. **66**, 1219.
Nagatani, T., 1997c, J. Phys. Soc. Jpn. **66**, L1928.
Nagatani, T., 1998a, Physica A **248**, 353.
Nagatani, T., 1998b, Phys. Rev. E **58**, 4271.
Nagatani, T., 1998c, Physica A **258**, 237.
Nagatani, T., 2000, Physica A **284**, 405.
Nagatani, T., H. Emmerich, and K. Nakanishi, 1998, Physica A **255**, 158.
Nagatani, T., and T. Seno, 1994, Physica A **207**, 574.
Nagel, K., 1994, Int. J. Mod. Phys. C **5**, 567.
Nagel, K., 1995, Ph.D. thesis (University of Cologne).
Nagel, K., 1996, Phys. Rev. E **53**, 4655.
Nagel, K., and C. Barrett, 1997, Int. J. Mod. Phys. C **8**, 505.
Nagel, K., and H. J. Herrmann, 1993, Physica A **199**, 254.
Nagel, K., and M. Paczuski, 1995, Phys. Rev. E **51**, 2909.
Nagel, K., and S. Rasmussen, 1994, in *Proceedings of the Alife 4 [Artificial Life IV] Meeting*, edited by R. A. Brooks and P. Maes (MIT, Cambridge, MA), p. 222.
Nagel, K., and M. Schreckenberg, 1992, J. Phys. I **2**, 2221.
Nagel, K., D. E. Wolf, P. Wagner, and P. Simon, 1998, Phys. Rev. E **58**, 1425.
Nakahara, A., and T. Isoda, 1997, Phys. Rev. E **55**, 4264.
Navin, P. D., and R. J. Wheeler, 1969, Traffic Eng. Control **39**, 31.
Nelson, P., 1995, Transp. Theory Stat. Phys. **24**, 383.
Nelson, P., 2000, Phys. Rev. E **61**, R6052.
Nelson, P., D. D. Bui, and A. Sopasakis, 1997, in *Transportation Systems*, edited by M. Papageorgiou and A. Pouliezos (IFAC, Technical University of Crete, Chania), Vol. 2, p. 799.
Nelson, P., and A. Sopasakis, 1998, Transp. Res., Part B: Methodol. **32B**, 589.
Neubert, L., H. Y. Lee, and M. Schreckenberg, 1999, J. Phys. A **32**, 6517.
Neubert, L., L. Santen, A. Schadschneider, and M. Schreckenberg, 1999, Phys. Rev. E **60**, 6480.
Newell, G. F., 1961, Oper. Res. **9**, 209.
Newell, G. F., 1993, Transp. Res., Part B: Methodol. **27B**, 281.
Nicolas, M., J.-M. Chomaz, and E. Guazzelli, 1994, Phys. Fluids **6**, 3936.
Nicolas, M., J.-M. Chomaz, D. Vallet, and E. Guazzelli, 1996, in *Traffic and Granular Flow*, edited by D. E. Wolf, M. Schreckenberg, and A. Bachem (World Scientific, Singapore), p. 267.
Nicolis, G., and I. Prigogine, 1977, *Self-Organization in Nonequilibrium Systems. From Dissipative Structures to Order through Fluctuations* (Wiley, New York).
Nowak, M. A., and R. M. May, 1992, Nature (London) **359**, 826.
Oeding, D., 1963, *Verkehrsbelastung und Dimensionierung von Gehwegen und anderen Anlagen des Fußgängerverkehrs* (Bundesministerium für Verkehr, Abt. Straßenbau, Bonn).
O'Flaherty, C. A., and M. H. Parkinson, 1972, Traffic Eng. Control **13**, 434.
Okazaki, S., and S. Matsushita, 1993, in *Engineering for Crowd Safety*, edited by R. A. Smith and J. F. Dickie (Elsevier, Amsterdam), p. 271.
Olami, Z., H. J. S. Feder, and K. Christensen, 1992, Phys. Rev. Lett. **68**, 1244.
Older, S. J., 1968, Traffic Eng. Control **10**, 160.
Ozaki, H., 1993, in *Proceedings of the 12th International Symposium on the Theory of Transportation and Traffic*, edited by C. F. Daganzo (American Elsevier, New York), p. 349.
Pampel, F., 1955, *Ein Beitrag zur Berechnung der Leistungsfähigkeit von Straßen* (Kirschbaum, Bielefeld).
Papageorgiou, M., 1983, *Applications of Automatic Control Concepts to Traffic Flow Modeling and Control* (Springer, Berlin).
Papageorgiou, M., 1995, Transp. Res. C **3**, 19.
Papageorgiou, M., 1999, in *Handbook of Transportation Science*, edited by R. W. Hall (Kluwer Academic, Boston), p. 231.
Papageorgiou, M., and A. Pouliezos, 1997, Eds., *Transportation Systems* (IFAC, Technical University of Crete, Chania), Vol. 2.
Pasteels, J. M., and J. L. Deneubourg, 1987, Eds., *From Individual to Collective Behavior in Social Insects* (Birkhäuser, Basel).
Pauls, J., 1984, Fire Technol. **20**, 27.
Pave, A., 1993, Ed., *Modelling and Simulation 1993* (Society for Computer Simulation International, Ghent).
Paveri-Fontana, S. L., 1975, Transp. Res. **9**, 225.
Payne, H. J., 1971, in *Mathematical Models of Public Systems*, edited by G. A. Bekey (Simulation Council, La Jolla, CA), Vol. 1, p. 51.

Payne, H. J., 1979a, in *Research Directions in Computer Control of Urban Traffic Systems*, edited by W. S. Levine, E. Lieberman, and J. J. Fearnsides (American Society of Civil Engineers, New York), p. 251.
Payne, H. J., 1979b, Transp. Res. Rec. **722**, 68.
Payne, H., 1984, Transp. Res. Rec. **971**, 140.
Peliti, L., 1985, J. Phys. (Paris) **46**, 1469.
Peng, G., and H. J. Herrmann, 1994, Phys. Rev. E **49**, 1796.
Peng, G., and H. J. Herrmann, 1995, Phys. Rev. E **51**, 1745.
Pennec, T. L., K. J. Måløy, A. Hansen, M. Ammi, D. Bideau, and X.-L. Wu, 1996, Phys. Rev. E **53**, 2257.
Persaud, B. N., 1986, Ph.D. thesis (University of Toronto).
Persaud, B. N., and F. L. Hall, 1989, Transp. Res., Part A **23A**, 103.
Persaud, B. N., and V. F. Hurdle, 1988, Transp. Res. Rec. **1194**, 191.
Persaud, B., S. Yagar, and R. Brownlee, 1998, Transp. Res. Rec. **1634**, 64.
Peytchev, E. T., and A. Bargiela, 1995, in *Modelling and Simulation ESM 1995*, edited by M. Snorek, M. Sujansky, and A. Verbraeck (Society for Computer Simulation International, Istanbul), p. 330.
Phillips, W. F., 1977, *Kinetic Model for Traffic Flow*. Technical Report DOT/RSPD/DPB/50-77/17 (National Technical Information Service, Springfield, VA).
Phillips, W. F., 1979a, Transp. Plan. Technol. **5**, 131.
Phillips, W. F., 1979b, in *Proceedings of the 1978 IEEE Conference on Decision and Control* (IEEE, New York), p. 1032.
Pipes, L. A., 1953, J. Appl. Phys. **24**, 274.
Pöschel, T., 1994, J. Phys. I **4**, 499.
Pöschel, T., and H. J. Herrmann, 1995, Europhys. Lett. **29**, 123.
Poethke, H. J., 1982, Ph.D. thesis (Rheinisch-Westfälische Technische Hochschule, Aachen).
Polus, A., J. L. Schofer, and A. Ushpiz, 1983, J. Transp. Eng. **109**, 46.
Popkov, V., L. Santen, A. Schadschneider, and G. M. Schütz, 2000, J. Phys. A **34**, L45.
Popkov, V., and G. M. Schütz, 1999, Europhys. Lett. **48**, 257.
Predtetschenski, W. M., and A. I. Milinski, 1971, *Personenströme in Gebäuden—Berechnungsmethoden für die Projektierung* (Müller, Köln-Braunsfeld).
Prigogine, I., 1961, in *Theory of Traffic Flow*, edited by R. Herman (Elsevier, Amsterdam), p. 158.
Prigogine, I., 1976, in *Evolution and Consciousness. Human Systems in Transition*, edited by E. Jantsch and C. H. Waddington (Addison-Wesley, Reading, MA), p. 93.
Prigogine, I., and F. C. Andrews, 1960, Oper. Res. **8**, 789.
Prigogine, I., and R. Herman, 1971, *Kinetic Theory of Vehicular Traffic* (Elsevier, New York).
Putensen, K., 1994, *Ein makroskopisches Modell des Verkehrsablaufs auf Stadtstraßen und seine Anwendung in der Leittechnik* (Schriftenreihe der Arbeitsgruppe Automatisierungstechnik, TU Hamburg-Harburg).
Quarantelli, E., 1957, Sociol. Soc. Res. **41**, 187.
Rajewsky, N., L. Santen, A. Schadschneider, and M. Schreckenberg, 1998, J. Stat. Phys. **92**, 151.
Rajewsky, N., and M. Schreckenberg, 1997, Physica A **245**, 139.
Rapoport, A., 1986, *General System Theory. Essential Concepts and Applications* (Abacus, Tunbridge Wells, Kent).
Rathi, A. K., E. B. Lieberman, and M. Yedlin, 1987, Transp. Res. Rec. **1112**, 61.
Raub, R. A., and R. C. Pfefer, 1998, Transp. Res. Rec. **1634**, 86.
Rauch, E. M., M. M. Millonas, and D. R. Chialvo, 1995, Phys. Lett. A **207**, 185.
Rechenberg, I., 1973, *Evolutionsstrategie: Optimierung technischer Systeme nach Prinzipien der biologischen Evolution* (Frommann-Holzboog, Stuttgart).
Redelmeier, D. A., and R. J. Tibshirani, 1999, Nature (London) **401**, 35.
Reimann, P., 2000, Phys. Rep. (in press).
Reiss, H., A. D. Hammerich, and E. W. Montroll, 1986, J. Stat. Phys. **42**, 647.
Reuschel, A., 1950a, Österr. Ing.-Archiv **4**, 193.
Reuschel, A., 1950b, Z. Oesterr. Ing.-Archit.-Ver. **95**, 59–62, 73–77.
Reynolds, C. W., 1987, Comput. Graph. **21**, 25.
Reynolds, C. W., 1994, in *From Animals to Animats 3: Proceedings of the Third International Conference on Simulation of Adaptive Behavior (SAB94)*, edited by D. Cliff, P. Husbands, J.-A. Meyer, and S. Wilson (MIT, Cambridge, MA), p. 402.
Reynolds, C. W., 1999, in *Proceedings of the 1999 Game Developer's Conference*, edited by A. Yu (Miller Freeman, San Francisco), p. 763.
Richards, P. I., 1956, Oper. Res. **4**, 42.
Rickert, M., and K. Nagel, 1997, Int. J. Mod. Phys. C **8**, 483.
Rickert, M., K. Nagel, M. Schreckenberg, and A. Latour, 1996, Physica A **231**, 534.
Rickert, M., and P. Wagner, 1996, Int. J. Mod. Phys. C **7**, 133.
Risken, H., 1989, *The Fokker-Planck Equation*, 2nd ed. (Springer, New York).
Ristow, G. H., and H. J. Herrmann, 1994, Phys. Rev. E **50**, R5.
Robertson, D. I., 1969a, Traffic Eng. Control **10**, 276.
Robertson, D. I., 1969b, *TRANSYT—A Traffic Network Study Tool*. Report No. TRRL-LR-253 (Transport and Road Research Laboratory, Crowthorne).
Rodríguez-Iturbe, I., and A. Rinaldo, 1997, *Fractal River Basins: Chance and Self-Organization* (Cambridge University, Cambridge, England).
Rørbech, J., 1976, Transp. Res. Rec. **596**, 22.
Rosato, A., K. J. Strandburg, F. Prinz, and R. H. Swendsen, 1987, Phys. Rev. Lett. **58**, 1038.
Roters, L., S. Lübeck, and K. D. Usadel, 1999, Phys. Rev. E **59**, 2672.
Roters, L., S. Lübeck, and K. D. Usadel, 2000, Phys. Rev. E **61**, 3272.
Roy, J. R., 1992, in *Proceedings of the IV. World Congress of the Regional Science Association International* (Palma de Mallorca).
Rudavets, M. G., 1993, J. Phys.: Condens. Matter **5**, 1039.
Rysgaard, R., 1998, in *Proceedings of the 3rd International Symposium on Highway Capacity and Quality of Service*, edited by R. Rysgaard (Road Directorate, Denmark), p. 49.
Sandahl, J., and M. Percivall, 1972, Traffic Q. **26**, 359.
Sandow, S., and S. Trimper, 1993a, J. Phys. A **26**, 3079.
Sandow, S., and S. Trimper, 1993b, Europhys. Lett. **21**, 799.
Santra, S. B., S. Schwarzer, and H. Herrmann, 1996, Phys. Rev. E **54**, 5066.
Sasamoto, T., and M. Wadati, 1997, J. Phys. Soc. Jpn. **66**, 279.
Sasvari, M., and J. Kertész, 1997, Phys. Rev. E **56**, 4104.
Sauermann, G., and H. J. Herrmann, 1998, in *Traffic and Granular Flow '97*, edited by M. Schreckenberg and D. E. Wolf (Springer, New York), p. 481.
Schadschneider, A., 1999, Eur. Phys. J. B **10**, 573.

Schadschneider, A., 2001, in *Pedestrian and Evacuation Dynamics*, edited by M. Schreckenberg and S. D. Sharma (Springer, Berlin), p. 75.
Schadschneider, A., and M. Schreckenberg, 1993, J. Phys. A **26**, L679.
Schadschneider, A., and M. Schreckenberg, 1997a, Ann. Phys. (Leipzig) **6**, 541.
Schadschneider, A., and M. Schreckenberg, 1997b, J. Phys. A **30**, L69.
Schadschneider, A., and M. Schreckenberg, 1998, J. Phys. A **31**, L225.
Schelhorn, T., D. O'Sullivan, M. Haklay, and M. Thurstain-Goodwin, 1999, *STREETS: An agent-based pedestrian model* presented at the conference *Computers in Urban Planning and Urban Management* (Venice, Italy).
Schick, K. L., and A. A. Verveen, 1974, Nature (London) **251**, 599.
Schmidt-Schmiedebach, R., 1973, Ph.D. thesis (University of Munich).
Schmittmann, B., and R. K. P. Zia, 1995, *Statistical mechanics of driven diffusive systems*, Vol. 17 of *Phase Transitions and Critical Phenomena*, edited by C. Domb and J. L. Lebowitz (Academic, London).
Schmittmann, B., and R. K. P. Zia, 1998, Phys. Rep. **301**, 45.
Schreckenberg, M., A. Schadschneider, K. Nagel, and N. Ito, 1995, Phys. Rev. E **51**, 2939.
Schreckenberg, M., and S. D. Sharma, 2001, Eds., *Pedestrian and Evacuation Dynamics* (Springer, Berlin).
Schreckenberg, M., and D. E. Wolf, 1998, Eds., *Traffic and Granular Flow '97* (Springer, Singapore).
Schubert, H., 1967, *Planungsmaßnahmen für den Fußgängerverkehr in den Städten* (Bundesministerium für Verkehr, Abt. Straßenbau, Bonn).
Schütt, H., 1990, *Entwicklung und Erprobung eines sehr schnellen, bitorientierten Verkehrssimulationssystems für Straßennetze* (Technische Universität, Hamburg-Harburg).
Schütz, G., 1993, J. Stat. Phys. **71**, 471.
Schütz, G., 1998, Eur. Phys. J. B **5**, 589.
Schütz, G. M., 2000a, *Exactly solvable models for many-body systems far from equilibrium*, Vol. 19 of *Phase Transitions and Critical Phenomena*, edited by C. Domb and J. Lebowitz (Academic, London).
Schütz, G. M., 2000b, Phys. Bl. **56**, 69.
Schütz, G., and E. Domany, 1993, J. Stat. Phys. **72**, 277.
Schütz, G., and S. Sandow, 1994, Phys. Rev. E **49**, 2726.
Schuster, H. G., 1988, *Deterministic Chaos*, 2nd ed. (VCH—Verlag Chemie, Weinheim).
Schwarz, T., 1995, Master's thesis (University of Stuttgart).
Schwefel, H.-P., 1977, *Numerische Optimierung von Computer-Modellen mittels Evolutionsstrategien* (Birkhäuser, Stuttgart).
Schweitzer, F., 1997a, Ed., *Self-Organization of Complex Structures: From Individual to Collective Dynamics* (Gordon and Breach, London).
Schweitzer, F., 1997b, in *Stochastic Dynamics*, edited by L. Schimansky-Geier and T. Pöschel (Springer, Berlin), p. 358.
Schweitzer, F., 2001, *Brownian Agents and Active Particles* (Springer, Berlin).
Schweitzer, F., W. Ebeling, H. Rosé, and O. Weiss, 1998, Evol. Comput. **5**, 419.
Schweitzer, F., W. Ebeling, and B. Tilch, 1998, Phys. Rev. Lett. **80**, 5044.
Schweitzer, F., K. Lao, and F. Family, 1997, BioSystems **41**, 153.
Schweitzer, F., and L. Schimansky-Geier, 1994, Physica A **206**, 359.
Schweitzer, F., L. Schimansky-Geier, W. Ebeling, and H. Ulbricht, 1988, Physica A **150**, 261.
Schweitzer, F., B. Tilch, and W. Ebeling, 2000, Eur. Phys. J. B **14**, 157.
Schwerdtfeger, T., 1987, Ph.D. thesis (University of Karlsruhe).
Sela, N., and I. Goldhirsch, 1995, Phys. Fluids **7**, 507.
Sela, N., I. Goldhirsch, and S. H. Noskowicz, 1996, Phys. Fluids **8**, 2337.
Semenzato, R., 1981a, Transp. Theory Stat. Phys. **9**, 83.
Semenzato, R., 1981b, Transp. Theory Stat. Phys. **9**, 95.
Seppäläinen, T., and J. Krug, 1999, J. Stat. Phys. **95**, 525.
Shimoyama, N., K. Sugawara, T. Mizuguchi, Y. Hayakawa, and M. Sano, 1996, Phys. Rev. Lett. **76**, 3870.
Shvetsov, V., and D. Helbing, 1999, Phys. Rev. E **59**, 6328.
Sick, B., 1989, Master's thesis (University of Ulm).
Siggia, E. D., 1977, Phys. Rev. B **16**, 2319.
Simon, P. M., and H. A. Gutowitz, 1998, Phys. Rev. E **57**, 2441.
Simon, P. M., and K. Nagel, 1998, Phys. Rev. E **58**, 1286.
Smilowitz, K., and C. F. Daganzo, 1999, PATH Working Paper UCB-ITS-PWP-99-5 (Institute of Transportation Studies, University of California, Berkeley, CA).
Smith, R. A., and J. F. Dickie, 1993, Eds., *Engineering for Crowd Safety* (Elsevier, Amsterdam).
Smulders, S., 1986, *Modelling and Simulation of Freeway Traffic Flow*. Report OS-R8615 (Centre for Mathematics and Computer Science, Amsterdam).
Smulders, S. A., 1987, in *Proceedings of the 10th International Symposium on Transportation and Traffic Theory*, edited by N. H. Gartner and N. H. M. Wilson (Elsevier, New York), p. 139.
Smulders, S., 1989, Ph.D. thesis (University of Twente).
Smulders, S., 1990, Transp. Res., Part B: Methodol. **24B**, 111.
Snorek, M., M. Sujansky, and A. Verbraeck, 1995, Eds., *Modelling and Simulation ESM 1995* (Society for Computer Simulation International, Istanbul).
Sparmann, U., 1978, Ed., *Spurwechselvorgänge auf zweispurigen BAB-Richtungsfahrbahnen* (Bundesministerium für Verkehr, Abt. Straßenbau, Bonn-Bad Godesberg).
Spektrum der Wissenschaft, 1995, *Dossier: Verkehr und Auto* (Spektrum der Wissenschaft, Heidelberg).
Spitzer, F., 1970, Adv. Math. **5**, 246.
Spohn, H., 1991, *Large Scale Dynamics of Interacting Particles* (Springer, Berlin).
Stanley, H. E., 1971, *Introduction to Phase Transitions and Critical Phenomena* (Oxford University, Oxford).
Stanley, H. E., and N. Ostrowsky, 1986, Eds., *On Growth and Form* (Nijhoff, Boston).
Stauffer, D., 1991, J. Phys. A **24**, 909.
Stauffer, D., and A. Aharony, 1994, *Introduction to Percolation Theory* (Taylor & Francis, London).
Stauffer, D., and H. E. Stanley, 1996, *From Newton to Mandelbrot* (Springer, Berlin).
Stevens, A., 1992, Ph.D. thesis (Ruprecht-Karls-University Heidelberg).
Stevens, A., and F. Schweitzer, 1997, in *Dynamics of Cell and Tissue Motion*, edited by W. Alt, A. Deutsch, and G. Dunn (Birkhäuser, Basel), p. 183.
Still, G. K., 1993, Fire **84**, 40.
Still, G. K., 2000, Ph.D. thesis (University of Warwick).

Stinchcombe, R. B., 1983, *Dilute Magnetism*, Vol. 7 of *Phase Transitions and Critical Phenomena*, edited by C. Domb and J. Lebowitz (Academic, New York), p. 151.
Stinchcombe, R. B., and G. Schütz, 1995a, Phys. Rev. Lett. **75**, 140.
Stinchcombe, R. B., and G. Schütz, 1995b, Europhys. Lett. **29**, 663.
Stølum, H.-H., 1996, Nature (London) **271**, 1710.
Stuttgarter Zeitung, April 16, 1996, p. 12.
Sugiyama, Y., A. Nakayama, and K. Hasebe, 2001, in *Pedestrian and Evacuation Dynamics*, edited by M. Schreckenberg and S. D. Sharma (Springer, Berlin), p. 155.
Sugiyama, Y., and H. Yamada, 1997, Phys. Rev. E **55**, 7749.
Swinney, H. L., and J. P. Gollub, 1985, Eds., *Hydrodynamic Instabilities and the Transition to Turbulence* (Springer, Berlin).
Taale, H., and F. Middelham, 1995, in *Modelling and Simulation ESM 1995*, edited by M. Snorek, M. Sujansky, and A. Verbraeck (Society for Computer Simulation International, Istanbul), p. 335.
Tadaki, S.-I., M. Kikuchi, Y. Sugiyama, and S. Yukawa, 1998, J. Phys. Soc. Jpn. **67**, 2270.
Takayasu, M., and H. Takayasu, 1993, Fractals **1**, 860.
Tan, M.-L., Y. H. Qian, I. Goldhirsch, and S. A. Orszag, 1995, J. Stat. Phys. **81**, 87.
Thom, R., 1975, *Structural Stability and Morphogenesis* (Benjamin, Reading, MA).
Thompson, P. A., and E. W. Marchant, 1993, in *Engineering for Crowd Safety*, edited by R. A. Smith and J. F. Dickie (Elsevier, Amsterdam), p. 259.
Tilch, B., 2001, unpublished.
Tilch, B., and D. Helbing, 2000, in *Traffic and Granular Flow '99: Social, Traffic, and Granular Dynamics*, edited by D. Helbing, H. J. Herrmann, M. Schreckenberg, and D. E. Wolf (Springer, Berlin), p. 333.
Timmermans, H., X. van der Hagen, and A. Borgers, 1992, Transp. Res., Part B: Methodol. **26B**, 45.
Toda, M., 1983, *Nonlinear Waves and Solutions* (Kluwer, Dordrecht).
Todosiev, E. P., 1963, *The Action-Point Model of the Driver-Vehicle System*. Technical Report 202A-3 (Ohio State University, Columbus, OH).
Todosiev, E. P., and L. C. Barbosa, 1963/64, Traffic Eng. **34**, 17.
Tokihiro, T., D. Takahashi, J. Matsukidaira, and J. Satsuma, 1996, Phys. Rev. Lett. **76**, 3247.
Tomer, E., L. Safonov, and S. Havlin, 2000, Phys. Rev. Lett. **84**, 382.
Toner, J., and Y. Tu, 1995, Phys. Rev. Lett. **75**, 4326.
Transportation Research Board, 1985, *Highway Capacity Manual*. Special Report 209 (Transportation Research Board, Washington, D.C.).
Transportation Research Board, 1996, *Traffic Flow Theory and Traffic Flow Simulation Models* (Transportation Research Board, Washington, D.C.), Vol. 1566.
Treiber, M., and D. Helbing, 1999a, J. Phys. A **32**, L17.
Treiber, M., and D. Helbing, 1999b, e-print cond-mat/9901239.
Treiber, M., and D. Helbing, 2001, Automatisierungstechnik **49** (11), 478.
Treiber, M., A. Hennecke, and D. Helbing, 1999, Phys. Rev. E **59**, 239.
Treiber, M., A. Hennecke, and D. Helbing, 2000, Phys. Rev. E **62**, 1805.
Treiterer, J., and J. A. Myers, 1974, in *Proceedings of the 6th International Symposium on Transportation and Traffic Theory*, edited by D. Buckley (Reed, London), p. 13.
Treiterer, J., and J. I. Taylor, 1966, Highw. Res. Rec. **142**, 1.
Uhlenbeck, G. E., and G. W. Ford, 1963, *Lectures in Statistical Mechanics* (American Mathematical Society, Providence).
Umbanhowar, P. B., F. Melo, and H. L. Swinney, 1996, Nature (London) **382**, 793.
Vallacher, R., and A. Nowak, 1994, Eds., *Dynamic Systems in Social Psychology* (Academic, New York).
van Kampen, N. G., 1981, *Stochastic Processes in Physics and Chemistry* (North-Holland, Amsterdam).
Vicsek, T., 1992, *Fractal Growth Phenomena*, 2nd ed. (World Scientific, Singapore).
Vicsek, T., A. Czirók, E. Ben-Jacob, I. Cohen, and O. Shochet, 1995, Phys. Rev. Lett. **75**, 1226.
Vilfan, I., R. K. P. Zia, and B. Schmittmann, 1994, Phys. Rev. Lett. **73**, 2071.
Virkler, M. R., and S. Elayadath, 1994, in *Proceedings of the Second International Symposium on Highway Capacity*, edited by R. Akçelik (Transportation Research Board, Washington, D.C.), Vol. 2, p. 671.
Volmuller, I., and R. Hamerslag, 1984, Eds., *Proceedings of the 9th International Symposium on Transportation and Traffic Theory* (VNU Science, Utrecht).
von Bertalanffy, L., 1968, *General System Theory* (Braziller, New York).
Voss, R. F., 1985, in *Scaling Phenomena in Disordered Systems*, edited by R. Pynn and A. Skjeltrop (Plenum, New York), p. 1.
Vumbaco, B. J., 1981, Ed., *Special Report 194* (National Academy of Sciences, Washington, D.C.).
Wagner, C. K. J., 1997a, Ph.D. thesis (Technische Universität, Munich).
Wagner, C., 1997b, Physica A **245**, 124.
Wagner, C., 1997c, Phys. Rev. E **55**, 6969.
Wagner, C., 1998a, Physica A **260**, 218.
Wagner, C., 1998b, J. Stat. Phys. **90**, 1251.
Wagner, C., C. Hoffmann, R. Sollacher, J. Wagenhuber, and B. Schürmann, 1996, Phys. Rev. E **54**, 5073.
Wagner, P., K. Nagel, and D. E. Wolf, 1997, Physica A **234**, 687.
Wagner, P., and J. Peinke, 1997, Z. Naturforsch., A: Phys. Sci. **52a**, 600.
Wang, B. H., and P. M. Hui, 1997, J. Phys. Soc. Jpn. **66**, L1238.
Wang, B. H., Y. R. Kwong, and P. M. Hui, 1998, Phys. Rev. E **57**, 2568.
Wang, B.-H., L. Wang, P. M. Hui, and B. Hu, 1998, Phys. Rev. E **58**, 2876.
Wegener, R., and A. Klar, 1996, Transp. Theory Stat. Phys. **25**, 785.
Weidlich, W., 1991, Phys. Rep. **204**, 1.
Weidlich, W., 1992, unpublished.
Weidmann, U., 1993, *Transporttechnik der Fußgänger* (Institut für Verkehrsplanung, Transporttechnik, Straßen- und Eisenbahnbau, ETH Zürich).
Weiss, G. H., 1994, *Aspects and Applications of Random Walk* (North-Holland, Amsterdam).
Westland, D., 1998, in *Proceedings of the 3rd International Symposium on Highway Capacity*, edited by R. Rysgaard (Road Directorate, Denmark), p. 1095.
Whitham, G. B., 1974, *Linear and Nonlinear Waves* (Wiley, New York).

Whitham, G. B., 1979, *Lectures on Wave Propagation* (Springer, Berlin).
Whitham, G. B., 1990, Proc. R. Soc. London, Ser. A **428**, 49.
Whyte, W. H., 1988, *City. Rediscovering the Center* (Doubleday, New York).
Wiedemann, R., 1974, *Simulation des Straßenverkehrsflusses* (Institut für Verkehrswesen, Universität Karlsruhe, Karlsruhe).
Wiedemann, R., and T. Schwerdtfeger, 1987, *Makroskopisches Simulationsmodell für Schnellstraßennetze mit Berücksichtigung von Einzelfahrzeugen (DYNEMO)* (Bundesministerium für Verkehr, Abt. Straßenbau, Bonn-Bad Godesberg).
Williams, J. C., H. S. Mahmassani, and R. Herman, 1987, Transp. Res. Rec. **1112**, 78.
Windover, J. R., 1998, Ph.D. thesis (University of California, Berkeley, CA).
Woesler, R., P. Schütz, M. Bode, M. Or-Guil, and H.-G. Purwins, 1996, Physica D **91**, 376.
Wolf, D. E., 1999, Physica A **263**, 438.
Wolf, D. E., and P. Grassberger, 1997, Eds., *Friction, Arching, Contact Dynamics* (World Scientific, Singapore).
Wolf, D. E., M. Schreckenberg, and A. Bachem, 1996, Eds., *Traffic and Granular Flow* (World Scientific, Singapore).
Wolfram, S., 1984, Nature (London) **311**, 419.
Wolfram, S., 1986, *Theory and Applications of Cellular Automata* (World Scientific, Singapore).
Wolfram, S., 1994, *Cellular Automata and Complexity* (Addison-Wesley, Reading, MA).
Wolpert, D. H., and K. Tumer, 1999, e-print cs.LG/9908014, Technical Report NASA-ARC-IC-99-63,-124.
Wu, X.-L., K. J. Måløy, A. Hansen, M. Ammi, and D. Bideau, 1993, Phys. Rev. Lett. **71**, 1363.
Yaguchi, H., 1986, Hiroshima Math. J. **16**, 449.
Yang, Q., 1997, Ph.D. thesis (Massachusetts Institute of Technology).
Yang, Q., and H. N. Koutsopoulos, 1996, Transp. Res., Part C: Emerg. Technol. **4**, 113.
Yoshikawa, K., N. Oyama, M. Shoji, and S. Nakata, 1991, Am. J. Phys. **59**, 137.
Youssefmir, M., B. A. Huberman, and T. Hogg, 1998, Comput. Econ. **12**, 97.
Yuhaski, S. J., Jr., and J. M. Macgregor Smith, 1989, Queueing Syst. **4**, 319.
Yukawa, S., and M. Kikuchi, 1995, J. Phys. Soc. Jpn. **64**, 35.
Yukawa, S., and M. Kikuchi, 1996, J. Phys. Soc. Jpn. **65**, 916.
Zeeman, E. C., 1977, Ed., *Catastrophe Theory* (Addison-Wesley, London).
Zhang, H. M., 2000, Transp. Res., Part B: Methodol. **34B**, 583.
Zhang, X., and G. Hu, 1995, Phys. Rev. E **52**, 4664.